UNIVERSITY OF
STIRLING

INVESTIGATING THE LONG-CHAIN POLYUNSATURATED FATTY ACID BIOSYNTHESIS OF THE AFRICAN CATFISH *CLARIAS GARIEPINUS* (BURCHELL, 1822)

THESIS SUBMITTED TO THE UNIVERSITY OF STIRLING
FOR THE DEGREE OF DOCTOR OF PHILOSOPHY

by

ANGELA O. OBOH

FEBRUARY 2018

INSTITUTE OF AQUACULTURE, SCHOOL OF NATURAL SCIENCES,
UNIVERSITY OF STIRLING, STIRLING, SCOTLAND, UK

DECLARATION

This thesis has been composed in its entirety by the candidate. Except where specifically acknowledged, the work described in this thesis has been conducted independently and and has not been submitted for any other degree.

Name: Angela O. Oboh

Sign:

Date:

Name: Óscar Monroig

Sign:

Date:

Name: Douglas R. Tocher

Sign:

Date:

ACKNOWLEDGEMENTS

I would like to express my gratitude to my supervisors Dr Óscar Monroig and Prof. Douglas R. Tocher for their guidance, encouragement and help throughout this project. I am especially indebted to Dr. Óscar Monroig, who taught me most of the experimental methodologies used in this work. I would like to thank Dr. Monica Betancor and Dr Naoki Kabeya who also helped me understand aspects of the laboratory work and for their contributions to the success of this project. I would like to express my appreciation to Dr Juan Carlos Navarro (Instituto de Acuicultura Torre de la Sal (CSIC), Spain) for his support in analysing the fatty acids of the yeast samples reported in Chapter 4 of this thesis. I am thankful to Prof. Brett Glencross for his time and support as well. I am grateful to the staff of the molecular and nutrition laboratories and the tropical aquarium including Dr John Taggart, Mrs Jacquie Ireland, Mr Keith Ransom, Mr. James Dick, Dr Matthew Sprague, Mrs Fiona Strachan, Mrs Elizabeth Mackinlay and Mrs Irene Younger for their advice, support and willingness to help in the laboratory.

I am grateful to the Commonwealth Scholarship Commission for funding this PhD.

I would like to thank all my friends and colleagues at Stirling, especially my office mates through the years, for their friendship and support, and for all the very interesting conversations.

I am grateful to my parents, brothers, sisters and extended family members for their love, support and prayers throughout the duration of my studies.

Finally, I give all the glory to God who saw me through to the end of this project and who never left me alone through this period of my life.

ABSTRACT

Investigating the biosynthesis of long-chain ($C_{20–24}$) polyunsaturated fatty acids (LC-PUFA), physiologically important compounds including arachidonic acid (ARA), eicosapentaenoic acid (EPA) and docosahexaenoic acid (DHA), in fish is crucial to identify dietary requirements for essential fatty acids (EFA). Moreover, knowledge of the $C_{20–24}$ LC-PUFA biosynthetic capability of farmed fish species enables us to understand their ability to utilise commonly used raw materials such as vegetable oils, which naturally lack LC-PUFA but include C_{18} PUFA that are metabolic precursors of LC-PUFA. Studies have shown that the potential of a species for LC-PUFA biosynthesis is associated with the complement and function of fatty acyl desaturase (*fads*) and elongase of very long chain fatty acid (*elovl*) genes existing in that species. The present study therefore aimed to investigate these genes in the African catfish (*Clarias gariepinus*), the most commercially important farmed fish in sub-Saharan Africa. A *fads2*, a *fads6* and four *elovl* (*elovl2*, *elovl4a*, *elovl4b*, *elovl8*) cDNAs were cloned and functionally characterised by heterologous expression in yeast. The Fads2 was a bifunctional desaturase enzyme with Δ6Δ5 and Δ8 activities, and thus catalysing all the desaturation reactions required for ARA and EPA biosynthesis from C_{18} precursor fatty acids. Moreover, the *C. gariepinus* Fads2 enzymes also desaturated 24:5n-3 to 24:6n-3, a Δ6 desaturation required for the biosynthesis of DHA through the so-called "Sprecher pathway". Functional characterisation of Fads6 by heterologous expression in yeast did not reveal its function. With regards to elongases, the *C. gariepinus* Elovl2 demonstrated the ability to elongate C_{20} and C_{22} PUFA and thus complements the Elovl5 with elongase capability towards C_{18} and C_{20} PUFA. The Elovl8 was capable of only limited elongation of C_{18} and C_{20} PUFA. Elovl4a and Elovl4b, enable the biosynthesis of very long-chain ($>C_{24}$) fatty acids, compounds with major roles in vision and fertility of vertebrates. The present study confirmed that *C. gariepinus* possess all the enzymatic capabilities required for the biosynthesis of ARA, EPA and DHA and, therefore, its physiological EFA requirements could be satisfied with dietary provision of C_{18} PUFA.

TABLE OF CONTENTS

DECLARATION 1
ACKNOWLEDGEMENTS 2
ABSTRACT 3
TABLE OF CONTENTS 4
LIST OF ABBREVIATIONS 9
LIST OF FIGURES 12
LIST OF TABLES 15
CHAPTER 1. 17
GENERAL INTRODUCTION 17
1.1 Current Status of Fish Production 18
1.1.1 Production of the African Catfish, *Clarias gariepinus* 19
1.1.2 *Clarias gariepinus* Nutrition 23
1.1.3 Lipid Sources and Essential Lipids for *C. gariepinus* Feed Production 24
1.2 Fatty Acids: Classification and Nomenclature 25
1.3 Fish Essential Fatty Acid Requirements 27
1.4 Biological Functions of Fatty Acids in Fish 32
1.5 Fatty Acid Synthesising Enzymes 34
1.5.1 Fatty Acyl Desaturases 34
1.5.2 The Desaturation of Fatty Acids 36
1.5.3 Classification and Activities of Fads enzymes 37
1.5.4 Elongation of Very Long-chain Fatty Acid (Elovl) protein 39
1.5.5 Classification and Activities of Elongation of Very Long-chain Fatty acid (Elovl) Enzymes 40
1.5.6 Biosynthesis of Long-Chain Polyunsaturated Fatty Acids (LC-PUFA) in Fish 42
1.5.7 LC-PUFA Biosynthetic Capabilities of *Clarias gariepinus* 44
1.6 Objectives of This Study 45
CHAPTER 2. 47
GENERAL MATERIALS AND METHODS 47
2.1 Materials 48
2.2 Preparation of Media, Buffers and Gels 48
2.2.1 Preparation of 50x TRIS/acetate/EDTA (TAE) Buffer (500 ml) 48

2.2.2 Preparation of Luria-Bertini (LB) Medium and Agar (400 ml) 49
2.2.3 Preparation of Competent *Escherichia coli* Cells 49
2.2.4 Preparation of Yeast Extract Peptone Dextrose (YPD) Medium and Agar (100 ml) 50
2.2.5 Preparation of Competent *Saccharomyces cerevisiae* Cells 50
2.2.6 Preparation of Na Salts of Fatty Acids 51
2.2.7 Preparation of *S. cerevisiae* Minimal Medium (SCMM^{-ura}) (400 ml) 51
2.2.8 Preparation of *S. cerevisiae* Minimal Medium Plates (200 ml) 52
2.3 Gene Molecular Cloning 52
2.3.1 Experimental Samples 52
2.3.2 RNA Extraction 52
2.3.3 First Strand cDNA Synthesis 54
2.3.4 Amplification of cDNA Fragments 54
2.3.5 RNA Ligase Mediated Rapid Amplification of cDNA Ends (RLM-RACE) PCR 57
2.3.6 Cloning of PCR Products into PCR 2.0 Vector 58
2.4 Sequence and Phylogenetic Analysis 60
2.5 Functional Characterisation of Genes by Heterologous Expression in *Saccharomyces cerevisiae* 61
2.5.1 Cloning of the PCR Product into pYES2 Vector 61
2.5.2 Transformation of Yeast Competent Cells with Plasmid Constructs 61
2.5.3 Yeast Culture 62
2.6 Fatty Acid Analysis of Yeast 62
2.6.1 Total Lipid Extraction 62
2.6.2 Preparation and Purification of Fatty Acid Methyl Esters 63
2.7 Tissue Expression Analysis of *C. gariepinus* Genes 64
2.8 Statistical Analysis 66
CHAPTER 3 67
BIOSYNTHESIS OF LONG-CHAIN POLYUNSATURATED FATTY ACIDS IN THE AFRICAN CATFISH CLARIAS GARIEPINUS: MOLECULAR CLONING AND FUNCTIONAL CHARACTERISATION OF FATTY ACYL DESATURASE (FADS2) AND ELONGASE (ELOVL2) cDNAS 67
3.1 Introduction 68
3.2 Materials and Methods 71
3.2.1 Sample Collection and RNA Preparation 71

3.2.2 Molecular Cloning of Fads2 and Elovl2 cDNAs 72
3.2.3 Sequence and Phylogenetic Analysis 75
3.2.4 Functional Characterisation of *C. gariepinus* Fads2 and Elovl2 by Heterologous Expression in *Saccharomyces cerevisiae* 75
3.2.5 Fatty Acid Analysis of Yeast 76
3.2.6 Gene Expression Analysis 76
3.2.7 Statistical Analysis 77
3.3 Results 78
3.3.1 Sequence and Phylogenetic Analysis 78
3.3.2 Functional Characterisation of *C. gariepinus* Fads2 and Elovl2 in *S. cerevisiae* 81
3.3.3 Tissue Expression Analysis of *C. gariepinus fads2*, *elovl2* and *elovl5* 86
3.4 Discussion 87
CHAPTER 4. 95
ELONGATION OF VERY LONG-CHAIN (> C_{24}) FATTY ACIDS IN CLARIAS GARIEPINUS: CLONING, FUNCTIONAL CHARACTERISATION AND TISSUE EXPRESSION OF ELOVL4 ELONGASES 95
4.1 Introduction 96
4.2 Materials and Methods 99
4.2.1 Sample Collection and RNA Preparation 99
4.2.2 Molecular Cloning of Elovl4 cDNA 99
4.2.3 Sequence and Phylogenetic Analysis 100
4.2.4 Functional Characterisation of *C. gariepinus* Elovl4a and Elovl4b by Heterologous Expression in *Saccharomyces cerevisiae* 100
4.2.5 Fatty Acid Analysis of Yeast 102
4.2.6 Gene Expression Analysis 103
4.2.7 Statistical Analysis 104
4.3 Results 104
4.3.1 Elovl4 Sequence and Phylogenetic Analysis 104
4.3.2 Functional Characterisation of *C. gariepinus* Elovl4 in Yeast 107
4.3.3 Tissue Expression Analysis of *C. gariepinus elovl4a* and *elovl4b* 112
4.4 Discussion 113
CHAPTER 5. 119
TWO ALTERNATIVE PATHWAYS FOR DOCOSAHEXAENOIC ACID (DHA, 22:6n-3) BIOSYNTHESIS ARE WIDESPREAD AMONG TELEOST FISH 119

5.1 Introduction 120
5.2 Materials and Methods 123
5.2.1 Fish Lineages 123
5.2.2 Determination of Δ6 Desaturase Activity of Fish Fads2 towards C_{24} PUFA in Co-Transformant *Saccharomyces cerevisiae* 123
5.2.3 In silico Retrieval of Putative Δ4 Desaturases 126
5.2.4 Phylogenetic Analysis of Fads Desaturases 126
5.2.5 Fatty Acid Analysis of Yeast 127
5.3 Results 127
5.3.1 Determination of Δ6 Desaturase Activity of Fish Fads towards C_{24} PUFA 127
5.3.2 Putative Δ4 desaturase Collection and Phylogenetics 130
5.4 Discussion 133
CHAPTER 6. 139
DETERMINING THE FUNCTION OF NOVEL FADS AND ELOVL ENZYMES IN THE AFRICAN CATFISH CLARIAS GARIEPINUS 139
6.1 Introduction 140
6.2 Materials and Methods 142
6.2.1 Molecular Cloning of Novel *fads* and *elovl* cDNAs 142
6.2.2 Sequence and Phylogenetic Analysis 144
6.2.3 Synteny Analysis 144
6.2.4 Functional Characterisation of *C. gariepinus* Novel *fads* and *elovl* by Heterologous Expression in *Saccharomyces cerevisiae* 145
6.2.5 Fatty Acid Analysis of Yeast 146
6.2.6 4,4-dimethyloxazoline (DMOX) Derivative Analysis with Gas Chromatography-Mass Spectrometry (GC-MS) 146
6.3 Results 147
6.3.1 Sequence and Phylogenetic Analysis of Fads6 147
6.3.2 Synteny Analysis of *fads6* 150
6.3.3 Functional Characterisation of Fads6 by Heterologous Expression in *Saccharomyces cerevisiae* 151
6.3.4 Sequence and Phylogenetic Analysis of Elovl8 152
6.3.5 Synteny Analysis of *elovl8* 156
6.3.6 Functional Characterisation of Elovl8 by Heterologous Expression in *Saccharomyces cerevisiae* 160
6.4 Discussion 165

6.4.1 Fads6 166
6.4.2 Elovl8 168
6.4.3 Conclusions 170
CHAPTER 7. 171
GENERAL DISCUSSION AND CONCLUSIONS 171
7.1 Introduction 172
7.2 Desaturases in LC-PUFA biosynthesis pathways 174
7.3 Elongases in LC-PUFA pathways 175
7.4 Tissues expression patterns of genes encoding LC- and VLC-PUFA biosynthesising enzymes 177
7.5 Novel enzymes Fads6 and Elovl8 178
7.6 Conclusion 178
REFERENCES 181

LIST OF ABBREVIATIONS

aa, amino acid

ABO, accessory breathing organ

ACP, acyl carrier protein

ALA, α-linolenic acid

ANOVA, analysis of variance

ARA, arachidonic acid

BHT, butylated hydroxytoluene

bp, base pair

cDNA, complementary DNA

CIP, calf intestine alkaline phosphatase

DHA, docosahexaenoic acid

DMOX, 4,4-dimethyloxazoline

DPA, docosapentaenoic acid

DTA, docosatetraenoic acid

EDTA, ethylenediaminetetraacetic acid

EFA, essential fatty acid

Elovl, elongation of very long-chain fatty acid protein

EPA, eicosapentaenoic acid

ER, endoplasmic reticulum

EST, expressed sequence tag

FA, fatty acid

FAD, flavin adenine dinucleotide

Fads, fatty acyl desaturase

FAME, fatty acid methyl ester

FAS, fatty acid synthase

FM, fishmeal

FO, fish oil

GC-MS, gas chromatography-mass spectrometry

LA, linoleic acid

LB, luria-Bertini

LC-PUFA, long-chain (C_{20-24}) polyunsaturated fatty acid

NAD+, nicotinamide adenine dinucleotide

NADP, nicotinamide adenine dinucleotide phosphate

ND, not detected

NMI, non-methylene interrupted

NTC, no template control

$OD_{600,}$ optical density measured at a wavelength of 600 nm

OFN, oxygen-free nitrogen

OLE1, stearoyl-CoA Δ9 desaturase

ORF, open reading frame

PCR, polymerase chain reaction

PUFA, polyunsaturated fatty acid

qPCR, quantitative real-time polymerase chain reaction

RLM-RACE, RNA ligase mediated rapid amplification of cDNA ends

SCD, stearoyl CoA desaturases

$SCMM^{-ura}$, *Saccharomyces cerevisiae* minimal medium minus uracil

SRA, sequence read archive

TAP, tobacco acid pyrophosphatase

THA, tetracosahexaenoic acid

TLC, thin-layer chromatography

TPA, tetracosapentaenoic acid

TSA, transcriptome shotgun assembly

VLC-PUFA, very long-chain (> C_{24}) polyunsaturated fatty acid

VLC-SFA, very long-chain (> C_{24}) saturated fatty acid

VO, vegetable oil

LIST OF FIGURES

Chapter 1

Figure 1.1. Morphological characteristics of the African catfish *Clarias gariepinus*…..20

Figure 1.2 Main global producers of *Clarias gariepinus*……21

Figure 1.3. The biosynthetic pathways of long-chain polyunsaturated fatty acids (LC-PUFA) from dietary α-linolenic (18:3n-3) and linoleic (18:2n-6) acids in teleosts…….29

Figure 1.4. The predicted topology of membrane desaturase in relation to the membrane……35

Figure 1.5. The sequence of desaturation reaction……..36

Figure 1.6. The steps of fatty acid elongation of long-chain fatty acids……..39

Chapter 2

Figure 2.1. A typical agarose gel image. Gel image for the screening of *Clarias gariepinus fads2* first fragment ligated into PCR 2.0 vector ……...…56

Chapter 3

Figure 3.1. Phylogenetic tree comparing the deduced amino acid sequence of *Clarias gariepinus* Fads2 with Fads from a range of vertebrates. ……..79

Figure 3.2. Phylogenetic tree comparing the deduced amino acid sequence of *Clarias gariepinus* Elovl2 with Elovl2, Elovl4 and Elovl5 from a range of vertebrates…….81

Figure 3.3. Functional characterisation of the newly cloned *Clarias gariepinus* Fads2 in yeast (*Saccharomyces cerevisiae*)...……..83

Figure 3.4. Functional characterisation of the newly cloned *Clarias gariepinus* Elovl2 in yeast (*Saccharomyces cerevisiae*)……...……85

Figure 3.5. Tissue distribution of *fads2, elovl2* and *elovl5* transcripts in *Clarias gariepinus*. 87

Chapter 4

Figure 4.1. Phylogenetic tree comparing the deduced amino acid sequences of *Clarias gariepinus* Elovl4a and Elovl4b (highlighted in bold) with Elovl4, Elovl2 and Elovl5 sequences from a range of vertebrates……..……104

Figure 4.2 ClustalW amino acid alignment of the deduced *Clarias gariepinus* Elovl4 proteins with orthologues from *Danio rerio* (Elovl4a, gb|NP_957090.1|; Elovl4b, gb

|NP_956266.1|), *Nibea mitsukurii* (gb|AJD80650.1|) and *Clupea harengus* (gb|XP_012692914.1|)……..105
Figure 4.3 Functional characterisation of the newly cloned *Clarias gariepinus* Elovl4a (a and b) and Elovl4b (c and d) in yeast (*Saccharomyces cerevisiae*)……..107
Figure 4.4. Tissue distribution of *Clarias gariepinus elovl4a* and *elovl4b* transcripts…. ……110

Chapter 5

Figure 5.1. Characterisation of fish fatty acyl desaturases 2 (Fads2) ability to desaturate 24:5n-3……..128
Figure 5.2. Phylogenetic tree comparing the amino acid sequences of teleost Fads2 with non-teleost vertebrate Fads-like from the cartilaginous fish and mammals (human and mouse)……...…130

Chapter 6

Figure 6.1. Amino acid alignment of the deduced *Clarias gariepinus* Fads6 proteins with Fads6 proteins from three teleost (*D. rerio*, *Fundulus heteroclitus*, *Labrus bergylta*), a mammalian (*Homo sapiens*), a reptilian (*Alligator sinensis*) and an avian (*Calypte anna*) species using Clustal Omega…….146
Figure 6.2. Phylogenetic tree comparing the deduced amino acid sequences of *Clarias gariepinus* Fads6 with desaturase sequences from a range of teleost species…….147
Figure 6.3. Schematic presentation of synteny blocks showing the mapping of *fads6* and other conserved genes across a range of vertebrate species……...149
Figure 6.4. Amino acid alignment of the deduced *Clarias gariepinus* Elovl8, Elovl4a and Elovl4b proteins using Clustal Omega……152
Figure 6.5. Phylogenetic tree comparing the deduced amino acid sequences of *Clarias gariepinus* Elovl8 with Elovl4, Elovl2 and Elovl5 sequences from a range of teleost species..…….153
Figure 6.6. Schematic presentation of synteny blocks showing the mapping of the *elovl8* gene cloned in this study that formed a group with *Danio rerio elovl8b* and other conserved genes across a range of vertebrate species……155
Figure 6.7. Schematic presentation of synteny blocks showing the mapping of *elovl8a* and flanking genes across a range of vertebrate species…….157

Figure 6.8. Schematic presentation of the synteny block of *Danio rerio* showing *elovl8a versus Ictalurus punctatus*…….158
Figure 6.9. Functional characterisation of *Clarias gariepinus* Elovl8 elongase in yeast (*Saccharomyces cerevisiae*)……..160
Figure 6.10. Mass spectrum of 4,4-dimethyloxazoline DMOX derivatives of 20:3n-3 elongated from 18:3n-3 by the *Clarias gariepinus* Elovl8…….161
Figure 6.11. Mass spectrum of 4,4-dimethyloxazoline DMOX derivatives of 20:3n-6 elongated from 18:3n-6 by the *Clarias gariepinus* Elovl8……..161
Figure 6.12. Mass spectrum of 4,4-dimethyloxazoline DMOX derivatives of 20:4n-3 elongated from 18:4n-3 by the *Clarias gariepinus* Elovl8…….162
Figure 6.13. Mass spectrum of 4,4-dimethyloxazoline DMOX derivatives of 22:4n-6 elongated from 20:4n-6 by the *Clarias gariepinus* Elovl8…….162

Chapter 7

Figure 7.1. The biosynthesis pathway of long-chain (C_{20-24}) polyunsaturated fatty acids from α-linolenic (18:3n-3) and linoleic (18:2n-6) acids in *Clarias gariepinus*……...174

LIST OF TABLES

Chapter 1

Table 1.1. Fatty acid nomenclature. .....….26

Chapter 2

Table 2.1. The quantity of fatty acid, 1M NaOH and 5.6 % Tergitol used in preparation of sodium (Na) salts of fatty acids.....51

Chapter 3

Table 3.1. Sequences of primers used for cDNA cloning and tissue expression analysis (qPCR) of *Clarias gariepinus fads2* and *elovl2*. 74

Table 3.2. Substrate conversions of *Saccharomyces cerevisiae* transformed with *Clarias gariepinus fads2* coding region and grown in the presence of exogenously added substrates (18:3n-3, 18:2n-6, 20:3n-3, 20:2n-6, 20:4n-3, 20:3n-6, 22:5n-3 or 22:4n-6). 84

Table 3.3. Substrate conversions of *Saccharomyces cerevisiae* transformed with *Clarias gariepinus elovl2* coding region and grown in the presence of exogenously added substrates (18:3n-3, 18:2n-6, 18:4n-3, 18:3n-6, 20:5n-3, 20:4n-6, 22:5n-3 or 22:4n-6)..86

Chapter 4

Table 4.1. Sequences of primers used for molecular cloning of full-length cDNA and tissue expression analysis (qPCR) of *Clarias gariepinus elovl4a* and *elovl4b*……...100

Table 4.2. Functional characterisation of *Clarias gariepinus* Elovl4 elongases: role in biosynthesis of very long-chain saturated fatty acids (VLC-PUFA) …….106

Table 4.3. Functional characterisation of *Clarias gariepinus* Elovl4 elongases: role in biosynthesis of very long-chain polyunsaturated fatty acids (VLC-PUFA)……..108-109

Chapter 5

Table 5.1. Fish fatty acyl desaturases (Fads) investigated for the ability to desaturate tetracosapentaenoic acid (24:5n-3) to tetracosahexaenoic acid (24:6n-3)……123

Table 5.2. Capability of fish Fads2 for Δ6 desaturation of C_{24} substrates 24:4n-6 and 24:5n-3 using a yeast *Saccharomyces cerevisiae* heterologous system as described in Materials and Methods……..127

Chapter 6

Table 6.1. Sequences of primers used for cDNA cloning of *Clarias gariepinus fads6* and *elovl8*. Restriction sites *Hin*dIII (forward) and *Xba*I (reverse) are underlined……...141

Table 6.2. Functional characterisation of the novel *Clarias gariepinus* Elovl8 elongase ……..159

CHAPTER 1.

GENERAL INTRODUCTION

1.1 Current Status of Fish Production

Fish is the most important source of long chain (C_{20-24}) polyunsaturated fatty acids (LC-PUFA), physiologically essential fatty acids (EFA) in human diet, in addition to being a rich source of other important nutrients including protein, vitamins and minerals (Bell and Koppe, 2010; Beveridge et al., 2013; Tocher, 2015). Whereas capture fisheries provided the bulk of fish supplied for human consumption in the past, aquaculture has increasingly contributed to global fish supply in the last few decades, rising from 26 % in 2000 to approximately 45 % of the global production of fish in 2015 (Beveridge et al., 2013; FAO, 2017). Freshwater species are among the farmed fish species driving global production and are projected to make up about 60 % of total aquaculture production by 2025 (De Silva, 2012; De Silva et al., 2010; FAO, 2016). Therefore, as the fastest growing food production sector in the world, aquaculture offers food security, chiefly through the significant production of low-value freshwater species (FAO, 2016; Tidwell and Allan, 2001). This is important for several reasons, one of which is that these species require little or no input of marine ingredients, namely fishmeal (FM) and fish oil (FO), finite and expensive raw materials (Rana et al., 2009). Thus, low-value freshwater fish species can be more tolerant of the current increasing use of vegetable products in fish feed, leading to lower production cost compared to the higher valued species.

FM and FO have traditionally been used in fish feeds as prime sources of proteins, amino acids, essential lipids and micronutrients (Tacon et al., 2011). However, the combination of stagnant production, increasing cost and competition that aquaculture has with livestock production and nutraceutical industries (FO use as supplements) has made identification and use of alternative protein and lipid sources in fish feed essential for ensuring the sustainable development of the industry (FAO, 2016; Ng et al., 2003; Tidwell and Allan, 2001). Thus, plant protein and oil sources that are readily available, more sustainable and

cheaper are increasingly used to replace the marine raw materials in aquafeeds. The disadvantage, however, is that substitution with plant ingredients may compromise levels of some essential nutrients in the feed. Therefore, replacement needs to take into account the nutritional profiles of marine *versus* plant ingredients.

Furthermore, low-value fish are the major species produced in developing countries. An example is the African catfish *Clarias gariepinus*, which accounts for almost 50 % of fish produced (including capture fisheries) in countries like Nigeria (FAO, 2016). Despite the recent rise in aquaculture production in Africa, a huge portion of fish consumed is still imported, frozen fish, as the combined fisheries and aquaculture production do not meet demand (FAO, 2014). Aquaculture has long been regarded as the means to bridge the gap between demand and supply of fish, and a focus on freshwater species that can be sustainably farmed arises as a reasonable way to achieve this goal.

1.1.1 Production of the African Catfish, *Clarias gariepinus*

The African Catfish, also known as the North African catfish, *Clarias gariepinus*, is a freshwater species of catfish belonging to the family Clariidae and order Siluriformes (Figure 1.1). The species has a number of favourable characteristics that make it an excellent species for farming and was adopted as the most desirable African catfish for aquaculture in the mid-1970s (Pouomogne, 2010; Van Weerd, 1995). *C. gariepinus* is fast growing, reaching over 1 kg in a year. They are hardy and can tolerate conditions of low dissolved oxygen because they possess large, multibranched accessory air-breathing organs also known as arborescent organs, above their gill arches (Figure 1.1). *C. gariepinus* can be fed a wide variety of feed ingredients and have been classified as euryphagous, opportunistic, omnivorous predators (Atanda, 2007; Hecht, 2013; Pouomogne, 2010). All these may account for why *C. gariepinus* is the most important commercially farmed fish

species in sub-Saharan Africa (FAO, 2012), and cultured in many parts of the world including countries in Europe, Asia and South America (Figure 1.2) (Pouomogne, 2010).

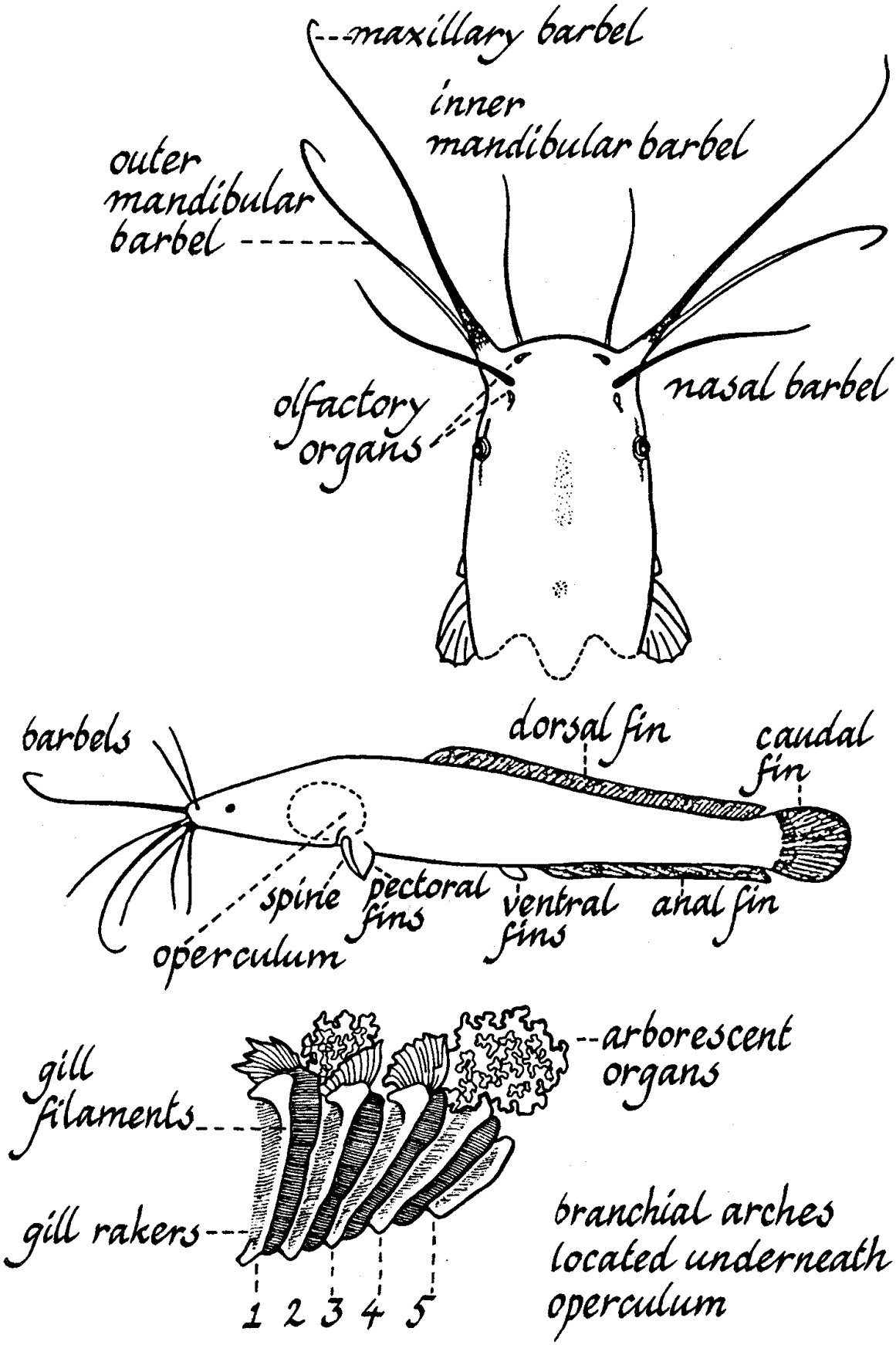

Figure 1.1. Morphological characteristics of the African catfish *Clarias gariepinus*. Source (De Graaf and Janssen, 1996).

Figure 1.2 Main producers of *Clarias gariepinus*. The map was constructed from FAO reported statistics for this species. (Source: Pouomogne, 2010)

Aquacultural production in Nigeria comprises mostly of African catfish (90 %) (Brummett, 2007). Even though tremendous progress has been made, and intensive fish farming increased markedly in recent years, Nigeria's potential to increase its aquaculture production to meet demand has not been achieved as growth in the sector is hindered by problems such as inadequate supply of high-quality fingerlings and high cost of feed (Atanda, 2007). The early stages of development of catfish are the most critical of all production stages with great losses (up to 70-90%) recorded, mostly related to nutritional causes (Atanda, 2007; Brummett, 2007). Efforts needed to improve the quality and output performance of *C. gariepinus* to enable the full expansion of this species includes production of high quality, cost effective feed for all stages of production.

Fish feed constitutes the highest recurrent cost in aquaculture, ranging from 30 to 60 % of the total production cost (De Silva and Anderson, 1995) and affects the profitability and success of any commercial fish production business. In addition, fish feed determine, together with other factors, the growth performance and health of fish. Fish feed can also influence the final profile of nutritents including fatty acids (FA) in the fish, thus determining the nutritional value for human consumers (Bell et al., 2002; Hoffman and Prinsloo, 1995a; Ng and Chong, 2004; Ng et al., 2003; Sprague et al., 2017; Tocher et al., 2002).

1.1.2 *Clarias gariepinus* Nutrition

The natural feed of *C. gariepinus* juveniles includes plankton, insects, molluscs, crustaceans and detritus, whereas adults feed preferentially on fish, although they are also capable of feeding on various other feed sources available (Van Weerd, 1995). Their natural feeding habits are indicative of their feed requirements and their ability to utilise a wide variety of feed ingredients. *C. gariepinus* is cultured in different systems ranging from extensive polyculture system in ponds to intensive culture in tanks under recirculatory conditions (De Graaf and Janssen, 1996; Hecht, 2013; Pouomogne, 2010). Consequently, feeding husbandry strategies range from provision of nutrients via pond fertilisation (extensive systems), supplemental diets in form of farm and industrial by-products (semi-intensive systems) to nutritionally balanced, complete feeds (intensive systems) (Hecht, 2013; Pouomogne, 2010). Farm and industrial by-products used include rice bran, wheat middling, brewery waste, cottonseed meal, corn meal and peanut (groundnut) meal. These may be fed directly or made into pelleted feeds, and typically consist of 28-35 % protein. Non-conventional feed ingredients also used include chicken entrails, abattoir waste, fish market waste, maggots, termites, earthworms and crickets (Hecht, 2013). Nutritionally balanced sinking or extruded fish pellets are used in intensive system. Nutrients required

for optimal growth and maintaining the health of fish typically include proteins (and their amino acids), lipids (and their fatty acids), vitamins and minerals. Nutritional studies have shown optimum growth rate for *C. gariepinus* is attained with feed containing 40-43 % crude protein, 10-12 % dietary lipid and 12-14 kJ/g digestible energy (Hecht, 2013; Pouomogne, 2010; Van Weerd, 1995).

1.1.3 Lipid Sources and Essential Lipids for *C. gariepinus* Feed Production

Lipids are important components in fish feed formulation. Lipids are high-energy organic molecules containing primarily carbon atoms in a variety of chain or ring conformations. They consists of five main classes: fatty acids (FA), triglycerides, phospholipids, sphingolipids and sterols (De Silva and Anderson, 1995). A variety of vegetable oils (VO) including groundnut oil, olive oil, palm oil, sunflower oil, soybean oil, as well as FO, have been investigated for use in feeds for the African catfish (Hoffman and Prinsloo, 1995a; Ng et al., 2003; Solomon et al., 2012). Interestingly, studies have shown that *C. gariepinus* fed FO as the only lipid source exhibited growth rates lower than those fed VO (Hoffman and Prinsloo, 1995a; Ng et al., 2003, 2004). This has also been reported in another catfish species, *Heterobranchus longifilis* (Legendre et al., 1995). A combination of FO and VO have been shown to give the best growth rates (Ng et al., 2003; Ochang et al., 2007; Solomon et al., 2012). These studies also show body FA composition of *C. gariepinus* is strongly influenced by dietary lipid source and thus, can be used to manipulate the FA composition of *C. gariepinus* (Hoffman and Prinsloo, 1995a, 1995b; Ng et al., 2003).

Dietary lipids supply FA, some of which are the essential compounds that fish cannot synthesise themselves to meet physiological demands, and therefore must be provided in the diet. The requirements for EFA have been shown to vary greatly among fish species and this is dependent upon a species capacity for endogenous FA synthesis (Lovell, 1998; Sargent et al., 2002). Therefore studies determining fish EFA requirements and their

endogenous LC-PUFA biosynthesis capacity at all developmental stages (larvae, juvenile, adult, or broodstock) are vital in fish nutrition for the provision of EFA for optimal growth (NRC, 2011). However, EFA for *C. gariepinus* and its capacity for FA synthesis has not been determined. For clarity purposes, we will first provide a description of the fatty acid nomenclature system used in this dissertation.

1.2 Fatty Acids: Classification and Nomenclature

FA are organic molecules with a carboxylic acid group at the end of an aliphatic chain containing four or more carbons, usually an even number up to 24 (Bell and Koppe, 2010; Castro et al., 2016). On the basis of number of carbon-carbon double bonds present, FA are designated saturated (no double bonds), monounsaturated (one carbon-carbon double bond) or polyunsaturated fatty acids (PUFA) (two or more carbon-carbon double bonds) (Sargent et al., 2002; Tocher, 2003). Long-chain polyunsaturated fatty acids (LC-PUFA) are herein defined as PUFA with aliphatic chains of between C_{20} to C_{24} and three or more double bonds, whereas PUFA with aliphatic chains greater than C_{24} are defined as very long-chain polyunsaturated fatty acids (VLC-PUFA) (Bell and Koppe, 2010; Castro et al., 2016).

There are two systems of naming unsaturated FA: the omega (ω or n-) nomenclature and the delta (Δ) nomenclature. The n- nomenclature system is based on FA chain lengths, number of double bonds and the position of the first double bond from the methyl end of the FA. Thus the n- nomenclature of docosahexaenoic acid (DHA) is 22:6n-3, meaning that it is a FA with 22 carbons, six double bonds, with the first double bond situated three carbon atoms from the methyl end. The Δ nomenclature on the other hand specifies the positions of all double bonds from the carboxyl group carbon, therefore DHA is $22{:}6\Delta^{4,7,10,13,16,19}$. The geometric configuration of most unsaturated FA is the *cis*

configuration, containing double bonds at three carbon intervals separated by a methylene group (Bell and Koppe, 2010). Therefore, all the double bond positions can be inferred once the bond closest to the n-carbon is known (Cook and McMaster, 2002; Lee et al., 2016; Sargent et al., 2002; Wallis et al., 2002). Despite the Δ nomenclature is more precise (it specifies the double bond positions along the FA), the n- nomenclature is the most frequently used in fish nutrition, except in specifying the activities of fatty acyl desaturase (Fads) enzymes (Castro et al., 2016). Both systems of classification have been used in this thesis.

FA are also known by their English names, which often reflect their origin such as "α-linolenic acid" from linseed oil (Sargent et al., 2002), and Greek-Latin names that reflect their number of carbon atoms and double bonds; thus "docosahexaenoic acid" reflects the number of carbon atoms (22) and double bonds (6) (Tocher, 2003). Some common FA mentioned in this study and their different names are presented in Table 1.1.

Table 1.1. Fatty acid nomenclature. The different system of nomenclature used for some of the fatty acids discussed in this study.

Common name	n- nomenclature	Δ nomenclature	Systematic name
Stearic acid	18:0		Octadecanoic acid
Oleic acid	18:1n-9	$18{:}1\Delta^{9}$	9-octadecenoic acid
Linoleic acid (LA)	18:2n-6	$18{:}2\Delta^{9,12}$	9,12-octadecadienoic acid
α-linolenic acid (ALA)	18:3n-3	$18{:}3\Delta^{9,12,15}$	9,12,15-octadecatrienoic acid
Stearidonic acid (SDA)	18:4n-3	$18{:}4\Delta^{6,9,12,15}$	6,9,12,15-octadecatetraenoic acid
Eicosatrienoic acid (ETE)	20:3n-3	$20{:}3\Delta^{11,14,17}$	11,14,17-eicosatrienoic acid
Eicosatetraenoic acid (ETA)	20:4n-3	$20{:}4\Delta^{8,11,14,17}$	8,11,14,17-eicosatetraenoic acid
Arachidonic acid (ARA)	20:4n-6	$20{:}4\Delta^{5,8,11,14}$	5,8,11,14-eicosatetraenoic acid
Eicosapentaenoic acid (EPA)	20:5n-3	$20{:}5\Delta^{5,8,11,14,17}$	5,8,11,14,17-eicosapentaenoic acid
Docosapentaenoic acid (DPA)	22:5n-3	$22{:}5\Delta^{7,10,13,16,19}$	7,10,13,16,19-docosapentaenoic acid
Docosahexaenoic acid (DHA)	22:6n-3	$22{:}6\Delta^{4,7,10,13,16,19}$	4,7,10,13,16,19-docosahexaenoic acid
Tetracosapentaenoic acid (TPA)	24:5n-3	$24{:}5\Delta^{9,12,15,18,21}$	9,12,15,18,21-tetracosapentaenoic acid
Tetracosahexaenoic acid (THA)	24:6n-3	$24{:}6\Delta^{6,9,12,15,18,21}$	6,9,12,15,18,21-tetracosahexaenoic acid

1.3 Fish Essential Fatty Acid Requirements

As stated above, PUFA that fish cannot endogenously synthesise and must obtain from their diet are regarded as EFA (Cook and McMaster, 2002). Basically, EFA have been described as any FA supplied in diets that significantly affects the growth of a species (Glencross, 2009). Various levels of EFA requirements for fish have been identified: maintenance, optimal, maximum growth, survival, body maintenance, least cost production or fish health levels (Hamre et al., 2013; Tocher, 2003). However, Tocher (2015) comprehensively classified EFA in fish into three levels with increasing

requirements. The physiological EFA requirement is the absolute dietary requirement of species of fish for PUFA that prevents the manifestation of EFA deficiency pathologies. The second level is that required for maintaining optimal health and growth performance of the fish. The third level, the highest of all three, is that required to guarantee the nutritional value of the fish for consumers in terms of deposition of health benefiting LC-PUFA (i.e. EPA and DHA) in fish muscle (fillet). The physiological EFA requirement and the level required for maintaining optimal health and growth performance of fish are species specific and dependent on the capacity for endogenous FA synthesis.

Lipogenesis is the term used to describe the endogenous synthesis of new lipids, the primary pathway being the biosynthesis of FA (Castro et al., 2016; NRC, 2011). The key pathway in lipogenesis is catalysed by a multi-enzyme complex known as fatty acid synthase (FAS) in the cytosol. This system of enzymes catalyses the synthesis of saturated long-chain fatty acids from acetyl CoA, malonyl CoA and nicotinamide adenine dinucleotide phosphate (NADPH) (Berg et al., 2012; Cook and McMaster, 2002; Leaver et al., 2008). The main product of FAS is palmitic acid (16:0) with minor amounts of stearic acid (18:0) also being attained. These saturated fatty acids can be biosynthesised *de novo* by all known organisms including fish (Castro et al., 2016). In eukaryotes, longer FA are formed by elongation reactions that add two-carbon units sequentially to the carboxyl ends of fatty acyl CoA substrates. These reactions are catalysed by enzymes known as elongases, located in the cytoplasmic face of the endoplasmic reticulum membrane (Berg et al., 2012; Cook and McMaster, 2002; Sargent et al., 2002; Tocher, 2003). These are important enzymes in this study and further details about them are given in Sections 1.5.4 and 1.5.5.

Fish are capable of desaturating stearic acid (18:0) and palmitic acid (16:0) with the microsomal stearoyl-CoA desaturases (Scd) to produce monounsaturated fatty acids such

as oleic acid (18:1n-9) and palmitoleic acid (16:1n-7), respectively. Both reactions imply the introduction of a double bond between carbons 9 and 10, and consequently Scd has Δ9 desaturase capability (Leaver et al., 2008). Polyunsaturated fatty acids can be synthesised by modification of the monounsaturated fatty acids by desaturases known as "methyl-end desaturases" that create a double bond between the existing double bond and the methyl end of the fatty acyl chain (Sperling et al., 2003). Thus, oleic acid is converted by the methyl-end desaturase Δ12 desaturase to linoleic acid (LA), the latter being subsequently converted to α-linolenic acid (ALA) by Δ15 desaturase (Figure 1.3). Δ12 and Δ15 desaturases can be found in a range of organisms such as plants, thus accounting for many VO being rich sources of these C_{18} PUFA (Lee et al., 2016; Wallis et al., 2002).

All vertebrates including fish have absolute dietary requirements for the C_{18} PUFA, LA (18:2n-6) and ALA (18:3n-3) because they lack the Δ12 and Δ15 desaturases required for their synthesis from oleic acid (Sargent et al., 2002; Tocher et al., 2003; Wallis et al., 2002). In addition, the longer chain derivatives of LA, namely arachidonic acid (ARA, 20:4n-6), and ALA, namely eicosapentaenoic acid (EPA, 20:5n-3) and DHA (22:6n-3), are essential for some fish species. These LC-PUFA play physiologically important roles in fish and the dietary requirement for them is primarily determined by a species ability to endogenously synthesise them from their dietary derived precursors LA and ALA (NRC, 2011). In fish species with high conversion capacity, the C_{18} PUFA found, for instance, in VO can meet their EFA requirement. Moreover, species with limited or no ability to biosynthesise LC-PUFA from their C_{18} PUFA precursors depend upon provision of LC-PUFA (ARA, EPA and DHA) in the diet, typically achieved by inclusion of marine ingredients, primarily FO.

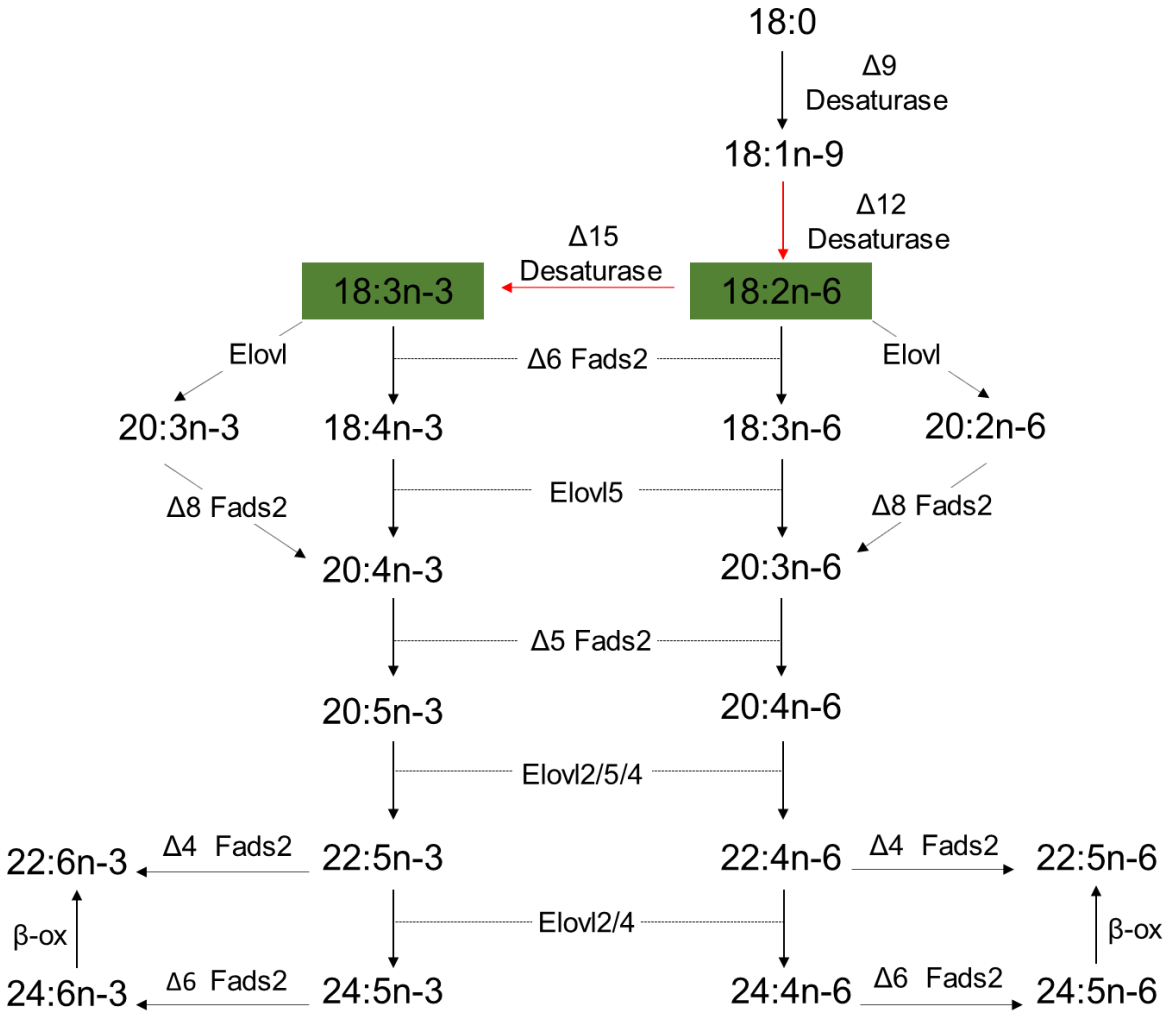

Figure 1.3. The biosynthetic pathways of long-chain polyunsaturated fatty acids (LC-PUFA) from dietary α-linolenic (18:3n-3) and linoleic (18:2n-6) acids in teleosts. Enzymatic activities shown in the diagram are predicted from heterologous expression in yeast (*Saccharomyces cerevisiae*) of fish fatty acyl desaturase 2 (Fads2) and Elongase of very long-chain fatty acid (Elovl) proteins. The red lines indicate desaturation reactions not possible in vertebrates and the fatty acids highlighted in green indicate the starting point of LC-PUFA, the C_{18} PUFA obtained from diets. β-ox, partial β-oxidation.

Generally, it has been suggested that LA and/or ALA can satisfy the EFA requirements of freshwater fish, whereas the EFA requirements are met in marine fish by dietary supply of ARA, EPA and DHA (Sargent et al., 2002; Tocher, 2010). However, several studies have established that in most fish species with the ability to convert ALA acid to EPA and DHA,

the C_{20-22} LC-PUFA are more effective nutritionally than the C_{18} PUFA (Buzzi et al., 1996; Sargent et al., 2002; Tocher, 2010; et al., 1997). Providing these species such as rainbow trout, *Oncorhnychus mykiss* (Buzzi et al., 1996; Wirth et al., 1997) and channel catfish *Ictalurus punctatus* (Satoh et al., 1989; Wilson and Moreau, 1996) with direct sources of EPA and DHA resulted in better growth. Hence for these species, as well, the LC-PUFA are at least 'semi essential' as the rate of conversion from C_{18} PUFA to C_{20-22} LC-PUFA may be insufficient to support optimal growth, particularly at certain life stages such as the larval stage, when fish are undergoing fast somatic growths and neural tissues accumulating LC-PUFA are rapidly developing (Brett and Müller-Navarra, 1997; Glencross, 2009). Consequently, at those life stages, there is a requirement for LC-PUFA regardless the ability of converting C_{18} PUFA into LC-PUFA that species has in later developmental stages (Brett and Müller-Navarra, 1997; Sargent et al., 2002; Tocher, 2010). It is interesting to note, however, that provision of dietary n-3 LC-PUFA to freshwater fish species such as *Oreochromis* sp. (Ng and Chong, 2004) and African catfishes (Hoffman and Prinsloo, 1995a; Legendre et al., 1995; Ng et al., 2003) did not increase their growth performance beyond those of fish fed the C_{18} PUFA diets. Therefore, a wide range of EFA requirements exists even in fish capable of endogenous LC-PUFA synthesis, underlining the need for species specific studies.

Differences among fish also occur in their requirements for n-3/n-6 FA series. Reported estimates for juveniles and subadults of freshwater fish species indicate that their EFA requirements can generally be satisfied by LA and ALA of about 1 % of the diet dry weight, with warmwater species such as tilapia having a higher requirement for LA (Ng and Chong, 2004; NRC, 2011; Sargent et al., 2002). Studies have, however, given conflicting results, pointing to a requirement for n-3 FA in some warmwater species but not for others (Chou and Shiau, 1999; Ng et al., 2003; Ng and Chong, 2004). For example, most tilapia species

studied suggest they require 0.5 – 1.0 % LA (Ng and Chong, 2004), but significant improvement in growth has been recorded in tilapia species fed cod liver oil compared to corn oil, indicating their requirement for n-3 FA or at least n-3 LC-PUFA for maximum growth (Chou and Shiau, 1999; Ng and Chong, 2004).

The requirements for EFA and their optimal ratios also vary quantitatively during ontogenesis and therefore, accurate definition of EFA requirements for a given species must include the determination of absolute requirement of specific PUFA, the optimal balance between FA, and how these requirements vary at different life stages (Sargent et al., 2002; Tocher, 2010). Furthermore, EFA requirements studied individually may give a different picture from one considering all EFA due to the effect of their interaction, further increasing the challenge of establishing EFA requirements. This interaction stems from the ability of biosynthetic enzymes, namely desaturases and elongases (see below) to act on different FA substrate leading to competition among FA for use as substrate (Geiger et al., 1993; Glencross, 2009; Sargent et al., 1999). Therefore, the presence or absence of certain FA in a species may affect the availability of another FA as substrate for longer chain FA synthesis. The optimum ratio of FA must therefore be taken into account in the determination of EFA requirements. This ratio changes with stage of development in different species making the study of the "singular and interactive requirements of each of the five key EFA" essential (Glencross, 2009; Sargent et al., 1999).

1.4 Biological Functions of Fatty Acids in Fish

FA can occur as free molecules in nature but they generally occur esterified into complex lipids including membrane phospholipids and triglycerides, which are basically two and three FA bonded to a glycerol molecule, respectively (De Silva and Anderson, 1995; NRC, 2011). Features of FA such as length, degree of unsaturation, position of their double bonds

and, as seen with eicosanoids the position of the last bond of PUFA (n-3 or n-6), determine their properties and functions (Calder, 2005; Qiu, 2003).

All FA can serve as important sources of cellular energy but some LC-PUFA also play essential roles in metabolism (NRC, 2011). FA catabolism is the major source of energy in fish species. FA catabolism takes place in mitochondria and peroxisomes, in a process known as β-oxidation, which involves the sequential cleavage of two-carbon units (NRC, 2011). With the exception of DHA, oxidation of FA is determined by substrate FA concentrations and enzyme specificities, although there is an order of preference with saturated and monounsaturated FA preferentially oxidised before PUFA, and PUFA before LC-PUFA (NRC, 2011). DHA is a poor substrate for mitochondrial β-oxidation as removal of the Δ4 double bond requires peroxisomal oxidation and are thus retained in tissues in spite of dietary concentration (NRC, 2011; Sargent et al., 2002; Tocher, 2003). Whereas triglycerides are an efficient form of high-energy storage molecules, phospholipids are the major lipid component of cell and organelle membrane where they perform structural roles as fundamental components of lipid bilayers (Guillou et al., 2010; Leaver et al., 2008; Los and Murata, 1998; Tocher and Glencross, 2015). PUFA determine the physical properties (melting temperature) of phospholipids hence determining the fluidity of cell membranes that are made of a phospholipid bilayers. Through their impacts on cell membrane fluidity, PUFA act as active antifreeze for membrane lipid. This is important for poikilotherms, in particular fish, that remain active at low temperatures (Brett and Müller-Navarra, 1997; Das, 2008; Nakamura and Nara, 2004).

LC-PUFA also have unique and important roles in controlling and regulating cellular metabolism and physiology. They regulate many membrane-associated processes such as permeability, cell division and inflammation (Guillou et al., 2010; Schmitz and Ecker, 2008; Vagner and Santigosa, 2011). They control FA synthesis by activating transcription

factors and regulating the expression of certain genes including those coding for fatty acid synthase (FAS) (Qiu, 2003). LC-PUFA also play important roles in the induction of maturation in teleosts, sperm performance (milt quantity and sperm motility), embryonic and larval development (Butts et al., 2015; Sorbera et al., 2001; Tocher and Glencross, 2015). Catabolism of lipids results in the release of free fatty acids utilised during embryogenesis and early larval development for energy and formation of developing larval tissues (Tocher, 2003). LC-PUFA has an effect on visual and neural development and therefore, survival of larvae (Glencross, 2009). ARA has been shown to induce oocyte maturation, whereas eggs with higher concentration of DHA have higher fertilisation, hatching and larval survival rates (Sorbera et al., 2001; Yanes-Roca et al., 2009).

DHA has important structural and functional roles in neural membranes and is pivotal for the proper development of neural tissues. ARA plays a role in cell signalling, immune response and, in fish, in the regulation of the ionic balance (Glencross, 2009; Tocher and Glencross, 2015). Eicosanoids derived from ARA and EPA including prostaglandins, leukotrienes and thromboxanes regulate many important signaling pathways such as regulation of steroid biosynthesis (Guillou et al., 2010). Eicosanoids derived from n-6 fatty PUFA (e.g. ARA) are more potent mediators of inflammation compared to the ones derived from n-3 FA (e.g. EPA) (Calder, 2005; Qiu, 2003; Simopoulos, 2002). Docosanoids derived from DHA are also less pro-inflammatory than eicosanoids derived from ARA (Farooqui, 2011).

1.5 Fatty Acid Synthesising Enzymes

1.5.1 Fatty Acyl Desaturases

Desaturases are non-heme, iron-containing enzymes that perform dehydrogenation reactions that result in the introduction of a double bond at specific positions in fatty acyl chains (Los and Murata, 1998; Shanklin et al., 2009). Desaturases can be divided into two

classes, membrane-bound and soluble desaturases, based on subcellular location (Castro et al., 2016). They are distinguished on the basis of their sequence similarity, homology and di-iron centres. Soluble desaturases are restricted to plant plastids and compose of the acyl-acyl carrier protein (ACP) desaturases. Whereas, acyl-lipid desaturases (present in cyanobacteria, fungi and plant endoplasmic reticulum (ER) and plastid) and the acyl-coenzyme A (CoA) desaturases make up the membrane-bound desaturases. The acyl-coenzyme A (CoA) desaturases use fatty acyl-CoA as substrates (Los and Murata, 1998; Nakamura and Nara, 2004; Pereira et al., 2003).

Membrane-bound desaturases, characterised by the possession of three histidine box motifs, can be further divided into two families: stearoyl-CoA desaturases (Scd) and fatty acyl desaturases (Fads) (Guillou et al., 2010). Scd are the Δ9 desaturases whereas the Fads include Δ6, Δ5 and Δ4 desaturases (Guillou et al., 2010; Li et al., 2010). Another classification, based on the end of the fatty acyl chain from which the desaturase counts in determining specificity, divides desaturases into methyl-end and front-end desaturases (Castro et al., 2016; Nakamura and Nara, 2004). The topology of Fads has been predicted (Figure 1.4). These predictions have been based on hydropathy analysis and on residues regarded as involved in binding the di-iron site, which are found in the same relative positions in both soluble and membrane-bound desaturases. Membrane-bound desaturases are thought to span the membrane four times in such a way that the histidine boxes lie on the cytoplasmic side where, together with the iron ions, they constitute the catalytic centre of the desaturase (Figure 1.4) (Los and Murata, 1998; Shanklin et al., 2009).

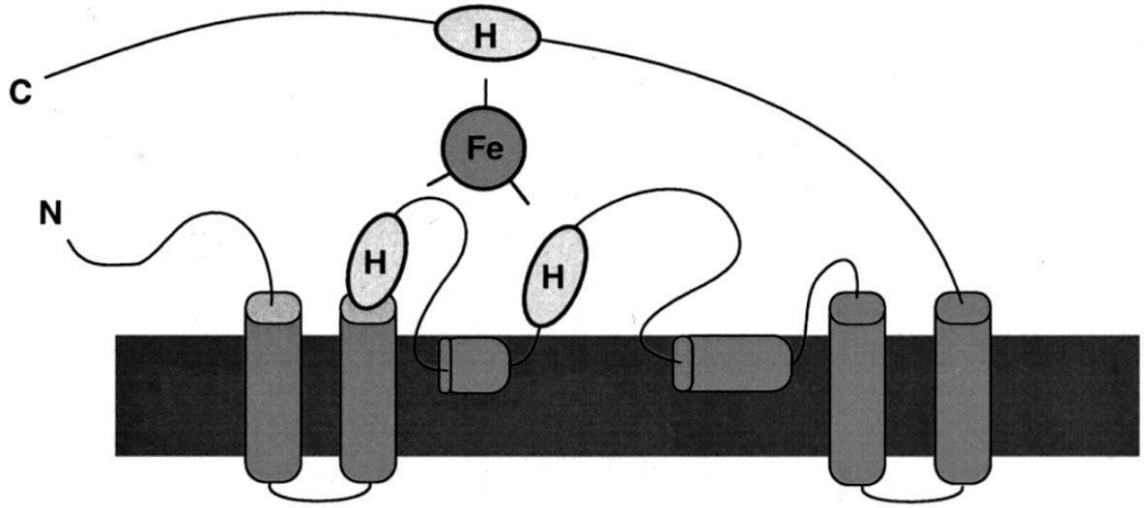

Figure 1.4. The predicted topology of membrane desaturase in relation to the membrane. The dark rectangular block represents the membrane and the four cylindrical shapes represent the transmembrane regions The histidine (H) boxes are outside the membrane, where they form the proposed catalytic centre with the iron (Fe) ions (Source: Los and Murata, 1998).

1.5.2 The Desaturation of Fatty Acids

Desaturation reactions are catalysed by three membrane-bound proteins: a desaturase, nicotinamide adenine dinucleotide (NADH)-cytochrome b_5 reductase and cytochrome b_5, and require molecular oxygen. At the start of this reaction (Figure 1.5), electrons are transferred from NADH to the flavin adenine dinucleotide (FAD) moiety of NADH-cytochrome b_5 reductase. The heme iron atom of cytochrome b_5 is then reduced to the Fe^{2+} state, and subsequently, the nonheme iron atom of the desaturase is converted into the Fe^{2+} state enabling it to interact with oxygen and the fatty acyl CoA substrate, resulting in the creation of a double bond and the release of two molecules of water. Two of the four electrons come from the single bond of the FA substrate, whereas the other two are from NADH (Berg et al., 2012; Cook and McMaster, 2002; Nakamura and Nara, 2004).

A.

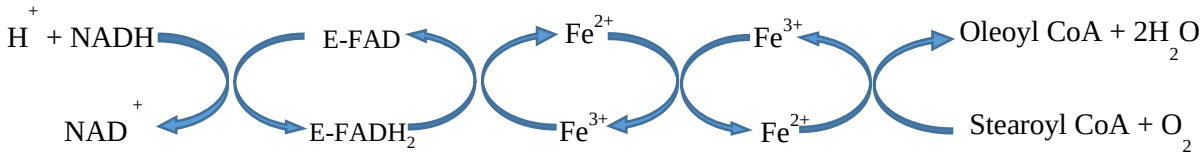

B.

$$\text{Stearoyl CoA} + \text{NADH} + H^+ + O_2 \longrightarrow \text{oleoyl CoA} + NAD^+ + 2H_2O$$

Figure 1.5. The sequence of desaturation reaction. A. Electron-transport chain in the desaturation of fatty acids. B. The equation for the desaturation of stearoyl CoA to oleoyl CoA.

1.5.3 Classification and Activities of Fads enzymes

Fads enzymes constitute a family of genes in vertebrates with three members named *FADS1*, *FADS2* and *FADS3* in mammals. The gene and protein nomenclature used in this thesis is the standard gene/protein nomenclature as defined by Castro et al. (2016). Following this system of nomenclature, the human gene is referred to as '*FADS*' and the predicted protein as 'FADS'; for mouse and rat, gene is referred to as '*Fads*', and protein as 'FADS'; for birds, gene is referred to as '*FADS*', whereas protein is as 'FADS'; for amphibians and fishes, gene is referred to as '*fads*', whereas protein as 'Fads'.

In mammals and cartilaginous fish species, *FADS1* (*fads1*) and *FADS2* (*fads2*) encode Δ5 and Δ6 desaturases, respectively (Guillou et al., 2010; Lee et al., 2016). The function of FADS3 was not known until recently, when it was demonstrated to display Δ13 desaturase activity of vaccenic acid in rodents (Garcia et al., 2017; Rioux et al., 2013). However, all teleost Fads desaturases studied so far are Fads2 with very diverse activities that have been attributed to the functionalisation of the protein during the evolution of teleost (Castro et al., 2016; Fonseca-Madrigal et al., 2014). Other Fads, with as yet unknown functions are

present in some vertebrates. These include the so-called "Fads6" (Guillou et al., 2010), and "*Fads4*" found in mammalian genomes (Castro et al., 2012), which, unlike the other three *Fads* (*Fads1*, *Fads2* and *Fads3*) that map together, are located on different chromosomes (Castro et al., 2012).

Fads2 are named by the fixed position of the double bond they create counting from the carboxyl (front) end of the FA, and are often termed as "front-end" desaturases (Nakamura and Nara, 2004). Therefore, Δ6, Δ8, Δ5 and Δ4 Fads2 create double bonds at positions 6, 8, 5 and 4, respectively, of the fatty acyl chain. Multiple isoforms of Fads2 have been isolated from teleost species such as *Salmo salar* (Hastings et al., 2005; Monroig et al., 2010b; Zheng et al., 2005), *Oncorhynchus mykiss* (Zheng et al., 2004; Hamid et al., 2016), *Siganus canaliculatus* (Li et al., 2010), *Chirostoma estor* (Fonseca-Madrigal et al., 2014), *Channa striata* (Kuah et al., 2015, 2016) and *Oreochromis niloticus* (Tanomman et al., 2013; Oboh et al., 2017), whereas only a single Fads2 have been isolated from others (Kabeya et al., 2017, 2015; Lopes-Marques et al., 2017; Mohd-Yusof et al., 2010; Morais et al., 2011; Wang et al., 2014; Xie et al., 2014; Zheng et al., 2004). Interestingly, Δ6 Fads2 catalyses the desaturation of 18 and 24-carbon PUFA in the biosynthesis pathways of both n-3 and n-6 LC-PUFA, but have been found to also desaturate 16:0 to 16:1n-10 in mice and humans (Miyazaki et al., 2006; Park et al., 2009). Many Δ6 Fads2 also exhibit Δ8 activity, catalysing the desaturation of 20:3n-3 and 20:2n-6, and presenting an alternative pathway to the already described Δ6Δ5 pathway of EPA and ARA synthesis (Figure 1.3) (Monroig et al., 2011a; Park et al., 2009). A number of characterised teleost Fads2 are bifunctional Δ6Δ5 Fads2. The first bifunctional Δ6Δ5 Fads2 cloned was from zebrafish *Danio rerio* (Hastings et al., 2001). Since then, more bifunctional Δ6Δ5 Fads2 have been isolated from *S. canaliculatus* (Li et al., 2010), *O. niloticus* (Tanomman et al., 2013), *C. estor* (Fonseca-Madrigal et al., 2014) and *C. striata* (Kuah et al., 2016).

Fads2 with Δ4 activity have been characterised in teleost species including *S. canaliculatus* (Li et al., 2010), *S. solea* (Morais et al., 2012), *C. estor* (Fonseca-Madrigal et al., 2014), *C. striata* (Kuah et al., 2015), *O. niloticus* and *Oryzias latipes* (Oboh et al 2017). These teleost Δ4 Fads2 also exhibit some Δ5 desaturase activity. Even the Δ5 Fads2 from *S. salar* exhibited a low level of Δ6 activity (Hastings et al., 2005). The existence of multiple Fads2 with different specificities in a species is increasingly observed among teleosts. Thus, many of the species in which Δ4 Fads2 have been characterised also possess the bifunctional Δ6Δ5 Fads2 (Fonseca-Madrigal et al., 2014; Kuah et al., 2016, 2015; Li et al., 2010).

1.5.4 Elongation of Very Long-chain Fatty Acid (Elovl) protein

Elongation of very long-chain fatty acids (Elovl) proteins catalyse the addition of two-carbon units to the carboxyl end of a fatty acyl CoA, with malonyl CoA as the two-carbon donor and NADPH as the reducing agent. Elongation primarily occurs on the cytoplasmic face of the endoplasmic reticulum (ER), although it also occurs in the mitochondria (Cook and McMaster, 2002). The FA substrate for elongation may have been endogenously synthesised or from dietary FA (Cook and McMaster, 2002; Guillou et al., 2010; Leonard et al., 2004).

Each round of elongation consists of a series of steps, namely condensation, reduction, dehydration and reduction reactions, which are catalysed by four enzymes similarly to the *de novo* synthesis of palmitic acid by FAS. The steps of the 2-carbon chain elongation of long-chain FA is presented in Figure 1.6. The first step (condensation reaction), catalysed by Elovl enzymes with a particular substrate specificity and generally accepted to be the rate-limiting step of the overall FA elongation pathway, results in addition of the 2-carbon moiety (Bell and Tocher, 2009; Leonard et al., 2004). In this step, the fatty acyl-CoA and malonyl-CoA are condensed to β-ketoacyl-CoA. β-Ketoacyl-CoA is then reduced to β-

hydroxy acyl-CoA by the β-ketoacyl reductase that utilises NADPH. The third step involves dehydration to enoyl-CoA by β-hydroxy acyl-CoA dehydratase and finally, a second reduction step catalysed by 2-trans-enoyl-CoA reductase generates the elongated fatty acyl$_{(n+2)}$-CoA by reducing enoyl-CoA in the presence of NAD(P)H (Castro et al., 2016; Cook and McMaster, 2002).

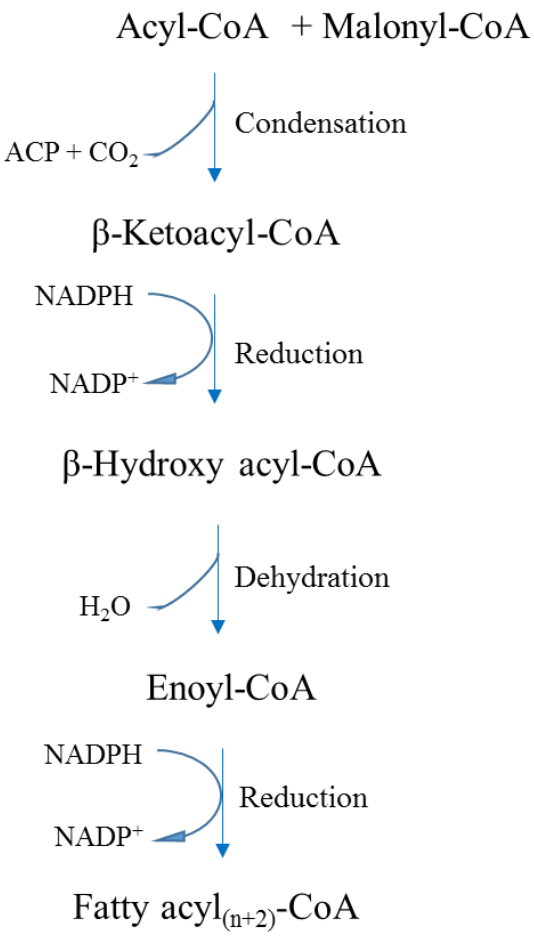

Figure 1.6. The steps of fatty acid elongation of long-chain fatty acids.

1.5.5 Classification and Activities of Elongation of Very Long-chain Fatty acid (Elovl) Enzymes

Seven Elovl proteins (Elovl 1-7) with similar motifs in their protein sequence make up the elongase protein family (Guillou et al., 2010; Jakobsson et al., 2006). Elovl2 and Elovl5 are involved in PUFA elongation, Elovl 1, 3, 6 and 7 elongate saturated and

monounsaturated fatty acid while Elovl4 is capable of elongating both VLC-SFA and VLC-PUFA (Agbaga et al., 2008; Guillou et al., 2010; Jakobsson et al., 2006). *Elovl5* genes have been cloned and characterised from teleost species including *S. salar* (Hastings et al., 2005; Morais et al., 2009), *D. rerio* (Agaba et al., 2004), *C. gariepinus*, *O. niloticus*, *Gadus morhua*, *Sparus aurata*, *Psetta maxima* (Agaba et al., 2005), *Thunnus maccoyii* (Gregory et al., 2010), *C. estor* (Fonseca-Madrigal et al., 2014), *Nibea mitsukurii* (Kabeya et al., 2015), *Larimichthys crocea* (Li et al., 2017) and *Paralichthys olivaceus* (Kabeya et al., 2017). Relevant to this study, cloning and functional characterisation of an Elovl5 from *C. gariepinus* has been carried out (Agaba et al., 2005). Elovl2 has been found in fewer fish species compared to Elovl5 and have so far, only been characterised in *S. salar* (Morais et al., 2009), *D. rerio* (Monroig et al., 2009) and *O. mykiss* (Gregory and James, 2014).

Functional characterisation of Elovl2, Elovl4 and Elovl5 shows they have to some extent overlapping functions, with Elovl5 mainly elongating PUFA of chain lengths C_{18} and C_{20} whereas Elovl2 and Elovl4 act on PUFA substrates of chain lengths C_{20} and C_{22} (Castro et al., 2016; Monroig et al., 2016b). Most teleost Elovl5 exhibit low ability to elongate C_{22} PUFA and although numerous researchers suggest only Elovl5 can provide all the required elongation activity for LC-PUFA synthesis, biosynthesis would be more efficient in teleost species with also Elovl4 and particularly, Elovl2. Fish Elovl2 mainly elongates C_{20} and C_{22} PUFA but are also able to elongate 18-carbon PUFA, albeit with comparatively lower efficiency. Fish Elovl2 are unable to act on saturated and monounsaturated fatty acids substrates and synthesis of PUFA of C_{24} or longer are negligible (Jakobsson et al., 2006; Monroig et al., 2011b). In contrast mouse Elovl2 is capable of VLC-PUFA biosynthesis (Zadravec et al., 2011).

Elovl4 have been shown to elongate VLC-PUFA, very long-chain (> C_{24}) polyunsaturated fatty acid and very long-chain (> C_{24}) saturated fatty acid (VLC-SFA) with chain lengths

of up to C_{36} (Agbaga et al., 2008; Carmona-Antoñanzas et al., 2011; Jin et al., 2017; Li et al., 2017; Monroig et al., 2010a). Two groups of the Elovl4 protein with different functional activities have been identified in fish, namely Elovl4a and Elovl4b. Elovl4b, which appear to be the most commonly studied (Carmona-Antoñanzas et al., 2011; Jin et al., 2017; Kabeya et al., 2015; Li et al., 2015, 2017; Monroig et al., 2010a, 2012, 2011c) efficiently synthesises both saturated VLC-SFA and VLC-PUFA up to C_{36}. *D. rerio* Elovl4a was only able to synthesise VLC-SFA whereas the black seabream *Acanthopagrus schlegelii* Elovl4a was able to elongate both VLC-SFA and VLC-PUFA (Jin et al., 2017; Monroig et al., 2010a). In addition to Elovl4a and Elovl4b, two identical isoforms termed Elovl4c-1 and Elovl4c-2 were cloned, but not functionally characterised, in *Gadus morhua*. Search of teleost genome reveal the existence of similar *elovl4*-like genes, which have not been functionally characterised.

1.5.6 Biosynthesis of Long-Chain Polyunsaturated Fatty Acids (LC-PUFA) in Fish

As already surmised, the ability to convert ALA and LA to LC-PUFA has been established in some fish species. The extent to which fish can convert C_{18} PUFA into $C_{20\text{-}24}$ LC-PUFA varies, depending on the species' complement and function of desaturases and elongases, diet, trophic level and even environmental conditions (Fonseca-Madrigal et al., 2014; Leaver et al., 2008; Sargent et al., 2002; Tocher, 2010). Environmental factors that could determine LC-PUFA synthesis capacity include salinity (Fonseca-Madrigal et al., 2014; Li et al., 2008), temperature and photoperiod (Tocher et al., 2000; Zheng et al., 2005). In addition, the rate differs substantially during development and with change in diets (Sargent et al., 2002). Freshwater fishes have long been recognised to have a higher capacity to bioconvert dietary LA and ALA to ARA, EPA and DHA than marine fishes. This capacity has been attributed to evolutionary pressures based on their natural diets and the gain and loss of genes (Castro et al., 2012; Leaver et al., 2008; Sargent et al., 2002).

The bioconversion from ALA to EPA and LA to ARA may involve the Δ6/Δ5 desaturation pathway (Sargent et al., 2002) or the proposed alternative Δ8/Δ5 desaturation pathway (Monroig et al., 2011a). The Δ6/Δ5 pathway involves a Δ6 desaturation of 18:3n-3 and 18:2n-6 to 18:4n-3 and 18:3n-6, respectively, a two-carbon chain elongation step to 20:4n-3 and 20:3n-6 and a Δ5 desaturation to 20:5n-3 and 20:4n-6, respectively (Vagner and Santigosa, 2011) (Figure 1.3). With the exception of *O. mykiss* Elovl2, the elongation step can be catalysed by Elovl5 and Elovl2, with Elovl5 being the most efficient (Gregory and James, 2014; Monroig et al., 2016b). Fish Elovl4 have also been shown to be capable of catalysing this elongation step. The alternative Δ8 desaturation pathway for the production of EPA and ARA was suggested following the cloning of a Fads2 gene with Δ8 desaturase activity from baboon neonate liver (Park et al., 2009), and from several fish species (Monroig et al., 2011a). In this pathway, the bioconversion from 18:3n-3 to EPA and from 18:2n-6 to ARA involves an initial elongation step to 20:3n-3 and 20:2n-6, respectively, followed by a Δ8 desaturation step to give 20:4n-3 and 20:3n-6 and finally a Δ5 desaturation step. All the known possible pathways for the biosynthesis of LC-PUFA from the C_{18} precursors (18:3n-3 and 18:2n-6) are presented in Figure 1.3. Irrespective of the pathway used, the steps and enzymes are the same for both n-3 and n-6 FA series (Figure 1.3).

DHA biosynthesis from EPA may occur through at least two routes; a direct route from a Δ4 desaturation of 22:5n-3 following the elongation from EPA, or the longer route entailing two consecutive elongation steps from EPA up to 24:5n-3 (Tetracosapentaenoic acid), a Δ6 desaturation to 24:6n-3 (Tetracosahexaenoic acid) and a chain shortening step in the peroxisomes to produce DHA (Figure 1.3) (Sprecher et al., 1995). With the exception of this final step which occurs in peroxisomes, all elongation and desaturation steps occur in the ER (Bell and Koppe, 2010). The second pathway is known as the "Sprecher

pathway". The Sprecher's pathway appears to be the more common of the two pathways in fish, as Δ4 Fads2 are not present in all groups of fish. Fish Elovl2, 4 and 5 have been shown to catalyse the elongation steps required with Elovl2 being the most efficient (Castro et al 2016; Monroig et al 2016b).

Studies in mammals established that the same Δ6 Fads2 is responsible for the two Δ6 desaturation reactions in the Sprecher's pathway, namely in the n-3 pathway for instance, 18:3n-3 to 18:4n-3 and 24:5n-3 to 24:6n-3. In fish it remained unclear if the same Δ6 Fads2 catalyses both desaturation steps or whether different Δ6 Fads2 (isoenzymes) are involved (Sargent et al., 2002; Vagner and Santigosa, 2011; Wallis et al., 2002). Competitive studies have shown Δ6 Fads2 displays a greater rate of desaturation of 18-carbon FA compared to 24-carbon FA (Geiger et al., 1993). The dual function of Δ6 Fads2 in the conversion of both 18 and 24-carbon FA it limits the rate of conversion from ALA to DHA (Portolesi et al., 2007). This explains why it is regarded as the rate-limiting factor of LC-PUFA synthesis (Bell and Tocher, 2009; Leonard et al., 2004; Li et al., 2008).

1.5.7 LC-PUFA Biosynthetic Capabilities of *Clarias gariepinus*

Understanding the abilities of farmed fish species to convert C_{18} PUFA to $C_{20\text{-}22}$ LC-PUFA has been the focus of many lipid nutrition studies as FM and FO rich in $C_{20\text{-}22}$ LC-PUFA are increasingly been replaced with more sustainable and cheaper plant based substitutes lacking in $C_{20\text{-}22}$ LC-PUFA. Therefore, understanding the LC-PUFA synthesis pathway in a species capable of utilising a variety of plant ingredients is crucial to understanding the extent to which a fish species can utilise alternative ingredients, particularly VO, and satisfy their EFA requirements. *C. gariepinus*, an important farmed species in which the LC-PUFA synthesis pathway has not been elucidated, although its Elovl5 has been cloned and functionally characterised by Agaba et al. (2005), is the model species used in the present study.

1.6 Objectives of This Study

The overall objective of this PhD study is to elucidate the complete LC-PUFA biosynthetic pathway in *C. gariepinus* by cloning and functional characterisation of all Fads- and Elovl-encoding genes with putative roles in these pathways. We hypothesise that characterisation of the full set of Fads and Elovl enzymes will allow us to identify the dietary EFA requirements of *C. gariepinus* that ultimately allow us to formulate diets with increased inclusion levels of plant ingredients.

The specific aims of this project include:

1. Molecular cloning of genes encoding Fads and Elovl involved in the LC-PUFA biosynthetic pathways of *C. gariepinus*
2. Functional characterisation of Fads and Elovl by heterologous expression in yeast
3. To establish the tissue expression pattern of the desaturases and elongases in *C. gariepinus*
4. To determine the Δ6 activity towards C_{24} substrates (24:5n-3 and 24:4n-6) of *C. gariepinus* Fads2 and Fads with diverse substrate specificities from fish species with different evolutionary and ecological backgrounds.

This thesis consists of a general introduction (Chapter 1), General Materials and Methods (Chapter 2), four result chapters (Chapters 3 - 6) that have been prepared as stand-alone manuscripts, and the final chapter (Chapter 7), is the General Discussion, which provides a concise synthesis of all the outcomes and conclusions of the data chapters.

The data chapters include:

Chapter 3. Biosynthesis of long-chain polyunsaturated fatty acids in the African catfish *Clarias gariepinus*: Molecular cloning and functional characterisation of fatty acyl desaturase (*fads2*) and elongase (*elovl2*) cDNAs

This chapter covers the molecular cloning and functional characterisation of *fads2* and *elovl2* genes from *C. gariepinus.* The tissue expression of these genes and the previously cloned *elovl5* were also investigated. Results from this chapter have been published in Aquaculture (2016, Vol. 462, p. 70–79).

Chapter 4. Elongation of very long-chain (> C24) fatty acids in *Clarias gariepinus*: cloning, functional characterisation and tissue expression of *elovl4* elongases

This chapter covers the molecular cloning and functional characterisation, two *elovl4* genes from *C. gariepinus* and investigated their tissue expression patterns. Results from this chapter has been published in Lipids (2017, Vol. 52, p. 837–848).

Chapter 5. Two alternative pathways for docosahexaenoic acid (DHA, 22:6n-3) biosynthesis are widespread among teleost fish

This chapter covers investigation of the pathways for DHA biosynthesis (Sprecher and Δ4 pathway) pathway existing in species representing major lineages along the tree of life of teleost fish. This chapter has been published in Scientific Reports (2017, Vol. 7, p. 3889)

Chapter 6. Determining the function of novel Fads and Elovl enzymes in the African catfish *Clarias gariepinus*

This chapter reports on the cloning and functional characterisation of a *fads* and an *elovl*-like genes from *C. gariepinus.*

CHAPTER 2.

GENERAL MATERIALS AND METHODS

2.1 Materials

RNA stabilisation buffer (3.6 M ammonium sulphate $(NH_4)_2SO_4$), 18 mM sodium citrate ($Na_3C_6H_5O_7$), 15 mM Ethylenediaminetetraacetic acid (EDTA), pH 5.2), RNA precipitation solution (1.2 M sodium chloride (NaCl) and sodium citrate sesquihydrate ($C_6H_6Na_2O_7$-1.5H_2O)) were prepared in the laboratory. TRI Reagent® was obtained from Sigma-Aldrich (St. Louis, USA). All FA substrates (> 98 - 99 % pure) used for the functional characterisation assays (listed in the materials and methods of the appropriate chapters), except for stearidonic acid (18:4n-3) and eicosatetraenoic acid (20:4n-3), were obtained from Nu-Chek Prep, Inc. (Elysian, MN, USA). Eicosatetraenoic acid was purchased from Cayman Chemical Co. (Ann Arbor, USA). Stearidonic acid (> 99 % pure) and yeast culture reagents including galactose, yeast nitrogen base (without amino acids), raffinose, tergitol NP-40 and yeast synthetic dropout medium supplement (without uracil) were obtained from Sigma-Aldrich (USA). *Escherichia coli* JM 109 cells used for the preparation of competent cells was obtained from Promega (Madison, USA). Thin-layer chromatography TLC silica gel plates (20 cm x 20 cm x 0.25 mm) and organic solvents were obtained from Merck (Darmstadt, Germany).

2.2 Preparation of Media, Buffers and Gels

2.2.1 Preparation of 50x TRIS/acetate/EDTA (TAE) Buffer (500 ml)

To prepare 500 ml 50x TAE buffer, the reagents required included 121 g Tris base (2-amino-2-hydroxymethyl-propane-1,3-diol), 50 ml 0.5M Na_2EDTA (pH 8.0) and 28.5 ml glacial acetic acid (100 %). First, 50 ml 0.5M Na_2EDTA was prepared by dissolving 9.3 g of EDTA in 50 ml of double distilled water (ddH_2O). This was stirred vigorously using a magnetic stirrer and the pH adjusted to 8.0 with NaOH. Subsequently, 121 g Tris base was then measured into a 500 ml beaker containing about 350 ml of ddH_2O, stirred and the prepared Na_2EDTA and 28.5 ml glacial acetic acid added to the mixture, stirred

properly and ddH_2O added to bring volume up to 500 ml.

2.2.2 Preparation of Luria-Bertini (LB) Medium and Agar (400 ml)

LB Medium: 8 g of LB medium (USB, Ohio, USA) was measured into a 500 ml bottle and 400 ml ddH_2O added and mixed. It was then autoclaved and stored at room temperature.

LB Agar: 12.8 g of LB agar (USB, Ohio, USA) was measured into a 500 ml bottle and 400 ml ddH_2O added and mixed. This was autoclaved, allowed to cool to about 55 ^oC and 400 µl of 100 mg/ml ampicillin solution added to it. Ampicillin solution (100 mg/ml) was prepared by dissolving 1 g of ampicillin in 10 ml ddH_2O and stored at -20 ^oC. About 20 ml of the prepared agar was poured into separate petri dishes, allowed to cool and stored at 4 ^oC.

2.2.3 Preparation of Competent *Escherichia coli* Cells

Day 1: Competent cells were prepared using *Escherichia coli* (JM 109, Promega). *E. coli* was inoculated into 1 ml LB medium. A volume of 20 µl of this broth was then plated in an ampicillin free agar plate and incubated overnight at 37 ^oC.

Day 2: Two separate colonies were inoculated into 5 ml LB medium in two 50 ml tubes. These were incubated overnight at 37 ^oC with shaking.

Day 3: Aliquots (0.5 ml) from day 2 were transferred to 250 ml autoclaved conical flasks containing 50 ml LB medium and incubated with shaking at 37 ^oC until bacteria attained log phase (about 2-3 h) with absorbance at 550 nm between 0.4-0.5. The culture was transferred to 50 ml tubes and centrifuged at 1200 g for 5 min at 4 ^oC and the supernatant discarded. The cell pellet was resuspended in 25 ml sterilised, ice cold 0.1 M $MgCl_2$, centrifuged at 1200 g for 5 min at 4 ^oC and the supernatant discarded. The cell pellet obtained was resuspended in 25 ml sterilised, ice cold 0.1 M $CaCl_2$, kept on ice for 30

min, centrifuged at 1200 g for 5 min at 4 ^{o}C and the supernatant discarded. Cells were finally resuspended in 5 ml of 0.1 M $CaCl_2$ containing 15 % glycerol. Aliquots of 100 µl were dispensed into 1.5 ml Eppendorf tubes and stored at -70 ^{o}C until further use.

2.2.4 Preparation of Yeast Extract Peptone Dextrose (YPD) Medium and Agar (100 ml)

YPD Medium: First, yeast extract (1 g) and peptone (2 g) were dissolved in 90 ml ddH_2O and autoclaved. Then, 10 ml of filtered 20 % Dextrose (D-glucose) was added to the mixture and stored at 4 ^{o}C.

YPD Agar: Yeast extract (1 g), peptone (2 g) and agar (2 g) were dissolved in 90 ml ddH_2O and autoclaved. After this, 10 ml of filtered 20 % Dextrose (D-glucose) was added to the mixture, the plates allowed to cool and stored at 4 ^{o}C.

2.2.5 Preparation of Competent *Saccharomyces cerevisiae* Cells

Competent *Saccharomyces cerevisiae* cells were prepared using the S. c. EasyComp^{TM} Transformation Kit (Invitrogen^{TM} Life Technologies, Carlsbad, USA), following the manufacturer's instructions. A single colony of yeast was inoculated into 10 ml YPD medium and grown overnight at 30 ^{o}C in a shaking incubator (250 - 300 rpm) till the optical density measured at a wavelength of 600 nm (OD_{600}) was between 3 and 5. The cells from the overnight culture were diluted to OD_{600} of between 0.2 to 0.4 in 10 ml YPD medium. The cells were then grown in a shaking incubator at 28-30 ^{o}C for 3 to 6 h until the OD_{600} reached between 0.6 and 1.0. After this, the cells were pelleted by centrifuging at 500 g for 5 min at room temperature. The supernatant was discarded and the pelleted cells resuspended and washed in 10 ml of Solution I. The mixture was centrifuged at 500 g for 5 min at room temperature and the supernatant was discarded. The pelleted cells were resuspended in 1 ml of Solution II and the resultant competent cells aliquoted into sterile tubes and stored at -70 ^{o}C. Aliquots of 50 µl of the competent cells were dispensed

into 1.5 ml Eppendorf tubes and freezed slowly by wrapping in several layers of paper towels and placing in a styrofoam box before placing in freezers.

2.2.6 Preparation of Na Salts of Fatty Acids

FA was measured into a tube and the appropriate volume of 1M NaOH added, mixed as well as possible to dissolve the FA. The correct volume of 5.6 % Tergitol was then added, mixed thoroughly and stored at -20 ^{o}C. The quantity of the reagents used differed with the FA and these are presented in Table 2.1.

Table 2.1. The quantity of fatty acid, 1M NaOH and 5.6 % Tergitol used in preparation of sodium (Na) salts of fatty acids.

Reagents	**C_{18}**	**C_{20}**	**C_{22}**	**C_{24}**
Fatty Acid (µl)	30	45	60	60
1M NaOH (µl)	200	250	300	500
5.6% Tergitol (µl)	800	750	700	1150
Final Concentration (mM)	100	150	200	200

2.2.7 Preparation of *S. cerevisiae* Minimal Medium (SCMM^{-ura}) (400 ml)

S. cerevisiae minimal medium minus uracil (SCMM^{-ura}) was prepared by mixing 2.68 g yeast nitrogen base (without amino acids), 0.768 g yeast synthetic dropout medium supplement (without uracil), into 320 ml ddH_2O, mixed, autoclaved and allowed to cool. A solution of 10 % (w/v) D-raffinose was prepared by measuring 11.8 g of 86 % D-raffinose in 80 ml ddH_2O, completely dissolved with the aid of a magnetic stirrer and a hotplate and filtering to sterilise through a 0.22 µm filter. This was added to the cool medium (approximately 55 ^{o}C), together with 4 ml 70 % Tergitol and stored at 4 ^{o}C.

2.2.8 Preparation of *S. cerevisiae* Minimal Medium Plates (200 ml)

SC minimal medium plates were prepared by dissolving 1.34 g yeast nitrogen base (without amino acids), 0.384 g yeast drop-out (without uracil) and 4 g agar in 180 ml ddH_2O, autoclaved and allowed to cool. A solution of 20 % (w/v) glucose was prepared by dissolving 4 g of glucose in 20 ml ddH_2O. It was filtered through a 0.22 µm filter to sterilise and then added to the mixture. This was poured into plates and allowed to cool. The SC minimal medium plates were kept at 4 ^oC until further use.

2.3 Gene Molecular Cloning

2.3.1 Experimental Samples

All experiments were subjected to ethical review and approved by the University of Stirling through the Animal and Welfare Ethical Review Body. The project was conducted under the UK Home Office in accordance with the amended Animals Scientific Procedures Act implementing EU Directive 2010/63. Adult specimens of the African catfish, *Clarias gariepinus* were used for this study. The fish were obtained from the tropical aquarium of the Institute of Aquaculture, University of Stirling. *C. gariepinus* (all greater than 1 kg in weight) were raised in the aquarium on standard salmonid diets. Fish were sacrificed with an overdose of tricaine methanesulfonate (MS222) and a sharp blow to the head. Approximately 50-100 mg of different tissue samples including brain, eye, intestine, gonad, heart, liver, kidney, adipose tissue, pituitary gland, stomach, spleen, skin, white muscle, head kidney, gill and the accessory breathing organ (ABO) were collected. The samples were immediately preserved overnight in RNA stabilisation buffer at 4 ^oC and subsequently stored in -70 ^oC freezers till required.

2.3.2 RNA Extraction

Total RNA was extracted following the RNA TRI Reagent (Sigma-Aldrich, USA) extraction protocol. About 25 mg tissue samples fixed in RNA later were homogenised

in 1 ml TRI Reagent in 1.5 ml Eppendorf tubes using a Mini-Beadbeater (Bio Spec Products Inc., Bartlesville, USA). Homogenised samples were incubated at room temperature for 5 min before they were centrifuged at 12,000 g for 10 min at 4 °C. The supernatants were then transferred into fresh Eppendorf tubes and 100 µl 1-bromo-3-chloropropane (BCP) added. The tubes were then vigorously shaken by hand for 15 s, incubated at room temperature for 15 min and centrifuged at 20,000 × g for 15 min at 4 ºC. The aqueous (upper) phase was transferred to fresh tubes and half the volume (per aqueous phase volume) of isopropanol and of RNA precipitation solution were added to precipitate the RNA. The mixtures were subsequently gently inverted six times, incubated for 10 min at room temperature and centrifuged at 20,000 × g for 10 min at 4 °C. The RNA precipitate formed gel-like pellets on the bottom of the tubes. The supernatant was removed (by pipetting) and pellet washed with 1 ml of 75 % ethanol in ddH_2O (v/v). The pellets were lifted from the bottom of the tube by flicking and inverting the tubes a few times so that the entire surface of the pellets was properly washed. The tubes were then centrifuged at 20,000 g for 5 min at room temperature and the ethanol carefully removed and discarded. The RNA pellets were air dried at room temperature until all visible traces of ethanol were gone. Subsequently, RNA pellets were resuspended in an appropriate amount of ddH_2O of 40-400 µl depending on the size of the RNA pellet. RNA solutions were incubated at room temperature for 30-60 min with gentle flicking of the tubes every 15 min to aid resuspension. The concentration and quality of RNA were assessed spectrophotometrically using the NanoDrop® (Labtech International ND-1000 spectrophotometer). The quality and integrity of RNA samples were further assessed by electrophoresis on 1 % agarose gel as described below. The RNA solutions were then stored at -70 ºC for further analysis.

2.3.3 First Strand cDNA Synthesis

First strand complementary DNA (cDNA) were synthesised using the High Capacity cDNA Reverse Transcription Kit (Applied Biosystems™, Foster city, USA) following the manufacturer's instructions. The reverse transcription kits and the RNA were allowed to thaw on ice. A total of 10 µl of RNA solution containing 1 µg RNA in ddH_2O were prepared in 0.2 ml PCR tubes. These were heated in a Biometra thermocycler for 5 min at 75 ^oC to denature RNA and held after that at 4 ^oC. The cDNA reverse transcriptase master mix were prepared according to manufacturer's instruction multiplied by the number of samples available. A volume of 10 µl of the cDNA reverse transcriptase mix containing 2 µl of reverse transcriptase buffer, 0.8 µl dNTP mix, 2 µl reverse transcriptase random primers, 1 µl reverse transcriptase and 4.2 µl nuclease-free water was added to the 10 µl solution of denatured RNA, mixed gently and centrifuged briefly. These were then put in a thermocycler set at 25 ^oC for 10 min, 37 ^oC for 2 h, 85 ^oC for 5 min and 4 ^oC for 4 min, after which the resultant cDNA were stored at -20 ^oC until further use.

2.3.4 Amplification of cDNA Fragments

Polymerase Chain Reaction (PCR) was performed to amplify first cDNA fragment using GoTaq® G2 Colorless Master mix (Promega). The total volume of reaction mixture used for PCR was 10 µl containing 5 µl GoTaq DNA polymerase, 1.0 µl cDNA, 3.0 µl nuclease free water and 0.5 µl of each primer (10 µM). PCR conditions consisted of an initial denaturation step at 95 °C for 2 min, followed by 33-37 cycles of denaturation at 95 °C for 30 s, annealing at 57-60 °C for 30 s, extension at 72 °C for 1-4 min, followed by a final extension at 72 °C for 7 min. PCR were typically run on agarose gels and the appropriate band cut and purified using the Illustra GFX PCR DNA/gel band purification

kit (GE Healthcare, Little Chalfont, UK). The PCR fragments were sent to GATC for sequencing (GATC Biotech Ltd., Konstanz, Germany).

2.3.4.1 Design of Primers and Primer Resuspension

Primers used for amplification of the first fragments of target genes were designed on conserved regions of those genes sequences after alignment (BioEdit v7.0.9, Tom Hall, Department of Microbiology, North Carolina State University, USA). Subsequently, primers were designed on previously obtained fragments such as primers used for RACE PCR and qPCR. The primers used in this study and their sequences are presented in the relevant chapters.

Primers were purchased from MWG as freeze-dried form. Upon reception, tubes containing primers were shortly centrifuged to collect primers at the bottom of the tube and the volume of ddH_2O required to give a final concentration of 100 pmol/µl in primer stock solutions. They were then vortexed to fully resuspend the primer. Working solutions of 10 pmol/µl were systematically prepared by transferring 20 µl of each primer solution into 180 µl of ddH_2O and stored at -20 ^oC.

2.3.4.2 Agarose Gel Electrophoresis

Agarose gels (1 %, w/v) were prepared by dissolving 0.25 g of agarose in 25 ml 0.5x TAE buffer in a 250 ml conical flask. Using an inverted 25 ml conical flask as a lid, it was heated in a microwave for about 1 min with gentle swirling of the flask at intervals, till agarose was completely dissolved. After allowing about 5-10 min for solution to cool sufficiently, 0.40 µl ethidium bromide (5 g/ml) was added and swirled gently to mix. The gel was then gently poured into an already prepared casting tray and an appropriate comb inserted to produce wells for loading samples. The gel was then allowed to set for at least 30 min.

Agarose gel was submerged in a tank containing 0.5x TAE buffer. The PCR products with loading dye added at 6x concentration were loaded into the wells. An appropriate DNA marker for estimating the band size, was also run alongside. The power supply was connected to the electrophoresis tank at 80 V to move the molecules through the agarose gel. After approximately 40 min, power supply was switch off and the gel viewed with the Syngene Transilluminator and the image of the gel taken. An example of a typical gel image is presented in Figure 2.1. PCR with potentially positive products were repeated in larger quantity (50 – 100 µl) and the appropriate band was cut out of the gel using a scalpel with the aid of the UV transilluminator in a dark room, purified and sequenced.

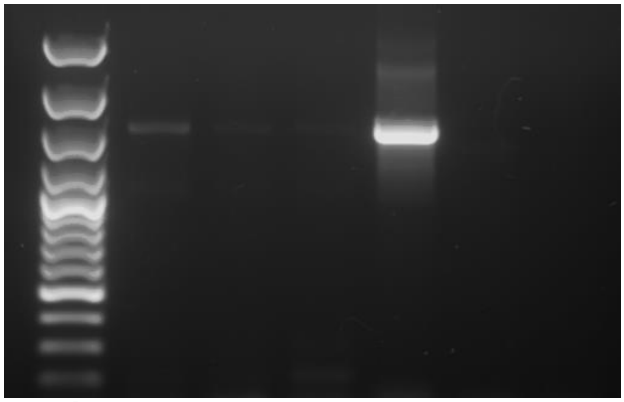

Figure 2.1 A typical agarose gel image. Gel image for the screening of *Clarias gariepinus fads2* first fragment ligated into PCR 2.0 vector.

2.3.4.3 Purification of DNA from TAE Agarose Gel

The PCR products or the gel cut-out bands were purified with the Illustra GFX PCR DNA and Gel band purification kit following the manufacturer's instruction. The recommended volume of capture buffer from the purification kit was added to the tube containing the product. If a gel, then it was dissolved completely by incubating in a hot block at 60 ^{o}C, for 15 min, mixing every 3 min and filtered through the column provided

with centrifugation at 16,000 g for 30 s. A volume of 500 µl of wash buffer was added to the column and centrifuged again for 30 s. The column was air dried completely in fume hood and 15-35 µl of ddH_2O was added to the middle, incubated at room temperature for 1 min and spun at 16,000 g for 1 min. The Nanodrop was used to quantify the concentration. It was then preserved at -20 ^oC for further use.

2.3.5 RNA Ligase Mediated Rapid Amplification of cDNA Ends (RLM-RACE) PCR

In order to obtain full-length cDNA sequences, RNA ligase mediated rapid amplification of cDNA ends (RLM-RACE) was used to synthesise both the 5'- and 3'-RACE cDNA using the FirstChoice® RLM-RACE kit (Ambion®, Life Technologies™, California, USA). For the 5'-RACE, approximately 10 µg in 16 µl of total RNA from one or several tissues (typically liver, intestine, eye and brain) were treated with Calf Intestine Alkaline Phosphatase (CIP) at 37 ^oC for 1 h. The CIP-treated RNA was then treated with Tobacco Acid Pyrophosphatase (TAP) to remove the cap structure from full-length mRNA, leaving a 5'-monophosphate. A 45 base RNA Adapter oligonucleotide was then ligated to the mRNA using T4 RNA ligase as described by the manufacturer. During the ligation reaction, the full length, decapped mRNA acquired the adapter sequence as its 5' end. A random-primed reverse transcription reaction allowed the synthesis of 5' RACE cDNA. Similarly, the manufacturer's protocol was followed to obtain the 3' RLM-RACE cDNA. A reverse transcription reaction consisting of 1 µg of total RNA from one or several *C. gariepinus* tissues, 4 µl dNTP mix, 2 µl 3' RACE adapter, 2 µl 10X RT buffer, 1 µl RNase inhibitor, 1 µl M-MLV reverse transcriptase and nuclease-free water to make the reaction up to 20 µl was assembled. This was mixed gently, centrifuged and incubated at 42 ^oC for 1 h. It was then preserved at -20 ^oC for further use.

Nested PCR was then carried out to amplify both the 5' and 3' end of the gene. The 5' (or 3') RACE outer primer and gene-specific primer were used in a PCR with the 5' (or 3')

RACE cDNA as template (first round PCR). The resulting PCR product was then used as template for the second round PCR with the 5' (or 3') RACE inner primer and a gene specific primer. The total volume of reaction mixture used for RACE PCR was 10 µl containing 5 µl GoTaq DNA polymerase, 1.0 µl template, 3.0 µl nuclease free water and 0.5 µl of each primer (10 µM). PCR conditions consisted of an initial denaturation step at 95 °C for 2 min, followed by 32 cycles of denaturation at 95 °C for 30 s, annealing at 57-60 °C for 30 s, extension at 72 °C for 1-3 min, followed by a final extension at 72 °C for 7 min. Gene-specific primers designed on the partial cDNA sequence obtained earlier with the set of primers supplied (5'-GCTGATGGCGATGAATGAACACTG-3' and 5'-CGCGGATCCGAACACTGCGTTTGCTGGCTTTGATG-3', outer and inner primer, respectively) corresponding to the 5' RACE Adapter sequence were used to perform nested PCR for 5' RLM-RACE. The 3' RACE primers provided in kit was used for 3' RLM-RACE (outer primer- 5'-GCGAGCACAGAATTAATACGACT-3' and inner primer- 5'-CGCGGATCCGAATTAATACGACTCACTATAGG-3').

2.3.6 Cloning of PCR Products into PCR 2.0 Vector

The first fragments, 5' and 3' RACE PCR fragments were (where necessary) cloned into PCR 2.1 vector (TA cloning® kit, Invitrogen, Life Technologies™, USA) and sequenced. Specifically, PCR products were ligated into the PCR 2.1 vector by combining 0.5 µl of the PCR product, 5.5 µl nuclease free water, 1 µl ligation buffer, 1 µl T4 DNA ligase and 1.5 µl PCR 2.1 vector in a tube at 14 ^{o}C for at least 4 h, preferably overnight. A volume of 5 µl of the ligation reaction was subsequently transformed into *E. coli* competent chemocompetent cells.

Transformation was done by the heat shock method using competent *E. coli* JM 109 cells (Promega) prepared as described in Section 2.2.3. Competent cells stored at -70 ^{o}C were thawed on ice and 5 µl of the DNA ligation reaction were added. This was incubated on

ice for 1 h, and then a heat shock was performed by placing the tube in a water bath at 42 ^{o}C for 1 min before the tube was placed on ice for 5 min. Subsequently, 900 µl of ampicillin free LB medium was added to each tube and incubated at 37 ^{o}C for 1 h with gentle shaking. They were then centrifuged at 1500 g for 2 min 30 s and 700 µl of the supernatant discarded. The cells were resuspended and 150 µl spread on an agar plate containing ampicillin (100 mg/ml) prepared as described in Section 2.2.2 and 32 µl of 50 mg/µl X-gal, sealed and incubated overnight at 37 ^{o}C. X-gal was used for blue-white screening of positive (white) and negative (blue) transformant colonies.

Positive colonies (number varying upon availability) were picked with a p10 tip, dipped in 60 µl of ddH_2O to deposit some genetic material and then rinsed in 15 µl of LB medium contained in a separate 0.2 ml tube for overnight cultures as explained below. The DNA contained in the *E. coli* cells deposited in the 60 µl of ddH_2O were subjected to 95 ^{o}C for 10 min and 4 ^{o}C for 1 min to partly extract DNA for further PCR screening using M13 forward and reverse primers. All PCR screenings were run on an agarose gel to idenfity the positive clones containing adequate band sizes as inserts.

A volume of 7.5 µl of LB medium containing positive colonies were incubated overnight at 37 ^{o}C with shaking in a 15 ml Falcon tube containing 3 ml of LB medium and 3 µl of 100 mg/µl ampicillin solution to give a final concentration of 100 mg/ml of ampicillin in the solution.

Plasmids were purified using GenElute^{TM} plasmid miniprep kit from Sigma-Aldrich (USA). The overnight recombinant *E. coli* culture were pelleted by centrifugation at 12,000 g for 1 min. The pellets were then resuspended with 200 µl of resuspension solution by vortexing to thoroughly resuspend the cells. The resuspended cells were lysed by the addition of 200 µl of lysis solution and mixed by gentle inversion 6-8 times. The

cells were then precipitated by the addition of 350 µl of the neutralisation and binding solution, and gently inverted 4-6 times and centrifuged at 12,000 g for 10 min. The lysates were then transferred to a binding column prepared with the column preparation solution and centrifuged at 12,000 g for 1 min. Then 750 µl of the wash solution were added to the column and centrifuged at 12,000 g for 1 min. After the flow-through was removed, the column was air dried before 40 µl of ddH_2O were added in order to elute the plasmids from column. After centrifuged at 12,000 g for 1 min, the concentrations were measured with the Nanodrop.

Finally, the plasmid prep samples were sequenced with the M13 primers (forward primer - GTAAAACGACGGCCAGTG, reverse primer - CAGGAAACAGCTATGACCAT) enabling to obtain the full sequence of insert. The full nucleotide sequences of the cDNA were obtained by aligning sequences of the first fragments, together with those of the 5' and 3' RACE PCR positive products using BioEdit.

2.4 Sequence and Phylogenetic Analysis

The deduced amino acid (aa) sequences of the *C. gariepinus* cDNAs were compared to related protein sequences from other vertebrate species and sequence identity scores were calculated using the EMBOSS Needle Pairwise Sequence Alignment tool (http://www.ebi.ac.uk/Tools/psa/emboss_needle/). Phylogenetic analysis of the deduced aa sequences of cDNAs from *C. gariepinus* and those from a variety of species across vertebrate lineages were carried out by constructing trees using the neighbour-joining method (Saitou and Nei, 1987) with the MEGA 4.0 or 6.0 software (www.megasoftware.net). Confidence in the resulting tree branch topology was measured by bootstrapping through 1,000 iterations.

2.5 Functional Characterisation of Genes by Heterologous Expression in *Saccharomyces cerevisiae*

2.5.1 Cloning of the PCR Product into pYES2 Vector

PCR fragments corresponding to the open reading frame (ORF) of *C. gariepinus* gene were amplified from a mixture of cDNA synthesised from liver, intestine, eye and brain total RNA, using the high fidelity *Pfu* DNA polymerase (Promega, USA) with primers containing restriction sites. PCR conditions consisted of an initial denaturation step at 95 °C for 2 min, followed by 35 cycles of denaturation at 95 °C for 30 s, annealing at 57-60 °C for 30 s, extension at 72 °C for 3-4 min followed by a final extension at 72 °C for 7 min. The DNA fragments obtained were purified as above, digested with the appropriate restriction enzymes (New England Biolabs, UK), and ligated into similarly digested pYES2 yeast expression vector (Invitrogen, UK). The PCR products were ligated into pYES2 vector by combining 7 µl of the PCR product, 1 µl ligation buffer, 1 µl ligase and 1 µl pYES2 vector in a tube and incubating at room temperature for 5 h.

Transformation was then performed by the heat shock method using competent *E. coli* JM 109 cells as described in Section 2.3.6. Screening for the presence of recombinant plasmids was done via PCR using the pYES2 primers (AACCCCGGATCGGACTACTA - forward and GGGAGGGCGTGAATGTAAG -reverse).

2.5.2 Transformation of Yeast Competent Cells with Plasmid Constructs

Yeast competent cells InvSc1 (Invitrogen) were transformed with the plasmid constructs or with empty vector (control) using the S.c. EasyComp™ Transformation Kit (Invitrogen). The yeast competent cells (50 µl) (Section 2.25) were thawed at room temperature, and 2 µl of the recombinant plasmid DNA and 500 µl of Solution III were added and vortexed to mix the reaction. The transformation reaction mixture was then incubated for 1 h at 30 ^{o}C with vortexing every 15 min. Subsequently 50 µl of the reaction

were spread on *S. cerevisiae* minimal medium minus uracil (SCMM^{-ura}) plates and incubated at 30 ^{o}C for three days for selection of yeast containing the pYES2 constructs.

2.5.3 Yeast Culture

One single yeast colony was selected in each functional characterisation assay run (Chapters 3-6) and grown in 5 ml of SCMM^{-ura} medium for 2 days at 30 °C. Subsequently subcultures starting at an optical density measured at a wavelength of 600 nm (OD_{600}) of 0.4 were run in individual Erlenmeyer flasks containing 5 ml of SCMM^{-ura} medium. The subcultures were grown for 4-5 h before galactose (2 %, w/v) (for the induction of gene expression) and a certain amount of PUFA substrate were added. For all genes, final concentration of PUFA substrates were 0.6 mM (C_{18}), 1.0 mM (C_{20}) and 1.2 mM (C_{22}) to compensate for differential uptake related to fatty acyl chain (Zheng et al., 2009). The PUFA substrate used for a particular gene are listed in the appropriate chapters. After 2 days, yeast cultures were harvested into 15 ml plastic tubes, centrifuged at 500 g for 3 min and supernatant discarded. 2 ml of methanol containing 0.01 % butylated hydroxytoluene (BHT) (w/v) was added and the yeast resuspended by vortexing and transfered to glass tubes. 4 ml chloroform containing 0.01 % BHT was added to the samples and they were homogenised using the Ultraturrax^{TM}. The samples were flushed with oxygen-free nitrogen (OFN) and stored in chloroform:methanol (2:1, v/v) at -20 °C for at least one day until further use.

2.6 Fatty Acid Analysis of Yeast

2.6.1 Total Lipid Extraction

Total lipids of yeast were extracted according to the method of Folch et al. (1957). The yeast samples were homogenised in chloroform:methanol (2:1, v/v) containing 0.01 BHT as antioxidant and 0.25 volumes (1.5 ml) of 0.88 % (w/v) KCl was added, thoroughly mixed and left to stand on ice for 5 min then centrifuged at 500 g for 3 min for phase

separation. The bottom phase was carefully removed and the infranatant filtered through a chloroform: methanol (2:1) pre-washed 9 cm Whatman no.1 filter paper into clean test tubes. Solvent was evaporated under a stream of OFN on an N-Evap evaporator (Organomation Associates, Inc. USA).

2.6.2 Preparation and Purification of Fatty Acid Methyl Esters

Lipids extracted from yeast samples were used to prepare fatty acid methyl esters (FAME). FAME extraction, purification and analysis were performed as described by Li et al. (2010). Briefly, 1 ml of toluene and 2 ml of 2 % (v/v) sulphuric acid in methanol were added and mixed thoroughly, and subsequently the tubes were flushed with OFN, stoppered and incubated overnight (approximately 16 h) at 50 ^{o}C in the hot-block. For FAME extraction, 2 ml 2 % (w/v) potassium hydrogen ($KHCO_3$) and 5 ml isohexane: diethyl ether (1:1, v/v) + 0.01 % (w/v) BHT were added to the tubes, vortexed and centrifuged at 500 g for 2 min. The upper organic layer was transferred to new tubes and the solvent evapourated off under a stream of OFN. The methyl esters were redissolved in 100 µl of isohexane and purified by thin-layer chromatography (TLC) plates. TLC plates were then chromatographed in isohexane/diethyl ether/acetic acid (90:10:1, v/v/v) up to 1-1.5 cm from the top of the plate. The plates were then removed from the tank and the solvent allowed to evaporate in the fume cupboard.

The FAME bands were visualised by spraying the sides of the plates with 1 % (w/v) iodine in chloroform and then scraped from the TLC plate into test tubes using a straight edged scalpel. FAME were eluted from the silica with 10 ml isohexane: diethyl ether (1:1, v/v) containing 0.01 BHT, vortexed and centrifuged to precipitate the silica. The solvent was transferred to new tubes, evaporated under OFN and redissolved in 100-150 µl of isohexane. FAME were stored -20^{o} C until GLC analysis. FA were identified by

comparison to known reference standards Restek (Thames Restek, Saunderton, UK). Gas chromatography-mass spectrometry (GC-MS) was used to confirm double bond positions of peaks that were too small or not distinct. In Chapter 6, 4,4-dimethyloxazoline (DMOX) derivatives, analysed by GC-MS were also used to confirm FA products. Further details on the preparation of DMOX derivatives are presented in Chapter 6.

The proportion of substrate FA converted was calculated as the proportion of exogenously added FA substrate desaturated or elongated [all product peak areas / (all product peak areas + substrate peak area)] × 100. GC-MS was used to confirm double bond positions when necessary.

2.7 Tissue Expression Analysis of *C. gariepinus* Genes

Gene expression was measured by quantitative real-time PCR (qPCR) using Biometra Thermocycler (Analytik Jena Company, Thuringia, Germany) and Luminaris Colour Higreen qPCR master mix (Thermo Scientific, Carlsbad, CA, USA) following the manufacturer's instructions. Extraction of RNA from tissues and cDNA synthesis were carried out as described above. PCR amplicons of each gene cloned into PCR 2.1 vector (TA cloning® kit, Invitrogen, Life Technologies™, USA) (Section 2.6.1) were linearised, DNA concentration quantified and serial-diluted to generate a standard curve of known copy numbers for quantification. A restriction enzyme (New England Biolabs) that cut the plasmid construct in only one position was used for linearization by incubating for 2 h at 37 ^{o}C the following mixture: plasmid product (1 µg in 39 µl of dd$H_2$0), 10x buffer (5 µl), 10x BSA (5 µl) and enzyme (1 µl).

The DNA concentration (Nanodrop) and size (bp) of plasmid + gene were determined in order to establish the quantity of linearised plasmid construct used for the preparation of the 1E8 copies qPCR standard. In order to prepare solutions of known copy numbers,

DNA concentration of linearised PCR 2.1 vectors containing a fragment of either candidate or reference genes was determined, and their molecular weights estimated as 660 g × length in base pair (bp) of the plasmid constructs. Further serial dilutions (1E7 to 1E0 copies) were prepared from 1E8 copies standard solution by adding 10 µl of it to 90 µl of ddH_2O and allowing to construct standard curves for each gene to evaluate the transcript copy numbers in each sample. Primer efficiency was also tested with normal PCR using GoTaq. The recipe for the primer efficiency test included standards (1/5, 1/10, 1/20, 1/50, 1/100, 1/200 and 1/500) prepared from a mix of cDNA (5 µl each) from all the tissues. PCR amplifications were run in an agarose gel and a single band and the absence of primer dimers was used to determine the reaction efficiency.

QPCR amplifications including standards were run in duplicates. QPCR were performed in a final volume of 20 µl containing 5 µl diluted (1/20) cDNA, 1 µl (10 µM) of each primer, 3 µl nuclease free water and 10 µl Luminaris Color Higreen qPCR master mix. For the reference gene, 2 µl diluted (1/20) cDNA and 6 µl nuclease free water were used. The qPCR conditions were 50 °C for 2 min, 95 °C for 10 min followed by 35 cycles of denaturation step at 95 °C for 15 s, annealing at 59 °C for 30 s and extension at 72 °C for 30 s. After amplification, a dissociation curve of 0.5 °C increments from 60 to 90 °C was performed, enabling confirmation of a single product in each reaction. Identity of the qPCR products was further confirmed by DNA sequencing of selected samples (GATC Biotech Ltd.). Negative controls (no template control, NTC) containing no cDNA were systematically run. Absolute copy number of the target and reference gene in each sample was calculated from the linear standard curve constructed. Normalisation of each target gene was carried out by dividing the absolute copy number of the candidate gene by the absolute copy number of the reference gene, 28S rRNA (gb|AF323692.1|). Primers used

for qPCR analysis were designed on the 3' end of the cDNA of the gene of interest and are presented in the appropriate Chapters.

2.8 Statistical Analysis

Tissue expression (qPCR) results were expressed as mean normalised ratios (±SE) corresponding to the ratio between the copy numbers of the target genes and the copy numbers of the reference gene. Differences in gene expression among tissues were analysed by one-way analysis of variance (ANOVA) followed by Tukey's HSD test at a significance level of $P \leq 0.05$ (IBM SPSS Statistics 21).

CHAPTER 3.

BIOSYNTHESIS OF LONG-CHAIN POLYUNSATURATED FATTY ACIDS IN THE AFRICAN CATFISH CLARIAS GARIEPINUS: MOLECULAR CLONING AND FUNCTIONAL CHARACTERISATION OF FATTY ACYL DESATURASE (FADS2) AND ELONGASE (ELOVL2) cDNAS

3.1 Introduction

Fish, like all vertebrates, are dependent on dietary sources of polyunsaturated fatty acids (PUFA) such as α-linolenic (ALA, 18:3n-3) and linoleic (LA, 18:2n-6) acids as they lack the Δ12 and Δ15 desaturases required for the synthesis of LA and ALA from oleic acid (18:1n-9) (Tocher, 2010; Tocher and Glencross, 2015). However, whereas the C_{18} PUFA, ALA and LA, can satisfy essential fatty acid (EFA) requirements of some fish species, long-chain (C_{20-24}) polyunsaturated fatty acids (LC-PUFA) including eicosapentaenoic acid (EPA, 20:5n-3), docosahexaenoic acid (DHA, 22:6n-3) and arachidonic acid (ARA, 20:4n-6), which play physiologically important roles, are required in the diet to meet the EFA requirements of other species. This reflects the differing ability of fish species to endogenously synthesise LC-PUFA from C_{18} precursors, associated with the complement of fatty acyl desaturases (Fads) and elongation of very long-chain fatty acids (Elovl) enzymes they possess (Bell and Tocher, 2009; Castro et al., 2016; Tocher, 2010). This has important implications with regards to feed formulation for fish farming. Species with active and complete biosynthetic pathways can convert C_{18} PUFA contained in vegetable oils (VO) that are now common ingredients in aquafeeds, to LC-PUFA, and thus are less dependent on the inclusion of fish oil (FO) to supply LC-PUFA in their diets.

The LC-PUFA biosynthesis pathways involves successive desaturation and elongation of the C_{18} precursors catalysed by Fads and Elovl elongases (Castro et al., 2016; Monroig et al., 2011a; Tocher, 2003; Vagner and Santigosa, 2011). Fads enzymes introduce double bonds (unsaturations) at specific positions of the fatty acyl chain (Nakamura and Nara, 2004). It has been shown that all *fads* so far studied in teleost genomes are paralogues of *fads2*, a gene encoding an enzyme that typically acts as Δ6 Fads in vertebrates, while *fads1*, another vertebrate *fads* encoding an enzyme with Δ5 activity,

appears to be absent in teleosts (Castro et al., 2016, 2012). While most fish Fads2 enzymes functionally characterised are typically Δ6, others have been characterised as bifunctional Δ6Δ5 Fads2 (Fonseca-Madrigal et al., 2014; Hastings et al., 2001; Li et al., 2010; Tanomman et al., 2013) or monofunctional Δ5 Fads (Hamid et al., 2016). In recent years, Fads2 with Δ4 activities have been found in a variety of teleost species (Fonseca-Madrigal et al., 2014; Kuah et al., 2015; Li et al., 2010; Morais et al., 2012). Furthermore, fish Fads2, as described in mammals (Park et al., 2009), also display Δ8 activity, an activity that appeared to be relatively higher in marine fish compared to freshwater fish species (Monroig et al., 2011a).

Elovl enzymes catalyse the condensation step in the elongation pathway resulting in the addition of a two-carbon unit to the pre-existing FA (Guillou et al., 2010). Functional characterisation of fish Elovl2, Elovl4 and Elovl5, elongase enzymes that function in the LC-PUFA biosynthesis pathway, show that they display somewhat overlapping activities (Castro et al., 2016). Thus Elovl5 generally elongate C_{18} and C_{20} PUFA, whereas Elovl2 and Elovl4 are more efficient towards C_{20} and C_{22} PUFA (Gregory and James, 2014; Monroig et al., 2011c, 2009; Morais et al., 2009). While both *elovl5* and *elovl4* genes are present in teleost genomes (Monroig et al., 2016b), *elovl2* appears to be lost in Acanthopterygii, a phylogenic group that, with the exception of salmonids, includes the vast majority of the most important farmed fish species (Castro et al., 2016). To the best of our knowledge, Elovl2 cDNAs have been characterised only in Atlantic salmon (*Salmo salar*) (Morais et al., 2009), *D. rerio* (Monroig et al., 2009) and rainbow trout (*Oncorhynchus mykiss*) (Gregory and James, 2014).

Evidence indicates that the complement and functionalities of *fads* and *elovl* genes existing in any teleost species has been shaped by evolutionary drivers leading to the retention, subfunctionalisation or loss of these genes (Castro et al., 2016). Moreover, the

habitat (marine *vs* freshwater), and specifically the availability of LC-PUFA in food webs, has also been implicated as influencing the LC-PUFA biosynthetic capability of fish (Bell and Tocher, 2009; Castro et al., 2016; Monroig et al., 2011b). Freshwater fish, having evolved on diets low in LC-PUFA, are believed to have all the genes and/or enzymatic functionalities required for endogenous LC-PUFA production (NRC, 2011; Tocher, 2015). Whereas, many marine species have not retained all the genes and/or enzymatic functionalities required for endogenous LC-PUFA production as a consequence of LC-PUFA being readily available in their natural diets (NRC, 2011; Tocher, 2015). However, such dichotomy has been recently seen as too simplistic and other factors including trophic level (Li et al., 2010) and trophic ecology (Morais et al., 2015, 2012) also appear to influence LC-PUFA biosynthesis capacity of fish species. Within an aquaculture nutrition context, investigations of the *fads* and *elovl* gene repertoire involved in LC-PUFA biosynthesis, as well as the functions of the enzyme they encode, are necessary to ascertain whether the EFA requirements of a species can be satisfied by C_{18} PUFA or whether dietary LC-PUFA are required.

The African catfish *Clarias gariepinus*, a freshwater species belonging to the family Clariidae and order Siluriformes, is the most important aquaculture species in Sub-Saharan Africa (FAO, 2012). Yet, neither its LC-PUFA biosynthetic pathway nor EFA requirement is fully understood. Studies on *C. gariepinus* and other African catfishes suggest they can effectively utilise C_{18} PUFA contained in VO to cover their physiologically important LC-PUFA requirements (Baker and Davies, 1996; Sotolu, 2010; Szabó et al., 2009). Intriguingly, lower growth performance has been reported for *C. gariepinus* fed diets with FO compared to those fed diets containing VO (Hoffman and Prinsloo, 1995a; Ng et al., 2003) in contrast to most fish species including those with

full LC-PUFA biosynthetic capability like salmonids (Sargent et al., 2002; Tocher and Glencross, 2015).

The aim of this study was to investigate the functions of the genes encoding putative Fads and Elovl enzymes that account for the LC-PUFA biosynthetic capability of *C. gariepinus* and thus understand the potential of this species to utilise diets containing VO and low contents of LC-PUFA. Here, we report the cloning and functional characterisation of *fads2* and *elovl2* genes from *C. gariepinus*. We further investigated the mRNA tissue distribution of the newly cloned genes, as well as that of the previously cloned *elovl5* (Agaba et al., 2005).

3.2 Materials and Methods

3.2.1 Sample Collection and RNA Preparation

Tissue samples were obtained from adult *C. gariepinus* (~1.8 kg) raised in the tropical aquarium of the Institute of Aquaculture, University of Stirling, UK, on standard salmonid diets. Eight *C. gariepinus* individuals were sacrificed with an overdose of tricaine methanesulfonate (MS222) and a sharp blow to the head. Tissue samples including liver, intestine, pituitary, testis, ovary, skin, muscle, gills, kidney and brain were collected. The samples were immediately preserved in an RNA stabilisation buffer (3.6 M ammonium sulphate, 18 mM sodium citrate, 15 mM EDTA, pH 5.2) and stored at -70 °C prior to extraction of total RNA following homogenisation in TRI Reagent® (Sigma-Aldrich, St. Louis, USA). Purity and concentration of total RNA was assessed using the NanoDrop® (Labtech International ND-1000 spectrophotometer) and integrity was assessed on an agarose gel. First strand complementary DNA (cDNA) was synthesised using High Capacity cDNA Reverse Transcription Kit (Applied Biosystems™, USA) following the manufacturer's instructions.

3.2.2 Molecular Cloning of Fads2 and Elovl2 cDNAs

Amplification of partial fragments of the genes was achieved by polymerase chain reaction (PCR) using a mixture of cDNA from eye, liver, intestine and brain as template and primers FadCGF2F1 and FadCGF2R1 for *fads2*, and EloCGE2F1 and EloCGE2R1 for *elovl2* (Table 3.1). For clarity, it should be noted that the standard gene/protein nomenclature has been used in this study (Castro et al., 2016). Following conventions accepted for zebrafish, proteins are termed with regular fonts (e.g. Fads2) whereas genes are italicised (e.g. *fads2*). Primers used for amplification of the first fragment of target genes were designed on conserved regions of fish orthologues of *fads2* and *elovl2* according to the following strategy. For *fads2*, sequences from the broadhead catfish (*Clarias microcephalus*) (gb|KF006248.1|), spot pangasius (*Pangasius larnaudii*) (gb|KC994461.1|), striped catfish (*Pangasianodon hypophthalamus*) (gb|JX035811.1|) and *Clarias* hybrid (*C. macrocephalus* and *C. gariepinus*) (gb|KC994463.1|) were aligned with the ClustalW tool (BioEdit v7.0.9, Tom Hall, Department of Microbiology, North Carolina State University, USA) for degenerate primer design. For *elovl2*, homologous sequences from *D. rerio* (gb|NM_001040362.1|), *S. salar* (gb|NM_001136553.1|) and Mexican tetra (*Astyanax mexicanus*) (gb|XM_007260074.2|) were retrieved from *National Center for Biotechnology Information* (NCBI) (http://ncbi.nlm.nih.gov), aligned (BioEdit) and conserved regions used to retrieve expressed sequence tags (ESTs) from catfish species. Six Channel catfish (*I. punctatus*) ESTs (GenBank accession numbers GH651976.1, GH651977.1, FD328544.1, FD284236.1, FD284235.1 and BM438219.1) were obtained and aligned with BioEdit. Subsequently, the consensus *elovl2*-like sequences from *I. punctatus*, and those from *D. rerio, S. salar* and *A. mexicanus*, were aligned for degenerate primer design. PCR conditions consisted of an initial denaturation step at 95 °C for 2 min,

followed by 33 cycles of denaturation at 95 °C for 30 s, annealing at 57 °C for 30 s, extension at 72 °C for 1 min 30 s, followed by a final extension at 72 °C for 7 min. The PCR fragments were purified using the Illustra GFX PCR DNA/gel band purification kit (GE Healthcare, Little Chalfont, UK), and sequenced (GATC Biotech Ltd., Konstanz, Germany). The primers used in this study and their sequences are presented in Table 3.1.

In order to obtain full-length cDNA sequences, Rapid Amplification of cDNA Ends (RACE) was performed with the FirstChoice® RLM-RACE RNA ligase mediated RACE kit (Ambion®, Life Technologies™, USA). The 5' RACE outer primer and gene-specific primer FadCGRF2R3 were used in a PCR using the 5' RACE cDNA as template (first round PCR) for *fads2*. The resulting PCR product was then used as template for the second round PCR with the 5' RACE inner primer and the gene-specific primer FadCGRF2R2. A similar approach was followed to perform 3' RACE PCR, with primers FadCGRF2F1 and FadCGRF2F2 used for first and second round PCR, respectively. For *elovl2*, the primers CGRE2R3 and CGRE2R2 were designed and used for first and second round PCR, respectively, for the 5' RACE PCR, while CGRE2F1 and CGRE2F2 were used for first and second round PCR, respectively, for the 3' RACE PCR. The first fragments, 5' and 3' RACE PCR fragments were then cloned into PCR 2.1 vector (TA cloning® kit, Invitrogen, Life Technologies™, USA) and sequenced as above. The full nucleotide sequences of the *fads2* and *elovl2* cDNAs were obtained by aligning sequences of the first fragments, together with those of the 5' and 3' RACE PCR positive products (BioEdit).

Table 3.1. Sequences of primers used for cDNA cloning and tissue expression analysis (qPCR) of *Clarias gariepinus fads2* and *elovl2*. Restriction sites *Bam*HI and *Xho*I are underlined.

Name	Direction	Sequence
Initial cDNA cloning		
FadCGF2F1	Forward	5'-ATGGGCGGCGGAGGACAC-3'
FadCGF2R1	Reverse	5'-GCATCTAGCCACAGCTCACC-3'
EloCGE2F1	Forward	5'-TACTTGGGACCAAAGTACATGA-3'
EloCGE2R1	Reverse	5'-AGATAGCGTTTCCACCACAG-3'
5′ RACE PCR		
FadCGRF2R2	Reverse	5'-CGATCACAACCCACTGATCA-3'
FadCGRF2R3	Reverse	5'-CGTCCTCCAGGATGTCTTTT-3'
EloCGRE2R3	Reverse	5'-AGCTTGCTGAAATAAGCTCCACT-3'
EloCGRE2R2	Reverse	5'-TGTAGAAGGACAGCATGGTGAC-3'
3′ RACE PCR		
FadCGRF2F1	Forward	5'-CAGTCGCCATTCAACGATT-3'
FadCGRF2F2	Forward	5'-GAACACCATCTCTTTCCCATG-3'
EloCGRE2F1	Forward	5'-TTGTCCACCATTCCTTCAATG-3'
EloCGRE2F2	Forward	5'-ACTGAACAGCTTCATCCATGTG-3'
ORF cloning		
FadCGF5UF1	Forward	5'-AGAGGAGCGCAGTGATGAG-3'
FadCGF3UR1	Reverse	5'-GTGGGAATTACAGAATTGTTATGG-3'
FadCGFVF	Forward	5'-CCCGGATCCAAGATGGGCGGCGGAGGAC-3'
FadCGFVR2	Reverse	5'-CCGCTCGAGTTATTTGTGGAGGTATGCATC-3'
EloCGE2VF	Forward	5'-CCCGGATCCAACATGGATTTTATTGTGAAGAA-3'
EloCGE2VR	Reverse	5'-CCGCTCGAGTCACTGCAGCTTATGTTTGGC-3'
EloCGE25UF	Forward	5'-CCAGTTACATTAAGAGGCACCG-3'
EloCGE23UR	Reverse	5'-AGATTAGTCAACATGAAAGGTGAA-3'
Quantitative PCR		
FadCGqF2F1	Forward	5'-TCCTATATGCTGGAACTAATGTGG-3'
FadCGqF2R1	Reverse	5'-AGGATGTAACCAACAGCATGG-3'
EloCGqE2F1	Forward	5'-GCAGTACTCTGGGCATTTGTC-3'
EloCGqE2R1	Reverse	5'-GGGACATTGGCGAAAAAGTA-3'
EloCGqE5F1	Forward	5'-ACTCACAGTGGAGGAGAGC-3'
EloCGqE5R1	Reverse	5'-GGAATGGTGGTAAACGTGCA-3'
28SrRNAF1	Forward	5'-GTCCTTCTGATGGAGGCTCA-3'
28SrRNAR1	Reverse	5'-CGTGCCGGTATTTAGCCTTA-3'

3.2.3 Sequence and Phylogenetic Analysis

The deduced amino acid (aa) sequences of the *C. gariepinus fads2* and *elovl2* cDNAs were compared to corresponding orthologues from other vertebrate species and sequence identity scores were calculated using the EMBOSS Needle Pairwise Sequence Alignment tool (http://www.ebi.ac.uk/Tools/psa/emboss_needle/). Phylogenetic analysis of the deduced aa sequences of *fads2* and *elovl2* cDNAs from *C. gariepinus* and those from a variety of species across vertebrate lineages were carried out by constructing trees using the neighbour-joining method (Saitou and Nei, 1987), with the MEGA 4.0 software (www.megasoftware.net/mega4/mega.html). Confidence in the resulting tree branch topology was measured by bootstrapping through 1,000 iterations.

3.2.4 Functional Characterisation of *C. gariepinus* Fads2 and Elovl2 by Heterologous Expression in *Saccharomyces cerevisiae*

PCR fragments corresponding to the open reading frame (ORF) of *C. gariepinus fads2* and *elovl2* were amplified from a mixture of cDNA synthesised from liver, intestine, eye and brain total RNA, using the high fidelity *Pfu* DNA polymerase (Promega, USA) with primers containing *Bam*HI (forward) and *Xho*I (reverse) restriction sites (Table 3.1). PCR conditions consisted of an initial denaturation step at 95 °C for 2 min, followed by 35 cycles of denaturation at 95 °C for 30 s, annealing at 57 °C for 30 s, extension at 72 °C for 3 min 30 s followed by a final extension at 72 °C for 7 min. The DNA fragments obtained were purified, digested with the appropriate restriction enzymes, and ligated into similarly digested pYES2 yeast expression vector (Invitrogen) as described in Section 2.6.1 of the General Materials and Methods chapter.

Yeast competent cells InvSc1 (Invitrogen) were transformed with the plasmid constructs pYES2-*fads2* (desaturase) or pYES-*elovl2* (elongase) or with empty vector (control) using the S.c. EasyComp™ Transformation Kit (Invitrogen). Selection of yeast

containing the pYES2 constructs was performed on *S. cerevisiae* minimal medium minus uracil ($SCMM^{-ura}$) plates. One single yeast colony was grown in $SCMM^{-ura}$ broth for 2 days at 30 ^{o}C, and subsequently subcultured in individual Erlenmeyer flasks until an optical density measured at a wavelength of 600 nm (OD_{600}) reached 1, after which galactose (2 %, w/v) and a PUFA substrate were added. Further details have been given in Section 2.6.3. For the *fads2*, Δ6 (18:3n-3 and 18:2n-6), Δ8 (20:3n-3 and 20:2n-6), Δ5 (20:4n-3 and 20:3n-6), and Δ4 (22:5n-3 and 22:4n-6) Fads substrates were used. For *elovl2*, substrates included C_{18}, (18:3n-3, 18:2n-6, 18:4n-3 and 18:3n-6), C_{20} (20:5n-3 and 20:4n-6) and C_{22} (22:5n-3 and 22:4n-6) PUFA. After 2 days, the yeasts were harvested, washed and homogenised in chloroform/methanol (2:1, v/v) containing 0.01 % butylated hydroxytoluene (BHT) and stored at -20 °C until further use.

3.2.5 Fatty Acid Analysis of Yeast

Total lipids extracted according to Folch et al. (1957) from yeast samples were used to prepare fatty acid methyl esters (FAME). FAME extraction, purification and analysis were performed as described by Li et al. (2010). Substrate FA conversion was calculated as the proportion of exogenously added FA substrate desaturated or elongated [all product peak areas / (all product peak areas + substrate peak area)] x 100 (Monroig et al., 2016b). GC-MS was used to confirm double bond positions when necessary (Li et al., 2010).

3.2.6 Gene Expression Analysis

Expression of the newly cloned *fads2* and *elovl2* genes, as well as that of the previously characterised elongase *elovl5* (Agaba et al., 2005), were determined by quantitative real-time PCR (qPCR). Extraction of RNA from tissues and cDNA synthesis were carried out as described above (Section 3.2.1). QPCR amplifications were carried out in duplicate using Biometra Thermocycler (Analytik Jena company, Germany) and Luminaris Color

Higreen qPCR master mix (Thermo Scientific, Carlsbad, CA, USA) following the manufacturer's instruction. The qPCR was performed in a final volume of 20 µl containing 5 µl diluted (1/20) cDNA, 1 µl (10 µM) of each primer, 3 µl nuclease free water and 10 µl Luminaris Color Higreen qPCR master mix. The qPCR conditions were 50 °C for 2 min, 95 °C for 10 min followed by 35 cycles of denaturation at 95 °C for 15 s, annealing at 59 °C for 30 s and extension at 72 °C for 30 s. After the amplifications, a dissociation curve of 0.5 °C increments from 60 to 90 °C was performed, enabling confirmation of a single product in each reaction. Negative controls (no template control, NTC) containing no cDNA were systematically run. Absolute copy number of the target and reference gene in each sample was calculated from the linear standard curve constructed. Normalisation of each target gene was carried out by dividing the absolute copy number of the candidate gene by the absolute copy number of the reference gene 28S rRNA (gb|AF323692.1|). In order to prepare solutions of known copy numbers, DNA concentration linearised PCR 2.1 vectors containing a fragment of either candidate or reference genes was determined, and their molecular weights were estimated as 660 g bp x length (bp) of the plasmid constructs. Primers used for qPCR analysis are also presented in Table 3.1.

3.2.7 Statistical Analysis

Tissue expression (qPCR) results were expressed as mean normalised ratios (±SE) corresponding to the ratio between the copy numbers of the target genes (*fads2*, *elovl2* and *elovl5*) and the copy numbers of the reference gene, 28S rRNA. Differences in gene expression among tissues were analysed by one-way analysis of variance (ANOVA) followed by Tukey's HSD test at a significance level of $P \leq 0.05$ (IBM SPSS Statistics 21).

3.3 Results

3.3.1 Sequence and Phylogenetic Analysis

C. gariepinus Fads2 sequence was deposited in the GenBank database with the accession number KU925904. The full length of the *C. gariepinus* Fads2 was 1,812 bp, comprising of a 5′ untranslated region (UTR) of 162 bp, an ORF of 1,338 bp encoding a putative protein of 445 aa, and a 3′ UTR of 312 bp. The deduced *C. gariepinus* Fads2 enzyme showed distinctive structural features of fatty acyl desaturases including the three histidine boxes HDFGH, HFQHH, and QIEHH (aa 181-185, 218-222 and 383-387, respectively) and cytochrome b_5-domain (aa 26-77) containing the heme binding motif HPGG (aa 54-57). Pairwise aa sequence comparisons of *C. gariepinus* Fads2 with other Fads2-like proteins showed highest identities with Fads from members of the catfish family such as *C. macrocephalus* (97 %) and *P. hypophthalamus* (91.5 %). Comparisons with bifunctional Δ6Δ5 Fads2 of *D. rerio* (gb|AF309556.1|) and *C. estor* (gb|AHX39207.1|), bifunctional Δ5Δ4 Fads2 of *C. striata* (gb|ACD70298.1|) and *S. canaliculatus* (gb|ADJ29913.1|) and Δ4 Fads2 of *S. senegalensis* (gb|AEQ92868.1|) and *C. estor* (gb|AHX39206.1|) showed identities ranging from 65.2-70.2 %. Lowest identities were observed when *C. gariepinus* Fads was compared to Fads1-like sequences from different vertebrate lineages. Phylogenesis of *C. gariepinus* Fads with Fads from a variety of vertebrate species showed it clustered with all other Fads2 in one group that was separate from the Fads1 group confirming that the newly cloned *fads* was a *fads2* (Figure 3.1).

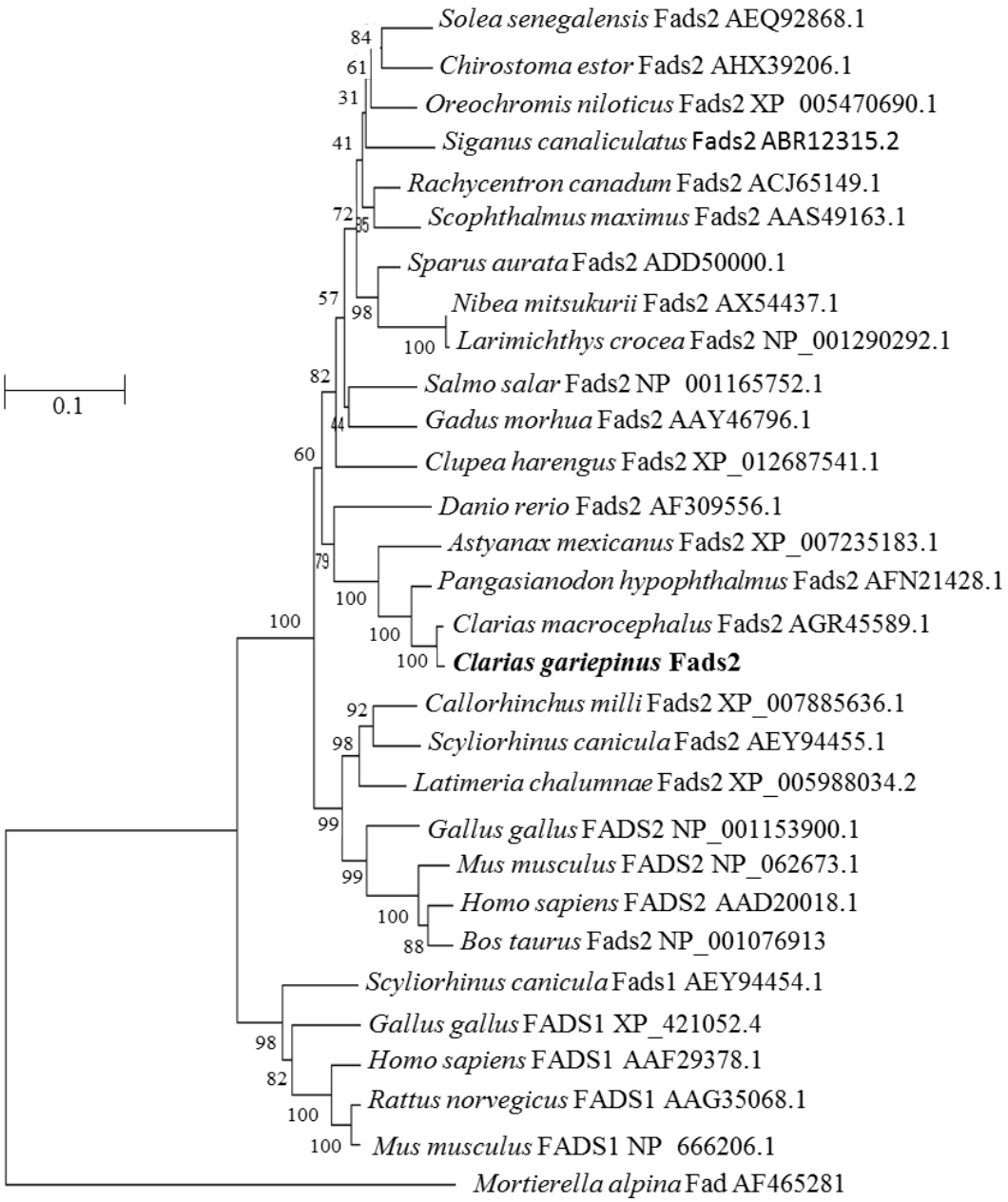

Figure 3.1. Phylogenetic tree comparing the deduced amino acid sequence of *Clarias gariepinus* Fads2 with Fads from a range of vertebrates. The tree was constructed using the neighbour-joining method (Saitou and Nei, 1987) with the MEGA 4.0 software. The numbers represent the frequency (%) with which the tree topology presented was replicated after 1,000 iterations.

The *C. gariepinus* Fads2 clustered most closely with Fads2 from bony fish species (with the exception of the sarcopterygian, *Latimeria chalumnae* which formed a separate

cluster with Fads2 from chondrichthyes (*C. milli and S. canicula*), mammalian (*H. sapiens, M. musculus* and *B.* t*aurus*) and avian species (*G. gallus*) (Figure 3.1).

C. gariepinus Elovl2 sequence was deposited in the GenBank database with the accession number KU902414. The full-length cDNA sequence of *C. gariepinus elovl2* was 1,432 bp (5′ UTR 91 bp, ORF 864 bp, 3′ UTR 477 bp) encoding a protein of 287 aa. Analysis of the deduced aa sequence of *C. gariepinus* Elovl2 revealed characteristic features of fatty acyl elongases such as the highly conserved histidine box (HVYHH, aa 151-155) and the carboxyl-terminal region, but the aa residues at the carboxyl terminus were KHKLQ, more similar to the KXRXX found in Elovl5 than to the KKXX in *H. sapiens* and *S. salar* Elovl2 (Morais et al., 2009). Comparisons of *C. gariepinus* Elovl2 with homologues from *A. mexicanus* (gb|XP_007260136.1|), *S. salar* (gb|ACI62500.1|), *D. rerio* (gb|XP_005162628.1|), *Clupea harengus* (gb|XP_012671565.1|), and *H. sapiens* (gb|NP_060240.3|) showed identities of 81.7, 72.9, 72.7, 69.1 and 64.8 %, respectively. *C. gariepinus* Elovl2 shared 52 % identity with *C. gariepinus* Elovl5. Phylogenetic analysis of the Elovl2 with members of the Elovl family confirmed that the newly cloned elongase was indeed an Elovl2 elongase. Thus, the *C. gariepinus* Elovl2 clustered together with all the Elovl2 and more distantly from Elovl5 sequences including that from *C. gariepinus* (Agaba et al., 2005) and even more distantly to Elovl4 enzymes (Figure 3.2).

.

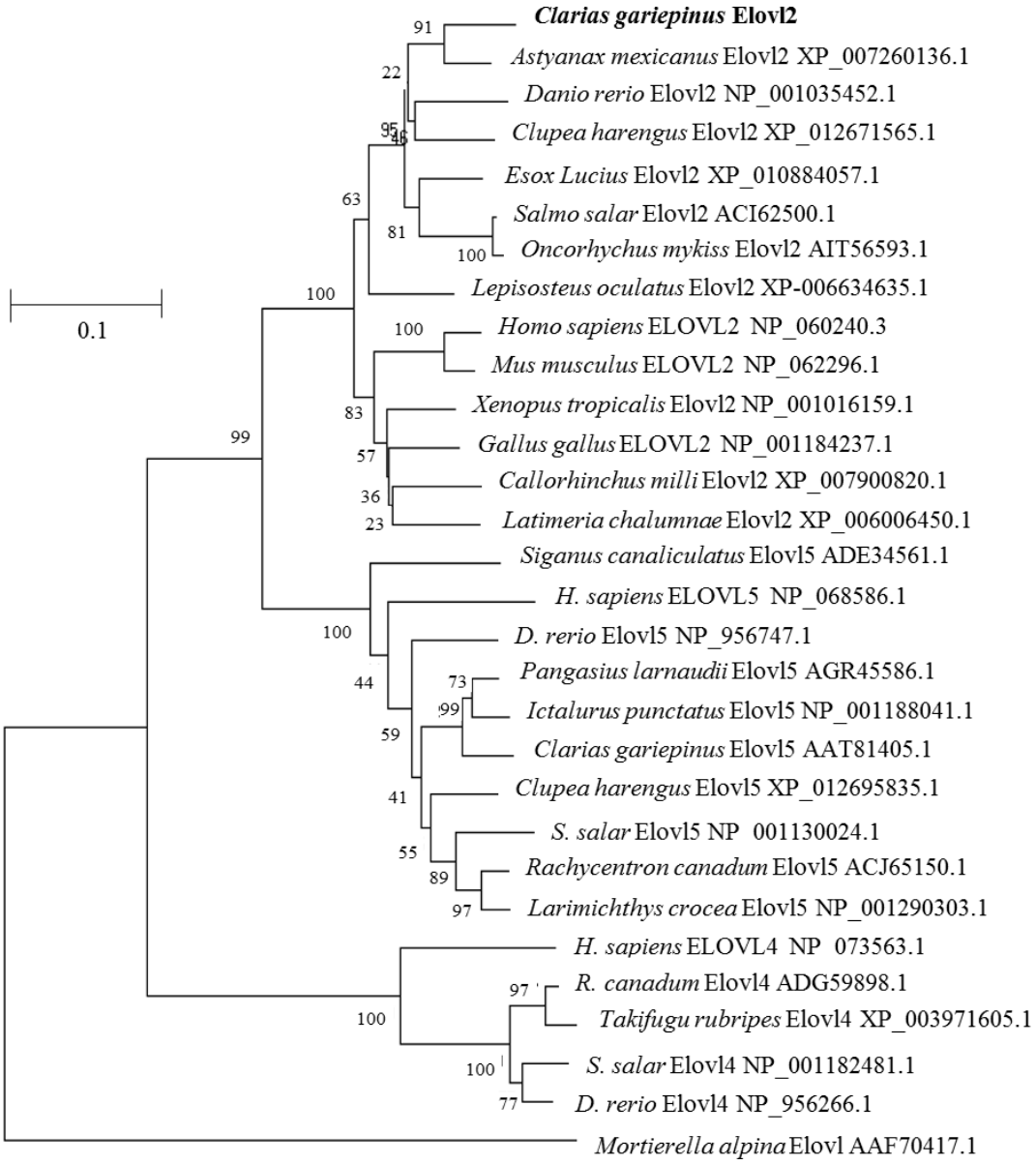

Figure 3.2. Phylogenetic tree comparing the deduced amino acid (aa) sequence of *Clarias gariepinus* Elovl2 with Elovl2, Elovl4 and Elovl5 from a range of vertebrates. The tree was constructed using the neighbour-joining method (Saitou and Nei, 1987) with the MEGA 4.0 software. The numbers represent the frequencies (%) with which the tree topology presented was replicated after 1,000 iterations.

3.3.2 Functional Characterisation of *C. gariepinus* Fads2 and Elovl2 in *S. cerevisiae*

Consistent with previous studies (Hastings et al., 2001), control yeast transformed with the empty pYES2 vector did not show any activity towards any of the PUFA substrates

assayed (data not shown). Functional characterisation by heterologous expression in yeast revealed that the *C. gariepinus* Fads2 had the ability to introduce double bonds at Δ5, Δ6 and Δ8 positions in the appropriate PUFA substrates (Figure 3.3; Table 3.2). The FA composition of the yeast transformed with pYES2-*fads2* showed peaks corresponding to the four main yeast endogenous FA, namely 16:0, 16:1n-7, 18:0 and 18:1n-9, the exogenously added PUFA and the corresponding PUFA product(s) (Figure 3.3; Table 3.2). Thus, the C_{18} PUFA substrates 18:3n-3 and 18:2n-6 were desaturated to 18:4n-3 (42 % conversion) and 18:3n-6 (23 %), respectively, indicating the encoded protein had Δ6 Fads activity (Figure 3.3A; Table 3.2). Moreover, the transgenic yeast was able to desaturate 20:4n-3 and 20:3n-6 to 20:5n-3 (19 %) and 20:4n-6 (14 %), respectively, indicating the *C. gariepinus* Fads2 also had Δ5 activity (Figure 3.3C; Table 3.2), and thus these results confirm that this Fads2 from *C. gariepinus* is a bifunctional Δ6Δ5 Fads. Additionally, the *C. gariepinus* Fads2 showed Δ8 Fads activity as the yeast transformed with pYES2-*fads2* were able to desaturate 20:3n-3 and 20:2n-6 to 20:4n-3 and 20:3n-6, respectively (Figure 3.3B and Table 3.2). No additional peaks were observed when yeast expressing the *C. gariepinus fads2* were grown in the presence of 22:5n-3 and 22:4n-6 (Figure 3.3D; Table 3.2).

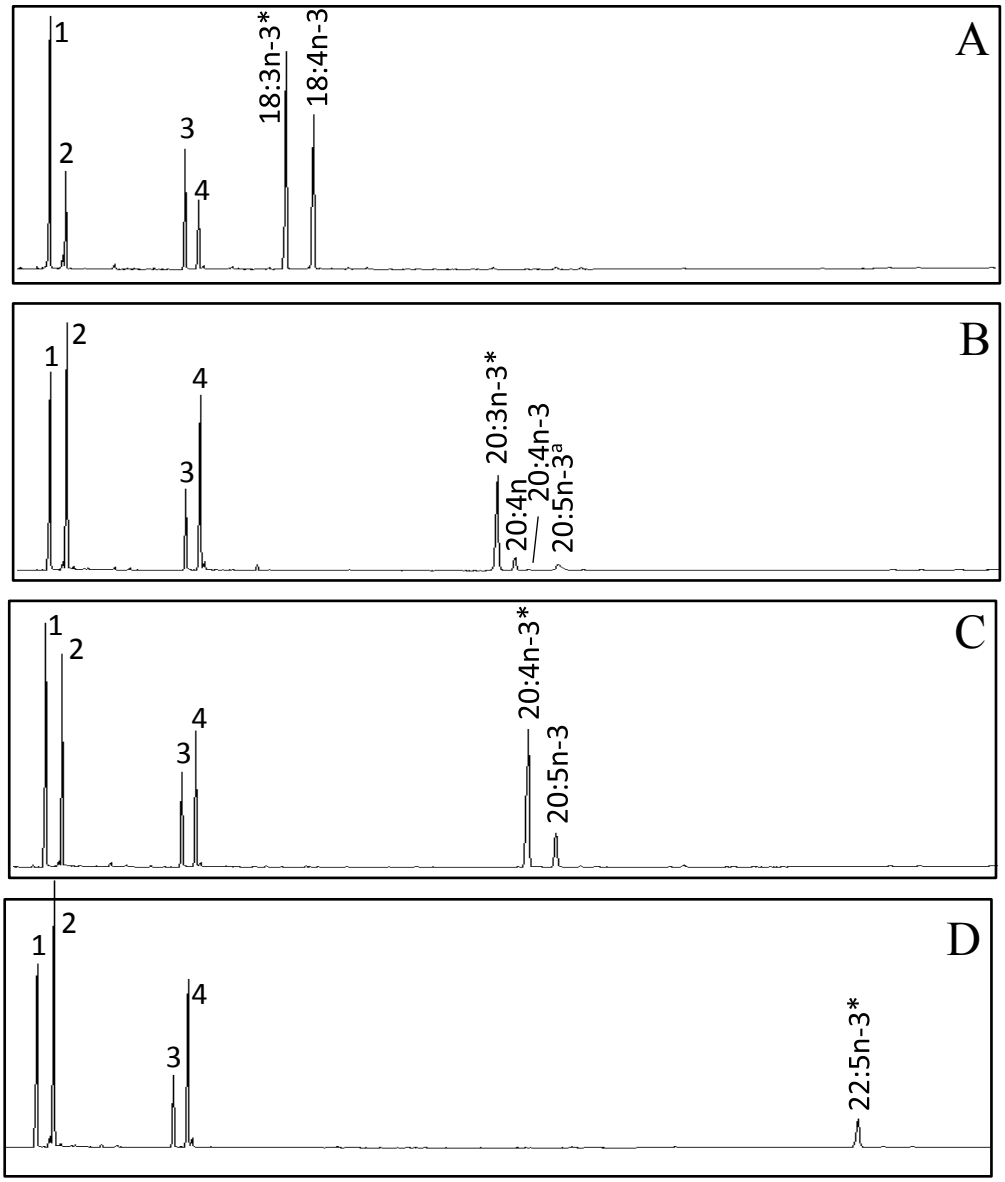

Figure 3.3. Functional characterisation of the newly cloned *Clarias gariepinus* Fads2 in yeast (*Saccharomyces cerevisiae*). The fatty acid (FA) profiles of yeast transformed with pYES2 containing the coding sequence of *fads2* were determined after the yeast were grown in the presence of one of the exogenously added substrates 18:3n-3 (A), 20:3n-3 (B), 20:4n-3 (C) and 22:5n-3 (D). Peaks 1-4 represent the *S. cerevisiae* endogenous FA, namely 16:0 (1), 16:1 isomers (2), 18:0 (3) and 18:1n-9 (4). Additionally, peaks derived from exogenously added substrates (*) or desaturation products are indicated accordingly. The peak indicated as "20:4*" is a non-methylene interrupted FA ($^{\Delta 6,11,14,17}$ 20:4 or $^{\Delta 5,11,14,17}$ 20:4) (panel B).

Table 3.2. Substrate conversions of *Saccharomyces cerevisiae* transformed with *Clarias gariepinus fads2* coding region and grown in the presence of exogenously added substrate (18:3n-3, 18:2n-6, 20:3n-3, 20:2n-6, 20:4n-3, 20:3n-6, 22:5n-3 or 22:4n-6). Conversions were calculated according to the formula [individual product peak area / (all products peak areas + substrate peak area)] × 100.

FA substrate	FA Product	Conversion (%)	Activity
18:3n-3	18:4n-3	42.0	Δ6
18:2n-6	18:3n-6	22.5	Δ6
20:3n-3	20:4n-3	12.9 [a]	Δ8
20:2n-6	20:3n-6	2.5 [a]	Δ8
20:4n-3	20:5n-3	18.7	Δ5
20:3n-6	20:4n-6	13.8	Δ5
22:5n-3	22:6n-3	Nd	Δ4
22:4n-6	22:5n-6	Nd	Δ4

[a] Conversions of Δ8 substrates (20:3n-3 and 20:2n-6) by Fads2 include stepwise reactions due to multifunctional desaturation abilities. Thus, the conversion rates of 20:3n-3 and 20:2n-6 include the Δ8 desaturation toward 20:4n-3 and 20:3n-6, respectively, and their subsequent Δ5 desaturations to 20:5n-3 and 20:4n-6, respectively.
FA, Fatty acid; Nd, not detected.

The *C. gariepinus* Elovl2 showed the ability to elongate C_{18-22} PUFA substrates (Figure 3.4; Table 3.3), with highest conversions towards the C_{20} substrates 20:5n-3 (73.4 %) (Figure 3.4B) and 20:4n-6 (56 %). Conversion of the C_{22} substrate was 36.7 % for 22:5n-3 (Figure 3.4C) and 9.7 % for 22:4n-6 (Table 3.3). Elongations of C_{18} PUFA were generally lower compared to those for C_{20} and C_{22} substrates. Stepwise elongations derived from further activity of the *C. gariepinus* Elovl2 towards products of initial substrate elongation resulted in the production of several polyenes up to 24 carbons (Figure 3.4; Table 3.3).

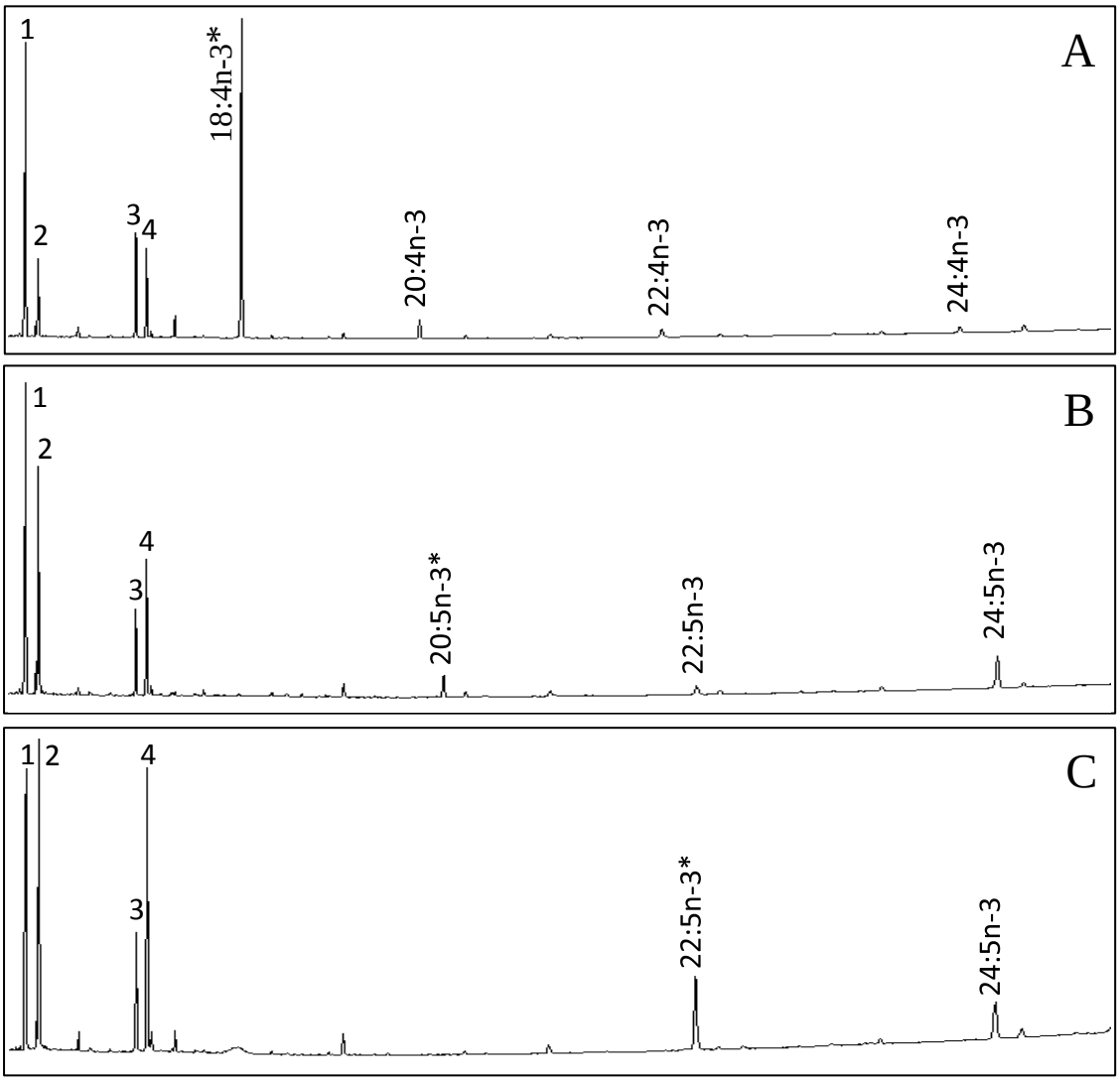

Figure 3.4. Functional characterisation of the newly cloned *Clarias gariepinus* Elovl2 in yeast (*Saccharomyces cerevisiae*). The fatty acid (FA) profiles of yeast transformed with pYES2 containing the coding sequence of *elovl2* were determined after the yeast were grown in the presence of one of the exogenously added substrates 18:3n-3 (A), 18:4n-3 (B), 20:5n-3 (C) and 22:5n-3 (D). Peaks 1-4 represent *S. cerevisiae* endogenous FA namely 16:0 (1), 16:1 (2), 18:0 (3) and 18:1n-9 (4). Additionally, peaks derived from exogenously added substrates (*) or elongation products are indicated accordingly.

Table 3.3. Substrate conversions of *Saccharomyces cerevisiae* transformed with *Clarias gariepinus elovl2* coding region and grown in the presence of exogenously added substrates (18:3n-3, 18:2n-6, 18:4n-3, 18:3n-6, 20:5n-3, 20:4n-6, 22:5n-3 or 22:4n-6). Conversions were calculated for each stepwise elongation according to the formula [peak areas of first products and longer chain products / (peak areas of all products with longer chain than substrate + substrate peak area)] x 100.

Fatty Acid Substrate	Fatty Acid Product	Conversion (%)
18:3n-3	20:3n-3	7.5
18:2n-6	20:2n-6	3.0
18:4n-3	20:4n-3	15.2
18:3n-6	20:3n-6	20.5
20:5n-3	22:5n-3	73.4
20:4n-6	22:4n-6	56.0
22:5n-3	24:5n-3	36.7
22:4n-6	24:4n-6	9.7

3.3.3 Tissue Expression Analysis of *C. gariepinus fads2, elovl2* and *elovl5*

Tissue distribution analysis of *C. gariepinus fads2*, *elovl2* and *elovl5* transcripts confirmed that these genes were expressed in all tissues analysed (Figure 3.5). Liver and brain were found to contain the highest transcript levels of the *C. gariepinus fads2*, followed by pituitary, intestine and kidney. Liver, brain and pituitary were also found to contain the highest transcript levels of the *C. gariepinus elovl2*. Generally, gonads including testis and ovary showed the lowest transcript levels for both *fads2* and *elovl2* (Figure 3.5). Intestine and liver exhibited the highest level of *elovl5*, while the lowest expression levels were found in muscle.

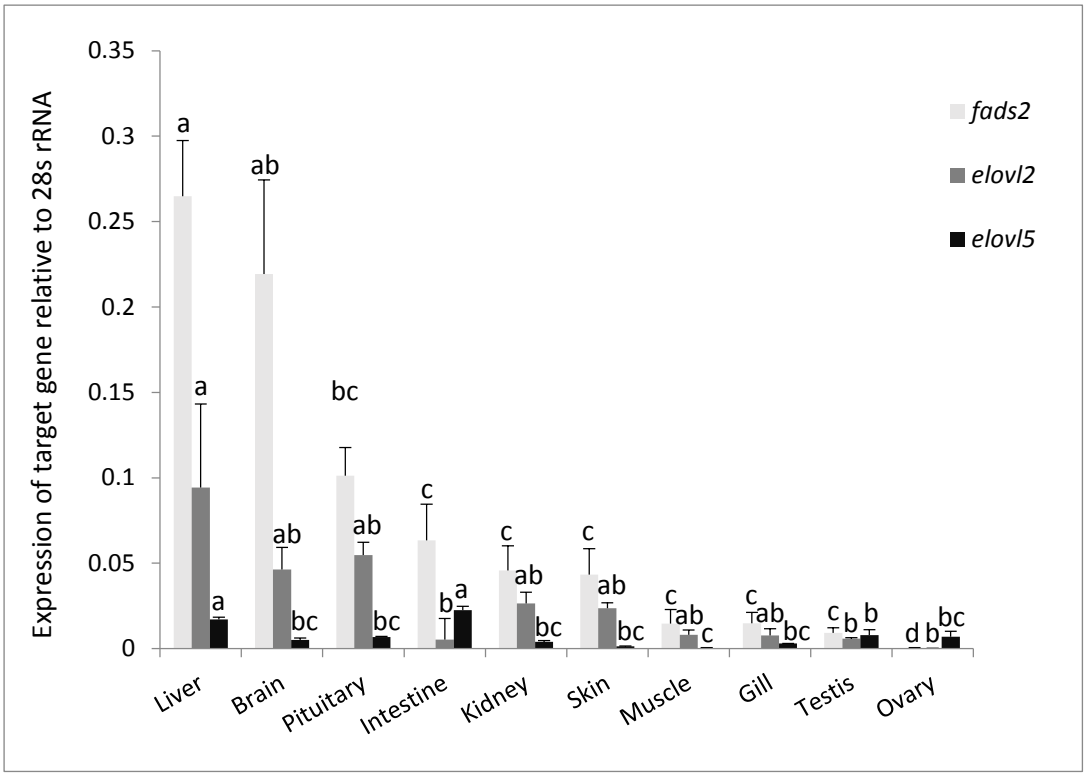

Figure 3.5. Tissue distribution of *fads2*, *elovl2* and *elovl*5 transcripts in *Clarias gariepinus.* Expression levels quantified for each transcript were normalised expression levels of the reference gene (28s rRNA) of the same tissue. The data are reported as mean values with their standard errors (n = 4). Within each target gene, different letters indicate statistically significant differences between expression levels (ANOVA and Tukey's HSD *post hoc* tests).

3.4 Discussion

Elucidating the LC-PUFA biosynthesis pathway in farmed fish is crucial for formulating diets that satisfy physiological requirements and thus ensure normal growth and development. These studies are particularly relevant in the current scenario whereby FO are being replaced by VO in aquafeed, the latter naturally devoid of essential LC-PUFA and thus potentially compromising both health of the fish and nutritional value for human consumers (Monroig et al., 2011b; Tocher and Glencross, 2015). Relevant to the present study, identification and production of fish that can efficiently utilise VO-based diets due to their high capacity for LC-PUFA biosynthesis is a valid strategy to expand aquaculture

considering that marine ingredients (FO and FM) will be increasingly limited in the future (Tocher, 2015). *C. gariepinus* feed and grow well on a variety of feed ingredients and are, therefore, a good model for studying the endogenous capacity for LC-PUFA synthesis of freshwater fish.

Phylogenetic analysis of the *fads*-like desaturase cDNA isolated from *C. gariepinus*, together with the possession of all the main structural features common to the Fads2 protein family confirmed it to be a Fads2. Sequence and phylogenetic analysis also showed that the *C. gariepinus* Fads2 shared highest aa sequence similarities with other catfish species, with relatively low scores when compared with Fads from more distantly related fish lineages (Betancur-R et al., 2013). Nevertheless, recent advances in functional analysis of fish Fads have concluded that some Fads2 have acquired novel functions (subfunctionalisation) during evolution and thus phylogeny of fish Fads2 does not necessarily correlate with their functionalities (Castro et al., 2016). The herein reported functions of the *C. gariepinus* Fads2 further confirm such a conclusion.

Functional characterisation demonstrated that the *C. gariepinus* Fads2 is a bifunctional Δ6Δ5 desaturase able to operate towards a range of substrates including n-3 (18:3n-3 and 20:4n-3) and n-6 (18:2n-6 and 20:3n-6) PUFA. Similar substrate specificities were previously described in *D. rerio*, which represented the first ever report of dual Δ6Δ5 functionality in a vertebrate Fads (Hastings et al., 2001). More recent studies have now shown that bifunctionality appear to be a more common feature of fish Fads2 than originally thought. Thus dual Δ6Δ5 Fads have been described in *S. canaliculatus* (Li et al., 2010), Nile tilapia (*Oreochromis niloticus*) (Tanomman et al., 2013) and *C. estor* (Fonseca-Madrigal et al., 2014). Interestingly, fish Fads2 with Δ4 capability reported in *S. canaliculatus* (Li et al., 2010), *S. senegalensis* (Morais et al., 2012) and *C. striata* (Kuah et al., 2015) showed as well some minor Δ5 activity and can thus be regarded as

dual Δ5Δ4 Fads (Castro et al., 2016). In contrast, other teleost Fads2 are single function Δ6 desaturases (González-Rovira et al., 2009; Mohd-Yusof et al., 2010; Monroig et al., 2013a; Zheng et al., 2009), in agreement with Fads activities reported in mammalian FADS2 (Castro et al., 2016). Such substrate plasticity exhibited amongst fish Fads2 is believed to be the result of a combination of multiple evolutionary drivers including habitat, trophic level and ecology underlying the specific phylogenetic position of each fish species (Castro et al., 2016, 2012; Li et al., 2010; Monroig et al., 2011b). In contrast, Fads1, another "front-end" Fads encoding a Δ5 Fads in mammals (Castro et al., 2016, 2012), appears to have been lost during evolution of teleost and is absent in the vast majority of farmed fish species (Castro et al., 2016).

The *C. gariepinus* Fads2 also exhibited Δ8 desaturation capability, an intrinsic feature of vertebrate Fads2 (Monroig et al., 2011a; Park et al., 2009). Although conversions in yeast might quantitatively vary from those occurring *in vivo*, it appeared that the *C. gariepinus* Fads2 had lower efficiency as Δ8 Fads than as Δ6 Fads, in agreement with the "Δ8 pathway" being regarded as a minor pathway compared to the more prominent Δ6 desaturation pathway (Monroig et al., 2011a; Park et al., 2009). Interestingly, the Δ8 desaturation capabilities of *C. gariepinus* Fads2 towards 20:3n-3 (12.9 %) was relatively high leading to lower Δ6Δ8 ratio (3.26), a parameter used to compare Δ8 desaturation capability among fish Fads2 enzymes (Monroig et al., 2011a). Thus, the Δ6/Δ8 ratio of *C. gariepinus* Fads2 is more similar to that of marine species like gilthead seabream (*Sparus aurata*) (2.7) and turbot (*Psetta maxima*) (4.2). Whereas it is notably lower than those of freshwater or salmonid Fads2 including *D. rerio* (22.4) and *S. salar* (12 and 14.7 for Fad_b and Fad_c, respectively) (Monroig et al., 2011a). These results suggest that the Δ8 pathway, while possibly not to such an extent as the Δ6 pathway, can still contribute to the initial steps of LC-PUFA biosynthesis in *C. gariepinus*. Note that Δ8 activity

introduces the same double bond as Δ6 activity, after elongation rather than before, and so a Fads having Δ6Δ8 activity is not regarded as "bifunctional".

The ability of the *C. gariepinus* Fads2 to desaturate a range of Δ5, Δ6 and Δ8 Fads substrates from both n-3 and n-6 series clearly shows it is a multifunctional enzyme. This is emphasised by the stepwise desaturation reactions that occurred when transgenic yeast expressing the *C. gariepinus* Fads2 were grown in the presence of certain FA substrates such as 20:3n-3 and 20:2n-6. *C. gariepinus* Fads2 enzyme activity toward 20:3n-3 led to the production of either 20:4n-3 (Δ8 desaturation) that was subsequently desaturated to 20:5n-3 (Δ5 desaturation), or the non-methylene interrupted (NMI) FA products $^{\Delta5,11,14,17}$20:4 or $^{\Delta6,11,14,17}$20:4 resulting from direct Δ5 or Δ6 desaturation, respectively. While the biological significance of these pathways is difficult to determine, particularly for NMI FA biosynthesis, the results further confirm that all the Fads capabilities (Δ5, Δ6 and Δ8) are present in the characterised Fads2. NMI fatty acids are principal constituents of plasmalogens and may play structural and protective roles in cell membrane (Monroig et al., 2013b; Kraffe et al., 2004; Barnathan, 2009). In marine invertebrates, NMI fatty acids are thought to confer resistance in tissues exposed most often to environmental physicochemical variations or to attack by microbial lipases (Kraffe et al., 2004).

Moreover, we can further confirm that all the elongase activities required in the LC-PUFA biosynthesis pathways also exist in *C. gariepinus*. Agaba et al. (2005) characterised an Elovl5 from *C. gariepinus* that, like the vast majority of fish Elovl5 investigated to date, showed C_{18} and C_{20} PUFA as preferred substrates, with markedly lower affinity towards C_{22} substrates (Castro et al., 2016). In contrast, the *C. gariepinus* Elovl2 showed higher elongation efficiencies towards C_{20} and C_{22} PUFA compared to C_{18} substrates. Generally, these results are consistent with the activities shown by the only

three fish Elovl2 enzymes characterised to date, i.e. *S. salar*, *D. rerio* and *O. mykiss* (Gregory and James, 2014; Monroig et al., 2009; Morais et al., 2009). Although, similar to the human orthologue, the latter did not show any activity on C_{18} FA substrates (Leonard et al., 2002). The presence of Elovl2 and particularly its ability to elongate C_{22} PUFA to a greater extent compared to Elovl5 elongases has been acknowledged as evidence supporting LC-PUFA biosynthetic capability in freshwater species and salmonids (Morais et al., 2009). The plethora of genomic and transcriptomic sequences currently available from a varied range of fish species and lineages strongly suggests that, rather than the habitat (freshwater *versus* marine) of fish, it is the phylogeny of each species that actually correlates with the presence or absence of Elovl2 within their genomes. Here we show that marine species such as the Atlantic herring *Clupea harengus* (Figure 3.2) possess a putative Elovl2, whereas freshwater species including *O. niloticus* or medaka (*O. latipes*) appear to have lost Elovl2 from their genomes.

The functions of the herein reported Fads2 and Elovl2, together with the previously characterised Elovl5 (Agaba et al., 2005), allow us to predict the biosynthetic pathways of LC-PUFA in *C. gariepinus.* Thus, the dual Δ6Δ5 Fads2 catalyses the initial desaturation of 18:3n-3 and 18:2n-6 (Δ6 desaturation), as well as the desaturation of 20:4n-3 and 20:3n-6 (Δ5 desaturation) as shown in Figure 1.3. Although we cannot confirm whether the *C. gariepinus* Fads2 can desaturate 24:5n-3 and 24:4n-6 (Δ6 desaturation) required to synthesise 22:6n-3 and 22:5n-6, respectively, through the so-called "Sprecher pathway" (Sprecher, 2000). Such ability of vertebrate Fads2 has been demonstrated in *O. mykiss*, *S. salar* and *D. rerio* (Bell and Tocher, 2009; Buzzi et al., 1996; Tocher et al., 2003). Further studies will aim to elucidate whether the newly cloned Fads2 or other Fads potentially co-existing in the *C. gariepinus* genome, have the ability to desaturate C_{24} PUFA in position Δ6. The Elovl2 was able to catalyse the elongation of

C_{18} (18:3n-3, 18:2n-6, 18:4n-3 and 18:3n-6), C_{20} (20:5n-3 and 20:4n-6) and C_{22} (22:5n-3 and 22:4n-6) PUFA. Its activity towards C_{18} PUFA was however very low compared to activity towards C_{20} and C_{22} PUFA. This, together with the activity of Elovl5, which is high towards C_{18} and C_{20} PUFA (Agaba et al., 2005), confirm that the activities required to catalyse all the elongation steps required for LC-PUFA synthesis are present in *C. gariepinus.*

Expression analysis showed *fads2*, *elovl2* and *elovl5* were expressed in all tissues analysed. Consistent with the vast majority of freshwater species studied, the tissue distribution patterns of *C. gariepinus fads2* and *elovl2* mRNAs showed liver as a major metabolic site for LC-PUFA biosynthesis. In contrast, marine fish species typically have brain as the tissue with highest expression levels of LC-PUFA biosynthesis genes, with production of DHA from EPA in brain being hypothesised as driving the retention of at least part of the LC-PUFA biosynthetic pathway in species with high inputs of dietary LC-PUFA (Monroig et al., 2011b). An exception to this pattern is represented by the Nile tilapia *fads2*, with highest expression in the brain (Tanomman et al., 2013). *C. gariepinus fads2* expression in liver was approximately four-fold greater than in intestine, in contrast to salmonid *fads2* that have been reported to be most highly expressed in intestine (Zheng et al., 2005). The expression of *elovl5* was also high in liver but was highest in the intestine.

In conclusion, we have successfully cloned and characterised *fads2* and *elovl2* genes that encode enzymes with a broad range of substrate specificities from *C. gariepinus*. These two enzymes, and the previously reported Elovl5, enable the African catfish *C. gariepinus* to carry out all the desaturation and elongation reactions required for endogenous LC-PUFA synthesis from C_{18} precursors, namely ALA and LA. These

results strongly suggest that *C. gariepinus* has the ability to effectively utilise VO rich in C_{18} PUFA to satisfy essential LC-PUFA requirements

CHAPTER 4.

ELONGATION OF VERY LONG-CHAIN (> C_{24}) FATTY ACIDS IN CLARIAS GARIEPINUS: CLONING, FUNCTIONAL CHARACTERISATION AND TISSUE EXPRESSION OF ELOVL4 ELONGASES

4.1 Introduction

Elongation of very long-chain fatty acid (Elovl) proteins catalyse the condensation reaction, regarded as the first and rate-limiting step of four sequential reactions required for the elongation of fatty acids (FA) (Guillou et al., 2010; Jakobsson et al., 2006). Seven members (Elovl 1-7) with similar motifs make up the Elovl protein family in vertebrates, although only Elovl2, Elovl4 and Elovl5 have been proven to have polyunsaturated fatty acids (PUFA) as substrates for elongation (Guillou et al., 2010; Jakobsson et al., 2006). Importantly, the complement of Elovl, along with that of fatty acyl desaturases (Fads), determines the ability of species to biosynthesise physiologically essential fatty acids (EFA) such as eicosapentaenoic acid (EPA, 20:5n-3), arachidonic acid (ARA, 20:4n-6) and docosahexaenoic acid (DHA, 22:6n-3) (Bell and Tocher, 2009). Fish have arguably been the group of organisms in which the most comprehensive characterisation of Elovl gene repertoire and function has been conducted, particularly farmed species (Castro et al., 2016). These studies have shown that Elovl5 elongates predominantly C_{18} and C_{20} PUFA, whilst Elovl2 preferentially elongates C_{20} and C_{22} PUFA (Castro et al., 2016), thus denoting somewhat overlapping functionalities that are likely to derive from a common evolutionary origin (Monroig et al., 2016b). However, the substrate specificities of Elovl4 proteins from vertebrates including fish have remained more elusive (Castro et al., 2016).

Cloning and functional characterisation of a teleost Elovl4 was first carried out in zebrafish *D. rerio* (Monroig et al., 2010a). It was shown that two Elovl4 genes, termed Elovl4a and Elovl4b, were present, in contrast to mammals in which only a single Elovl4 had been reported (Agbaga et al., 2008). Interestingly, both *D. rerio* Elovl4s showed the ability to elongate saturated FA, but only Elovl4b appeared to have a role in the biosynthesis of very long-chain (> C_{24}) polyunsaturated fatty acids (VLC-PUFA)

(Monroig et al., 2010a). Since this pioneer study in fish, further *elovl4* cDNA sequences have been studied in a variety of species including Atlantic salmon, Nibe croaker, orange-spotted grouper and rabbitfish (Carmona-Antoñanzas et al., 2011; Kabeya et al., 2015; Li et al., 2015; Monroig et al., 2012). Interestingly, with the exception of the zebrafish *elovl4a* (Monroig et al., 2010a), all *elovl4* cDNA cloned from other teleost fish species have been confirmed to be orthologues of the zebrafish *elovl4b*, although *in silico* searches indicated that virtually all teleosts possess at least one copy of both *elovl4a* and *elovl4b* (Castro et al., 2016). Recently, two further elongases termed *elovl4c-1* and *elovl4c-2* were identified from the Atlantic cod, *Gadus morhua*, although their functionalities remain to be elucidated (Xue et al., 2014). In addition to the differences in substrate specificities, further evidence suggesting that Elovl4a and Elovl4b participate in different biological processes was provided by tissue expression patterns suggesting *elovl4a* was highly expressed in brain, whereas *elovl4b* was highly expressed in eye (retina) and gonads (Monroig et al., 2010a; Xue et al., 2014). These results were consistent with studies on mammals indicating that these tissues are important sites for very long-chain FA biosynthesis. Thus, very long-chain (> C_{24}) saturated fatty acids (VLC-SFA) have been shown to play key roles in skin permeability barrier formation and thus essential for neonatal survival (Cameron et al., 2007; Uchida and Holleran, 2008; Vasireddy et al., 2007), whereas VLC-PUFA are essential in phototransduction and male fertility (Agbaga et al., 2010; Guillou et al., 2010; McMahon and Kedzierski, 2010; Zadravec et al., 2011).

An interesting trait that apparently differentiates fish Elovl4 from non-fish vertebrate Elovl4 orthologues is the ability of the former to catalyse the elongation of C_{22} PUFA substrates to C_{24} products. In particular, all fish Elovl4b characterised to date have shown the ability to efficiently elongate 22:5n-3 to 24:5n-3, a critical enzymatic step in the

biosynthesis of DHA through the Sprecher pathway (Sprecher, 2000). The acquisition or retention of such an ability by some fish Elovl4 has been hypothesised to compensate the loss of *elovl2* during the evolution history of some teleost lineages encompassing the vast majority of farmed marine fish species (Li et al., 2015; Monroig et al., 2012, 2011c, 2010a; Wang et al., 2015). Indeed, the apparent absence of *elovl2*, along with that of key desaturation activities, has been regarded as molecular evidence accounting for the low capacity of marine fish species to biosynthesise EPA, ARA and DHA (Morais et al., 2009).

Our overall aim is to elucidate the repertoire and function of genes encoding *elovl* and *fads* enzymes involved in the biosynthesis of LC-PUFA in the African catfish, *Clarias gariepinus*, a commercially important species in Sub-Saharan African aquaculture (FAO, 2016). *C. gariepinus* are freshwater fish with a variety of characteristics that makes them ideal for fish farming. African catfish *C. gariepinus* is a fast-growing species, can be cultured at high densities and tolerates poor water quality due to the possession of accessory air-breathing organs (De Graaf and Janssen, 1996; Pouomogne, 2010). *C. gariepinus* is an omnivorous fish and, while in the wild they feed on insects, crustaceans, worms, gastropods, fishes and plants, they accept a wide range of feed ingredients in captivity (Pouomogne, 2010). With regards to PUFA biosynthesising enzymes, Agaba et al. (2005) characterised an Elovl5 from *C. gariepinus* that was primarily active towards C_{18-20} PUFA substrates. More recently, we successfully isolated and functionally characterised an Elovl2 elongase with preference towards C_{20-22} PUFA substrates, as well as a Fads2 desaturase with dual Δ6Δ5 activity (Chapter 3). In the present study, we characterised, both molecularly and functionally, two *elovl4* cDNA from *C. gariepinus* and investigated their tissue expression patterns.

4.2 Materials and Methods

4.2.1 Sample Collection and RNA Preparation

Tissue samples used in this study were obtained from eight adult *C. gariepinus* specimens (~1.8 kg) and preserved as described in Section 3.2.1. The *C. gariepinus* were raised in the tropical aquarium of the Institute of Aquaculture, University of Stirling, UK, on standard salmonid diets. Total RNA extraction and first strand complementary DNA (cDNA) synthesis is also as described in Section 3.2.1.

4.2.2 Molecular Cloning of Elovl4 cDNA

Amplification of partial fragments of the genes was achieved by polymerase chain reaction (PCR) using a mixture of cDNA from eye and brain as template. For amplification of the first fragment of the *C. gariepinus elovl4a*, the primers UniE4aF (5'-CTCTTCCTCTGGCTGGGG-3') and UniE4aR (5'-TATGTCTGGTAGTAGAAGTTCC-3') were designed on conserved regions after alignment (BioEdit v7.0.9, Tom Hall, Department of Microbiology, North Carolina State University, USA) of *elovl4a*-like sequences from *D. rerio* (gb|NM_200796.1|), *G. morhua* (KF964008.1), *Takifugu rubripes* (gb|XM_003965960.1|) and *I. punctatus* (gb|JT417431.1|). Similarly, *elovl4b* homologous sequences from *Siganus canaliculatus* (gb|JF320823.1|), *Rachycentron canadum* (gb|HM026361.1|), *Salmo salar* (gb|NM_001195552.1|) and *I. punctatus* (gb|JT405661.1|) were aligned to design primers UniE4bF (5'-TAGCAGACAAGCGGGTGG-3') and UniE4bR (5'-CAAAGAGGATGATGAAGGTGA-3') used for the amplification of the first fragment of *C. gariepinus elovl4b*. PCR conditions consisted of an initial denaturation step at 95 °C for 2 min, followed by 35 cycles of denaturation at 95 °C for 30 s, annealing at 55 °C for 30 s, extension at 72 °C for 55 s, followed by a final extension at 72 °C for 7 min.

PCR fragments were purified using the Illustra GFX PCR DNA/gel band purification kit (GE Healthcare, UK), and sequenced at GATC Biotech Ltd (Germany).

Gene-specific primers were designed to obtain full-length cDNA by 5' and 3' Rapid Amplification of cDNA Ends (RACE) PCR (FirstChoice® RLM-RACE RNA ligase mediated RACE kit, Ambion®, Life Technologies™, USA). Positive RACE PCR products were identified by sequencing (GATC Biotech Ltd). The full nucleotide sequences of both *elovl4* cDNA sequences were obtained by aligning sequences of the first fragments, together with those of the 5' and 3' RACE PCR positive products (BioEdit). All primers used in RACE PCR are listed in Table 4.1.

4.2.3 Sequence and Phylogenetic Analysis

The deduced amino acid (aa) sequences of both *C. gariepinus elovl4* cDNA sequences were compared to corresponding orthologues from other vertebrate species by calculating the identity scores using the EMBOSS Needle Pairwise Sequence Alignment tool (http://www.ebi.ac.uk/Tools/psa/emboss_needle/). Phylogenetic analysis of the deduced aa sequences of the Elovl4 proteins from *C. gariepinus* and Elovl from a variety of vertebrate species was performed by constructing a tree using the neighbor-joining method (Saitou and Nei, 1987) with MEGA 6.0 software (www.megasoftware.net). Confidence in the resulting tree branch topology was measured by bootstrapping through 1,000 iterations.

4.2.4 Functional Characterisation of *C. gariepinus* Elovl4a and Elovl4b by Heterologous Expression in *Saccharomyces cerevisiae*

PCR fragments corresponding to the open reading frame (ORF) of *C. gariepinus* newly cloned *elovl4* cDNA were amplified from a mixture of cDNA synthesised from eye and brain RNA, using the high fidelity *Pfu* DNA polymerase (Promega, USA) with primers containing *Bam*HI (forward) and *Xho*I (reverse) restriction sites (Table 4.1). PCR

conditions consisted of an initial denaturation at 95 °C for 2 min, followed by 32 cycles of denaturation at 95 °C for 30 s, annealing at 55 °C for 30 s, extension at 72 °C for 2 min followed by a final extension at 72 °C for 7 min. The DNA fragments obtained were purified, digested with the appropriate restriction enzymes (New England Biolabs, UK), and ligated into the similarly digested pYES2 expression vector (Invitrogen, UK) to produce the plasmid constructs pYES2-*elovl4a* and pYES2-*elovl4b*.

Yeast competent cells InvSc1 (Invitrogen) were transformed with pYES2-*elovl4a* and pYES2-*elovl4b* using the S.c. EasyComp^{TM} Transformation Kit (Invitrogen). Selection of yeast containing the pYES2 constructs was done on *S. cerevisiae* minimal medium minus uracil (SCMM^{-ura}) plates. One single yeast colony was grown in SCMM^{-ura} broth for 2 days at 30 °C, and subsequently subcultured in individual Erlenmeyer flasks until optical density measured at a wavelength of 600 nm (OD_{600}) reached 1, after which galactose (2 %, w/v) and a PUFA substrate at a final concentration of 0.6 mM (C_{18}), 1.0 mM (C_{20}) and 1.2 mM (C_{22}) were added. The FA substrates included stearidonic acid (18:4n-3), gamma-linolenic acid (18:3n-6), EPA (20:5n-3), ARA (20:4n-6), docosapentaenoic acid (22:5n-3), docosatetraenoic acid (22:4n-6) and DHA (22:6n-3). In addition to exogenously added PUFA substrates, some Elovl4 have been shown to elongate saturated FA (Monroig et al., 2010a). Consequently, the ability of *C. gariepinus* Elovl4 enzymes to elongate yeast endogenous saturated FA was investigated. For that purpose, the saturated FA profiles of yeast transformed with empty pYES2 vector and those of yeast transformed with either pYES2-*elovl4a* or pYES2-*elovl4b* were compared after growing the yeast without addition of any substrate. After 2 days, yeast were harvested, washed twice with doubled distilled water and freeze-dried until further analysis.

Table 4.1. Sequences of primers used for molecular cloning of full-length cDNA and tissue expression analysis (qPCR) of *Clarias gariepinus elovl4a* and *elovl4b*. Restriction sites for *Bam*HI (forward) and *Xho*I (reverse) are underlined.

Name	Direction	Sequence
Initial cDNA cloning		
UniE4aF	Forward	5'-CTCTTCCTCTGGCTGGGG -3'
UniE4aR	Reverse	5'-TATGTCTGGTAGTAGAAGTTCC-3'
UniE4bF	Forward	5'-TAGCAGACAAGCGGGTGG-3'
UniE4bR	Reverse	5'-CAAAGAGGATGATGAAGGTGA-3'
5' RACE		
CGRE4aR3	Reverse	5'-GCAAGGAAGAGCTCTTTGAAG-3'
CGRE4aR2	Reverse	5'-ACAATTAGGGTCTTCCTGAGCT-3'
CGRE4bR3	Reverse	5'-GCAGCACCATGCTGAAGT-3'
CGRE4bR2	Reverse	5'-TGAAAGCGTCTCGGTGCT-3'
3' RACE		
CGRE4aF1	Forward	5'-TCATTGTCCTCTTTGGGAACT-3'
CGRE4aF2	Forward	5'-GCACTGGTGTCTGATTGGTTAT-3'
CGRE4bF2	Forward	5'-CTCACTCGCTGTACTCCGG-3'
CGRE4bF3	Forward	5'-CCAGTTCCATGTCACAATCG-3'
ORF cloning		
CGE4aVF	Forward	5'-CCCGGATCCAAGATGGATATTGTAACAC-3'
CGE4aVR	Reverse	5'-CCGCTCGAGCTAGTCCCGCTTTGCCCTGCC-3'
CGE4bVF	Forward	5'-CCCGGATCCAACATGGAAACGGTGCTTC-3'
CGE4bVR	Reverse	5'-CCGCTCGAGTCACTCCCTCTTTGTTCGTTCC-3'
qPCR		
CGqE4aF1	Forward	5'-GAGATGCAGAAGCAGGCATA-3'
CGqE4aR1	Reverse	5'-TTGAGCCTCCTCCAAACAGT-3'
CGqE4bF1	Forward	5'-GAGGAACGCACTGGGAACT-3'
CGqE4bR1	Reverse	5'-AAACGCCATCTATCCCATTG-3'
28SrRNAF1	Forward	5'-GTCCTTCTGATGGAGGCTCA-3'
28SrRNAR1	Reverse	5'-CGTGCCGGTATTTAGCCTTA-3'

4.2.5 Fatty Acid Analysis of Yeast

Total lipids extracted from freeze-dried samples of yeast (Folch et al., 1957) were used to prepare fatty acid methyl esters (FAME) as described in detail previously (Section 3.2.5). Identification of the peaks was carried out as described by Li et al. (2015). Briefly, FAME were identified and quantified after splitless injection and run in temperature

programming, in an Agilent 6850 gas chromatograph system, equipped with a Sapiens-5MS (30 m x 0.25 µm x 0.25 µm) capillary column (Teknokroma, Spain) coupled to a 5975 series mass spectrometer detector (Agilent Technologies, USA). The elongation of endogenous saturated FA was assessed by comparison of the areas of the FA of control yeast with those of yeast transformed with either pYES2-*elovl4a* or pYES2-*elovl4b*. As described in detail by Li et al. (2015), the elongation conversions of exogenously added PUFA substrates (18:4n-3, 18:3n-6, 18:4n-3, 20:5n-3, 20:4n-6, 22:5n-3 and 22:6n-3) were calculated by the step-wise proportion of substrate FA converted to elongated product as [areas of first product and longer chain products/(areas of all products with longer chain than substrate + substrate area)] x 100.

4.2.6 Gene Expression Analysis

Expression of the newly cloned *C. gariepinus elovl4* cDNAs was measured by quantitative real-time PCR (qPCR). RNA extraction from *C. gariepinus* tissues (four male and four females) and cDNA synthesis were carried out as described above (Section 4.2.1). PCR amplicons of each gene cloned into PCR 2.1 vector (TA cloning® kit, Invitrogen, Life Technologies™, USA) were linearised, quantified and serial-diluted to generate a standard curve of known copy numbers for quantification. All qPCR amplifications were carried out in duplicate using Biometra Thermocycler (Analytik Jena Company, Germany) and Luminaris Color Higreen qPCR master mix (Thermo Scientific, Carlsbad, CA, USA) following the manufacturer's instructions. The qPCR conditions, confirmation of qPCR products and calculation of absolute copy number of target and reference gene in each sample were performed as described in Section 3.2.6. Primers used for qPCR analysis are presented in Table 4.1.

4.2.7 Statistical Analysis

Tissue expression (qPCR) results were expressed as mean normalised ratios (n = 4) (± SE) corresponding to the ratio between the copy numbers of the target genes (*elovl4a* and *elovl4b*) and the copy numbers of the reference gene, 28S rRNA. Differences in gene expression among tissues were analysed by one-way analysis of variance (ANOVA) followed by Tukey's HSD test at a significance level of $P \leq 0.05$ (IBM SPSS Statistics 21, USA).

4.3 Results

4.3.1 Elovl4 Sequence and Phylogenetic Analysis

The sequence and phylogenetic analysis revealed that *C. gariepinus* possesses two *elovl4* cDNAs with homology to the *D. rerio* Elovl4 proteins (Monroig et al., 2010a) and, for consistency, were termed as *elovl4a* and *elovl4b*. The full-length of the *C. gariepinus elovl4a* cDNA consisted of 1,403 bp that contained an ORF of 945 bp encoding a putative protein of 314 aa. Whereas the full-length of the *C. gariepinus elovl4b* was 1,181 bp, with a 915 bp ORF encoding a putative protein of 304 aa. Both cDNA sequences have been deposited with the GenBank database under the accession number KY801284 (*elovl4a*) and KY801285 (*elovl4b*).

Phylogenetic analysis showed that *C. gariepinus* Elovl4 proteins grouped together with orthologues from a variety of vertebrates, with Elovl2 and Elovl5 sequences clustering separately (Figure 4.1). Within the teleost Elovl4, two distinct clusters containing each of the two Elovl4 from *C. gariepinus* could be identified. In one cluster, the *C. gariepinus* Elovl4a grouped closely with Elovl4a-like sequences from *D. rerio* (gb|NP_957090.1|), *G. morhua* (gb|AIG21330.1|), *C. harengus* (gb|XP_012692914.1|), *Oreochromis niloticus* (gb|XP_003443720.1|) and *T. rubripes* (gb|XP_003966009.1|). In the other, the *C. gariepinus* Elovl4b grouped with Elovl4b-like sequences from *D. rerio*

(gb|NP_956266.1|), *N. mitsukuri* (gb|AJD80650.1|), *R. canadum* (ADG59898.1) and *G. morhua* (gb|AIG213329.1|). These results confirmed that the newly cloned *elovl* cDNA from *C. gariepinus* encoded Elovl4a and Elovl4b proteins. Interestingly, the two so-called "Elovl4c" previously reported in *G. morhua* (Xue et al., 2014), grouped separately from all vertebrate Elovl4 (Figure 4.1).

Sequence analysis of the *C. gariepinus* putative Elovl4a and Elovl4b proteins showed that both possessed all the characteristic features of Elovl family members including a single histidine dideoxy binding motif HXXHH, the putative endoplasmic reticulum (ER) retrieval signal with an arginine (R) and lysine (K) residue at the carboxyl terminus, RXKXX) and multiple regions containing similar motifs such as (i) KXXEXXDT, (ii) QXXFLHXXHH, (iii) NXXXHXXMYXYY, (iv) TXXQXXQ (Figure 4.2) (Agaba et al., 2005; Jakobsson et al., 2006). The deduced aa sequences from the *C. gariepinus* Elovl4a and Elovl4b were 70.7 % similar to each other. Comparing the aa sequences of *C. gariepinus* Elovl4 deduced proteins with other fish Elovl4 sequences revealed that Elovl4a shared highest identities with *Clupea harengus* (gb|XP_012692914.1|) (87.0 %) and *D. rerio* Elovl4a (85.7 %), whereas *C. gariepinus* Elovl4b shared highest identities with *D. rerio* Elovl4b (83.6 %) and *Nibea mitsukuri* Elovl4 (gb|AJD80650.1|) (81.0 %). The aa sequence of *C. gariepinus* Elovl4a shared 41.5 % and 38.0 %, respectively, with previously described *C. gariepinus* Elovl5 and Elovl2 elongases, while identity scores of 43 % and 40.8 %, respectively, were obtained for Elovl4b

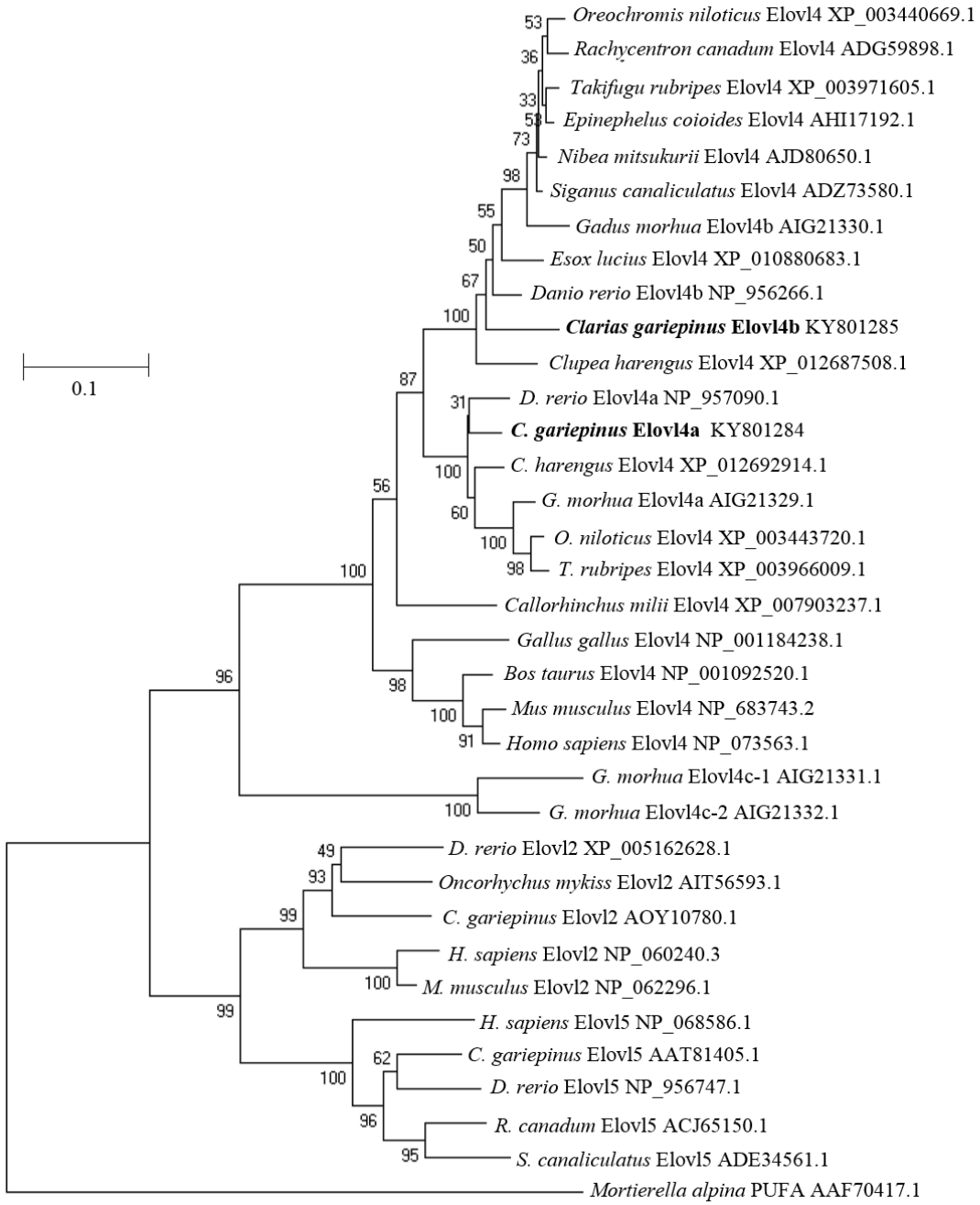

Figure 4.1. Phylogenetic tree comparing the deduced amino acid sequences of *Clarias gariepinus elovl4a* and *elovl4b* (highlighted in bold) with Elovl4, Elovl2 and Elovl5 sequences from a range of vertebrates. The tree was constructed using the neighbor-joining method (Saitou and Nei, 1987) with the MEGA 6.0 software. The numbers represent the frequencies (%) with which the tree topology presented was replicated after 1,000 iterations. The *Mortierella alpina* PUFA elongase was included in the analysis as outgroup sequence to construct the rooted tree.

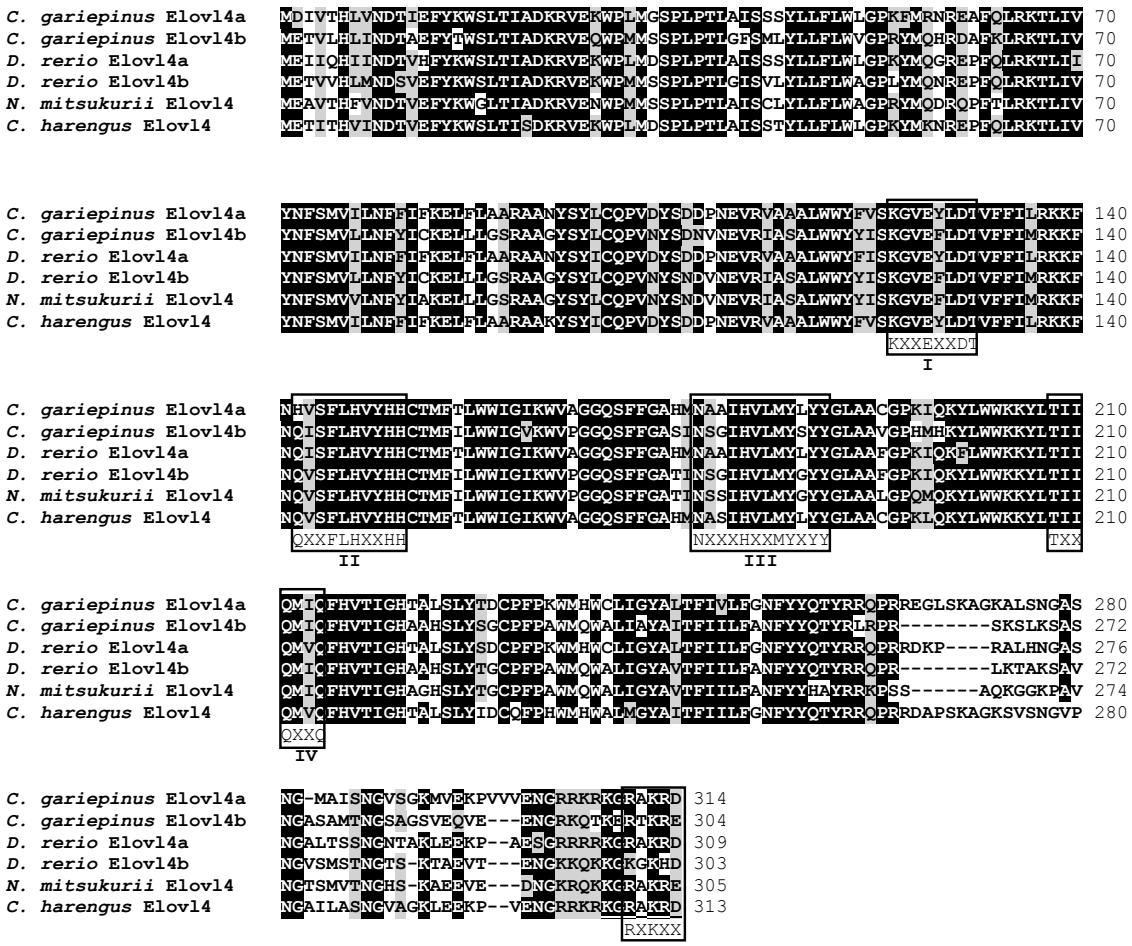

Figure 4.2. ClustalW amino acid alignment of the deduced *Clarias gariepinus* Elovl4 proteins with orthologues from *Danio rerio* (Elovl4a, gb|NP_957090.1|; Elovl4b, gb |NP_956266.1|), *Nibea mitsukurii* (gb|AJD80650.1|) and *Clupea harengus* (gb|XP_012692914.1|). Identical residues are shaded black and similar residues (based on the Blosum62 matrix, using ClustalW default parameters) are shaded grey. Indicated are four (i-iv) conserved motif of elongases: (i) KXXEXXDT, (ii) QXXFLHXXHH, (iii) NXXXHXXMYXYY and (iv) TXXQXXQ. The putative endoplasmic reticulum (ER) retrieval signal RXKXX at C-terminus is also indicated (Agaba et al., 2005).

4.3.2 Functional Characterisation of *C. gariepinus* Elovl4 in Yeast

The role of the *C. gariepinus* Elovl4 enzymes in the elongation of very long-chain saturated FA was assessed by comparison of the saturated ($\geq C_{24}$) FA profiles of control yeast transformed with empty pYES2 with those of yeast transformed with either pYES2-*elovl4a* or pYES2-*elovl4b* and grown in all cases in the absence of exogenously added

FA. The results confirmed that the *C. gariepinus* Elovl4 enzymes were involved in the biosynthesis of very long-chain saturated FA since yeast expressing both *elovl4a* and *elovl4b* generally contained higher levels of saturated FA ≥ C_{28}. More specifically, yeast expressing the *C. gariepinus elovl4a* had significantly higher levels of 28:0, 30:0 and 32:0 compared to control yeast, whereas yeast expressing the *C. gariepinus elovl4b* contained higher levels of 28:0 and 32:0 compared to controls (Table 4.2).

Table 4.2. Functional characterisation of *Clarias gariepinus* Elovl4 elongases: role in biosynthesis of very long-chain saturated fatty acids (FA). Results are expressed as an area percentage of total saturated FA ≥ C_{24} found in yeast transformed with either *C. gariepinus elovl4* coding regions or empty pYES2 vector (Control).

FA	Control	Elovl4a	Elovl4b
24:0	1.19±0.10[a]	1.60±0.25[b]	1.51±0.08[b]
26:0	23.46±1.15[a]	22.49±0.76[a]	26.82±4.81[a]
28:0	0.95±0.19[a]	4.42±0.62[b]	2.23±0.33[b]
30:0	0.23±0.06[a]	2.51±0.44[b]	0.48±0.05[a]
32:0	0.04±0.01[a]	0.40±0.02[b]	0.11±0.04[b]

The role of the *C. gariepinus* Elovl4 enzymes in VLC-PUFA biosynthesis was investigated by growing transgenic yeast expressing the *C. gariepinus elovl4a* and *elovl4b* cDNA in the presence of potential PUFA substrates. While transgenic yeast were able to elongate exogenously added PUFA substrates with chain lengths ranging from C_{18} to C_{22}, the conversions were markedly higher for longer chain substrates (Figure 4.3; Table 4.3). For Elovl4a, step-wise elongation products derived from exogenously supplemented PUFA and with C_{28-34} were very efficiently elongated as denoted by high conversions that were often above 80 % (Table 4.3). In contrast, the *C. gariepinus* Elovl4b was generally less active in the yeast expression system, leading to elongation

products with a maximum length of C_{34} and with generally lower conversions compared to Elovl4a (Table 4.3). As an exception, the Elovl4b was very efficient in utilising 22:6n-3 to produce intermediate elongation products up to 32:6n-3. It is important to note that both Elovl4 enzymes were able to produce 24:5n-3 from 22:5n-3 supplied directly or converted from exogenously supplied 20:5n-3 (Table 4.3).

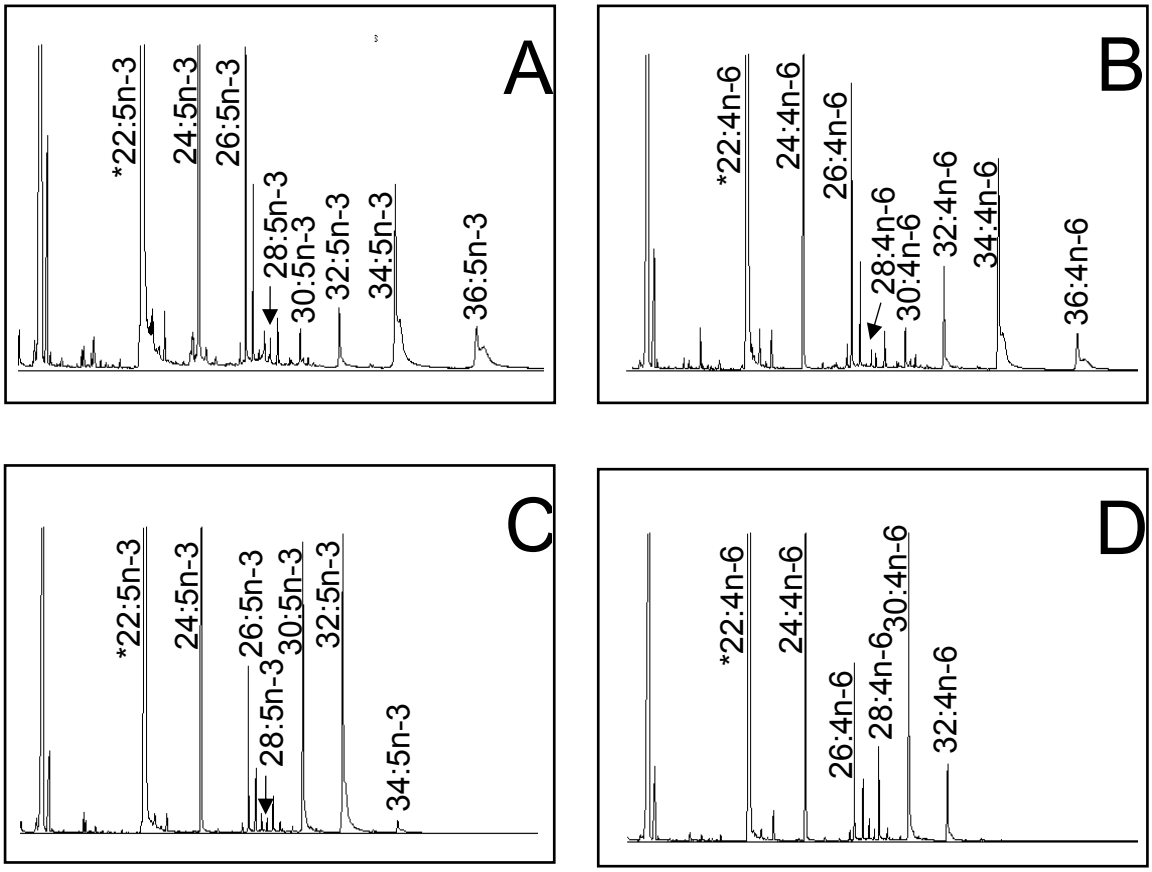

Figure 4.3. Functional characterisation of the newly cloned *Clarias gariepinus* Elovl4a (a and b) and Elovl4b (c and d) in yeast (*Saccharomyces cerevisiae*). The fatty acid profiles of yeast transformed with pYES2 containing the coding sequence of *elovl4a* and *elovl4b* were determined after the yeast were grown in the presence of one of the exogenously added substrates 22:5n-3 (A and C), and 22:4n-6 (B and D). The first peak (with asterisk) is derived from the exogenously added substrates. The elongation products are indicated accordingly in each panel.

Table 4.3. Functional characterisation of *Clarias gariepinus* Elovl4 elongases: role in biosynthesis of very long-chain polyunsaturated fatty acids (VLC-PUFA). *Saccharomyces cerevisiae* transformed with empty pYES2 vector (control) or pYES2 vector containing *C. gariepinus elovl4* coding region were grown in the presence of one exogenously added polyunsaturated fatty acid (PUFA) substrate C_{18} (18:4n-3 and 18:3n-6), C_{20} (20:5n-3 and 20:4n-6) and C_{22} (22:5n-3, 22:4n-6 and 22:6n-3). Conversions were calculated for each stepwise elongation according to the formula [areas of first products and longer chain products / (areas of all products with longer chain than substrate + substrate area)] x 100. The substrate FA varies as indicated in each step-wise elongation.

		% Conversion		
FA substrate	**Product**	**Elovl4a**	**Elovl4b**	**Elongation**
18:4n-3	20:4n-3	3.7	2.0	C18→36
	22:4n-3	26.8	6.4	C20→36
	24:4n-3	53.1	7.9	C22→36
	26:4n-3	62.9	6.8	C24→36
	28:4n-3	100.0	3.7	C26→36
	30:4n-3	100.0	48.9	C28→36
	32:4n-3	91.2	48.4	C30→36
	34:4n-3	83.6	1.4	C32→36
	36:4n-3	7.7	N.D.	C34→36
18:3n-6	20:3n-6	6.0	3.0	C18→36
	22:3n-6	49.5	9.9	C20→36
	24:3n-6	73.2	12.2	C22→36
	26:3n-6	80.2	29.4	C24→36
	28:3n-6	100.0	100.0	C26→36
	30:3n-6	100.0	100.0	C28→36
	32:3n-6	100.0	51.7	C30→36
	34:3n-6	69.5	N.D.	C32→36
	36:3n-6	8.1	N.D.	C34→36
20:5n-3	22:5n-3	20.4	6.3	C20→36
	24:5n-3	41.4	13.2	C22→36
	26:5n-3	55.8	4.7	C24→36
	28:5n-3	100.0	100.0	C26→36
	30:5n-3	100.0	19.3	C28→36

	32:5n-3	83.3	69.9	C30→36
	34:5n-3	93.4	12.0	C32→36
	36:5n-3	48.1	N.D.	C34→36
20:4n-6	22:4n-6	26.0	7.5	C20→36
	24:4n-6	54.6	15.9	C22→36
	26:4n-6	70.4	10.9	C24→36
	28:4n-6	85.4	9.9	C26→36
	30:4n-6	99.2	63.1	C28→36
	32:4n-6	96.5	28.4	C30→36
	34:4n-6	87.1	N.D.	C32→36
	36:4n-6	27.4	N.D.	C34→36
22:5n-3	24:5n-3	14.2	5.2	C22→36
	26:5n-3	51.1	3.9	C24→36
	28:5n-3	83.4	2.4	C26→36
	30:5n-3	98.3	31.0	C28→36
	32:5n-3	96.5	64.4	C30→36
	34:5n-3	89.8	5.6	C32→36
	36:5n-3	34.3	N.D.	C34→36
22:4n-6	24:4n-6	19.1	7.6	C22→36
	26:4n-6	69.9	9.9	C24→36
	28:4n-6	87.0	9.3	C26→36
	30:4n-6	99.2	67.7	C28→36
	32:4n-6	96.1	24.0	C30→36
	34:4n-6	83.8	N.D.	C32→36
	36:4n-6	24.3	N.D.	C34→36
22:6n-3	24:6n-3	0.8	0.9	C22→32
	26:6n-3	N.D.	100.0	C24→32
	28:6n-3	N.D.	100.0	C26→32
	30:6n-3	N.D.	100.0	C28→32
	32:6n-3	N.D.	43.7	C30→32

* N.D., not detected

4.3.3 Tissue Expression Analysis of *C. gariepinus elovl4a* and *elovl4b*

Tissue distribution analysis of *elovl4* mRNAs measured by qPCR indicated both genes were expressed in all tissues analysed, with high expression of *elovl4a* detected in pituitary and brain, whereas *elovl4b* expression was highest in female gonad and pituitary (Figure 4.4). Lowest expression signals for both *elovl4* were recorded in liver.

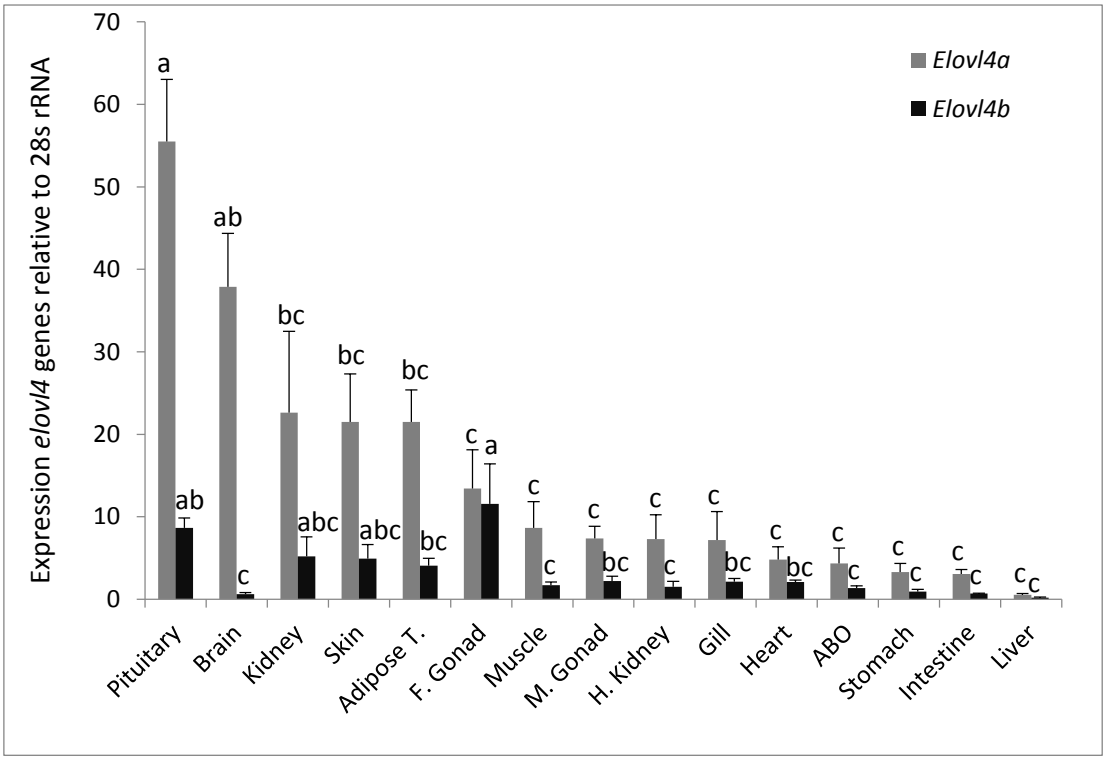

Figure 4.4. Tissue distribution of *Clarias gariepinus elovl4a* and *elovl4b* transcripts. Expression levels quantified for each target gene were normalised with the expression of the reference gene 28s rRNA. Data are reported as mean values with their standard errors (n = 4). Within each target gene, different letters indicate statistically significant differences in expression level among tissues (ANOVA and Tukey's HSD post hoc tests). ABO - accessory breathing organ, Adipose T. - adipose tissue, F. Gonad – female gonad, M. Gonad – male gonad

4.4 Discussion

Elovl enzymes with a role in long-chain (C_{20-24}) PUFA (LC-PUFA) biosynthesis have been investigated extensively in fish (Castro et al., 2016), particularly in farmed species in which current diet formulations including vegetable oils might compromise the provision of EFA (Tocher, 2015). While Elovl5 and Elovl2 have been regarded as key elongases within LC-PUFA biosynthetic pathways, Elovl4 has received less attention despite the key role that these elongases has in crucial physiological processes including vision, reproduction and neuronal functions of vertebrates (Agbaga et al., 2008; Agbaga, 2016; Mandal et al., 2004). The present study confirmed that the *C. gariepinus* Elovl4 enzymes play critical roles in the biosynthesis of very long-chain saturated fatty acids (VLC-SFA) and PUFA (VLC-PUFA), and may also participate in the biosynthesis of DHA from EPA.

Phylogenetic analysis confirmed two isoforms of Elovl4 (Elovl4a and Elovl4b) were isolated. The Elovl4 proteins, although similar, were separated into different branches of the phylogenetic tree. The Elovl4a protein formed a group with *D. rerio* Elovl4a and other Elovl4s separate from the group consisting of *C. gariepinus* Elovl4b and Elovl4b from fish species including *D. rerio*. This is in agreement with *in silico* studies that suggested all teleosts possess both types of Elovl4 (Castro et al., 2016). The functionally uncharacterised putative Elovl4c reported in *G. morhua* formed a group separate from all other Elovl4 sequences and therefore it is uncertain if these are true Elovl4 proteins. Functional characterisation of these genes is required to confirm this.

Different functions were determined for the *C. gariepinus* Elovl4 isoforms. It was confirmed that the *C. gariepinus* Elovl4a and Elovl4b participate in the biosynthesis of VLC-SFA. Thus, yeast expressing both *elovl4a* and *elovl4b* had increased levels of VLC-

SFA with C_{28-32} compared to control yeast. These results were consistent with elongation abilities of some teleost Elovl4 reported previously although, in some species like *S. salar* and *R. canadum*, Elovl4 were able to elongate up to 36:0 (Carmona-Antoñanzas et al., 2011; Monroig et al., 2011c, 2010a). VLC-SFA play important roles in skin permeability of mammals (Cameron et al., 2007; Vasireddy et al., 2007) and are incorporated into sphingolipids in the brain, although their role in the brain is yet to be ascertained (Agbaga, 2016). In fish, the physiological functions of VLC-SFA have been barely investigated, although it is reasonable to believe that these compounds also have important roles in brain function of teleosts. This is supported by the high expression signal of both *elovl4* isoforms in the head region of zebrafish embryos (Monroig et al., 2010a), and the high expression levels in brain of certain *elovl4* with the ability to biosynthesise VLC-SFA like Elovl4a from zebrafish (Monroig et al., 2010a) and the herein characterised *C. gariepinus*. The existence of neurons within the hypophysis, specifically in the posterior part (neurohypophysis), may likely explain the high expression of *elovl4a* and *elovl4b* observed in the present study. Other *C. gariepinus* tissues analysed also contained transcripts of *elovl4a*, indicating a widespread distribution as previously reported for the zebrafish *D. rerio elovl4a*, the only *elovl4a*-like sequence so far characterised in teleosts (Monroig et al., 2010a). With regards to *elovl4b*, transcripts were also detected in all tissues analysed, thus confirming a widespread distribution as described in cobia (Monroig et al., 2011c) and Atlantic salmon (Carmona-Antoñanzas et al., 2011). In contrast, relatively restricted tissue distributions of *elovl4b* were described in zebrafish (Monroig et al., 2010a) and rabbitfish (Monroig et al., 2012), species in which photoreception tissues such as eye (retina) and pineal gland appear to be the major sites of Elovl4b activity (Monroig et al., 2012, 2010a). Unfortunately, we could not analyse the expression of the target genes in eye or pineal,

although preliminary experiments indicated that both *C. gariepinus elovl4* were expressed in eye. Furthermore, the *C. gariepinus elovl4b* was highly expressed in female gonad suggesting that, in addition to the role it may play in male reproduction of mammals, as VLC-PUFA determines male fertility (Agbaga, 2016; Zadravec et al., 2011), fish Elovl4b might also have important functions in female reproduction. The above described expression patterns of the *C. gariepinus elovl4* genes, together with those tissues containing marked amounts of VLC-PUFA (Agbaga, 2016; Poulos, 1995), are in agreement with the roles that both Elovl4 play in the biosynthesis of VLC-PUFA in *C. gariepinus*.

Both Elovl4 showed the ability to biosynthesise VLC-PUFA of up to 34 - 36 carbons through consecutive elongations from all PUFA assayed including compounds with different chain lengths (C_{18-22}) and series (n-3 and n-6). While this is a common trait among Elovl4b-like enzymes (Carmona-Antoñanzas et al., 2011; Li et al., 2015; Monroig et al., 2012, 2011c, 2010a), the ability of the *C. gariepinus* Elovl4a to produce VLC-PUFA up to 36 carbons was somewhat unexpected since the only Elovl4a characterised so far from *D. rerio* showed little ability to biosynthesise VLC-PUFA (Monroig et al., 2010a). Whereas current evidence does not allow us to clarify which of the two Elovl4a phenotypes (*D. rerio* or *C. gariepinus*) is more prevalent among teleosts, the apparent differences might be in response to ecological and evolutionary factors as previously hypothesised for both elongases (Monroig et al., 2016b; Morais et al., 2009) and desaturases (Fonseca-Madrigal et al., 2014; Li et al., 2010). Irrespective of the mechanism driving the distinct phenotype among Elovl4a enzymes, it is clear that the *C. gariepinus* orthologue was very efficient in the production of VLC-PUFA from exogenously supplemented PUFA substrates. Such elongation capabilities largely apply to the *C. gariepinus* Elovl4b, although a distinctive trait of Elovl4b is its ability to

efficiently elongate exogenously added 22:6n-3 to 32:6n-3, a VLC-PUFA that has been detected in retinal phosphatidylcholine of gilthead seabream *Sparus aurata* (Monroig et al., 2016a). Despite the ability of the *C. gariepinus* Elovl4b to produce 32:6n-3 from DHA (22:6n-3), the latter does not appear to be a preferred substrate for biosynthesis of n-3 VLC-PUFA in bovine and rat retina (Rotstein et al., 1996; Suh and Clandinin, 2005). It was demonstrated that, while exogenously supplemented EPA and 22:5n-3 acted as precursors for VLC-PUFA biosynthesis, DHA was incorporated directly into retinal phospholipids without further metabolism.

Irrespective of whether teleost Elovl4 can utilise DHA or not, their ability to elongate 22:5n-3 to 24:5n-3 suggested that Elovl4 can play a role in DHA biosynthesis through the Sprecher pathway (Sprecher, 2000). This pathway requires the production of 24:5n-3 for further Δ6 desaturation and partial β-oxidation to DHA, and Elovl2 has been identified as a major candidate elongase accounting for the provision of 24:5n-3 from 22:5n-3 (Castro et al., 2016). *C. gariepinus* possess an Elovl2 with the abovementioned ability to elongate 22:5n-3 to 24:5n-3 (Chapter 3), indicating that Elovl2 and Elovl4 have partly overlapping functions as previously described between Elovl2 and Elovl5 (Monroig et al., 2016b). In contrast, teleosts within the Acanthopterygii clade have apparently lost Elovl2 (Leaver et al., 2008), and consequently the presence of Elovl4 with the ability to elongate 22:5n-3 is clearly advantageous to compensate for this loss (Castro et al., 2016). Studies in mammals have not fully clarified whether ELOVL4 participates in DHA biosynthesis. High expression of *ELOVL4* in tissues where DHA accounted for a large proportion of the PUFA content including retina, brain and testis, along with the crucial role DHA plays in the development and function of these tissues suggested a role of mammalian ELOVL4 in DHA biosynthesis (Agbaga et al., 2008; Mandal et al., 2004; Zhang et al., 2001, 2003). Moreover, Vasireddy et al. (2007) reported a reduction in DHA

and 22:5n-3 in non-polar lipids and free FA of whole skin of mouse without a functional *ELOVL4* compared to skin from wild type controls. On the contrary, Agbaga et al. (2010, 2008) concluded ELOVL4 did not participate in DHA biosynthesis in mammals or may play a redundant role, the latter hypothesis aligning well with the overlapping roles between Elovl2 and Elovl4 described above.

In conclusion, the present study demonstrated that *C. gariepinus* possess two distinct *elovl4*-like elongases with high homology to the previously described zebrafish Elovl4a and Elovl4b. Both *C. gariepinus* Elovl4 participate in the biosynthesis of both VLC-SFA and VLC-PUFA. While previous studies on teleosts had reported on the ability of Elovl4b-like elongases to operate efficiently towards both saturated and polyunsaturated FA, the herein described ability of the *C. gariepinus* Elovl4a to elongate PUFA was in contrast to that of *D. rerio* Elovl4a, the only Elovl4a-like elongase functionally characterised to date. The tissue distribution of *C. gariepinus elovl4* mRNA largely followed previous observations in other teleosts, with neuronal and reproductive tissues exhibiting the highest expression levels.

CHAPTER 5.

TWO ALTERNATIVE PATHWAYS FOR DOCOSAHEXAENOIC ACID (DHA, 22:6n-3) BIOSYNTHESIS ARE WIDESPREAD AMONG TELEOST FISH

5.1 Introduction

Long chain (C_{20-24}) polyunsaturated fatty acids (LC-PUFA) including arachidonic acid (ARA, 20:4n-6), eicosapentaenoic acid (EPA, 20:5n-3) and docosahexaenoic acid (DHA, 22:6n-3) play numerous physiologically important roles essential to health in humans (Brenna, 2002; Cardoso et al., 2016). Although humans have some ability to synthesise LC-PUFA from the C_{18} precursors linoleic acid (LA, 18:2n-6) and α-linolenic acid (ALA, 18:3n-3), dietary supply of these LC-PUFA is still required to meet physiological demands (Brenna, 2002). Fish are the primary source of n-3 LC-PUFA for humans (Shepherd et al., 2017) and this has prompted increasing interest in LC-PUFA metabolism in fish (Tocher, 2003), with biosynthesis being one of the most targeted pathways under investigation (Castro et al., 2016; Tocher, 2015). The biosynthesis of C_{20-22} LC-PUFA in vertebrates including fish involves alternating steps of desaturation and elongation of the dietary essential C_{18} fatty acids (FA), LA and ALA. Fatty acyl desaturases (Fads) catalyse the introduction of a double bond at a specific position of the acyl chain and have been named accordingly as Δ6, Δ5, Δ4 and Δ8 desaturases (Meesapyodsuk and Qiu, 2012). Elongation of very long-chain fatty acid (Elovl) proteins catalyse the condensation and rate-limiting reaction of the FA elongation pathway (Guillou et al., 2010; Jakobsson et al., 2006). Biosynthesis of ARA and EPA from the C_{18} precursors LA and ALA, respectively, follows the same pathways and involves the same enzymes (Figure 1.3). The pathways revealed from studies in vertebrates are the so-called "Δ6 pathway" (Δ6 desaturation – elongation – Δ5 desaturation) and the "Δ8 pathway" (elongation – Δ8 desaturation – Δ5 desaturation) (Figure 1.3) (Castro et al., 2016; Monroig et al., 2011a; Park et al., 2009; Tocher, 2010; Vagner and Santigosa, 2011).

Since the studies of Sprecher and co-workers in rats (Sprecher, 2000, 1992; Sprecher et al., 1995), it had been generally accepted that the biosynthesis of DHA in vertebrates was achieved by two consecutive elongations from EPA to produce tetracosapentaenoic acid (TPA, 24:5n-3), which then undergoes a Δ6 desaturation to tetracosahexaenoic acid (THA, 24:6n-3), the latter being β-oxidised to DHA in peroxisomes (Ferdinandusse et al., 2001). This pathway, known as the "Sprecher pathway", was subsequently confirmed to be operative in rainbow trout *Oncorhynchus mykiss* (Buzzi et al., 1997, 1996). The first question that arose after the demonstration of this pathway was whether the same or different Δ6 Fads catalysed the reactions with C_{18} and C_{24} substrates (Sprecher et al., 1995). It was demonstrated that the same Δ6 Fads carried out the conversions of 18:3n-3 to 18:4n-3 and 24:5n-3 to 24:6n-3 in humans (De Antueno et al., 2001) and rat (D'andrea et al., 2002; Geiger et al., 1993). In fish species, it is still unclear whether the same Fads catalyses the two Δ6 desaturation reactions or if two Δ6 Fads (isoenzymes) are involved (Sargent et al., 2002; Tocher et al., 2003; Vagner and Santigosa, 2011). Studies using yeast as a heterologous expression system confirmed that the bifunctional Δ6Δ5 Fads from zebrafish (*Danio rerio*) had ability to desaturate both C_{18} and C_{24} substrates at the Δ6 position (Tocher et al., 2003). However, the Nibe croaker (*Nibea mitsukurii*) Δ6 Fads catalysed the desaturation of C_{18} but not C_{24} substrates (Kabeya et al., 2015). These findings suggested that the DHA biosynthetic capability varied among teleost fish and, interestingly, recent findings have demonstrated that, unlike other vertebrates, teleost fish have acquired alternative pathways for DHA biosynthesis during evolution (Castro et al., 2016).

The "Δ4 pathway", first described in the marine protist *Thraustochytrium* sp. (Qiu et al., 2001), is a more direct pathway involving one single elongation of EPA to docosapentaenoic acid (DPA, 22:5n-3), which is subsequently desaturated at the Δ4

position to produce DHA. Although for many years Δ4 desaturases had not been found in any vertebrate species, a Fads2 with Δ4 desaturase activity was first discovered in rabbitfish (*Siganus canaliculatus*) (Li et al., 2010). Since then, Fads with Δ4 desaturases have been found in several teleost species such as Senegalese sole (*Solea senegalensis*) (Morais et al., 2012), pike silverside (*Chirostoma estor*) (Fonseca-Madrigal et al., 2014) and striped snakehead (*Channa striata*) (Kuah et al., 2015). Recently, human cells expressing the baboon *FADS2* had the ability for direct Δ4 desaturation of 22:5n-3 to 22:6n-3 (Park et al., 2015). Thus, the existence of the Δ4 pathway among teleosts appeared to be more widespread than initially believed.

It is interesting to note that, unlike other vertebrates, current evidence suggests that all *fads*-like genes found in teleost fish are Fads2 orthologues (Castro et al., 2012). Thus the functional diversity among fish Fads2 described above has been hypothesised to be dependent upon various factors including the phylogenetic position of species, in combination with environmental and ecological factors (Castro et al., 2016). In the present study, we aimed to elucidate the pathways for DHA biosynthesis existing in species representing major lineages along the tree of life of teleost fish (Betancur-R et al., 2013). In particular, we have investigated the prevalence of the Sprecher pathway among teleost fish by determining the Δ6 activity towards C_{24} substrates (24:5n-3 and 24:4n-6) of desaturases with different substrate specificities (Δ6, Δ5 and Δ4), and derived from fish species with different evolutionary and ecological backgrounds. Furthermore, we have taken advantage of the now known key amino acid (aa) residues determining Δ4 desaturase ability of Fads (Lim et al., 2014) to identify teleost taxa, with publically available genomic or transcriptomic databases, in which their desaturase repertoire enables them to biosynthesise DHA through the more direct Δ4 pathway.

5.2 Materials and Methods

5.2.1 Fish Lineages

A comprehensive set of Fads2-like sequences was collected by screening genomic and transcriptomic databases from fish species representing a sample group of lineages such as the basal gnathostome *S. canicula*; early diverging post-3R teleosts Osteoglossiformes (*A. gigas*) and Anguilliformes (*A. japonica*); and various other teleostei such as Cypriniformes (*D. rerio*), Siluriformes (*C. gariepinus*) and Salmoniformes (*S. salar* and *O. mykiss*), to relatively modern groups like Anabantiformes (*C. striata*), Atheriniformes (*C. estor*), Cichliformes (*O. niloticus*, *M. zebra* and *H. burtoni*), Blenniiformes (*Tomicodon* sp., *Acyrtus* sp. and *Enneanectes* sp.), Beloniformes (*O. latipes*), Cyprinodontiformes (*P. reticulata*, *F. heteroclitus* and *A. limnaeus*), Pleuronectiformes (*S. senegalensis*), Spariformes (*S. aurata*), Centrarchiformes (*M. salmoides*) and Eupercaria (*S. canaliculatus* and *N. mitsukurii*). The desaturase sequences from fish species listed above were used for phylogenetic analysis and selected sequences were subjected to functional characterisation as described.

5.2.2 Determination of Δ6 Desaturase Activity of Fish Fads2 towards C_{24} PUFA in Co-Transformant *Saccharomyces cerevisiae*

We first investigated the ability for Δ6 desaturase activity towards C_{24} PUFA substrates, i.e. 24:4n-6 and 24:5n-3, the latter being an intermediate in the Sprecher pathway for DHA biosynthesis. Such activities were tested in a total of 15 Fads sequences belonging to 12 species of fish (Table 5.1), through a newly developed yeast-based assayed as follows. Yeast competent cells Inv*Sc*1 (Invitrogen) were co-transformed with two different plasmid constructs prepared as described below. First, the *D. rerio elovl2* open reading frame (ORF) (Monroig et al., 2009) was ligated into the yeast expression vector p415TEF (a centromeric plasmid with a *LEU2* selectable marker) to produce the construct p415TEF-*elovl2*, in which the expression of the *D. rerio elovl2* was controlled

under the yeast *TEF1* promoter (constitutive expression). Second, the ORF of the corresponding fish Fads (Table 5.1) was cloned into the episomal yeast vector pYES2, in which the Fads expression was under the control of the *GAL1* promoter (inducible expression). Selection of transformant yeast containing both constructs was performed by growing the co-transformed yeast on *S. cerevisiae* minimal medium minus uracil minus leucine (SCMM$^{-ura-leu}$) plates. One single colony was grown in SCMM$^{-ura-leu}$ broth for 24 h at 30 ºC, and subsequently subcultured in individual Erlenmeyer flasks at 0.1 OD_{600} (t_0) and supplemented with either 0.75 mM Na salts of 22:4n-6 (docosatetraenoic acid, DTA) or 22:5n-3 (DPA) (0.75 mM). Co-transformed yeast were then grown for 24 h (t_0 + 24 h) allowing the *D. rerio* Elovl2 to convert the exogenously added C_{22} substrates (DTA or DPA) into their corresponding C_{24} elongation products 24:4n-6 and 24:5n-3, respectively. In order to test the ability of the fish desaturases to introduce Δ6 double bonds into the newly synthesised 24:4n-6 and 24:5n-3 in yeast, the *fads* expression was then induced (t_0 + 24 h) by addition of 2 % galactose, after which the recombinant yeast were further grown for 48 h (t_0 + 72 h) before collection. As positive controls, a subculture aliquot of the same colony used for the above described assay was supplemented with an n-3 PUFA substrate for which the corresponding assayed Fads had previously shown activity (Table 5.1) and galactose (2 %) at t_0. More specifically, co-transformant yeasts were grown in the presence of 18:3n-3 as controls for Δ6 (e.g. AgΔ6Fads2) or Δ6Δ5 (e.g. DrΔ6Δ5Fads2) desaturases, 20:4n-3 for Δ5 desaturases (e.g. SsΔ5Fads2) and 22:5n-3 for Δ4 desaturases (e.g. CeΔ4Fads2). The yeast co-transformed with empty p415TEF and pYES2 vectors were also prepared as negative controls.

Table 5.1. Fish fatty acyl desaturases (Fads) investigated for the ability to desaturate tetracosapentaenoic acid (24:5n-3) to tetracosahexaenoic acid (24:6n-3). Their known desaturation activities and the studies in which they were published are indicated accordingly.

Species	Desaturase name[a]	Reported activity[b]	GenBank Accession no.	Reference
Scyliorhinus canicula	ScyΔ6Fads2	Δ6	JN657544	Castro et al., 2012
Arapaima gigas	AgΔ6Fads2	Δ6	AOO1978	Lopes-Marques et al., 2017
Anguilla japonica	AjΔ6Fads2	Δ6	AHY22375	Wang et al., 2014
Danio rerio	DrΔ6Δ5Fads2	Δ6, Δ5	AAG25710	Hastings et al., 2001
Clarias gariepinus	CgΔ6Δ5Fads2	Δ6, Δ5	AMR43366	Chapter 3
Salmo salar	SsΔ6Fads2	Δ6[c]	AAR21624	Zheng et al., 2005
S. salar	SsΔ5Fads2	Δ5	AAL82631	Hastings et al., 2001
Oncorhynchus mykiss	OmΔ6Fads2	Δ6	AAK26745	Zheng et al., 2005
Chirostoma estor	CeΔ6Δ5Fads2	Δ6, Δ5	AHX39207	Fonseca-Madrigal et al., 2014
C. estor	CeΔ4Fads2	Δ4	AHX39206	Fonseca-Madrigal et al., 2014
Siganus canaliculatus	ScΔ6Δ5Fads2	Δ6, Δ5	ABR12315	Li et al., 2010
S. canaliculatus	ScΔ4Fads2	Δ4	ADJ29913	Li et al., 2010
Sparus aurata	SaΔ6Fads2	Δ6	AAL17639	Zheng et al., 2004
Nibea mitsukurii	NmΔ6Fads2	Δ6	AJD80650	Kabeya et al., 2015

[a] Scy, *Scyliorhinus canicula*; Ag, *Arapaima gigas*; Aj, *Anguilla japonica*; Dr, *Danio rerio*; Cg, *Clarias gariepinus*; Ss, *Salmo salar*; Om, *Oncorhychus mykiss*; Ce, *Chirostoma estor*; Sc, *Siganus canaliculatus*; Sa, *Sparus aurata*; Nm, *Nibea mitsukurii*; On, *Oreochromis niloticus*

[b] Δ8 desaturase activities of some of these desaturases and reported in the corresponding publication are not indicated in the interests of clarity

[c] Refers to "Fads2_a" as termed by Monroig et al. (2010b)

5.2.3 In silico Retrieval of Putative Δ4 Desaturases

For retrieval of putative Δ4 desaturase sequences from databases, an alignment of the four functionally characterised Δ4 desaturases from rabbitfish (ADJ29913), Senegalese sole (AEQ92868), pike silverside (AHX39206) and striped snakehead (ACD70298) was performed using the Clustal Omega Multiple Sequence Alignment tool (http://www.ebi.ac.uk/Tools/msa/clustalo/). The conserved aa sequence PPLLIPVFYNFNIMXTMISR, which included the four key aa residues (underlined) accounting for Δ4 regioselectivity (Lim et al., 2014), was used as a query for blast searches. The majority of the putative Δ4 desaturase sequences were obtained from the NCBI Non-redundant protein sequences (nr) database using the blastp algorithm. We further explored the Expressed Sequence Tags (EST) and Transcriptome Shotgun Assembly (TSA) databases using the tblastn algorithm. In addition, the Fish-T1K website (http://www.fisht1k.org) was also used for the tblastn search. Among the retrieved sequences, we selected only those that contained "Y" and "N" in positions 1 and +4, respectively, within the four aa domain YXXN, as these have been reported previously to be crucial for Δ4 function (Lim et al., 2014).

5.2.4 Phylogenetic Analysis of Fads Desaturases

A phylogenetic tree was built to compare the deduced aa sequences of the fish Fads considered in the present study. The neighbour-joining method (Saitou and Nei, 1987), with the CLC Main Workbench 7 (CLC bio, Aarhus, Denmark), was used to construct the phylogenetic tree, with confidence in the resulting tree branch topology measured by bootstrapping through 1,000 iterations. The alignment of Fads aa sequences used for constructing the phylogenetic tree was performed with MAFFT using the L-INS-i method (Katoh and Toh, 2008). Non-teleost fish sequences from *S. canicula* and mammalian (human and mouse) Fads2 sequences were also included in the analysis.

5.2.5 Fatty Acid Analysis of Yeast

Total lipids extracted from yeast samples (Folch et al., 1957) were used to prepare fatty acid methyl esters (FAME). FAME extraction, purification and analysis were performed as described by Li et al. (2010). Substrate FA conversions for the Δ6 desaturase activity towards C_{24} substrates were calculated using the same formula as above (Section 4.2.5) considering the areas of 24:5n-3 and 24:4n-6 produced endogenously by the *D. rerio* Elovl2 as substrates for calculations. When necessary, GC-MS was used to confirm the identity of the products (Li et al., 2010).

5.3 Results

5.3.1 Determination of Δ6 Desaturase Activity of Fish Fads towards C_{24} PUFA

The capabilities of fish Fads to desaturate C_{24} PUFA (24:4n-6 and 24:5n-3) at Δ6 position were determined by co-transforming yeast with *D. rerio elovl2* and the individual fish *fads* to be assayed. Control yeast co-transformed with empty p415TEF and pYES2 vectors did not show any activity towards any of the PUFA substrates assayed (data not shown) and the yeast showed typical FA profiles consisting primarily of 16:0, 16:1 isomers, 18:0 and 18:1n-9 (Figure 5.2). Independent of the desaturase cloned into the inducible expression vector pYES2, all the co-transformant yeast were able to elongate the exogenously added 22:4n-6 and 22:5n-3 to 24:4n-6 and 24:5n-3, respectively, confirming the activity of the *D. rerio* Elovl2 cloned into the constitutive expression vector p415TEF. Importantly, the incubation of all the co-transformant yeast in the presence of the corresponding FA substrate as controls (i.e. 18:3n-3 for Δ6 and Δ6Δ5 desaturases, 20:4n-3 for Δ5 desaturases, and 22:5n-3 for Δ4 desaturases) confirmed that the desaturases were functional, with activities as previously reported (Table 5.2).

The ability for Δ6 desaturation of C_{24} PUFA such as 24:4n-6 and 24:5n-3 varied among fish Fads (Figure 5.2; Table 5.2). Interestingly, none of the three Δ4 Fads2 assayed (*C.*

estor, *S. canaliculatus* and *Oreochromis niloticus*) showed any ability to desaturate either 24:4n-6 or 24:5n-3 (Table 5.2). However, most of the fish Fads2 with Δ6 and/or Δ5 specificities were capable of desaturating both 24:4n-6 and 24:5n-3 to their corresponding Δ6 desaturated products, namely 24:5n-6 and 24:6n-3, respectively (Figure 5.2; Table 5.2). Due to the intrinsic variability of desaturation activities in the yeast system, we normalised the Δ6 desaturase activities measured on C_{24} substrates with those obtained on the corresponding control FA substrate. For that purpose, we calculated the ratio "$\Delta_{24:5n-3}/\Delta_{control}$" (Table 5.2) that allowed comparisons among the fish Fads investigated herein. Generally, desaturases from species within relatively ancient fish lineages including *Scyliorhinus canicula*, *Arapaima gigas*, *Anguilla japonica*, *Clarias gariepinus*, *Salmo salar* and *O. mykiss* showed high capacity for Δ6 desaturation towards 24:5n-3, with $\Delta_{24:5n-3}/\Delta_{control}$ ratios ≥ 0.82 (Table 5.2). On the other hand, more modern species such as *S. canaliculatus*, *Sparus aurata* and *N. mitsukurii* had Fads2 with $\Delta_{24:5n-3}/\Delta_{control}$ ratios ≤ 0.43 (Table 5.2). It is interesting to note that the *S. salar* Δ5 (SsΔ5Fads2) showed the ability to desaturate 24:5n-3 to 24:6n-3 (Figure 5.2E; Table 5.2), denoting Δ6 desaturase activity. In order to confirm these results, we incubated the SsΔ5Fads2 co-transformant yeast in the presence of 18:3n-3 and confirmed the presence of Δ6 desaturated product 18:4n-3 (3.5 % conversion). Among all the non-Δ4 Fads2, the *N. mitsukurii* NmΔ6Fads2 was the only tested desaturase with no activity on either 24:4n-6 nor 24:5n-3 (Figure 5.2C).

Table 5.2. Capability of fish Fads2 for Δ6 desaturation of C_{24} substrates 24:4n-6 and 24:5n-3 using a yeast *Saccharomyces cerevisiae* heterologous system as described in Materials and Methods. Fatty acid (FA) conversions were calculated as the percentage of 24:4n-6 and 24:5n-3 desaturated to 24:5n-6 and 24:6n-3, respectively, as [product area / (product area + substrate area)] x 100. Conversions towards the control FA substrate (18:3n-3 as controls for Δ6 and Δ6Δ5 desaturases, 20:4n-3 for Δ5 desaturases and 22:5n-3 for Δ4 desaturases) are also indicated. In order to normalise the % conversions obtained throughout the Fads2 dataset, ratios between the activities on 24:5n-3 and those on the control FA ("$\Delta_{24:5n-3}/\Delta_{control}$") are also presented.

	% Conversion			
Desaturase[a]	**24:4n-6→24:5n-6**	**24:5n-3→24:6n-3**	**Control→Product**	**$\Delta_{24:5n-3}/\Delta_{control}$**
ScyΔ6Fads2	29.3	34.3	41.9	0.82
AgΔ6Fads2	25.4	19.0	15.3	1.24
AjΔ6Fads2	14.0	15.8	17.8	0.89
DrΔ6Δ5Fads2	10.4	15.8	11.9	1.33
CgΔ6Δ5Fads2	29.9	28.1	31.5	0.89
SsΔ6Fads2	18.5	26.0	23.9	1.09
SsΔ5Fads2	1.4	6.4	3.4	1.88
OmΔ6Fads2	7.5	19.7	20.4	0.97
CeΔ6Δ5Fads2	4.2	9.0	22.9	0.39
CeΔ4Fads2	ND	ND	9.9	0.00
ScΔ6Δ5Fads2	6.0	7.4	36.4	0.20
ScΔ4Fads2	ND	ND	6.9	0.00
SaΔ6Fads2	4.8	6.5	15.0	0.43
NmΔ6Fads2	ND	ND	10.5	0.00
OnΔ4Fads2	ND	ND	4.5	0.00

ND, Not detected

[a] Scy, *Scyliorhinus canicula;* Ag, *Arapaima gigas*; Aj, *Anguilla japonica*; Dr, *Danio rerio*; Cg, *Clarias gariepinus*; Ss, *Salmo salar*; Om, *Oncorhychus mykiss*; Ce, *Chirostoma estor*; Sc, *Siganus canaliculatus*; Sa, *Sparus aurata*; Nm, *Nibea mitsukurii*; On, *Oreochromis niloticus*

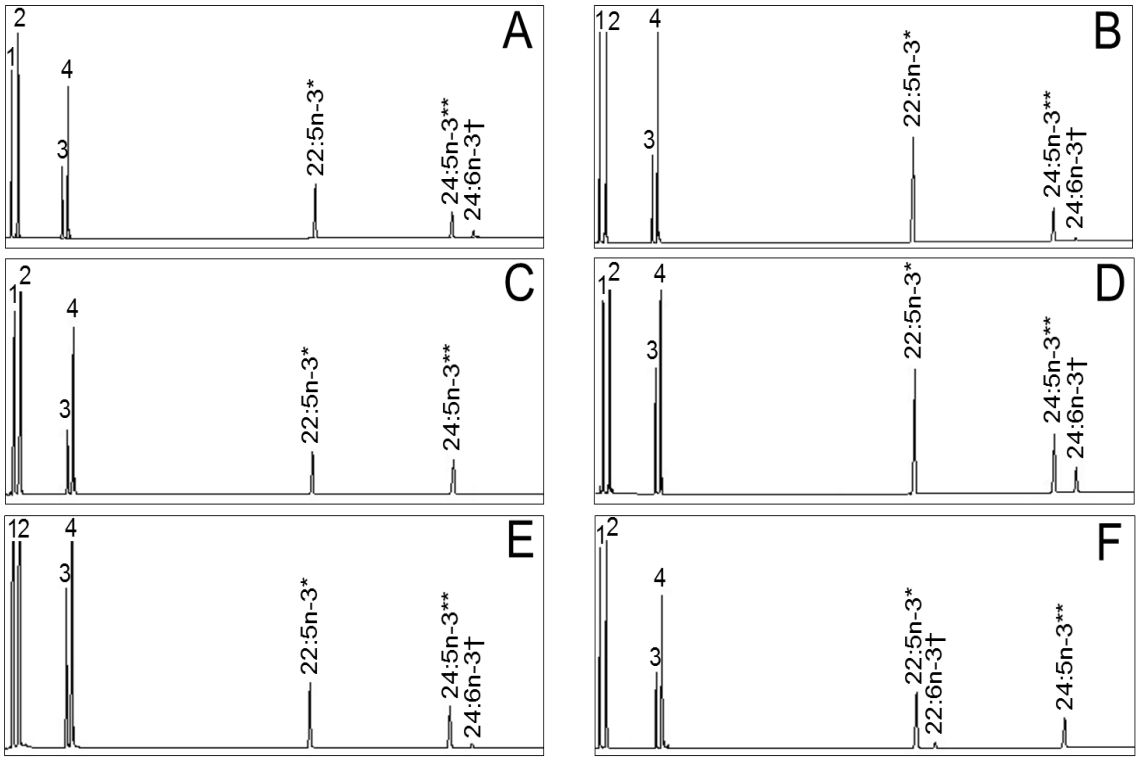

Figure 5.1. Characterisation of fish fatty acyl desaturases 2 (Fads2) ability to desaturate 24:5n-3. Fatty acid (FA) profiles of yeast (*Saccharomyces cerevisiae*) co-transformed with the *Danio rerio elovl2*, and the *Arapaima gigas* Δ6 *fads2* (A), *Sparus aurata* Δ6 *fads2* (B), *Nibea mitsukurii* Δ6 *fads2* (C), *Clarias gariepinus* Δ6Δ5 *fads2* (D), *Salmo salar* Δ5 *fads2* (E) and *Chirostoma estor* Δ4 *fads2* (F) and grown in the presence of an exogenously added FA substrates (indicated as "*" in all panels). Peaks 1-4 represent the *S. cerevisiae* endogenous FA, namely 16:0 (1), 16:1 isomers (2), 18:0 (3) and 18:1n-9 (4). Elongation (**) and desaturation (†) products from exogenously added or endogenously produced FA are indicated accordingly.

5.3.2 Putative Δ4 desaturase Collection and Phylogenetics

The phylogenetic tree comparing the deduced aa sequence of the fish Fads with those of human and rat is shown in Figure 5.3. All Fads1 clustered together and were separate from all Fads2 in the tree. All teleost Fads2 studied in the present study strongly clustered within the teleost group (99 % bootstraps), with desaturases from early divergent teleost species (e.g. *A. gigas*, *A. japonica*, *C. gariepinus*, *S. salar* and *O. mykiss*) clustering

separately from desaturases from species belonging to more recent lineages (95 % bootstraps) (Figure 5.3). Among the latter, one can find all the sequences with YXXN residues determining Δ4 activity (Lim et al., 2014) including desaturases from *S. canaliculatus*, *S. senegalensis*, *C. estor*, *O. latipes* and *O. niloticus*. Clearly, all Fads2-like proteins from Nile tilapia and other cichlids formed a monophyletic clade (99 % bootstraps), itself comprising a subgroup with Fads2 sequences possessing the abovementioned distinctive YXXN motif for Δ4 desaturases and another group that includes the Δ6Δ5 Fads2 from Nile tilapia (Figure 5.3).

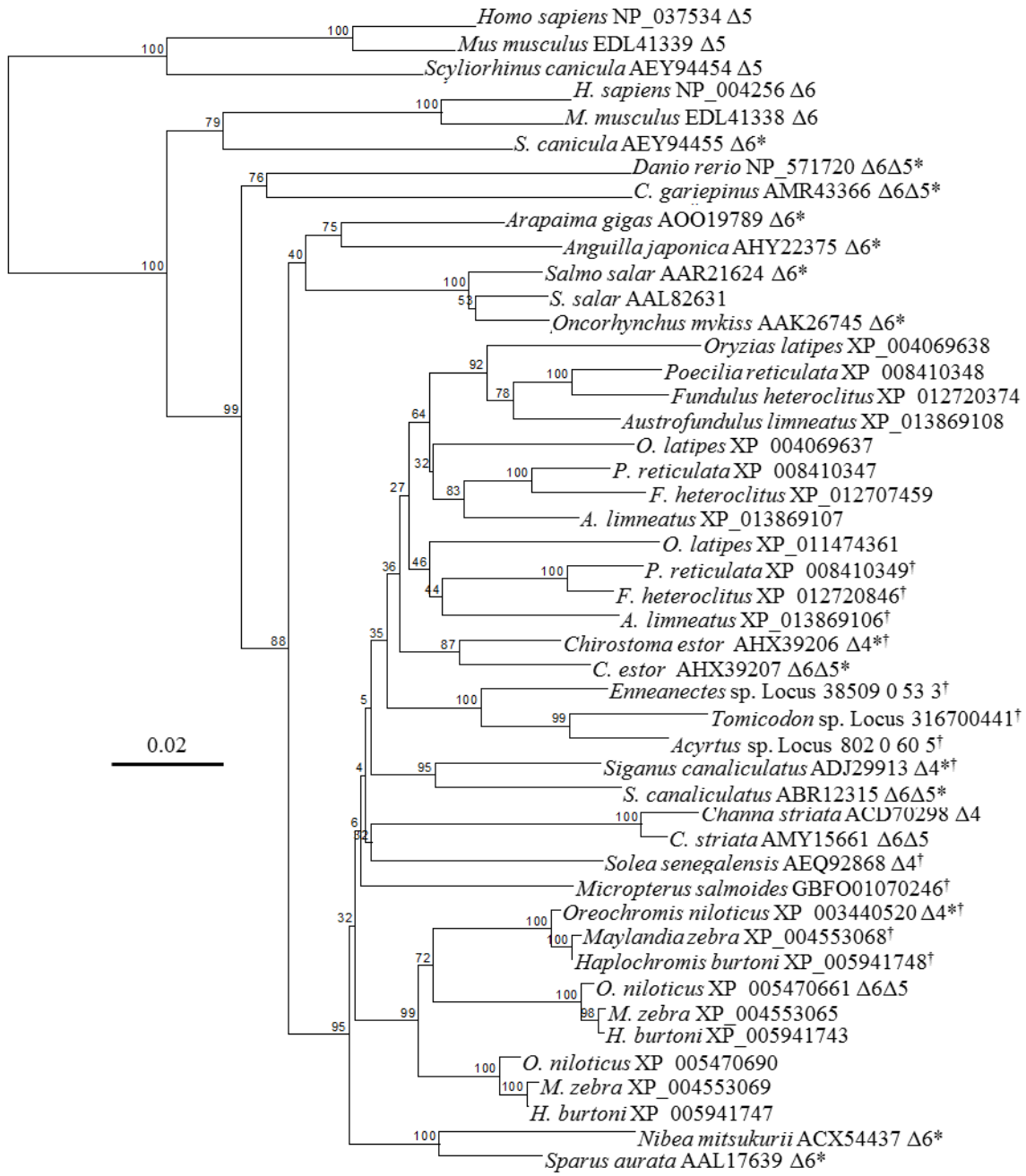

Figure 5.2. Phylogenetic tree comparing the amino acid sequences of teleost Fads2 with non-teleost vertebrate Fads-like from the cartilaginous fish and mammals (human and mouse). The numbers represent the frequencies (%) with which the tree topology presented was replicated after 1,000 iterations. The functionally characterised Fads were shown with their corresponding regioselectivity (Δ6, Δ5, Δ6Δ5 and Δ4). Asterisks ("*") indicate Fads2 that have been subjected to further functional analysis in the present study. Crosses ("†") indicate Fads2 that possess the YXXN amino acid residues determining Δ4 desaturase activity (Castro et al., 2012). Branches including Teleostei and Acanthopterygii Fads2 sequences are indicated.

5.4 Discussion

It has been largely accepted that DHA biosynthesis in vertebrates proceeds through the Sprecher pathway (Castro et al., 2016; Guillou et al., 2010). While most earlier investigations focussed on mammals, studies in *O. mykiss* confirmed that the Sprecher pathway also operated in fish (Buzzi et al., 1997, 1996). It was subsequently demonstrated that the same Δ6 Fads-like enzyme that acts on C_{18} PUFA precursors at the initiation of the LC-PUFA biosynthesis (Figure 1.3) was also responsible for the desaturation of 24:5n-3 required in the Sprecher pathway (D'andrea et al., 2002; De Antueno et al., 2001). Despite the plethora of studies reporting on the functions of fish Fads6, the capability of fish Fads to operate towards 24:5n-3, and therefore to contribute to DHA biosynthesis through the Sprecher pathway, had not been fully established. For that purpose, we herein conducted a retrospective study investigating the ability to operate as Δ6 desaturases towards 24:5n-3 and 24:4n-6 of a range of previously characterised Fads2 from fish belonging to lineages distributed along the phylogenetic tree of teleosts (Betancur-R et al., 2013).

Using a newly developed method involving yeast, we were able to establish that, with the exception of the Nibe croaker Fads2, all teleost non-Δ4 desaturases tested in this study had the ability to efficiently convert 24:5n-3 and 24:4n-6 into 24:6n-3 and 24:5n-6, respectively, confirming their ability for Δ6 desaturation of C_{24} PUFA substrates. Such ability was observed in Fads2 from species spread across the evolutionary history of teleosts from basal (e.g. *A. gigas* and *A. japonica*) and recent (e.g. *S. canaliculatus* and *S. aurata*) lineages, and with different regioselectivities including Δ6 desaturases (e.g. *O. mykiss* and *S. aurata*) and bifunctional Δ6Δ5 desaturases (e.g. *C. estor* and *S. canaliculatus*). Since all these Fads2 also showed Δ6 desaturase activity towards C_{18} PUFA (18:3n-3 and 18:2n-6), the present results confirmed that the same Fads2 can

function as Δ6 desaturases at both steps of the LC-PUFA biosynthetic pathway as described above for mammals (D'andrea et al., 2002; De Antueno et al., 2001). This is in agreement with studies on zebrafish Δ6Δ5 Fads2, which showed the ability to operate as Δ6 desaturase on C_{18} (Hastings et al., 2001) and C_{24} PUFA substrates, using for the latter a yeast supplemented with 24:5n-3 (Tocher et al., 2003). Interestingly, we could also confirm that the previously characterised Δ5 Fads2 from Atlantic salmon *S. salar* (Hastings et al., 2005), also showed Δ6 activity on C_{24} PUFA (24:4n-6 and 24:5n-3) and 18:3n-3, suggesting that this enzyme is indeed a bifunctional Δ6Δ5 desaturase. Bifunctionality appears a relatively widespread feature among fish Fads2 as a consequence of sub- (acquisition of additional substrate specificities) and neo-functionalisation (substitution and/or acquisition of new substrate specificities) events that have occurred in teleost Fads2 (Castro et al., 2016; Fonseca-Madrigal et al., 2014). More specifically, bifunctional Δ6Δ5 Fads2 have been found in *D. rerio* (Hastings et al., 2001), *S. canaliculatus* (Li et al., 2010), *O. niloticus* (Tanomman et al., 2013), *C. estor* (Fonseca-Madrigal et al., 2014) and *C. striata* (Kuah et al., 2016). Moreover, all the Δ4 Fads2 found so far in fish also exhibited some Δ5 desaturase activity (Fonseca-Madrigal et al., 2014; Kuah et al., 2015; Li et al., 2010; Morais et al., 2012), although none of them had Δ6 activity, which is consistent with the lack of Δ6 desaturase activity towards C_{24} PUFA substrates observed in all the Δ4 Fads2 assayed in the present study. Interestingly, our results show that the two pathways of DHA biosynthesis, namely the Sprecher and Δ4 pathways, co-exist within some species such as *S. canaliculatus* and *C. estor* since, in addition to the role of their Δ6Δ5 Fads2 in the Sprecher pathway uncovered in the present study, the existence of Δ4 desaturases in their genomes potentially enables them to further operate via the Δ4 pathway (Fonseca-Madrigal et al., 2014; Li et al., 2010).

The Δ4 pathway was first reported in the rabbitfish *S. canaliculatus* (Li et al., 2010), with further Δ4 desaturases subsequently described in *S. senegalensis, C. estor* and *C. striata* (Fonseca-Madrigal et al., 2014; Kuah et al., 2015; Morais et al., 2012). In the present study, we have expanded the number of fish lineages and species in which putative Δ4 desaturases exist. In particular, putative Δ4 desaturases were identified in 11 species belonging to Cichliformes (*O. niloticus*, *Maylandia zebra* and *Haplochromis burtoni*), Beloniformes (*O. latipes*), Blenniiformes (*Tomicodon* sp., *Acyrtus* sp. and *Enneanectes* sp.), Cyprinodontiformes (*Poecilia reticulata, Fundulus heteroclitus* and *Austrofundulus limnaeus*) and Centrarchiformes (*Micropterus salmoides*). It is very likely that the number of species with Δ4 Fads2 will expand when further genomic and/or transcriptomic data become available. This is particularly true for species within groups such as Cichliformes and Beloniformes, in which we found putative Δ4 Fads2 in all species studied in each group. Overall, these results clearly showed that the presence of Δ4 Fads2 among teleosts was far more common than initially believed when the first vertebrate Δ4 desaturase was discovered in *S. canaliculatus* (Li et al., 2010). However, the presence of Fads2 appears to be restricted to teleost species within groups regarded herein as "recent lineages", indicating that the acquisition of the Δ4 pathway occurred later during the evolution of teleosts (Castro et al., 2016; Fonseca-Madrigal et al., 2014).

In more basal teleost lineages, namely Osteoglossiformes (e.g. *A. gigas*), Anguilliformes (e.g. *A. japonica*), Cypriniformes (e.g. *D. rerio*), Siluriformes (e.g. *C. gariepinus*) and Salmoniformes (e.g. *S. salar* and *O. mykiss*), the Sprecher pathway appears to be the only possible route available for DHA biosynthesis. This is supported by, not only the apparent absence of Δ4 Fads2 in their genomes, but also the relatively higher capacity for Δ6 desaturase towards 24:5n-3 of their Fads2, as denoted by normalising the Δ6 conversions of 24:5n-3 ($\Delta_{24:5n-3}$) with that towards a control substrate ($\Delta_{control}$). Thus,

Fads2 from early divergent teleosts, along with the cartilaginous fish *S. canicula*, had relatively high capacity for Δ6 desaturation towards 24:5n-3, with $\Delta_{24:5n-3}/\Delta_{control} \geq 0.82$. In contrast, Fads2 from other species (*S. aurata*, *C. estor* and *S. canaliculatus*) had lower $\Delta_{24:5n-3}/\Delta_{control} \leq 0.43$, indicating lower activity of the Sprecher pathway. While exceptions to this pattern are likely to exist given the functional diversity among teleost Fads2 (Castro et al., 2016; Fonseca-Madrigal et al., 2014), the apparent lower contribution of the Sprecher pathway to DHA biosynthesis in late-diverging teleosts coincided with the occurrence of Δ4 Fads2 enabling certain species an alternative route for DHA biosynthesis. The limited activity of the Sprecher pathway among these teleost species might be not only restricted to their lower desaturation capability on 24:5n-3 stated above, but also to the absence of key elongase enzymes such as Elovl2, responsible for the production of the Δ6 desaturase substrate 24:5n-3 (Bell and Tocher, 2009; Leaver et al., 2008; Monroig et al., 2010a). Although Elovl4 can partly compensate such an absence in certain tissues (Carmona-Antoñanzas et al., 2011; Li et al., 2015; Monroig et al., 2011c, 2010a), loss of Elovl2 in the genomes of Acanthopterygii, a group that includes all the late-diverging species considered in this study (Morais et al., 2009), can notably compromise the efficient production of 24:5n-3 as precursor for DHA biosynthesis via the Sprecher pathway. Lack of key enzymatic capabilities in LC-PUFA biosynthetic pathways has been speculated to be a consequence of species having readily available essential LC-PUFA in their diets (Bell and Tocher, 2009; Tocher et al., 2003). This is the case of marine teleosts, particularly higher trophic species, in which no selection pressure to retain complete and active LC-PUFA biosynthetic pathways has been exerted. For example, extreme cases of marine teleosts with loss of enzymatic activities include the pufferfish (e.g. *Tetraodon nigroviridis* and *Takifugu rubripes*), which lack Fads2 in their genomes (Morais et al., 2009). In the present study, we

observed that the marine carnivore Nibe croaker *N. mitsukurii* possess a Fads2 that was the only non-Δ4 Fads2 studied that showed no detectable activity towards 24:5n-3. These results were consistent with the inability of *N. mitsukurii* Fads2 to desaturate 24:5n-3 to 24:6n-3 in yeast (Kabeya et al., 2015) and the accumulation of 24:5n-3, but not DHA, in transgenic *N. mitsukurii* carrying an *elovl2* (Kabeya et al., 2014).

The present study demonstrated that, with the notable exception of Δ4 desaturases, fish Fads2 have the ability to operate as Δ6 desaturases towards C_{24} PUFA enabling them to synthesise DHA through the Sprecher pathway. However, the so-called "Δ4 pathway" represents an alternative route in some species. Through *in silico* searches, the present study revealed that the presence of Δ4 Fads was more common than initially believed, and reported three new orders and 11 species in which putative Δ4 desaturases were identified. Interestingly, functional characterisation of the *S. salar* Fads2 previously characterised as a Δ5 desaturase confirmed this enzyme has also Δ6 desaturase activity and should be therefore regarded as a bifunctional Δ6Δ5 desaturase. Overall our results demonstrate that two alternative routes for DHA biosynthesis can exist in teleost fish. Whereas the Sprecher pathway appeared to be widely spread across the entire clade, a more scattered distribution was observed for the Δ4 pathway.

CHAPTER 6.

DETERMINING THE FUNCTION OF NOVEL FADS AND ELOVL ENZYMES IN THE AFRICAN CATFISH CLARIAS GARIEPINUS

6.1 Introduction

Fatty acyl desaturases (Fads) and elongation of very long-chain fatty acid (Elovl) proteins play key roles in the biosynthesis of long-chain (C_{20-24}) polyunsaturated fatty acids (LC-PUFA). Teleost species synthesise, to varying extents, LC-PUFA from 18:2n-6 and 18:3n-3 via a range of fatty acid desaturases (typically with Δ8, Δ6, Δ5, Δ4 desaturase activities) and elongases (Elovl2, 4 and 5) (Chapter 1). With regards to desaturases, such membrane-bound enzymes are Fads2 orthologues (Castro et al., 2012) and have the ability to introduce double bonds at either one (monofunctional) or more positions (multifunctional) (Monroig et al., 2011b). They perform carboxyl-directed desaturations and are known as "front-end" desaturases. Cytochrome b_5, the ultimate electron donor in desaturation reactions in animals (Napier et al., 1997; Sperling and Heinz, 2001), is fused to the N-terminal region of Fads-like desaturases. The possession of a cytochrome b_5-like domain appears to be restricted to enzymes that modify the proximal portion of lipid substrates facing the membrane surface such as the front-end desaturases, Δ6, Δ5 and Δ4 Fads2 (Napier et al., 1999). The fusion of the electron donor to the desaturase protein is thought to have conferred some evolutionary advantages resulting in a more efficient functioning of these enzymes (Guillou et al., 2004; Napier et al., 1999; Sperling et al., 2003). In contrast, some members of the other family of membrane-bound desaturases, stearoyl-CoA desaturases (Scd), do not possess a cytochrome b_5-like domain (Mitchell and Martin, 1995). Sequence analysis reveals this is also the case of teleosts Scd, an enzyme reported to have Δ9 desaturase activity catalysing the desaturation of saturated fatty acids to produce monounsaturated fatty acids such as 18:1n-9 (oleic acid). Importantly, vertebrates including teleosts lack methyl-directed desaturases, namely Δ12 and Δ15 desaturases mainly found in lower eukaryotes and plants (Lee et al., 2016; Wallis et al., 2002), and therefore cannot convert oleic acid (18:1n-9) into linoleic acid (LA,

18:2n-6) and linolenic acid (ALA, 18:3n-3), the latter becoming dietary essential nutritients for vertebrates.

The sequential desaturations and elongations of LA and ALA to give longer chain PUFA have been described in various teleost species (Chapter 1). Thus, the desaturation reactions are performed by Fads2 exhibiting a range of activities (Δ6/Δ5/Δ4/Δ8). In addition to Scd and Fads, there might be further uncharacterised desaturases with potential roles in LC-PUFA. Searches in *D. rerio* and several teleost species genome allowed idenfication of a gene annotated as Fads6.

Elovl2, Elovl4 and Elovl5 elongases participate in LC-PUFA synthesis (Guillou et al., 2010; Jakobsson et al., 2006; Monroig et al., 2016b). Whereas teleost Elovl5 exhibits a substrate preference for C_{18} and C_{20} PUFA, Elovl2 are much more capable of elongating C_{20} and C_{22} PUFA. Teleost Elovl4a and Elovl4b enzymes have the unique ability to synthesise very long chain saturated and unsaturated fatty acids with chain lengths reaching up to C_{36} (Chapter 4). In addition to the Elovl4 enzymes characterised in a range of fish species including *Clarias gariepinus* (Chapter 4), two *elovl4*-like genes (termed *elovl4c-1* and *elovl4c-2*) were cloned from *G. morhua* (Xue et al., 2014). Interestingly, phylogenetic analysis of these *elovl4*-like genes showed they group separately from other *elovl4* genes (Xue et al., 2014). Preliminary studies indicated there might be similar *elovl* genes that have been annotated as "*elovl4*" (or "*elovl4*-like") in many fish species genomes such as *S. salar* (XP_014071374), *I. punctatus* (XP_017324302) and *O. niloticus* (XP_005479178.1). Interestingly, two isoforms of this gene can be found in *D. rerio* (NP_001191453 and NP_001070061) but they are annotated as "Elovl8". Irrespective of the annotation, the phylogeny of this novel *elovl* gene and whether its potential sequence similarity to characterised *elovl4* can be related to roles of this enzyme in the LC-PUFA biosynthetic pathways, remains to be studied. Consequently, the present

chapter describes the cloning and functional characterisation the novel elongase *elovl8* from *C. gariepinus*, as well as the abovementioned *fads6* desaturase.

6.2 Materials and Methods

6.2.1 Molecular Cloning of Novel *fads* and *elovl* cDNAs

Amplification of partial fragments of the genes was achieved by PCR using a mixture of cDNA from eye, liver, intestine and brain as template. Primers Fads6F and Fads6R for *fads6* were designed on conserved regions of *fads6* sequences from *D. rerio* (gb|XM_003199660.4|), *I. punctatus* (gb|XM_017482704.1|), *O. niloticus* (gb|XM_019362343.1), *T. rubripes* (gb|XM_003961066.2|) and *Labrus bergylta* (gb|XM_020659396.1|) (Table 6.1) retrieved from NCBI (http://ncbi.nlm.nih.gov). Degenerate primer design was approached as described in previous chapters (e.g. Section 3.2.2).

For *elovl8* genes, primers Elovl8F2 and Elovl8R1 (Table 6.1) that were designed on conserved regions of sequences from *elovl8*-like genes from *D. rerio* (*elovl8b*) (gb|NM_001024438.2|), *I. punctatus* (gb|XM_017468816.1|), *O. niloticus* (gb|XM_005479121.3|) and *T. rubripes* (gb|XM_003974099.2|). PCR conditions consisted of an initial denaturation step at 95 °C for 2 min, 33 cycles of denaturation (95 °C for 30 s), annealing (57 °C for 30 s) and extension (72 °C for 1 min 30 s) and a final extension (72 °C for 5 min). The PCR fragments were purified using the Illustra GFX PCR DNA/gel band purification kit (GE Healthcare, Little Chalfont, UK), and sequenced (GATC Biotech Ltd., Konstanz, Germany).

Sequences of the partial gene fragments were then used to generate full-length cDNA sequence with a blast search of the high-throughput DNA Sequence Read Archive (SRA) database on NCBI. *C. gariepinus* SRA data with accession number ERX538457

generated by transcriptomic profiling with Illumina HiSeq 2000 paired end sequencing was used.

Table 6.1. Sequences of primers used for cDNA cloning of *Clarias gariepinus fads6* and *elovl8.* Restriction sites *Hin*dIII (forward) and *Xba*I (reverse) are underlined.

Name	Direction	Sequence
Initial cDNA cloning		
Elovl8F2	Forward	5'-GTCAGCCTGTVGAYTACAGC-3'
Elovl8R1	Reverse	5'-TAGCTCTGRTARTARAAGTT-3'
Fads6F	Forward	5'-AGCAGCTGGTGGGASAGGA-3'
Fads6R	Reverse	5'-TGCTCCACRTGRCAGTTGAT-3'
ORF cloning		
CGE85UF1	Forward	5'-AAACAGGTTGAGGCTGTGGA-3'
CGE83UR1	Reverse	5'-ATTCTGCATGGTGTGTGTGG-3'
CGE85VF	Forward	5'-CCCAAGCTTAGAATGGCTTCGGCGTGGCA-3'
CGE83VR	Reverse	5'-CCGTCTAGATCAGGAGCGCTTGCTCTTGC-3'
CGF65UF1	Forward	5'-CTAAGAACTAGCAGAATCAGC-3'
CGF63UR1	Reverse	5'-CGTCTTGGCTTTGAGGATCT-3'
CGF65VF	Forward	5'-CCCAAGCTTAGCATGCAGAACATCCCAGA-3'
CGF63VR	Reverse	5'-CCGTCTAGATCACTGCACCCCGACCAGCT-3'

All significant alignments were downloaded and submitted for alignment to the CAP3 assembly program (http://biosrv.cab.unina.it/webcap3/). This process was repeated as many times as necessary to extend the cDNA sequence up to the start and stop codon. The sequence derived from SRA sequences were aligned with sequence of the known partial fragment to obtain the complete cDNA sequence. Using this method, the *fads6* full-length cDNA was generated. However, for the *elovl8* this method only extended the sequence, but was not able to generate the full sequence. So Elovl8 amino acid (aa)

sequences from *I. punctatus* were used as query sequence to blast (tblastn) *C. gariepinus* SRA sequence. In addition, very short nucleotide sequences (< 40 bp) were used as queries for a blast search. In order to ensure the nucleotide sequences generated using the SRA database were correct, new sets of primers were designed and PCR used to isolate the full sequences of both genes.

6.2.2 Sequence and Phylogenetic Analysis

The deduced aa sequences of the cDNAs were compared to corresponding orthologues from other species with a Pairwise Sequence Alignment tool (http://www.ebi.ac.uk/Tools/psa/emboss_needle/) and Omega multiple alignment tool (http://www.ebi.ac.uk/Tools/msa/clustalo/). Phylogenetic analysis of the deduced aa sequences of both cDNAs from *C. gariepinus* and those from a variety of species across vertebrate lineages were carried out by constructing trees using the neighbour-joining method (Saitou and Nei, 1987), with the MEGA 7.0 software. Confidence in the resulting tree branch topology was measured by bootstrapping through 1,000 iterations. *Morteriella alpina* desaturase and elongase was used as the outgroup sequence for rooting the *fads6* and *elovl8* phylogenetic trees, respectively.

6.2.3 Synteny Analysis

Synteny analysis was perfomed to predict and establish the presence and location of the *fads6* and *elovl8* genes. The gene database on NCBI was searched for the genes and the chromosome number and names of flanking genes recorded. For *elovl8*, flanking genes, common to all the species such as Selenoprotein pb (Sepp1b), Zinc Finger SWIM-Type Containing 5 (Zswim5) and Muty DNA glycosylase (Mutyh), were used to search the NCBI gene database. This search produced a number of results for different teleost species. As the complete genome for *C. gariepinus* is not yet available, *I. punctatus*, its closest relative with its full genome sequenced, was used to predict the presence of these

genes in *C. gariepinus*. Synteny analysis of other teleost species was also conducted for further comparison.

6.2.4 Functional Characterisation of *C. gariepinus* Novel *fads* and *elovl* by Heterologous Expression in *Saccharomyces cerevisiae*

Similarly to assasys performed to characterise the funcions of desaturases and elongases from *C. gariepinus* (Chapters 3 and 4), PCR fragments corresponding to the open reading frame (ORF) of *C. gariepinus fads6* and the *elovl8* were amplified from a mixture of cDNA synthesised from liver, intestine, eye and brain total RNA, using the high fidelity Pfu DNA polymerase (Promega, USA). Primers CGF65VF and CGF63VR were used for *fads6*, whereas CGE85VF and CGE83VR were used for *elovl8* (Table 6.1). Both sets of primers contained *Hin*dIII (forward) and *Xba*I (reverse) restriction sites. PCR conditions were exactly as mentioned above (Section 6.2.1) except for the extension time, which was 3 min 30 s. The DNA fragments obtained were purified, digested with the appropriate restriction enzymes, and ligated into similarly digested pYES2 yeast expression vector (Invitrogen), as described in Section 2.6.1.

Yeast competent cells InvSc1 (Invitrogen) were transformed with the plasmid constructs pYES2-*fads6* or pYES-*elovl8* or with empty vector (control) using the S.c. EasyComp™ Transformation Kit (Invitrogen). Selection of yeast containing the pYES2 constructs and culture of a single yeast colony was performed as described in detail in Chapter 2. For the *fads6*, the PUFA substrates tested included 18:3n-3, 18:2n-6, 20:3n-3, 20:2n-6, 20:4n-3, 20:3n-6, 22:5n-3 and 22:4n-6. For *elovl8*, substrates included 18:2n-6, 18:3n-3, 18:3n-6, 18:4n-3, 20:5n-3, 20:4n-6, 22:5n-3 and 22:6n-3. These sets of fatty acid (FA) substrates are confirmed substrates for LC-PUFA biosynthetic *fads* and *elovl* genes. The ability of the *C. gariepinus* Fads6 and Elovl8 enzymes to desaturate or elongate yeast endogenous saturated FA was determined by comparing the saturated FA profiles of

yeast transformed with empty pYES2 vector and those of yeast transformed with either pYES2-*fads6* or pYES2-*elovl8*, after growing the yeast without addition of any exogenous FA substrate. The yeast were harvested after 2 days. Further analysis of the yeast samples was as described in detail in Section 2.6.3.

6.2.5 Fatty Acid Analysis of Yeast

Total lipids were extracted from yeast samples according to Folch et al. (1957). Subsequently, preparation of fatty acid methyl esters (FAME), extraction, purification and analysis were performed as described in the preceding chapters. Substrate FA conversion were calculated as the proportion of exogenously added FA substrate [product peak areas / (product peak areas + substrate peak area)] × 100. GC-MS was used to confirm double bond positions.

6.2.6 4,4-dimethyloxazoline (DMOX) Derivative Analysis with Gas Chromatography-Mass Spectrometry (GC-MS)

GC analysis of FAME offer limited structural information, so in order to confirm FA products (position of the double bonds) of the *C. gariepinus elovl8 gene* in *S. cerevisiae*, the FAME were converted to 4,4-dimethyloxazoline (DMOX) derivatives and analysed by GC-MS. Briefly, 0.5 g of 2-amino-2-methyl-1-propanol was added to the FAME samples in test tubes. The tubes were flushed with nitrogen, stoppered and sealed with tape, and placed in a heating block at 180 °C overnight. The next day, samples were allowed to cool to room temperature and 5 ml diethyl ether/isohexane (1:1, v/v) and 5 ml water added were added to the tubes, thoroughly mixed and centrifuged for 3 min at 478 g. The organic layer was transferred to new tubes, dried down under nitrogen, dissolved in 100 µl isohexane and GC-MS analysis performed to confirm identity of FA products.

6.3 Results

6.3.1 Sequence and Phylogenetic Analysis of Fads6

C. gariepinus Fads6 consisted of an ORF of 1,068 bp encoding a putative protein of 355 aa. Sequence analysis showed it possessed three histidine boxes (HLASH, HVEMHH and HVEHH) containing eight histidine residues, a characteristic feature of membrane-bound desaturases. Comparison with other vertebrate Fads6 show the aa within the first and last histidine boxes are conserved. Interestingly, the third histidine box begins with H and not Q unlike teleost front-end desaturases. Furthermore, *C. gariepinus* Fads6 lacked a consensus sequence for cytochrome $b_{5,}$ domain present in all Fads2, predictable by the absence of a haem-binding motif His-Pro-Gly-Gly (HPGG), a highly conserved and invariant characteristic of cytochrome b_5 domains found in fused cytochrome b_5 desaturases (Dahmen et al., 2013; Napier et al., 1999, 1997). Searches in genome assemblies from several vertebrate species confirmed this absence in other vertebrate Fads6. However, two Avian species, Anna's hummingbird *Calypte anna* (Figure 6.1) and the common cuckoo *Cuculus canorus*, have HPGG in the N-terminal end, but it is not certain if this indicates presence of a cytochrome b_5-like domain. Although, it is unlikely, as the region (< 40 aa) is shorter than the cytochrome b_5 domains present in other cytochrome b_5 fusion desaturases. In addition, this region does not contain the other conserved aa that make up the haem-binding pocket (Mitchell and Martin, 1995). Moreover, a blast search performed with approximately 100 bp of the sequence including the HPGG motif revealed desaturases and not cytochrome b_5 sequences.

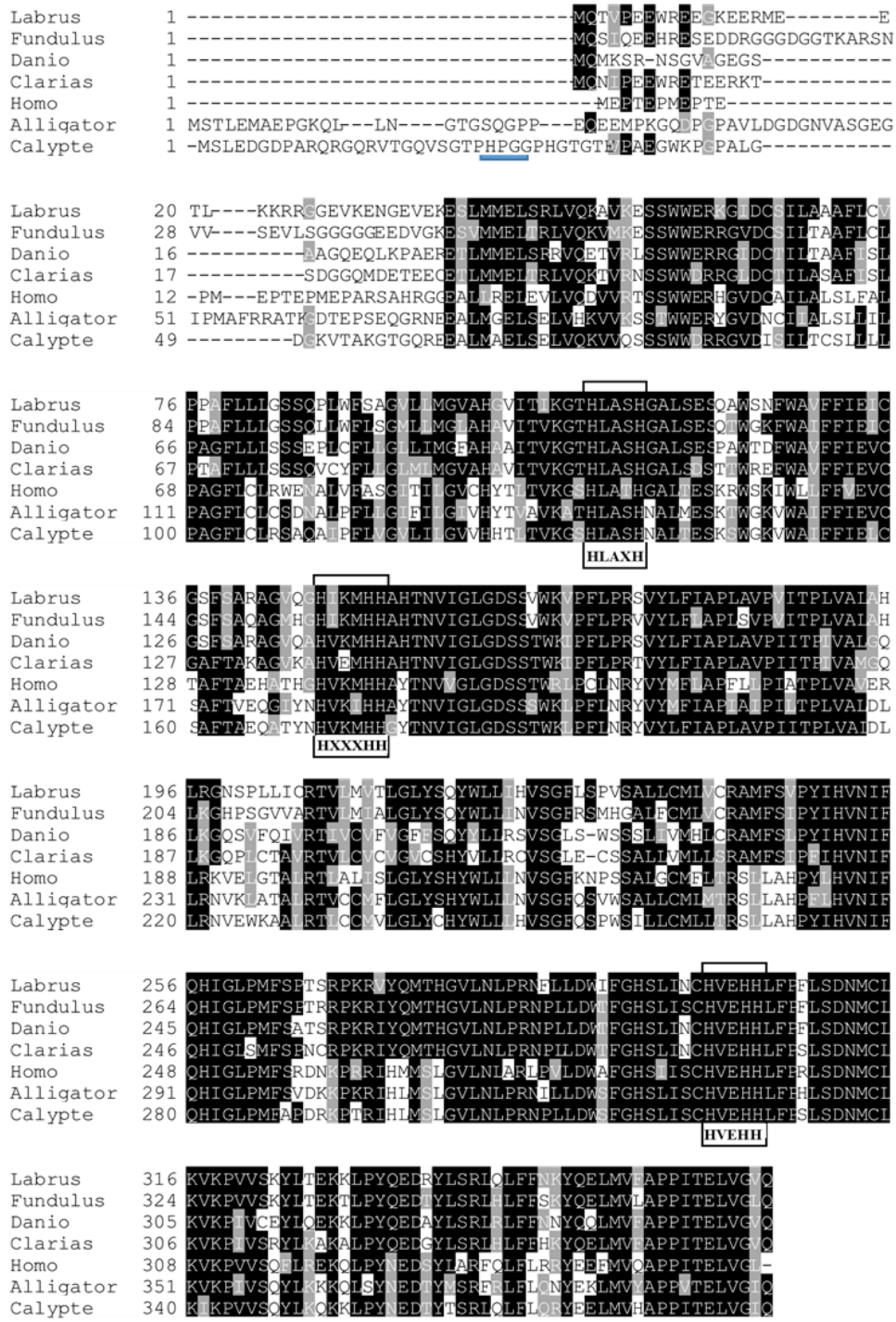

Figure 6.1. Amino acid alignment of the deduced *Clarias gariepinus* Fads6 proteins with Fads6 proteins from three teleost (*D. rerio*, *Fundulus heteroclitus*, *Labrus bergylta*), a mammalian (*Homo sapiens*), a reptilian (*Alligator sinensis*) and an avian (*Calypte anna*) species using Clustal Omega. Identical residues are shaded black and similar residues are shaded grey using BoxShade from the ExPASy Bioinformatics Resource Portal (http://www.ch.embnet.org/software/BOX_form.html). The three conserved histidine motif are seen in boxes. A HPGG motif is underlined in blue.

Pairwise comparison of the deduced Fads6 aa sequence to those of the *C. gariepinus* Fads2 that encodes a bifunctional Δ5/Δ6 desaturase (Chapter 3) revealed a low level of sequence homology (15.6 % identical). However, relatively higher sequence identities ranging from 53.7 % (*H. sapiens*), 68.4 % (*S. salar*), 72.6 % (*D. rerio*), to up to 91 % (*I. punctatus*) were found between *C. gariepinus* Fads6 and other vertebrate Fads6-like sequences (Figure 6.1). Phylogenetic analysis was conducted with the Fads6 from *C. gariepinus* and Fads2, Fads6 and Scd from a range of vertebrates. Fads6 and Scd formed a clade separate from Fads2 (Figure 6.2).

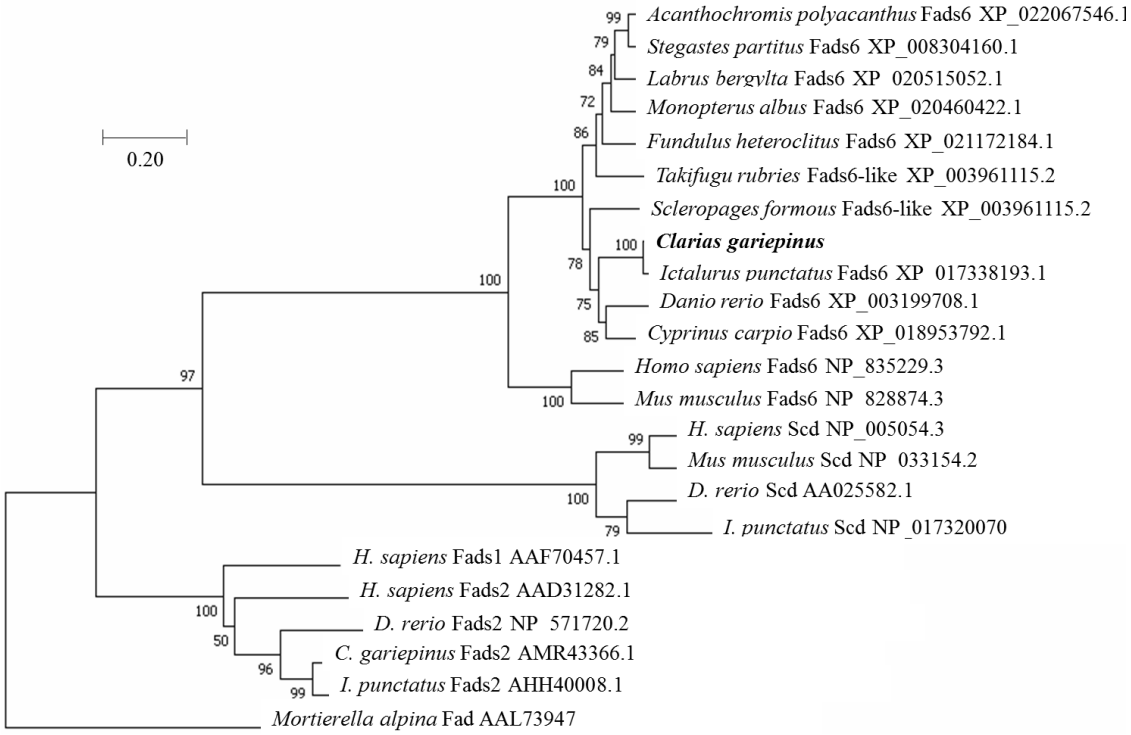

Figure 6.2. Phylogenetic tree comparing the deduced amino acid sequences of *Clarias gariepinus* Fads6 with desaturase sequences from a range of teleost species. The tree was constructed using the neighbour-joining method with the MEGA 7.0 software. The numbers represent the frequencies (%) with which the tree topology presented was replicated after 1,000 iterations. The *Mortierella alpina* PUFA desaturase was included in the analysis as an outgroup sequence to construct the rooted tree.

6.3.2 Synteny Analysis of *fads6*

Synteny analysis revealed Fads6 was present in species from all vertebrate classes and mapped on chromosomes different from Fads2. As the complete genome of *C. gariepinus* is not available, *I. punctatus,* a siluriforme and the closest relative of *C. gariepinus* with complete genome sequence, was used. The synteny map is schematically presented in Figure 6.3. Although the genes preceding *fads6* on the chromosomes were relatively similar across vertebrate species, the genes succeeding it were different between classes of vertebrates. The genes succeeding *fads6* in fish species were similar but differed from those in mammalian and avian species, except in the sarcopterygian, *L. chalumnae*, which had a gene composition more similar to tetrapods than to fish species. The arrangement of genes in *L. chalumnae* was exactly as occurs in *H. sapiens* and *Gallus gallus* (Figure 6.3). The order and orientation of the genes in fish species are relatively conserved except in *I. punctatus* where, although similar genes as in other species are present, the orientation is different (Figure 6.3).

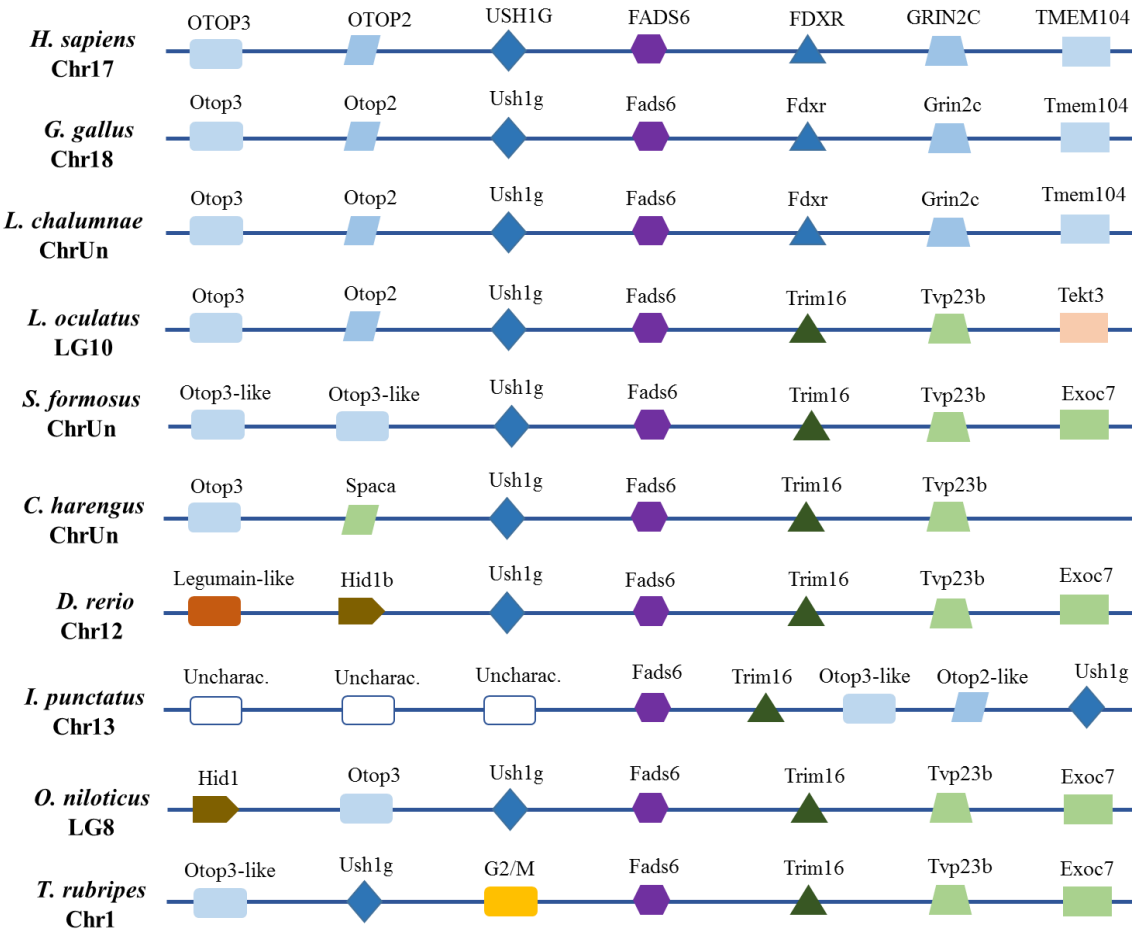

Figure 6.3. Schematic presentation of synteny blocks showing the mapping of *fads6* and other conserved genes across a range of vertebrate species. Abbreviations: Otop3, otopetrin 3; Otop2, otopetrin 2; Ush1g, usher syndrome type-1G; Fdxr, ferrodoxin reductase; Grin2c, glutamate ionotropic receptor NMDA type subunit 2C; Tmem104, transmembrane protein 104; Trim16, tripartite motif containing 16; Tvp23b, trans-golgi network vesicle protein 23; Tekt3, tektin-3; Exoc7, exocyst complex component 7; Hid1, high temperature induced dauer formation; Spaca, sperm acrosome membrane associated protein; G2/m, G2/m phase-specific E3 Ubiquitin-protein ligase like.

6.3.3 Functional Characterisation of Fads6 by Heterologous Expression in *Saccharomyces cerevisiae*

Heterologous expression of *fads6* in *S. cerevisiae* did not result in any detectable desaturation towards any of the exogenously added PUFA substrates. None of the known Fads2 desaturation activities, Δ6, Δ5, Δ4 or Δ8 were observed. In addition, the FA profile

of the yeast transformed with pYES2-*fads6* was not different from the control, indicating there was no activity towards yeast endogenous FA, predominantly saturated and monounsaturated FA. Therefore, no capability for *C. gariepinus* Fads6 to desaturate saturated or unsaturated FA could be detected by heterologous expression in *S. cerevisiae.*

6.3.4 Sequence and Phylogenetic Analysis of Elovl8

The *C. gariepinus elovl8* gene consists of an ORF of 795 bp encoding a putative protein of 264 aa. Sequence analysis showed it possessed all the characteristic motifs of Elovl family members including a single histidine motif HXXHH and the putative endoplasmic reticulum (ER) retrieval signal at the carboxyl terminus (Figure 6.4) (Agaba et al., 2005; Jakobsson et al., 2006; Leonard et al., 2004). Only two *elovl8* gene records (*D. rerio elovl8a*; 268 aa and *elovl8b*; 264 aa) are available on NCBI. Pairwise comparison of the deduced amino acid sequence of *C. gariepinus* Elovl8 to *D. rerio* Elovl8b aa sequence revealed that they share a high identity of 86.4 % and similarity of 95.1 %. *C. gariepinus* Elovl8 also shares high identity to *C. harengus* (XP_012677096: 82 %; XP_012683259; 73.5 %) and *S. salar* (XP_014071374: 78.7 %; XP_013995966; 67.9) Elovl4-like aa sequences and to both *G. morhua* Elovl4c-1 (75 % identity) and Elovl4c-2 (83 % identity). However, comparison of the *C. gariepinus* Elovl8 to *C. gariepinus* Elovl4a and Elovl4b revealed remarkably lower scores of about 40 % identity. Comparison of the *C. gariepinus* Elovl8 to other teleost Elovl4 gave similar values such as *D. rerio* (Elovl4a: 41.3 %, Elovl4a: 41 %), *A. schlegelli* (Elovl4a: 39.2 %, Elovl4b: 40.3 %), *C. harengus* (XP_012692914.1; 41 %) and *S. salar* (40.3 %) Elovl4.

Sequence analysis revealed the deduced Elovl8 aa sequence was remarkably shorter than both *C. gariepinus* Elovl4 proteins studied in Chapter 4 (40 and 50 aa compared to

Elovl4b and Elovl4a, respectively) (Figure 6.4). The missing base pairs are from the carboxyl terminus of the Elovl8 aa sequence.

Phylogenetic analysis of the *C. gariepinus* Elovl8 was performed by constructing tree comparing Elovl known to be involved in elongation of LC-PUFA, namely Elovl2, Elovl4 and Elovl5 sequences, collected from teleosts and other vertebrates (Figure 6.5). The topology of the tree showed two clades: one consisting of Elovl2 and Elovl5, and the other consisting of Elovl4 and Elovl8 (many annotated as "Elovl4-like", the designations as recorded on NCBI) (Figure 6.5). The Elovl8 proteins themselves were separated into two clusters, one group consisting of fishes of the class Chondricthyes and a sarcopterygian (*L. chalumnae*) whereas the other consisted mostly of teleost species. Most of the Elovl8-like elongases including *C. gariepinus* Elovl8 and both *G. morhua* Elovl4c-1 and Elovl4c-2 grouped with *D. rerio* Elovl8b sequence. In contrast, other Elovl8 from species such as *O. niloticus*, *C. harengus* and *Scleropages formosus* grouped with the *D. rerio* Elovl8a.

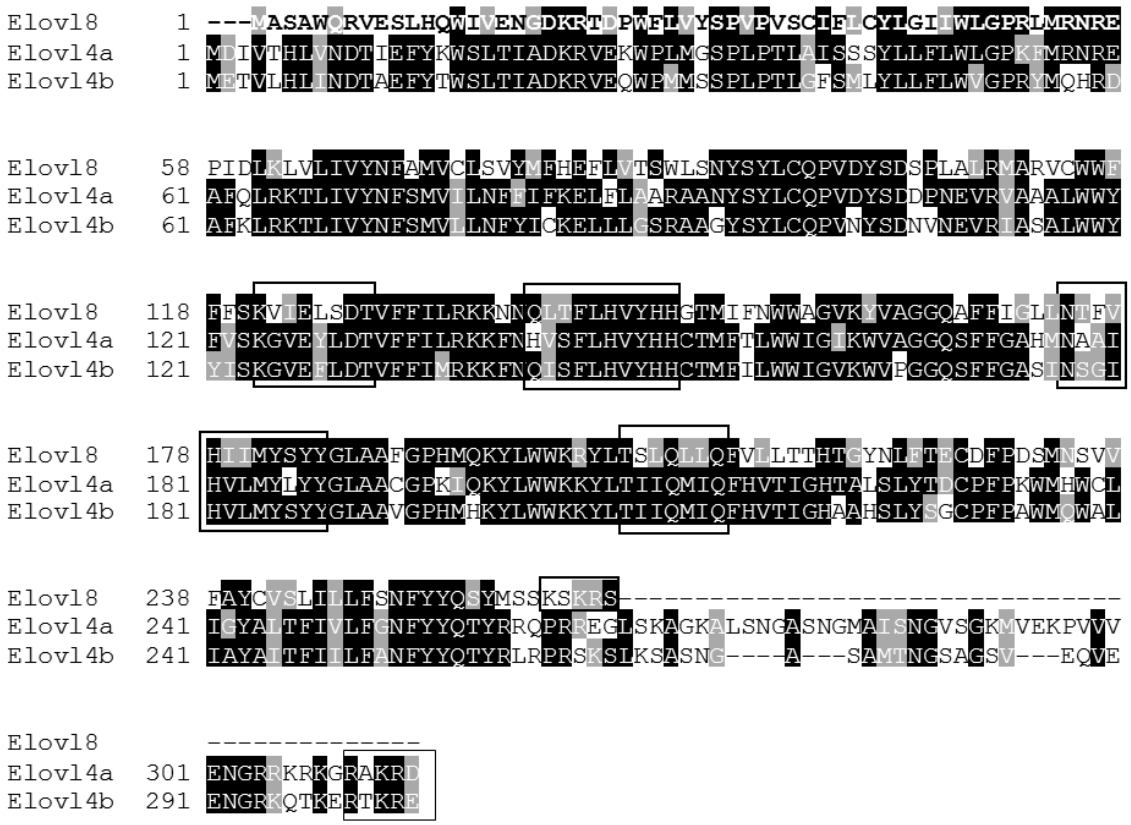

Figure 6.4. Amino acid alignment of the deduced *Clarias gariepinus* Elovl8, Elovl4a and Elovl4b proteins using Clustal Omega. Identical residues are shaded black and similar residues are shaded grey. The four conserved motif of elongases, with the second containing the single histidine motif and the putative endoplasmic reticulum (ER) retrieval signal at the C-terminus are placed in boxes.

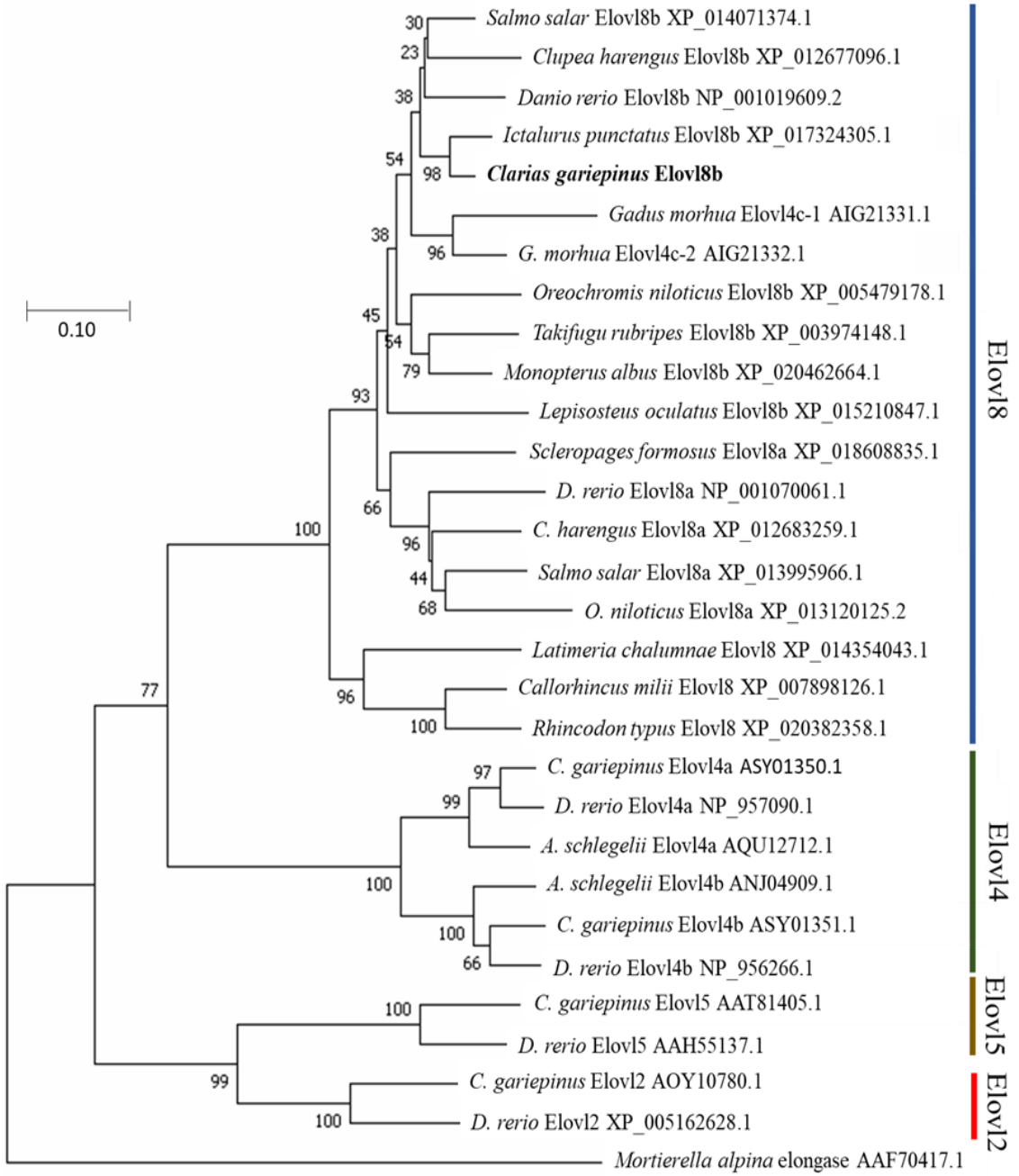

Figure 6.5. Phylogenetic tree comparing the deduced amino acid sequences of *Clarias gariepinus* Elovl8 with Elovl4, Elovl2 and Elovl5 sequences from a range of teleost species. The tree was constructed using the neighbour-joining method with the MEGA 7.0 software. The numbers represent the frequencies (%) with which the tree topology presented was replicated after 1,000 iterations. The *Mortierella alpina* PUFA elongase was included in the analysis as an outgroup sequence to construct the rooted tree.

6.3.5 Synteny Analysis of *elovl8*

Synteny analysis revealed the novel *elovl8* gene cloned from *C. gariepinus* and found as well in *I. punctatus*, is present in fish, mapping on different chromosomes from *elovl4a* or *elovl4b* gene and are flanked by genes including muty DNA glycosylase (*mutyh*), DNA methyltransferase 1-associated protein 1 (*dmap1*), zinc finger protein GLIS1 (*glis1*) and iodothyronine deiodinase 1 (*dio1*) (Figure 6.6). The *elovl8* was not found to locate in the chromosome containing any of these genes in *H. sapiens* (mammals), *G. gallus* (Aves) or *L. chalumna* (Pisces).

The order and orientation of flanking genes were similar among fish species and differed to some degree from the other vertebrate classes. *L. chalumnae* was the only exception, exhibiting a greater similarity to avian and mammalian species than to fish species. The composition of genes flanking the *elovl8* genes of *S. formosus* and *Lepisosteus oculatus* were similar and differed from both tetrapod and the other fish species. These species were included in the analysis because they are ancient, evolutionary important species.

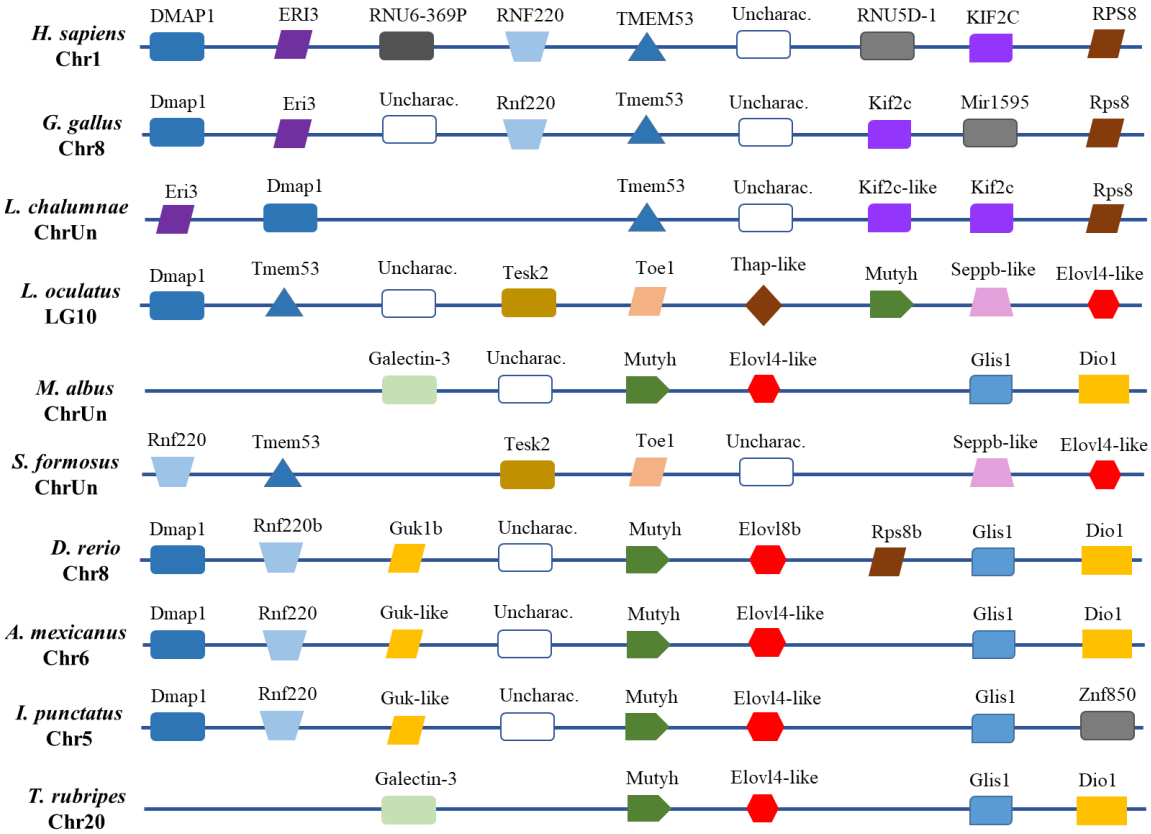

Figure 6.6. Schematic presentation of synteny blocks showing the mapping of the *elovl8* gene cloned in this study that formed a group with *Danio rerio elovl8b* and other conserved genes across a range of vertebrate species. The composition and orientation of the genes are relatively conserved especially amongst teleost species. Abbreviations: DMAP1, DNA methyltransferase 1-associated protein 1 (Dmap1); ERI3, exoribonuclease family member 3; RNU6-369P, RNA, U6 small nuclear 369, pseudogene; RNF220, ring finger protein 220; TMEM53, transmembrane protein 53; RNU5D-1, RNA, U5D small nuclear 1; KIF2C, kinensin family member 2c; RPS8, ribosomal protein S8; Mir1595, MicroRNA mir-1595; Mutyh, muty DNA glycosylase; Glis1, zinc finger protein GLIS1; Dio1, iodothyronine deiodinase 1; Tesk2, testis-specific kinase 2; Toe1, target of EGRI, member 1; Thap, THAP domain-containing protein 1; Seppb, selenoprotein pb; Rnf220, E3 ubiquitin-protein ligase Rnf220; Guk, guanylate kinase; Znf850, zinc finger protein 850.

Phylogenetic analysis revealed another *elovl8*-like gene different from *elovl4a*, *elovl4b* or the presently cloned *elovl8* gene. All efforts to clone this gene from *C. gariepinus* failed. Therefore, synteny analysis was conducted to determine its presence in catfish. The *D. rerio elovl8a* gene that formed a group with the second *elovl8*-like genes was used to begin the analysis and genes flanking these genes were then used to find species with these *elovl8* genes.

Synteny analysis revealed the second *D. rerio elovl8* gene (*elovl8a*) is located on chromosome 2 and flanked by *toe1*, *tesk2*, *seppb*, and zinc finger swim-type containing 5 (*zswim5*) (Figure 6.7). The analysis also indicated some teleost species, including *I. punctatus*, do not possess this gene, although similar genes flanking the *elovl8* gene on chromosome 2 of *D. rerio* can be found on chromosome 20 of *I. punctatus* (Figures 6.7 and 6.8). Synteny analysis of some other fish genomes demonstrated that species such as *A. mexicanus*, *Esox lucius*, *Lates calcarifer*, *L. bergylta* and *T. rubripes* do not contain orthologues of the *D. rerio elovl8a*. Interestingly, synteny analysis revealed the presence of orthologues in some fish species such as *C.harengus* (|XP_012683259|) and *O. niloticus* (|XP_013120125|).

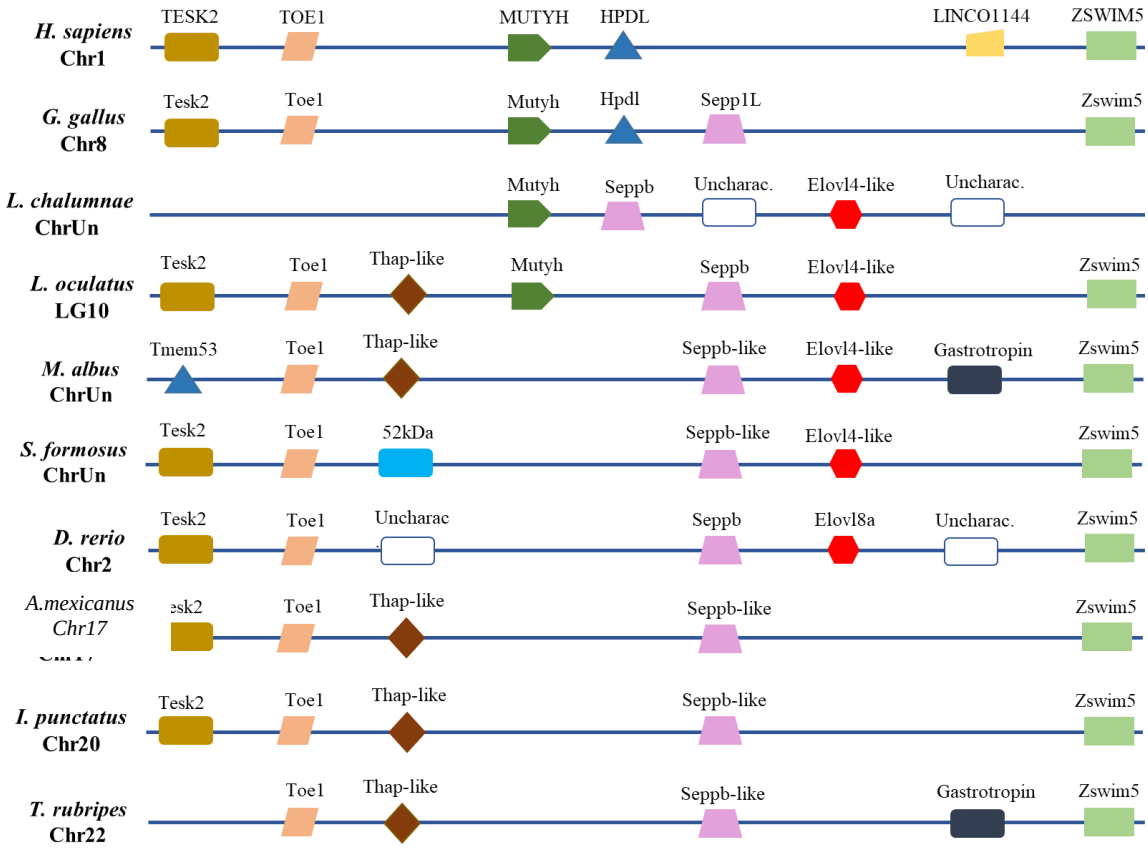

Figure 6.7. Schematic presentation of synteny blocks showing the mapping of Elovl8a and flanking genes across a range of vertebrate species. The orientation of the genes are relatively conserved especially amongst teleost species. Abbreviations: Tesk2, testis-specific kinase 2; Toe1, target of EGRI, member 1; Mutyh, muty DNA glycosylase; Hpdl, 4-hydroxyphenylpyruvate dioxygenase; LINCO1144, long intergenic non-protein coding RNA 1144; Zswim5, zinc finger swim-type containing 5; Seppb, selenoprotein pb; Thap, THAP domain-containing protein 1; 52kDa, 52kDa repressor of the inhibitor of the protein kinase.

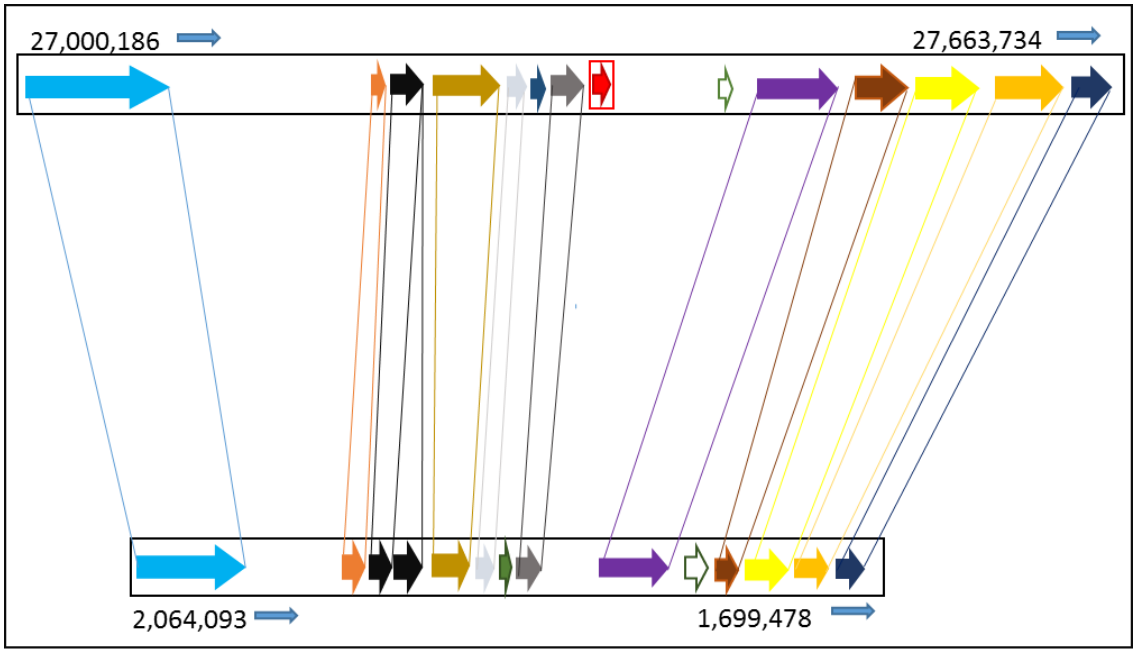

List of genes as they appear on the figure above.
***D. rerio Chromosome* 2:** 27,000,186 - 27,663,734
Cdh7, *dsela*, *tmx3*, *tesk2*, *toe1*, uncharacterised protein, *sepp1b*, *elovl8a*, uncharacterised protein, *zswim5*, *urod*, *lyn*, *tgs1*, *tmem68*

***I. punctatus Chromosome* 20:** 2,064,093 - 1,699,478
Cdh7, *dsela*, *tmx x1*, *tmx x2*, *tesk2*, *toe1*, *THAP domain containing protein 2-like*, *selenoprotein like*, *zswim5*, *uroporphyrinogen decarboxylase*, *urod*, *lyn-like x2*, *tgs1*, *tmem68*

*Full names of these genes can be found in the appendix

Figure 6.8. Schematic presentation of the synteny block of *Danio rerio* showing *elovl8a versus Ictalurus punctatus*. The block at the top represents *D. rerio* chromosome while the block below represents *I. punctatus* chromosome. Genes flanking *elovl8a* on chromosome 2 (NC_007113.7) in *D. rerio* are located on chromosome 20 of *I. punctatus* (NC_030435.1). Genes have been presented relatively in proportion to their sizes and have been allocated different colours. The order and orientation of the genes are relatively conserved. Corresponding genes appearing on both blocks have been linked by similarly coloured lines. *Elovl8a* is red in colour, in a red box, in the middle of *D. rerio* chromosome block. No corresponding gene is present in *I. punctatus* chromosome block below.

6.3.6 Functional Characterisation of Elovl8 by Heterologous Expression in *Saccharomyces cerevisiae*

Elongated products of 18:3n-3, 18:2n-6, 18:4n-3, 18:3n-6 and 20:4n-6, namely 20:3n-3, 20:2n-6, 20:4n-3, 20:3n-6 and 22:4n-6, respectively, were obtained from the

heterologous expression of the *C. gariepinus elovl8* in *S. cerevisiae* grown in the presence of these FA substrates (Table 6.2, Figure 6.9). However, it is worth noting that the relative conversions (Table 6.2) were remarkably lower than those obtained by elongation of these FA by *C. gariepinus* Elovl2 and Elovl4 (Chapters 3 and 4).

Table 6.2. Functional characterisation of the novel *Clarias gariepinus* Elovl8 elongase. *Saccharomyces cerevisiae* transformed with empty pYES2 vector (control) or pYES2 vector containing the *C. gariepinus elovl8* coding region were grown in the presence of one exogenously added fatty acid (FA) substrates (18:3n-3, 18:2n-6, 18:4n-3, 18:3n-6, 20:5n-3, 20:4n-6, 22:5n-3, 22:4n-6 and 22:6n-3). Conversions were calculated for each FA as the proportion of exogenously added FA substrate elongated [product peak area / (product peak areas + substrate peak area)] × 100. FA substrates not included in the table were not elongated.

Fatty Acid Substrate	Fatty Acid Product	Conversion (%)
18:2n-6	18:3n-6	1.37
18:3n-3	20:3n-3	2.24
18:4n-3	20:4n-3	1.44
18:3n-6	20:3n-6	1.50
20:4n-6	22:4n-6	2.58

The identity of the products was confirmed by preparing DMOX derivatives from yeast FAME samples (Figures 6.10 – 6.13). Two prominent peaks were used to confirm fatty acid DMOX derivatives: the base peak of the McLafferty ion (*m/z* = 113) and the peak at *m/z* = 126 (Christie, 2003). In addition to this, the general series of ions 14 amu apart except in regions with double bonds, where they were 12 amu apart, or the first gap from the molecular ion, which was 15 amu was also used for confirmation (Christie, 2003). Elongated products from substrates such as 20:5n-3, 22:5n-3, 22:6n-3 and 22:4n-6 were not detected.

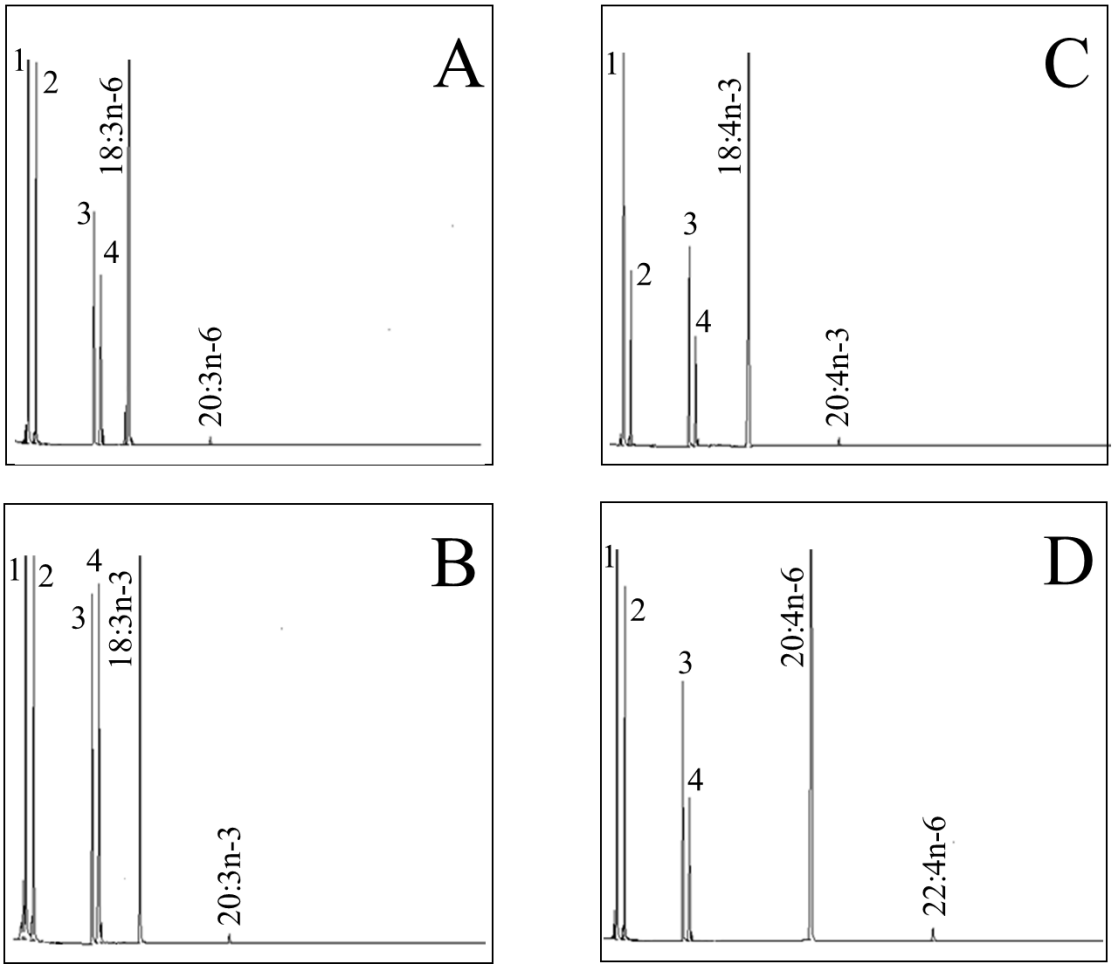

Figure 6.9. Functional characterisation of *Clarias gariepinus* Elovl8 elongase in yeast (*Saccharomyces cerevisiae*). The fatty acid profiles of yeast transformed with pYES2 containing the coding sequence of the *C. gariepinus elovl8* were determined after the yeast were grown in the presence of one of the exogenously added substrates 18:3n-6 (A), 18:3n-3 (B), 20:3n-3 (C) and 20:4n-6 (D). The first peak four peaks are derived from the exogenously added substrates. The elongation products are indicated accordingly in each panel.

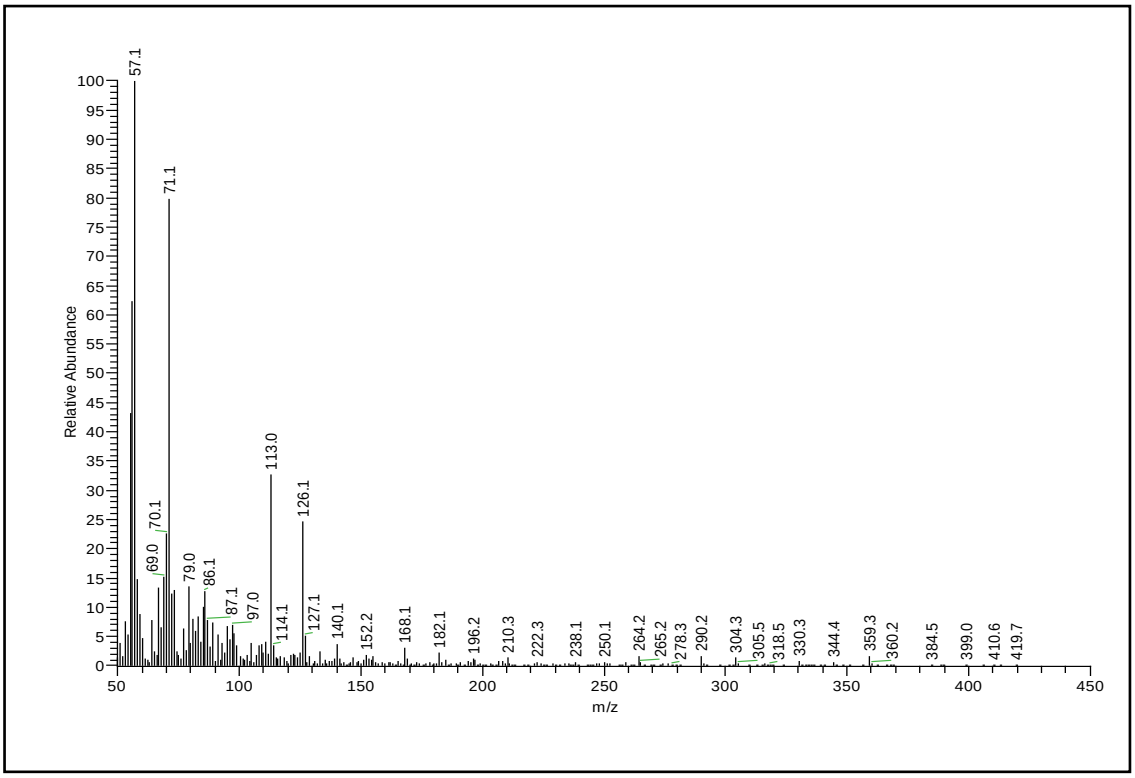

Figure 6.10. Mass spectrum of 4,4-dimethyloxazoline DMOX derivatives of 20:3n-3 elongated from 18:3n-3 by the *Clarias gariepinus* Elovl8.

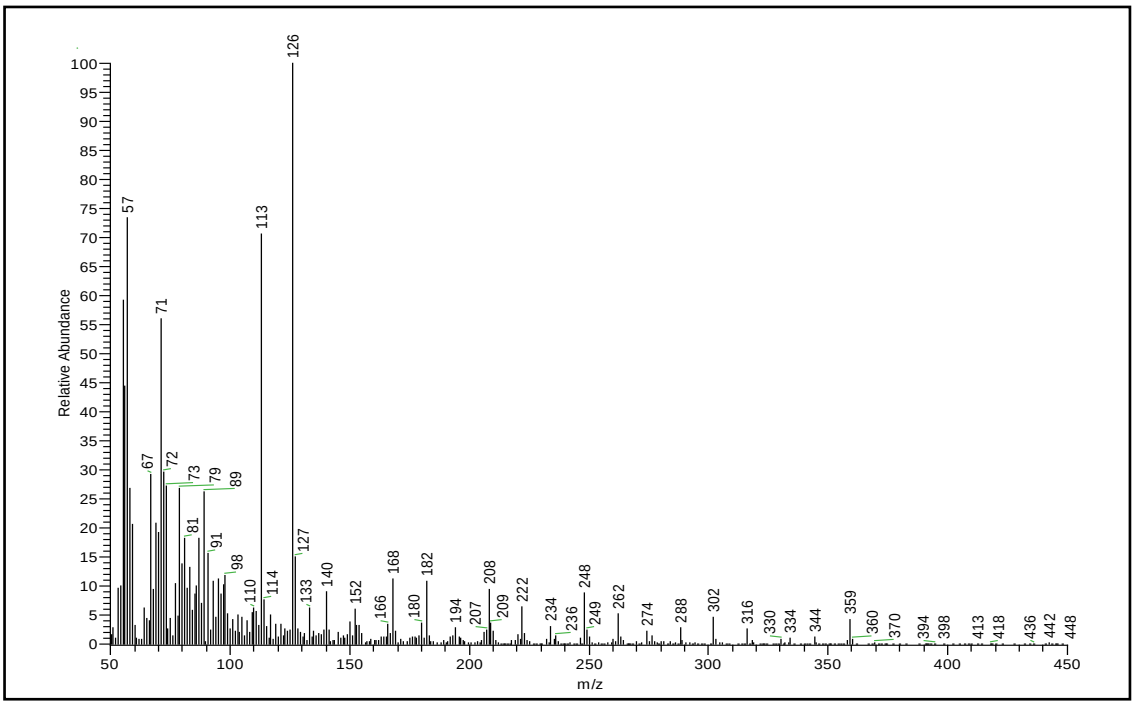

Figure 6.11. Mass spectrum of 4,4-dimethyloxazoline DMOX derivatives of 20:3n-6 elongated from 18:3n-6 by the *Clarias gariepinus* Elovl8.

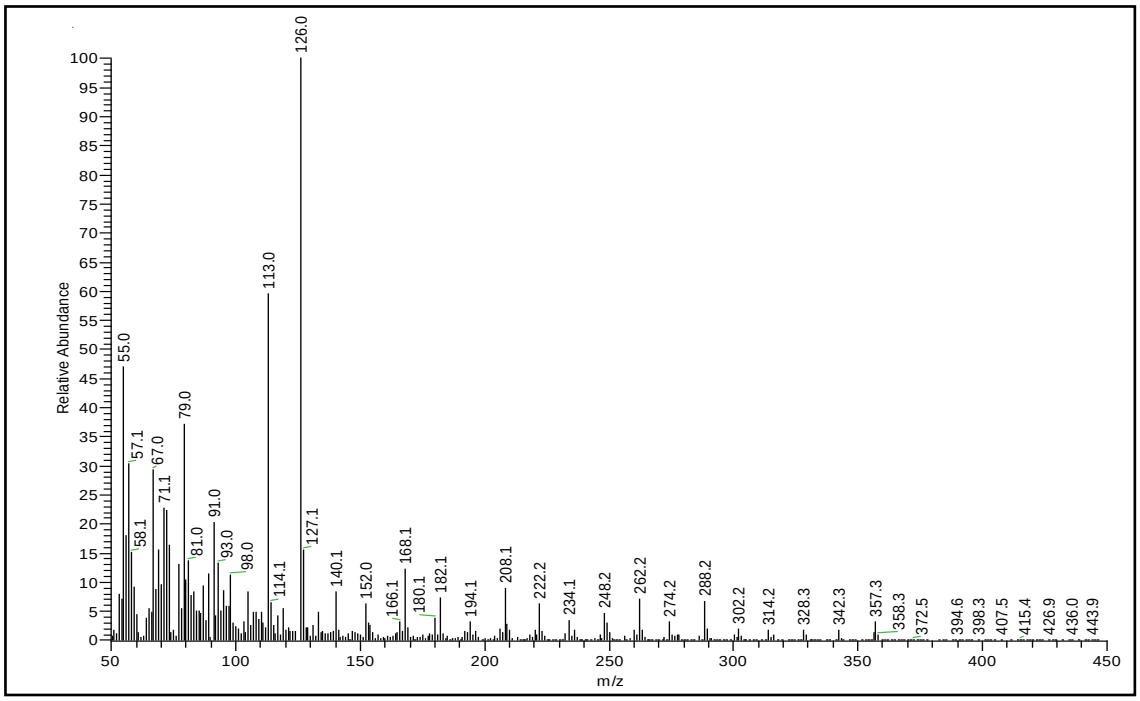

Figure 6.12. Mass spectrum of 4,4-dimethyloxazoline DMOX derivatives of 20:4n-3 elongated from 18:4n-3 by the *Clarias gariepinus* Elovl8.

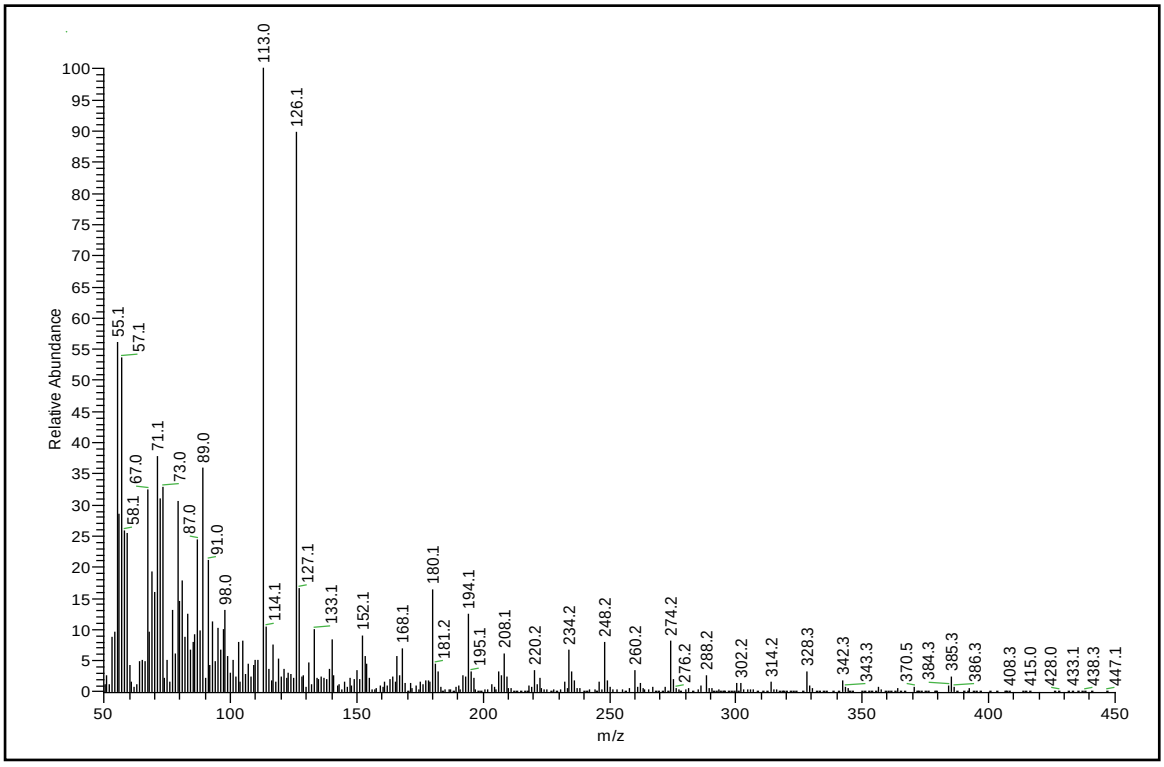

Figure 6.13. Mass spectrum of 4,4-dimethyloxazoline DMOX derivatives of 22:4n-6 elongated from 20:4n-6 by the *Clarias gariepinus* Elovl8.

6.4 Discussion

Heterologous expression of eukaryote LC-PUFA synthesis enzymes in *S. cerevisiae* has been instrumental in elucidating fatty acid synthesis pathways. The absence of LC-PUFA in *S. cerevisiae* due to their lack of the synthesising enzymes is beneficial in allowing the uncomplicated identification of genes with LC-PUFA biosynthesis activities (Leonard et al., 2004). In addition, *S. cerevisiae* has served as an appropriate eukaryote for the functional characterisation of FA enzymes because it presents a suitable membrane environment; the endoplasmic reticulum (ER) and provides the necessary system such as electron donor (cytochrome b_5), NADH, NADH: cytochrome b_5 oxidoreductase required for FA desaturation and elongation reactions to occur (Covello and Reed, 1996; Martin et al., 2007). Studies that involve the complementation of yeast mutants incapable of carrying out certain FA biosynthesising enzyme functions have also played an important role (Mitchell and Martin, 1995; Shanklin et al., 1994; Stukey et al., 1990; Tocher et al., 1998). Additionally, the development of mouse models lacking either a desaturase or an elongase, as well as cell culture studies has substantially advanced knowledge of these genes (Guillou et al., 2010; Leonard et al., 2004). In the present study, heterologous expression in *S. cerevisiae* was used to determine the functions of two uncharacterised genes, namely *fads6* and an *elovl8*.

The two genes studied herein, namely *fads6* and *elovl8*, were confirmed by sequence and phylogenetic analysis to be fatty acyl desaturase and elongase genes, respectively. However, heterologous expression in *S. cerevisiae* of the *elovl8* gene resulted in only low levels of elongated products, and heterologous expression of the *fads6* produced no desaturated products. Although functional characterisation of the *fads6* by heterologous expression in *S. cerevisiae* has not been successful, sequence and phylogenetic analysis

was used to infer its desaturase type and putative function. Possible reasons why functional characterisation in yeast did not exhibit any activity will also be discussed.

6.4.1 Fads6

Phylogenetic and sequence analysis of the Fads6 desaturase isolated from *C. gariepinus* revealed this was different from the previously characterised Fads2 (Chapter 3). Protein sequence analysis of the Fads6 desaturase showed it possessed some features characteristic of membrane bound desaturases such as the three histidine boxes (Diaz et al., 2002; Shanklin et al., 1994), but differed in the absence of an an N-terminal cytochrome b_5 domain and the aa that begins the third histidine box. The very low identity (15.6 %) between *C. gariepinus* Fads6 and Fads2 may be accounted for in part, by the difference in aa sequence length (355 bp for *C. gariepinus* and 445 bp for Fads2), which is basically the result of the absence of the cytochrome b_5 domain in Fads6. The high similarity amongst vertebrate Fads6 indicates they are highly conserved, suggesting they have functional role(s) in vertebrates.

In lacking a cytochrome b_5-like domain, the *C. gariepinus* Fads6 are similar to animal Scd (Chang et al., 2001; Hsieh et al., 2004, 2003, 2001; Mitchell and Martin, 1995). Whereas the absence of a cytochrome b_5-like domain does not preclude function as seen in Scd (which function efficiently inspite of their lack of a cytochrome b_5-like domain), the inability to elucidate the function of Fads6 by heterologous expression in *S. cerevisiae* may be related to electron transfer facilitated by cytochrome b_5. In desaturases that utilise cytochrome b_5 as their electron donor, the cytochrome b_5 can either be fused (cytochrome b_5 fusion desaturases) or free (Napier et al., 1997; Sperling and Heinz, 2001). Studies show fused desaturases cannot function if the cytochrome b_5-like domain is removed even in the presence of free microsomal cytochrome b_5 (Guillou et al., 2004; Mitchell and Martin, 1995; Napier et al., 1997; Sayanova et al., 1999). Aside from free microsomal

cytochrome b_5, Petrini et al. (2004) speculated that an alternative electron donor, possibly the cytochrome b_5 domain of stearoyl-CoA Δ9 desaturase (OLE1) was present in yeast during yeast assays. Using cytochrome b_5 mutant yeast, these authors showed that *Trypanosoma brucei* Δ12 desaturase could use the fused cytochrome b_5 of yeast as an alternate electron donor in the cytochrome b_5 mutant yeast. In another study, Dahmen et al. (2013) increased *Tetrahymena thermophila* Δ6 Fads activity in *S. cerevisiae* ten-fold by coexpression with *T. thermophila* cytochrome b_5 showing the importance of the interaction between cytochrome b_5 and desaturase. In the same study, increased desaturase activity by coexpression with *S. cerevisiae* cytochrome b_5 was only two-fold. These studies indicate cytochrome b_5 fusion domains have evolved to optimise interactions with their respective desaturase domains. This ability to utilise or interact with certain cytochrome b_5 could also be true for non-fused desaturases. Thus, failure of the heterologous expression of Fads6 in *S. cerevisiae* may be an indication of the inability of the free microsomal cytochrome b_5 to transfer electrons for the desaturation reaction and the inability of *C. gariepinus* Fads6 to make use of the alternate cytochrome b_5 source. All the above raises the question of whether coexpression of *C. gariepinus* Fads6 with *C. gariepinus* cytochrome b_5 would allow the desaturation reaction take place in yeast.

Furthermore, desaturases exhibit strong preference with regard to FA substrate chain length, location of double bonds in the chain, and their carrier molecule (Dahmen et al., 2013; Lou et al., 2014; Wang et al., 2013). According to Man et al. (2006), understanding the structure and orientation of membrane-bound desaturases will help to reveal interactions between the enzymes and their FA substrates. Indeed, some of these interactions and determinants of substrate chain length specificity have been elucidated with the provision of the three-dimensional structure information of mammalian SCD

(Bai et al., 2015; Wang et al., 2015), and by domain swapping and site-directed mutagenesis (Meesapyodsuk and Qiu, 2014). Failure of the heterologous expression of *C. gariepinus* Fads6 in yeast to yield any desaturated product maybe related to the form of FA substrate provided.

6.4.2 Elovl8

Synteny analysis showed that at least one of the *elovl8* genes was present in teleost species. Many teleost species including *I. punctatus* have just one of these *elovl8* genes and it is most likely that *C. gariepinus*, similarly, has just one too. Both *I. punctatus* and the *C. gariepinus* Elovl8 group with *D. rerio* Elovl8b (Figure 6.5). On the other hand, species like *D. rerio, C. harengus* and *O. niloticus* possess both types. Similar searches of both human and *G. gallus* genomes did not reveal any of these *elovl8* genes. However, in these species and in teleosts such as *C. milii, S. formosus* and *L. oculatus*, genes flanking both *elovl8* genes can all be found on one chromosome whether they possess one of the *elovl8* genes or not. The species that have both genes have them on different chromosomes. Synteny analysis and the inability to isolate the second Elovl8-like protein (Elovl8a) strongly suggest this protein does not exist in *C. gariepinus*. Similarly, search of other fish species genome showed this gene is absent in many species such as *A. mexicanus, E. lucius, L. calcarifer, L. bergylta* and *T. rubripes*.

Moreover, although the *L. oculatus* and *S. formosus* synteny showed many similarities, the phylogenetic analysis indicated the genes are different. Teleost species with both *elovl8* genes were mostly from the order Percomorpharia (including Carangaria, Ovalentaria and Eupercaria species) but also Salmoniformes and Cyprinodontiformes. The earliest species in which both *elovl8* genes were found was in *M. albus*. However, in this species, only one *elovl8* gene sequence, possibly an *elovl8a*-like was available. The genes were also present in species like *T. rubripes* (*elovl8b*-like) and *O. latipes* (both),

which do not possess *elovl2* genes (Leaver et al., 2008), and thus may play an important role in FA elongation in these species. Although *elovl8* genes were not found amongst genes flanking both *elovl8* genes in other vertebrate classes, we cannot conclude they do not exist in these classes since they may occur on other chromosomes, flanked by different genes.

C. gariepinus Elovl8 possessed characteristic features of Elovl enzymes such as a single histidine box and the carboxyl-terminal region that acts as an endoplasmic reticulum retention signal (Jakobsson et al., 2006; Leonard et al., 2004; Meyer et al., 2004). The low sequence identity score between the newly cloned Elovl and *C. gariepinus* Elovl4s (40 %) may be partly due to the missing aa sequences from the C-terminus (Figure 6.4). The *C. gariepinus* Elovl8 protein belonged to a group including both functionally uncharacterised putative Elovl4c reported in *G. morhua* (Xue et al., 2014) and the putative Elovl8b of *D. rerio*. This group was separate from other Elovl8-like proteins, which grouped with the putative Elovl8a of *D. rerio*. Pairwise analysis of aa sequences from both types (Elovl8a and Elovl8b) resulted in 66 - 73 % identities, showing a greater sequence identity between them than with either Elovl4a or Elovl4b. This suggests the Elovl8 protein (Elovl8a and Elovl8b) are different from Elovl4a and Elovl4b and have been wrongly annotated.

The *C. gariepinus* Elovl8 protein performed similar reactions as Elovl5, albeit at a much lower conversion than those of many of the previously reported Elovl-like elongases expressed in yeast. The *C. gariepinus* Elovl8 was capable of elongating 18:3n-3, 18:2n-6, 18:4n-3, 18:3n-6 and 20:4n-6, but there was no evidence of elongation of 20:5n-3, 22:5n-3, 22:6n-3, 22:4n-6 or saturated FA. Although the efficiency of these elongations was low in the case of the Elovl8 protein of *C. gariepinus*, this may not necessarily be the case in other species (Table 6.2; Figure 6.9). The lack of elongation capacity on

20:5n-3 (a preferred substrate for Elovl5 elongases), along with the remarkably low conversions, can indicate that Elovl8 might have only residual funcions within LC-PUFA biosynthesis.

The functional characterisation of this protein increases the number of Elovl enzymes already known to participate in LC-PUFA synthesis in fish. With the presence of a variety of Elovl proteins carrying out similar, overlapping functions, and the suggestion that Elovl4a and Elovl4b may be able to perform elongation reactions carried out by Elovl2, it is unlikely that PUFA elongation is the limiting factor in LC-PUFA synthesis in fish. However, in the presence of numerous *elovl* genes performing similar activities, there is the possibility that some of them may have become redundant leading to the low activity observed within Elovl8. This redundancy could also, potentially, lead to reduced or total loss of functionality, which could explain why the activity of this gene is low in this species, whereas Elovl2, Elovl4a, Elovl4b and Elovl5 display high efficiencies (Agaba et al., 2005; Chapters 3 and 4).

6.4.3 Conclusions

Molecular cloning and functional characterisation of *C. gariepinus* Fads6 and Elovl8 by heterologous expression in *S. cerevisiae* have been performed. The yeast assay successfully used for functionally characterise other enzymes (Chapters 3-5) did not reveal the function of *C. gariepinus* Fads6. The results showed *C. gariepinus* Elovl8 was capable of elongating some of the FA substrates assayed (18:3n-3, 18:2n-6, 18:4n-3, 18:3n-6 and 20:4n-6), but not efficiently. Synteny analysis showed the enzymes are ubiquitous and conserved in many groups of animals. Further study of these genes in other fish, particularly those lacking other desaturase and elongase enzymes may lead to better understanding of these enzymes.

CHAPTER 7.

GENERAL DISCUSSION AND CONCLUSIONS

7.1 Introduction

Studies elucidating long-chain (C_{20-24}) polyunsaturated fatty acid (LC-PUFA) synthesis pathways have been driven by the revelation of the relationship between n-3 LC-PUFA in diets and human health (Ayeloja et al., 2013; Bell et al., 2003; Cardoso et al., 2016; Monroig et al., 2011b). Moreover, in aquaculture, increasing substitution of fish oil (FO) rich in LC-PUFA with vegetable oil (VO) lacking LC-PUFA in fish diet that affect LC-PUFA profile of farmed fish (Bell et al., 2002; Tocher et al., 2002), have made these studies essential. These substitutions have no significant effect on the growth or feed conversion ratio of many freshwater and salmonid species (Al-Souti et al., 2012; Bell et al., 2002; Turchini et al., 2009), but result in decreased levels of n-3 LC-PUFA and the n-3/n-6 ratio, thereby compromising their benefits for the consumers (Ng et al., 2003, 2001; Simopoulos, 2016; Sprague et al., 2017; Turchini et al., 2009, 2006). Moreover, experimental studies have indicated that the rate at which dietary C_{18} PUFA is converted is not sufficient to increase LC-PUFA up to levels obtained in fish fed diets containing FO (Bell et al., 2002; Bell and Dick, 2004; Böhm et al., 2014; Tocher et al., 2002).

Many farmed freshwater fishes including carps, tilapia and catfish are lean fishes with generally lower than 5 % fat by weight in their muscle tissue (Ayeloja et al., 2013; Memon et al., 2011) and are not regarded as very rich sources of LC-PUFA, such as eicosapentaenoic acid (EPA) and docosahexaenoic acid (DHA). However, these species are still valuable sources of LC-PUFA and account for a large portion of the global fish supply (Al-souti and Claereboudt, 2014; Bahurmiz and Ng, 2007; Steffens, 1997; Turchini et al., 2009). Studies show greater use of VO in their diet further decreases the already low FA content and skews n-3/n-6 FA ratios, which are also health important indices (Al-Souti et al., 2012; Böhm et al., 2014; Tocher et al., 2002). With no cheaper or more sustainable alternatives to FO available yet, VO will continue to be used as a

substitute in aquafeed for the foreseeable future and therefore, practical culture strategies for improving and optimising the LC-PUFA content of VO-fed fish are still required. These include designing feed that optimise the conversion of C_{18} precursors to LC-PUFA, identification and selection of genetic strains with enhanced LC-PUFA body content and/or biosynthesis and even genetic manipulations (Bell et al., 2003; Betancor et al., 2016; Gjedrem, 2000; Kabeya et al., 2016, 2014; Klempova et al., 2013; Monroig et al., 2011b; Nguyen et al., 2010; Watters et al., 2012). Understanding the biochemistry of the enzymes involved in FA synthesis and elucidating the biosynthetic pathways is key to undertake, successfully, any of these proffered solutions.

It is against this background that the present study was developed. The overall objective of this research work was to investigate the repertoire of genes and enzymatic functionalities involved in the production of LC-PUFA from the C_{18} precursors in *C. gariepinus* and thus, elucidate its LC-PUFA synthesis pathway. This will enable the determination of their specific dietary EFA and thus allow the design of appropriate diets for their optimal growth and development. This is important considering the commercial and socio-economic value of this species and its role in food security in African countries.

Six genes, namely *fads2*, *fads6*, *elovl2*, *elovl4a*, *elovl4b* and an *elovl8b*, were cloned and functionally characterised from *C. gariepinus*. Two of these (*fads2* and *elovl2*), together with the previously cloned *elovl5* (Agaba et al., 2005) are known to participate in LC-PUFA biosynthesis. The *elovl4*s, *elovl4a* and *elovl4b* catalysed the production of very long-chain (> C_{24}) polyunsaturated fatty acid (VLC-PUFA), whereas *fads6* and *elovl8*, are novel genes that, to the best of our knowledge, have not yet been functionally characterised in any vertebrate. Results on desaturase and elongase activities within the LC-PUFA biosynthetic pathways of *C. gariepinus* and findings on the novel Fads6 and Elovl8 enzymes investigated are discussed in the sections below.

7.2 Desaturases in LC-PUFA biosynthesis pathways

The *C. gariepinus fads2* encoded an enzyme with Δ6 and Δ5 activities and thus is a bifunctional Δ6Δ5 Fads2. It is capable of converting 18:3n-3 and 18:2n-6 to 18:4n-3 and 18:3n-6, respectively (Δ6 desaturase activity), and 20:4n-3 and 20:3n-6 to 20:5n-3 and 20:4n-6, respectively (Δ5 desaturase activity), with a preference for n-3 over n-6 substrates. This expands the list of bifunctional Fads2 described in teleost species which include *Danio rerio* (Hastings et al., 2001), *Siganus canaliculatus* (Li et al., 2010), *Oreochromis niloticus* (Tanomman et al., 2013), *Chirostoma estor* (Fonseca-Madrigal et al., 2014) and *Channa striata* (Kuah et al., 2016).

C. gariepinus Fads2 also exhibited Δ8 desaturation capability, converting 20:3n-3 and 20:2n-6 to 20:4n-3 and 20:3n-6, respectively. This is consistent with the majority of teleost Δ6 Fads2 characterised till date (Fonseca-Madrigal et al., 2014; Kabeya et al., 2017, 2015; Monroig et al., 2011a; Wang et al., 2014). *C. gariepinus* Fads2 displayed higher efficiency towards the C_{18} PUFA (Δ6 activity) compared to 20:3n-3 and 20:2n-6 (Δ8 activity), in agreement with the "Δ8 pathway" being regarded as a minor pathway in comparison to the Δ6 desaturation pathway (Monroig et al., 2011a; Park et al., 2009).

Investigation of the Δ6 activity towards C_{24} substrates (24:5n-3 and 24:4n-6) of *C. gariepinus* Fads2 and Fads2 from a cross section of fish species revealed *C. gariepinus* Fads2 and all the other fish Δ6 Fads2 tested, except *N. mitsukurii* Δ6 Fads2, were capable of converting 24:5n-3 and 24:4n-6 to 24:6n-3 and 24:5n-6, respectively. *C. gariepinus* Fads2 was not capable of catalysing the Δ4 desaturation of 22:5n-4. Moreover, genome searches using the conserved, distinctive YXXN motif of Δ4 desaturase revealed Δ4 Fads2 only amongst recently evolved fish species along the entire tree of life of teleosts (Betancur-R et al., 2013). Indicating that more basal species including *C. gariepinus* are capable of DHA biosynthesis only through the Sprecher pathway. In contrast, both the

Sprecher and Δ4 pathways seem to co-exist in species such as *S. canaliculatus* and *C. estor*, that possess a complement of Fads2 enabling key desaturation reactions (Δ4 desaturation of 22:5n-4 and Δ6 desaturation of 24:5n-3) within both routes (Fonseca-Madrigal et al., 2014; Li et al., 2010). Perhaps to compensate for their lack of Fads2 with Δ4 desaturase activity, the more ancient teleosts species displayed relatively higher capacity for Δ6 desaturation towards 24:5n-3 than recently evolved teleost (Table 5.2).

Overall, *C. gariepinus* Fads2 displays the multi-functionality and plasticity associated with teleost Fads2 (Castro et al., 2016; Fonseca-Madrigal et al., 2014), and is capable of performing all the desaturation steps required for endogenous biosynthesis of LC-PUFA via the Sprecher pathway (Figure 7.1).

7.3 Elongases in LC-PUFA pathways

The molecular cloning of *elovl2* and *elovl4* genes, in addition to the previously cloned *elovl5* (Agaba et al., 2005), showed *C. gariepinus* has the complete set of Elovl enzymes required for LC-PUFA biosynthesis (Figure 7.1). Compared to Elovl5, Elovl2 have been characterised in few fish species, namely *S. salar*, *D. rerio* and *O. mykiss* (Gregory and James, 2014; Monroig et al., 2009 and Morais et al., 2009). Consistent with the activities shown by these teleost Elovl2, *C. gariepinus* Elovl2 predominantly elongates C_{20} and C_{22} PUFA, with a preference for n-3 over n-6 substrates. The presence of Elovl2 and its increased ability, compared to Elovl5 elongases, to elongate 22:5n-3 to 24:5n-3, a critical enzymatic step in the biosynthesis of DHA through the Sprecher pathway has been suggested to be evidence supporting LC-PUFA biosynthetic capability in freshwater species (Morais et al., 2009).

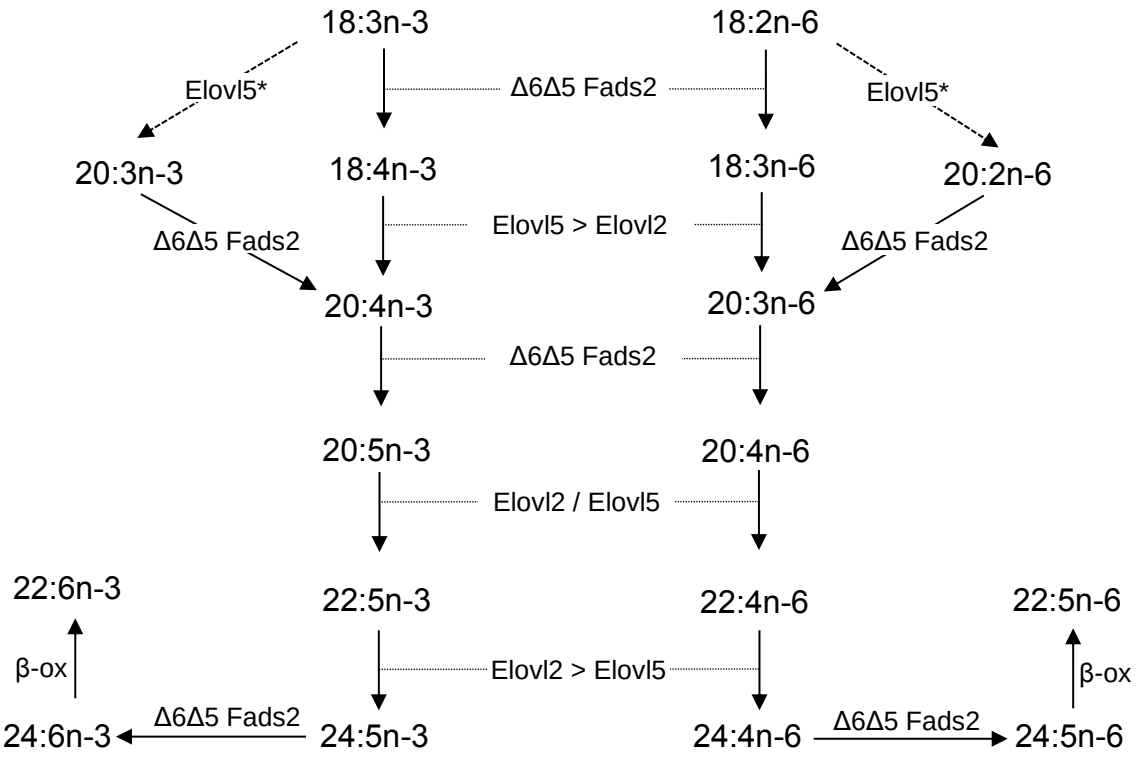

Figure 7.1. The biosynthesis pathway of long-chain (C_{20-24}) polyunsaturated fatty acids from α-linolenic (18:3n-3) and linoleic (18:2n-6) acids in *Clarias gariepinus*. Enzymatic activities shown in the scheme are predicted from heterologous expression in yeast of the herein investigated Δ6Δ5 fatty acyl desaturase 2 (Δ6Δ5 Fads2) and Elovl2 elongase, and the previously reported Elovl5 (Agaba et al., 2005). The Elovl4s have not been included in the figure, though they participate in the pathway. β-ox, partial β-oxidation; Elovl, fatty acyl elongase; Fads, fatty acyl desaturase. *Gene not cloned and functionally characterised in this study.

The cloning of two isoforms of Elovl4 (Elovl4a and Elovl4b) was consistent with *in silico* studies that suggest all teleosts possess both types of Elovl4 (Castro et al 2016). Both *C. gariepinus* Elovl4 enzymes were active towards saturated and unsaturated long-chain FA, producing elongated products of up to C_{32} (VLC-SFA) and C_{36} (VLC-PUFA). These results were consistent with elongation abilities of most teleost Elovl4 characterised so far (Jin et al., 2017; Li et al., 2015, 2017, Monroig et al., 2012, 2011c; Monroig et al.,

2010a), the majority of which are Elovl4b. Similarly to Elovl4a from *A. schlegelii*, but in contrast to the *D. rerio* orthologue, the latter having limited capability to biosynthesise VLC-PUFA (Monroig et al., 2010a), the *C. gariepinus* Elovl4a exhibited elongation abilities similar to Elovl4b, and thus was able to produce VLC-PUFA of up to $C_{36.}$ In addition, in contrast to Elovl4a, *C. gariepinus* Elovl4b efficiently elongated exogenously added 22:6n-3 to 32:6n-3, a VLC-PUFA that has been detected in retinal phosphatidylcholine of gilthead seabream *Sparus aurata* (Monroig et al., 2016a).

7.4 Tissues expression patterns of genes encoding LC- and VLC-PUFA biosynthesising enzymes

Tissue expression analysis showed *C. gariepinus fads2* and *elovl* genes were ubiquitously expressed, although expression was greater in certain tissues. Liver, brain and pituitary were found to contain the highest transcript levels of *C. gariepinus fads2* and *elovl2*. This is consistent with the pattern observed in freshwater and salmonid fish species (Hamid et al., 2016; Monroig et al., 2009). The expression of *elovl5* was also high in liver but was highest in the intestine while the lowest expression level was found in muscle. Gonads (testis and ovary) showed the lowest transcript levels for both *fads2* and *elovl2*. These results indicated, in agreement with previous studies, that LC-PUFA biosynthesis was highest in liver, brain and intestine (Monroig et al., 2009; Morais et al., 2009; Zheng et al., 2005).

Tissue distribution analysis of *elovl4* mRNAs in *C. gariepinus* showed high expression of *elovl4a* in pituitary and brain, whereas female gonad and pituitary had the highest expression levels of *elovl4b*. These expression patterns were consistent with the reported high expression of these genes in neuronal and reproductive tissues of teleosts (Carmona-Antoñanzas et al., 2011; Monroig et al., 2010a), tissues containing great amounts of VLC-PUFA (Agbaga, 2016; Poulos, 1995).

7.5 Novel enzymes Fads6 and Elovl8

Phylogenetic and synteny analysis of the novel Elovl8 enzymes revealed two forms (Elovl8a and Elovl8b) exist in teleosts. The herein cloned *C. gariepinus elovl8* gene was an orthologue of the *D. rerio* Elovl8b, but the Elovl8a is absent in *C. gariepinus*. The *C. gariepinus* Elovl8b elongated only C_{18} PUFAs and 20:4n-6, and at a much lower rate than the other *C. gariepinus* Elovl proteins. This reduced substrate specificity and functional activity, in comparison to the other characterised *C. gariepinus* Elovl proteins implies the Elovl8 may not contribute to the LC-PUFA synthesis in this species.

Sequence, phylogenetic and synteny analysis of the Fads6 indicate they are well conserved across vertebrate species and differ from Fads2. Heterologous expression of the *C. gariepinus fads6* in yeast produced no desaturated products. A number of reasons, some of which were discussed in Section 6.4.1, may have been responsible for this failure. This implies that a different method of functionally characterising genes, other than the yeast heterologous expression system may be required to elucidate the functions of Fads6.

7.6 Conclusion

In conclusion, *C. gariepinus* possesses all the desaturase and elongase enzymes required for the conversion of 18:3n-3 to EPA via the prominent 'Δ6Δ5 pathway' or the alternative 'Δ8Δ5 pathway', whereas conversion of EPA to DHA occurs via the Sprecher pathway but not the 'Δ4 pathway' (Figure 7.1). This also applies to the n-6 FA series beginning with 18:2n-6. These findings demonstrated that *C. gariepinus* has an active LC-PUFA biosynthesis pathway that potentially enables them to endogenously synthesise the physiologically important LC-PUFA ARA, EPA and DHA from the C_{18} PUFA precursors. Consequently, dietary C_{18} PUFA, linoleic acid (18:2n-6) and α-linolenic acid (18:3n-3), abundant in VO can satisfy their essential fatty acid requirements. This may

explain the reported ability of *C. gariepinus* to perform better when fed VO than FO (Hoffman and Prinsloo, 1995a; Ng et al., 2003, 2004). Although, feeding a combination of FO and VO diet has been shown to give the best growth rates (Ng et al., 2003; Ochang et al., 2007; Solomon et al., 2012). The differences in these studies may be attributable to the stage of development of the experimental fish. The rate of LC-PUFA biosynthesis may be insufficient to meet physiological demand at specific stages of development, with the consequence that dietary provision of LC-PUFA result in better growths at such stages. Although, quantitative EFA requirement could not be established in this study, it is required for the complete understanding of *C. gariepinus* ability to utilise VO and thus, to enable the formulation VO based diets that give optimal growth.

Future Perspectives

Considering the importance of *C. gariepinus* in the human diet, and the potential benefits complete understanding of its LC-PUFA biosynthetic pathways will have on its production, it is important that further studies that utilise the results from this study be carried out. These should include

1. Feed trials to demonstrate LC-PUFA biosynthetic capacities of *C. gariepinus* at different developmental stages.
2. Feed trials to determine quantitative EFA requirements *C. gariepinus* at different developmental stages.
3. Feed trials determining the best ratios of C_{18} PUFAs that can improve the n-3 LC-PUFA profile of farmed *C. gariepinus.*
4. Long term nutritional programmes aimed at the development of *C. gariepinus* strains with increased LC-PUFA biosynthetic capacities and optimization of these gains over several generations.

5. Further, long-term trials involving the identification and selection of genetic strains with enhanced LC-PUFA body content and/or LC-PUFA biosynthetic capacities.

REFERENCES

Agaba, M.K., Tocher, D.R., Dickson, C.A., Dick, J.R., Teale, A.J., 2004. Zebrafish cDNA encoding multifunctional fatty acid elongase involved in production of eicosapentaenoic (20:5n-3) and docosahexaenoic (22:6n-3) acids. Mar. Biotechnol. 6, 251–261.

Agaba, M.K., Tocher, D.R., Zheng, X., Dickson, C.A., Dick, J.R., Teale, A.J., 2005. Cloning and functional characterisation of polyunsaturated fatty acid elongases of marine and freshwater teleost fish. Comp. Biochem. Physiol. Part B Biochem. Mol. Biol. 142, 342–352.

Agbaga, M., 2016. Different mutations in ELOVL4 affect very long chain fatty acid biosynthesis to cause variable neurological disorders in humans, in: Bowes Rickman, C., LaVail, M.M., Anderson, R.E., Grimm, C., Hollyfield, J., Ash, J. (Eds.), Retinal Degenerative Diseases, Advances in Experimental Medicine and Biology, 854: 129–135.

Agbaga, M.P., Brush, R.S., Mandal, M.N.A., Henry, K., Elliott, M.H., Anderson, R.E., 2008. Role of Stargardt-3 macular dystrophy protein (ELOVL4) in the biosynthesis of very long chain fatty acids. Proc. Natl. Acad. Sci. 105, 12843–12848.

Agbaga, M.P., Mandal, M.N.A., Anderson, R.E., 2010. Retinal very long-chain PUFAs: New insights from studies on ELOVL4 protein. J. Lipid Res. 51, 1624–1642.

Al-Souti, A., Al-Sabahi, J., Soussi, B., Goddard, S., 2012. The effects of fish oil-enriched diets on growth, feed conversion and fatty acid content of red hybrid tilapia, *Oreochromis* sp. Food Chem. 133, 723–727.

Al-souti, A., Claereboudt, M., 2014. Total lipid and fatty acid content of tilapia (GIFT strain) grown in a semi-intensive system: A descriptive view. Res. Heal. Nutr. 2, 13–19.

Alimuddin, K.V., Satoh, S., Takeuchi, T., Yoshizaki, G., 2008. Cloning and over-expression of a masu salmon (*Oncorhynchus masou*) fatty acid elongase-like gene in zebrafish. Aquaculture 282, 13–18.

Atanda, A.N., 2007. Freshwater fish seed resources in Nigeria, in: Bondad Reantaso, M.G. (Ed.), Assessment of Freshwater Fish Seed Resources for Sustainable Aquaculture. FAO Fisheries Technical Paper. FAO Fisheries Technical Paper. No. 501. Rome, FAO, pp. 361-380.

Ayeloja, A.A., George, F.O.A., Dauda, T.O., Jimoh, W.A., Popoola, M.A., 2013. Nutritional comparison of captured *Clarias gariepinus* and *Oreochromis niloticus*. Int. Res. J. Nat. Sci. 1, 9–13.

Bahurmiz, O.M., Ng, W.K., 2007. Effects of dietary palm oil source on growth, tissue fatty acid composition and nutrient digestibility of red hybrid tilapia, *Oreochromis* sp., raised from stocking to marketable size. Aquaculture 262, 382–392.

Bai, Y., McCoy, J.G., Levin, E.J., Sobrado, P., Rajashankar, K.R., Fox, B.G., Zhou, M., 2015. X-ray structure of a mammalian stearoyl-CoA desaturase. Nature 524, 252–256.

Baker, R.T.M., Davies, S.J., 1996. Increased production of docosahexaenoic acid (22:6n-3), DHA) in catfish nutritionally stressed by the feeding of oxidized oils and the modulatory effect of dietary α-tocopheryl acetate. J. Fish Biol. 49, 748–752.

Barnathan, G, 2009. Non-methylene-interrupted fatty acids from marine invertebrates: Occurrence, characterization and biological properties. Biochimie 2009, 91, 671–678.

Bell, J.G., Henderson, R.J., Tocher, D.R., Mcghee, F., Dick, J.R., Porter, A., Smullen, R.P., Sargent, J.R., 2002. Substituting fish oil with crude palm oil in the diet of Atlantic salmon (*Salmo salar*) affects muscle fatty acid composition and hepatic fatty acid metabolism. JN, 222–230.

Bell, J.G., Koppe, W., 2010. Lipids in aquafeeds, in: Turchini, G.M., Ng, W.K., Tocher, D.R. (Eds.), Fish Oil Replacement and Alternative Lipid Sources in Aquaculture Feeds. CRC Press, UK, pp. 21–60.

Bell, M. V., Dick, J.R., 2004. Changes in capacity to synthesise 22:6n-3 during early development in rainbow trout (*Oncorhynchus mykiss*). Aquaculture 235, 393–409.

Bell, M. V., Tocher, D.R., 2009. Biosynthesis of polyunsaturated fatty acids in aquatic ecosystems: General pathways and new directions, in: Arts, M.T., Brett, M., Kainz, M. (Eds.), Lipids in Aquatic Ecosystems. Springer-Verlag, New York, pp. 211–236.

Bell, M. V, Dick, J.R., Porter, A.E., 2003. In vivo assays of docosahexaenoic acid biosynthesis in fish, in: Browman, H.I., Skiftesvik, A.B. (Eds.), The Big Fish Bang. Proceedings of the 26th Annual Larval Fish Conference. Institute of Marine Research, Postboks 1870 Nordnes, Bergen, Norway. ISBN 82-7461-059-8.

Berg, J.M., Tymoczko, J.L., Stryer, L., 2012. Biochemistry, 7th ed. W H Freeman, New York.

Betancor, M.B., Olsen, R.E., Solstorm, D., Skulstad, O.F., Tocher, D.R., 2016. Assessment of a land-locked Atlantic salmon (*Salmo salar* L.) population as a potential genetic resource with a focus on long-chain polyunsaturated fatty acid biosynthesis. Biochim. Biophys. Acta 1861, 227–238.

Betancur-R, R., Broughton, R.E., Wiley, E.O., Carpenter, K., López, J.A., Li, C., Holcroft, N.I., Arcila, D., Sanciangco, M., Cureton II, J.C., Zhang, F., Buser, T., Campbell, M.A., Ballesteros, J.A., Roa-Varon, A., Willis, S., Borden, W.C., Rowley, T., Reneau, P.C., Hough, D.J., Lu, G., Grande, T., Arratia, G., Ortí, G., 2013. The tree of life and a new classification of bony fishes. PLOS Curr. 732988, 1–45.

Beveridge, M.C.M., Thilsted, S.H., Phillips, M.J., Metian, M., Troell, M., Hall, S.J., 2013. Meeting the food and nutrition needs of the poor: The role of fish and the opportunities and challenges emerging from the rise of aquaculture. Fish Biol. 83, 1067–1084.

Böhm, M., Schultz, S., Koussoroplis, A.M., Kainz, M.J., 2014. Tissue-specific fatty acids response to different diets in common carp (*Cyprinus carpio* L.). PLoS One 9, e94759.

Brenna, J.T., 2002. Efficiency of conversion of α-linolenic acid to long chain n-3 fatty acids in man. Curr. Opin. Clin. Nutr. Metab. Care 5, 127–132.

Brett, M.T., Müller-Navarra, D.C., 1997. The role of highly unsaturated fatty acids in aquatic food web processes. Freshw. Biol. 38, 483–500.

Brummett, R.E., 2007. Freshwater fish seed resources in Nigeria, in: Bondad-Reantaso, M.G. (Ed.), Assessment of freshwater fish seed resources for sustainable aquaculture. FAO Fisheries Technical Paper. No. 501. Rome, FAO, p. 628.

Butts, I.A.E., Baeza, R., Stottrup, J.G., Krüger-Johnsen, M., Jacobsen, C., Perez, L., Asturiano, J.F., Tomkiewicz, J., 2015. Impact of dietary fatty acids on muscle composition, liver lipids, milt composition and sperm performance in European eel. Comp. Biochem. Physiol. Part A Mol. Integr. Physiol. 183, 87–96.

Buzzi, M., Henderson, R.J., Sargent, J.R., 1997. Biosynthesis of docosahexaenoic acid in trout hepatocytes proceeds via 24-carbon intermediates. Comp. Biochem. Physiol. Part B Biochem. Mol. Biol. 116, 263–267.

Buzzi, M., Henderson, R.J., Sargent, J.R., 1996. The desaturation and elongation of linolenic acid and eicosapentaenoic acid by hepatocytes and liver microsomes from rainbow trout (*Oncorhynchus mykiss*) fed diets containing fish oil or olive oil. Biochim. Biophys. Acta 1299, 235–244.

Calder, P.C., 2005. Polyunsaturated fatty acids and inflammation. Biochem. Soc. Trans. 33, 423–427.

Cameron, D.J., Tong, Z., Yang, Z., Kaminoh, J., Kamiyah, S., Chen, H., Zeng, J., Chen, Y., Luo, L., Zhang, K., 2007. Essential role of Elovl4 in very long chain fatty acid synthesis, skin permeability barrier function, and neonatal survival. Int. J. Biol. Sci. 3, 111–119.

Cardoso, C., Afonso, C., Bandarra, N.M., 2016. Seafood lipids and cardiovascular health. Nutrire 41, 7.

Carmona-Antoñanzas, G., Monroig, Ó., Dick, J.R., Davie, A., Tocher, D.R., 2011. Biosynthesis of very long-chain fatty acids (C >24) in Atlantic salmon: Cloning, functional characterisation, and tissue distribution of an Elovl4 elongase. Comp. Biochem. Physiol. Part B Biochem. Mol. Biol. 159, 122–129.

Castro, L.F.C., Monroig, Ó., Leaver, M.J., Wilson, J., Cunha, I., Tocher, D.R., 2012. Functional desaturase Fads1 (Δ5) and Fads2 (Δ6) orthologues evolved before the origin of jawed vertebrates. PLoS One 7, e31950.

Castro, L.F.C., Tocher, D.R., Monroig, Ó., 2016. Long-chain polyunsaturated fatty acid biosynthesis in chordates: Insights into the evolution of Fads and Elovl gene repertoire. Prog. Lipid Res. 62, 25–40.

Chang, B.E., Hsieh, S.L., Kuo, C.M., 2001. Molecular cloning of full-length cDNA encoding delta-9 desaturase through PCR strategies and its genomic organization and expression in grass carp (*Ctenopharyngodon idella*). Mol. Reprod. Dev. 58, 245–254.

Chou, B.S., Shiau, S.Y., 1999. Both n-6 and n-3 fatty acids are required for maximal growth of juvenile hybrid tilapia. N. Am. J. Aquac. 61, 13–20.

Christie, W.W., 2003. Lipid analysis: Isolation, separation, identification and structural analysis of lipids, 3rd ed., The oily press. Bridgwater, England.

Cook, H.W., McMaster, C.R., 2002. Fatty acid desaturation and chain elongation in eukaryotes, in: Vance, D.E., Vance, J.E. (Eds.), Lipids, Lipoproteins and Membranes (4th Ed.). Elsevier, pp. 181–204.

Covello, P.S., Reed, D.W., 1996. Functional expression of the extraplastidial *Arabidopsis thaliana* oleate desaturase gene (*FAD2*) in *Saccharomyces cerevisiae*. Plant Physiol. 111, 223–226.

D'andrea, S., Guillou, H., Jan, S., Catheline, D., Thibault, J.N., Bouriel, M., Rioux, V., Legrand, P., 2002. The same rat Δ6-desaturase not only acts on 18- but also on 24-carbon fatty acids in very-long-chain polyunsaturated fatty acid biosynthesis. Biochem. J. 364, 49–55.

Dahmen, J.L., Olsen, R., Fahy, D., Wallis, J.G., Browse, J., 2013. Cytochrome b_5 coexpression increases *Tetrahymena thermophila* Δ6 fatty acid desaturase activity in *Saccharomyces cerevisiae*. Eukaryot. Cell 12, 923–931.

Das, U.N., 2008. Can essential fatty acids reduce the burden of disease(s)? Lipids Health Dis. 7, 9.

De Antueno, R.J., Knickle, L.C., Smith, H., Elliot, M.L., Allen, S.J., Nwaka, S., Winther, M.D., 2001. Activity of human Δ5 and Δ6 desaturases on multiple n-3 and n-6 polyunsaturated fatty acids. FEBS Lett. 509, 77–80.

De Graaf, G.J., Janssen, J.A.L., 1996. Artificial reproduction and pond rearing of the African catfish *Clarias gariepinus* in sub-Saharan Africa-a handbook. FAO Fisheries Technical Paper. No 362. FAO, Rome.

De Silva, S.S., 2012. Aquaculture: A newly emergent food production sector-and perspectives of its impacts on biodiversity and conservation. Biodivers. Conserv. 21, 3187–3220.

De Silva, S.S., Anderson, T.A., 1995. Fish nutrition in aquaculture. Chapman & Hall, Suffolk, Great Britain.

De Silva, S.S., Francis, D.S., Tacon, G.J., 2010. Fish oils in aquaculture: In retrospect. Fish oil Replace. Altern. lipid sources Aquac. Feed. 439–485.

Diaz, A.R., Mansilla, M.C., Vila, A.J., De Mendoza, D., 2002. Membrane topology of the acyl-lipid desaturase from *Bacillus subtilis*. J. Biol. Chem. 277, 48099–48106.

FAO, 2017. World aquaculture 2015: a brief overview, by Rohana Subasinghe. FAO Fisheries and Aquaculture Circular No. 1140. Rome.

FAO, 2016. The State of World Fisheries and Aquaculture. Contributing to food security and nutrition for all. Rome.

FAO, 2014. The State of World Fisheries and Aquaculture. Opportunities and challenges. Rome.

FAO, 2012. The State of World Fisheries and Aquaculture. Rome.

Farooqui, A. A., 2011. Lipid mediators and their metabolism in the brain. Springer-Verlag New York.

Ferdinandusse, S., Denis, S., Mooijer, P.A.W, Zhang, Z., Reddy, J.K., Spector, A.A., Wanders, R.J.A., 2001. Identification of the peroxisomal β-oxidation enzymes involved in the biosynthesis of docosahexaenoic acid. J. Lipid Res. 42, 1987–1995.

Folch, J., Lees, M., Sloane-Stanley, G.H., 1957. A simple method for the isolation and purification of total lipids from animal tissues. J. Biol. Chem. 226, 497–509.

Fonseca-Madrigal, J., Navarro, J.C., Hontoria, F., Tocher, D.R., Martínez-Palacios, C.A., Monroig, Ó., 2014. Diversification of substrate specificities in teleostei Fads2: Characterization of Δ4 and Δ6Δ5 desaturases of *Chirostoma estor*. J. Lipid Res. 55, 1408–1419.

Garcia, C., Duby, C., Catheline, D., Toral, P.G., Bernard, L., Legrand, P., Rioux, V., 2017. Synthesis of the suspected trans-11, cis-13 conjugated linoleic acid isomer in ruminant mammary tissue by FADS3-catalyzed Δ13-desaturation of vaccenic acid. J. Dairy Sci. 100, 783–796.

Geiger, M., Mohammed, B.S., Sankarappa, S., Sprecher, H., 1993. Studies to determine if rat liver contains chain-length-specific acyl-CoA 6-desaturases. Biochim. Biophys. Acta 1170, 137–142.

Gjedrem, T., 2000. Genetic improvement of cold-water fish species. Aquacult. Res. 31, 25–33.

Glencross, B.D., 2009. Exploring the nutritional demand for essential fatty acids by aquaculture species. Rev. Aquac. 1, 71–124.

González-Rovira, A., Mourente, G., Zheng, X., Tocher, D.R., Pendón, C., 2009. Molecular and functional characterization and expression analysis of a Δ6 fatty acyl desaturase cDNA of European Sea Bass (*Dicentrarchus labrax* L.). Aquaculture 298, 90–100.

Gregory, M.K., James, M.J., 2014. Rainbow trout (*Oncorhynchus mykiss*) Elovl5 and Elovl2 differ in selectivity for elongation of omega-3 docosapentaenoic acid. Biochim. Biophys. Acta 1841, 1656–1660.

Gregory, M.K., See, V.H.L., Gibson, R. A., Schuller, K. A., 2010. Cloning and functional characterisation of a fatty acyl elongase from southern bluefin tuna (*Thunnus maccoyii*). Comp. Biochem. Physiol. Part B Biochem. Mol. Biol. 155, 178–185.

Guillou, H., D'Andrea, S., Rioux, V., Barnouin, R., Dalaine, S., Pedrono, F., Jan, S., Legrand, P., 2004. Distinct roles of endoplasmic reticulum cytochrome b_5 and

fused cytochrome b_5-like domain for rat Δ6-desaturase activity. J. Lipid Res. 45, 32–40.

Guillou, H., Zadravec, D., Martin, P.G.P., Jacobsson, A., 2010. The key roles of elongases and desaturases in mammalian fatty acid metabolism: Insights from transgenic mice. Prog. Lipid Res. 49, 186–199.

Hamid, N.K.A., Carmona-Antoñanzas, G., Monroig, Ó., Tocher, D.R., Turchini, G.M., Donald, J.A., 2016. Isolation and functional characterisation of a *fads2* in rainbow trout (*Oncorhynchus mykiss*) with Δ5 desaturase activity. PLoS One 11: e0150770.

Hamre, K., Yúfera, M., Rønnestad, I., Boglione, C., Conceição, L.E.C., Izquierdo, M., 2013. Fish larval nutrition and feed formulation: Knowledge gaps and bottlenecks for advances in larval rearing. Rev. Aquac. 5, S26–S58.

Hastings, N., Agaba, M.K., Tocher, D.R., Leaver, M.J., Dick, J.R., Sargent, J.R., Teale, A.J., 2001. A vertebrate fatty acid desaturase with Δ5 and Δ6 activities. Proc. Natl. Acad. Sci. 98, 14304–14309.

Hastings, N., Agaba, M.K., Tocher, D.R., Zheng, X., Dickson, C.A., Dick, J.R., Teale, A.J., 2005. Molecular cloning and functional characterization of fatty acyl desaturase and elongase cDNAs involved in the production of eicosapentaenoic and docosahexaenoic acids from α-linolenic acid in Atlantic salmon (*Salmo salar*). Mar. Biotechnol. 6, 463–474.

Hecht, T., 2013. A review of on-farm feed management practices for North African catfish in sub-Saharan Africa, in Hasan, M.R. and New, M.B. (Ed.), On-farm Feeding and Feed Management in Aquaculture. FAO Fisheries and Aquaculture Technical Paper No. 583. Rome, FAO. pp. 463-479.

Hoffman, L.C., Prinsloo, J.F., 1995a. The influence of different dietary lipids on the growth and body composition of the African sharptooth catfish, *Clarias gariepinus* (Burchell). S. Afr. J. Sci. 91, 315–320.

Hoffman, L.C., Prinsloo, J.F., 1995b. Genetic and nutritional influence on the total lipid fatty acid profile of *Clarias gariepinus* muscle. Aquat. Living Resour. 8, 415–421.

Hsieh, S.L., Chang, H.T., Wu, C.H., Kuo, C.M., 2004. Cloning, tissue distribution and hormonal regulation of stearoyl-CoA desaturase in tilapia, *Oreochromis mossambicus*. Aquaculture 230, 527–546.

Hsieh, S.L., Liao, W.L., Kuo, C.M., 2001. Molecular cloning and sequence analysis of stearoyl-CoA desaturase in milkfish, *Chanos chanos*. Comp. Biochem. Physiol. Part B Biochem. Mol. Biol. 130, 467–477.

Hsieh, S.L., Liu, R.W., Wu, C.H., Cheng, W.T., Kuo, C.M., 2003. cDNA nucleotide sequence coding for stearoyl-CoA desaturase and its expression in the zebrafish (*Danio rerio*) Embryo. Mol. Reprod. Dev. 66, 325–333.

Jakobsson, A., Westerberg, R., Jacobsson, A., 2006. Fatty acid elongases in mammals: Their regulation and roles in metabolism. Prog. Lipid Res. 45, 237–249.

Jin, M., Monroig, Ó., Navarro, J.C., Tocher, D.R., Zhou, Q.C., 2017. Molecular and functional characterisation of two *elovl4* elongases involved in the biosynthesis of very long-chain (> C_{24}) polyunsaturated fatty acids in black seabream *Acanthopagrus schlegelii*. Comp. Biochem. Physiol. Part B Biochem. Mol. Biol. 212, 41–50.

Kabeya, N., Chiba, M., Haga, Y., Satoh, S., Yoshizaki, G., 2017. Cloning and functional characterization of *fads2* desaturase and *elovl5* elongase from Japanese flounder *Paralichthys olivaceus*. Comp. Biochem. Physiol. Part B Biochem. Mol. Biol. 214, 36–46.

Kabeya, N., Takeuchi, Y., Yamamoto, Y., Yazawa, R., Haga, Y., Satoh, S., Yoshizaki, G., 2014. Modification of the n-3 HUFA biosynthetic pathway by transgenesis in a marine teleost, nibe croaker. J. Biotechnol. 172, 46–54.

Kabeya, N., Takeuchi, Y., Yazawa, R., Haga, Y., Satoh, S., Yoshizaki, G., 2016. Transgenic modification of the n-3 HUFA biosynthetic pathway in nibe croaker larvae: Improved DPA (docosapentaenoic acid; 22:5n-3) production. Aquac. Nutr. 22, 472–478.

Kabeya, N., Yamamoto, Y., Cummins, S.F., Elizur, A., Yazawa, R., Takeuchi, Y., Haga, Y., Satoh, S., Yoshizaki, G., 2015. Polyunsaturated fatty acid metabolism in a marine teleost, Nibe croaker *Nibea mitsukurii*: Functional characterization of

Fads2 desaturase and Elovl5 and Elovl4 elongases. Comp. Biochem. Physiol. Part B Biochem. Mol. Biol. 188, 37–45.

Katoh, K., Toh, H., 2008. Recent developments in the MAFFT multiple sequence alignment program. Brief. Bioinform. 9, 286–298.

Klempova, T., Mihalik, D., Certik, M., 2013. Characterization of membrane-bound fatty acid desaturases. Gen. Physiol. Biophys. 32, 445–458.

Kraffe, E., Soudant, P., Marty, Y., 2004. Fatty acids of serine, ethanolamine, and choline plasmalogens in some marine bivalves. Lipids 39, 59–66.

Kuah, M.K., Jaya-Ram, A., Shu-Chien, A.C., 2016. A fatty acyl desaturase (fads2) with dual Δ6 and Δ5 activities from the freshwater carnivorous striped snakehead *Channa striata*. Comp. Biochem. Physiol. Part A Mol. Integr. Physiol. 201, 146–155.

Kuah, M.K., Jaya-Ram, A., Shu-Chien, A.C., 2015. The capacity for long-chain polyunsaturated fatty acid synthesis in a carnivorous vertebrate: Functional characterisation and nutritional regulation of a Fads2 fatty acyl desaturase with Δ4 activity and an Elovl5 elongase in striped snakehead (*Channa striata*). Biochim. Biophys. Acta 1851, 248–260.

Leaver, M.J., Bautista, J.M., Björnsson, B.T., Jönsson, E., Krey, G., Tocher, D.R., Torstensen, B.E., 2008. Towards fish lipid nutrigenomics: Current state and prospects for fin-fish aquaculture. Rev. Fish. Sci. 16, 71–92.

Lee, J.M., Lee, H., Kang, S.B., Park, W.J., 2016. Fatty acid desaturases, polyunsaturated fatty acid regulation, and biotechnological advances. Nutrients 8, 23.

Legendre, M., Kerdchuen, N., Corraze, G., Bergot, P., 1995. Larval rearing of an African catfish *Heterobranchus longifilis* (Teleostei, Clariidae): Effect of dietary lipids on growth, survival and fatty acid composition of fry. Aquat. Living Resour. 8, 355–363.

Leonard, A.E., Kelder, B., Bobik, E.G., Chuang, L.T., Lewis, C.J., Kopchick, J.J., Mukerji, P., Huang, Y.S., 2002. Identification and expression of mammalian long-chain PUFA elongation enzymes. Lipids 37, 733–740.

Leonard, A.E., Pereira, S.L., Sprecher, H., Huang, Y.S., 2004. Elongation of long-chain fatty acids. Prog. Lipid Res. 43, 36–54.

Li, S., Monroig, Ó., Navarro, J.C., Yuan, Y., Xu, W., Mai, K., Tocher, D.R., Ai, Q., 2015. Molecular cloning and functional characterization of a putative Elovl4 gene and its expression in response to dietary fatty acid profiles in orange-spotted grouper *Epinephelus coioides*. Aquac. Res. 48, 537–552.

Li, S., Monroig, Ó., Wang, T., Yuan, Y., Navarro, J.C., Hontoria, F., Liao, K., Tocher, D.R., Mai, K., Xu, W., Ai, Q., 2017. Functional characterization and differential nutritional regulation of putative Elovl5 and Elovl4 elongases in large yellow croaker (*Larimichthys crocea*). Sci. Rep. 7, 2303.

Li, Y., Monroig, Ó., Zhang, L., Wang, S., Zheng, X., Dick, J.R., You, C., Tocher, D.R., 2010. A vertebrate fatty acyl desaturase with 4 activity. Proc. Natl. Acad. Sci. 107, 16840–16845.

Li, Y., Hu, C., Zheng, Y., Xia, X., Xu, W., Wang, S., Chen, W., Sun, Z., Huang, J., 2008. The effects of dietary fatty acids on liver fatty acid composition and Δ^6-desaturase expression differ with ambient salinities in *Siganus canaliculatus*. Comp. Biochem. Physiol. Part B Biochem. Mol. Biol. 151, 183–190.

Lim, Z.L., Senger, T., Vrinten, P., 2014. Four amino acid residues influence the substrate chain-length and regioselectivity of *Siganus canaliculatus* Δ4 and Δ5/6 desaturases. Lipids 49, 357–367.

Lopes-Marques, M., Ozório, R., Amaral, R., Tocher, D.R., Monroig, Ó., Castro, L.F.C., 2017. Molecular and functional characterization of a *fads2* orthologue in the Amazonian teleost, *Arapaima gigas*. Comp. Biochem. Physiol. Part B Biochem. Mol. Biol. 203, 84–91.

Los, D.A., Murata, N., 1998. Structure and expression of fatty acid desaturases. Biochim. Biophys. Acta 1394, 3–15.

Lou, Y., Schwender, J., Shanklin, J., 2014. FAD2 and FAD3 desaturases form heterodimers that facilitate Metabolic channeling *in vivo*. J. Biol. Chem. 289, 17996–18007.

Lovell, T., 1998. Nutrition and feeding of fish, 2nd ed. Kluwer Academic Publishers, Massachusetts, USA.

Man, W.C., Miyazaki, M., Chu, K., Ntambi, J.M., 2006. Membrane topology of mouse stearoyl-CoA desaturase 1. J. Biol. Chem. 281, 1251–1260.

Mandal, M.N.A., Ambasudhan, R., Wong, P.W., Gage, P.J., Sieving, P.A., Ayyagari, R., 2004. Characterization of mouse orthologue of *ELOVL4*: Genomic organization and spatial and temporal expression. Genomics 83, 626–635.

Martin, C.E., Oh, C.S., Jiang, Y., 2007. Regulation of long chain unsaturated fatty acid synthesis in yeast. Biochim. Biophys. Acta, 271–285.

McMahon, A., Kedzierski, W., 2010. Polyunsaturated very-long-chain C28-C36 fatty acids and retinal physiology. Br. J. Ophthalmol. 94, 1127–1132.

Meesapyodsuk, D., Qiu, X., 2014. Structure determinants for the substrate specificity of acyl-CoA Δ9 desaturases from a marine copepod. ACS Chem. Biol. 9, 922–934.

Meesapyodsuk, D., Qiu, X., 2012. The front-end desaturase: Structure, function, evolution and biotechnological use. Lipids 47, 227–237.

Memon, N.N., Talpur, F.N., Bhanger, M.I., Balouch, A., 2011. Changes in fatty acid composition in muscle of three farmed carp fish species (*Labeo rohita*, *Cirrhinus mrigala*, *Catla catla*) raised under the same conditions. Food Chem. 126, 405–410.

Meyer, A., Kirsch, H., Domergue, F., Abbadi, A., Sperling, P., Bauer, J., Cirpus, P., Zank, T.K., Moreau, H., Roscoe, T.J., Zähringer, U., Heinz, E., 2004. Novel fatty acid elongases and their use for the reconstitution of docosahexaenoic acid biosynthesis. J. Lipid Res. 45, 1899–1909.

Mitchell, A.G., Martin, C.E., 1995. A novel cytochrome b_5-like domain is linked to the carboxyl terminus of the *Saccharomyces cerevisiae* Δ-9 fatty acid desaturase. J. Biol. Chem. 270, 29766–29772.

Miyazaki, M., Bruggink, S.M., Ntambi, J.M., 2006. Identification of mouse palmitoyl-coenzyme A Δ9-desaturase. J. Lipid Res. 47, 700–704.

Mohd-Yusof, N.Y., Monroig, Ó., Mohd-Adnan, A., Wan, K.L., Tocher, D.R., 2010. Investigation of highly unsaturated fatty acid metabolism in the Asian sea bass, *Lates calcarifer*. Fish Physiol. Biochem. 36, 827–843.

Monroig, Ó., Hontoria, F., Varó, I., Tocher, D.R., Navarro, J.C., 2016a. Biosynthesis of very long-chain (> C24) polyunsaturated fatty acids in juveniles of Gilthead seabream (*Sparus aurata*). The 17th international symposium on fish nutrition and feeding, June 5–10, Sun Valley, Idaho, USA.

Monroig, Ó., Li, Y., Tocher, D.R., 2011a. Delta-8 desaturation activity varies among fatty acyl desaturases of teleost fish: High activity in delta-6 desaturases of marine species. Comp. Biochem. Physiol. B 159, 206–213.

Monroig, Ó., Lopes-Marques, M., Navarro, J.C., Hontoria, F., Ruivo, R., Santos, M.M., Venkatesh, B., Tocher, D.R., Castro, L.F.C., 2016b. Evolutionary functional elaboration of the Elovl2/5 gene family in chordates. Sci. Rep. 6, 20510.

Monroig, Ó., Navarro, J.C., Tocher, D.R., 2011b. Long-chain polyunsaturated fatty acids in fish: Recent advances on desaturases and elongases involved in their biosynthesis, in: Cruz-Suarez, L.E., Ricque-Marie, D., Tapia-Salazar, M., Nieto-Lopez, M.G., Villarreal-Cavazos, D.A., Gamboa-Delgado, J., Hernandez-Hernandez, L.H. (Eds.), XI International Symposium on Aquaculture Nutrition, 23-25 November 2011, San Nicolas de Los Garza, N.L. Universidad Autonoma de Nuevo Leon, Monterrey, Mexico. pp. 257–283.

Monroig, Ó., Rotllant, J., Cerdá-Reverter, J.M., Dick, J.R., Figueras, A., Tocher, D.R., 2010a. Expression and role of Elovl4 elongases in biosynthesis of very long-chain fatty acids during zebrafish *Danio rerio* early embryonic development. Biochim. Biophys. Acta 1801, 1145–1154.

Monroig, Ó., Rotllant, J., Sánchez, E., Cerdá-Reverter, J.M., Tocher, D.R., 2009. Expression of long-chain polyunsaturated fatty acid (LC-PUFA) biosynthesis genes during zebrafish *Danio rerio* early embryogenesis. Biochim. Biophys. Acta 1791, 1093–1101.

Monroig, Ó., Tocher, D.R., Hontoria, F., Navarro, J.C., 2013a. Functional characterisation of a Fads2 fatty acyl desaturase with Δ6/Δ8 activity and an

Elovl5 with C16, C18 and C20 elongase activity in the anadromous teleost meagre (*Argyrosomus regius*). Aquaculture 412–413, 14–22.

Monroig, Ó., Tocher, D.R., Navarro, J.C., 2013b. Biosynthesis of polyunsaturated fatty acids in marine invertebrates: Recent advances in molecular mechanisms. Mar. Drugs 11, 3998-4018.

Monroig, Ó., Wang, S., Zhang, L., You, C., Tocher, D.R., Li, Y., 2012. Elongation of long-chain fatty acids in rabbitfish *Siganus canaliculatus*: Cloning, functional characterisation and tissue distribution of Elovl5- and Elovl4-like elongases. Aquaculture 350–353, 63–70.

Monroig, Ó., Webb, K., Ibarra-Castro, L., Holt, G.J., Tocher, D.R., 2011c. Biosynthesis of long-chain polyunsaturated fatty acids in marine fish: Characterization of an Elovl4-like elongase from cobia *Rachycentron canadum* and activation of the pathway during early life stages. Aquaculture 312, 145–153.

Monroig, Ó., Zheng, X., Morais, S., Leaver, M.J., Taggart, J.B., Tocher, D.R., 2010b. Multiple genes for functional Δ6 fatty acyl desaturases (Fad) in Atlantic salmon (*Salmo salar* L.): Gene and cDNA characterization, functional expression, tissue distribution and nutritional regulation. Biochim. Biophys. Acta 1801, 1072–1081.

Morais, S., Castanheira, F., Martinez-Rubio, L., Conceição, L.E.C., Tocher, D.R., 2012. Long chain polyunsaturated fatty acid synthesis in a marine vertebrate: Ontogenetic and nutritional regulation of a fatty acyl desaturase with Δ4 activity. Biochim. Biophys. Acta 1821, 660–671.

Morais, S., Monroig, Ó., Zheng, X., Leaver, M.J., Tocher, D.R., 2009. Highly unsaturated fatty acid synthesis in Atlantic salmon: Characterization of ELOVL5- and ELOVL2-like elongases. Mar. Biotechnol. 11, 627–639.

Morais, S., Mourente, G., Martínez, A., Gras, N., Tocher, D.R., 2015. Docosahexaenoic acid biosynthesis via fatty acyl elongase and Δ4-desaturase and its modulation by dietary lipid level and fatty acid composition in a marine vertebrate. Biochim. Biophys. Acta 1851, 588–597.

Morais, S., Mourente, G., Ortega, A., Tocher, J.A., Tocher, D.R., 2011. Expression of fatty acyl desaturase and elongase genes, and evolution of DHA:EPA ratio during

development of unfed larvae of Atlantic bluefin tuna (*Thunnus thynnus* L.). Aquaculture 313, 129–139.

Nakamura, M.., Nara, T.Y., 2004. Structure, function and dietary regulation of Δ6, Δ5 and Δ9 desaturases. Annu. Rev. Nutr. 24, 345–376.

Napier, J.A., Sayanova, O., Sperling, P., Heinz, E., 1999. A growing family of cytochrome b_5-domain fusion proteins. Trends Plant Sci. 4, 2–4.

Napier, J.A., Sayanova, O., Stobart, A.K., Shewry, P.R., 1997. A new class of cytochrome b_5 fusion proteins. Biochem. J. 328, 717–718.

Ng, W.K., Chong, C., 2004. An overview of lipid nutrition with emphasis on alternative lipid sources in tilapia feeds, in: Bolivar, R.B., Mair, G.C., Fitzsimmons, K. (Eds.), New dimension in farmed tilapia. Proceedings Sixth International Symposium on Tilapia in Aquaculture, Philippines, pp. 241–248.

Ng, W.K., Lim, P.-K., Boey, P.-L., 2003. Dietary lipid and palm oil source affects growth, fatty acid composition and muscle α-tocopherol concentration of African catfish, *Clarias gariepinus*. Aquaculture 215, 229–243.

Ng, W.K., Lim, P.K., Sidek, H., 2001. The influence of a dietary lipid source on growth, muscle fatty acid composition and erythrocyte osmotic fragility of hybrid tilapia. Fish Physiol. Biochem. 25, 301–310.

Ng, W.K., Wang, Y., Ketchimenin, P., Yuen, K.H., 2004. Replacement of dietary fish oil with palm fatty acid distillate elevates tocopherol and tocotrienol concentrations and increases oxidative stability in the muscle of African catfish, *Clarias gariepinus*. Aquaculture 233, 423–437.

Nguyen, N.H., Ponzoni, R.W., Yee, H.Y., Abu-Bakar, K.R., Hamzah, A., Khaw, H.L., 2010. Quantitative genetic basis of fatty acid composition in the GIFT strain of Nile tilapia (*Oreochromis niloticus*) selected for high growth. Aquaculture 309, 66–74.

National Research Council (NRC), 2011. Nutrient Requirements of Fish and Shrimp. The National Academies Press, Washington, DC.

Oboh, A., Kabeya, N., Carmona-Antoñanzas, G., Castro, L.F.C., Dick, J.R., Tocher, D.R., Monroig, Ó., 2017. Two alternative pathways for docosahexaenoic acid (DHA, 22:6n-3) biosynthesis are widespread among teleost fish. Sci. Rep. 7, 3889.

Ochang, S.N., Fagbenro, O.A., Adebayo, O.T., 2007. Growth performance, body composition, haematology and product quality of the African catfish (*Clarias gariepinus*) feed diets with Palm oil. Pakistan J. Nutr. 6, 452–459.

Park, H.G., Park, W.J., Kothapalli, K.S.D., Brenna, J.T., 2015. The fatty acid desaturase 2 (*FADS2*) gene product catalyzes Δ4 desaturation to yield n-3 docosahexaenoic acid and n-6 docosapentaenoic acid in human cells. FASEB J. 29, 3911–3919.

Park, W.J., Kothapalli, K.S.D., Lawrence, P., Tyburczy, C., Brenna, J.T., 2009. An alternate pathway to long-chain polyunsaturates: the $FADS_2$ gene product Δ8-desaturates 20:2n-6 and 20:3n-3. J. Lipid Res. 50, 1195–1202.

Pereira, S.L., Leonard, A.E., Mukerji, P., 2003. Recent advances in the study of fatty acid desaturases from animals and lower eukaryotes. Prostaglandins Leukot. Essent. Fat. Acids 68, 97–106.

Petrini, G.A., Altabe, S.G., Uttaro, A.D., 2004. *Trypanosoma brucei* oleate desaturase may use a cytochrome *b5*-like domain in another desaturase as an electron donor. Eur. J. Biochem. 271, 1079–1086.

Portolesi, R., Powell, B.C., Gibson, R.A., 2007. Competition between 24:5n-3 and ALA for Δ6 desaturase may limit the accumulation of DHA in $HepG_2$ cell membranes. J. Lipid Res. 48, 1592–1598.

Poulos, A., 1995. Very long chain fatty acids in higher animals-A review. Lipids 30, 1-14.

Pouomogne, V., 2010. *Clarias gariepinus*, cultured aquatic species information programme. *Clarias gariepinus*. FAO, Rome. Accessed 7 Aug 2017.

Qiu, X., 2003. Biosynthesis of docosahexaenoic acid (DHA, 22:6-4,7,10,13,16,19): Two distinct pathways. Prostaglandins Leukot. Essent. Fat. Acids 68, 181–186.

Qiu, X., Hong, H., MacKenzie, S.L., 2001. Identification of a Δ4 fatty acid desaturase from *Thraustochytrium* sp. involved in the biosynthesis of docosahexanoic acid by heterologous expression in *Saccharomyces cerevisiae* and *Brassica juncea*. J. Biol. Chem. 276, 31561–31566.

Rana, K.J., Siriwardena, S., Hasan, M.R., 2009. Impact of rising feed ingredient prices on aquafeeds and aquaculture production, FAO Fisheries and Aquaculture Technical Paper.

Rioux, V., Pédrono, F., Blanchard, H., Duby, C., Boulier-Monthéan, N., Bernard, L., Beauchamp, E., Catheline, D., Legrand, P., 2013. Trans -vaccenate is Δ13-desaturated by FADS3 in rodents. J. Lipid Res. 54, 3438–3452.

Rotstein, N.P., Pennacchiotti, G.L., Sprecher, H., Aveldaño, M.I., 1996. Active synthesis of $C_{24:5,\ n-3}$ fatty acid in retina. Biochem. J. 316, 859–64.

Saitou, N., Nei, M., 1987. The neighbour-joining method: a new method for reconstructing phylogenetic trees. Mol Biol Evo 4, 406–425.

Sargent, J.R., Bell, J.G., Mcevoy, L., Tocher, D.R., Estevez, A., 1999. Recent developments in the essential fatty acid nutrition of fish. Aquaculture 177, 191–199.

Sargent, J.R., Tocher, D.R., Bell, J.G., 2002. The lipids, in: Halver, J.E., Hardy, R.W. (Eds.), Fish nutrition. Academic Press, San Diego, pp. 181–257.

Satoh, S., Poe, W.E., Wilson, R.P., 1989. Studies on the essential fatty acid requirement of channel catfish, *Ictalurus punctatus*. Aquaculture 79, 121–128.

Sayanova, O., Shewry, P.R., Napier, J.A., 1999. Histidine-41 of the cytochrome b_5 domain of the borage Δ^6 fatty acid desaturase is essential for enzyme activity. Plant Physiol. 121, 641–646.

Schmitz, G., Ecker, J., 2008. The opposing effects of *n-3* and *n-6* fatty acids. Prog. Lipid Res. 47, 147–155.

Shanklin, J., Guy, J.E., Mishra, G., Lindqvist, Y., 2009. Desaturases: Emerging models for understanding functional diversification of diiron-containing enzymes. J. Biol. Chem. 284, 18559–18563.

Shanklin, J., Whittle, E., Fox, B.G., 1994. Eight histidine residues are catalytically essential in a membrane-associated iron enzyme, stearoyl-CoA desaturase, and are conserved in alkane hydroxylase and xylene monooxygenase. Biochemistry 33, 12787–12794.

Shepherd, C.J., Monroig, Ó., Tocher, D.R., 2017. Future availability of raw materials for salmon feeds and supply chain implications: The case of Scottish farmed salmon. Aquaculture 467, 49–62.

Simopoulos, A.P., 2016. An increase in the Omega-6/Omega-3 fatty acid ratio increases the risk for obesity. Nutrients 8, 1–17.

Simopoulos, A.P., 2002. The importance of the ratio of omega-6/omega-3 essential fatty acids. Biomed. Pharmacother. 56, 365-379.

Solomon, S.G., Ataguba, G.A., Imbur, I., 2012. Growth performance of juvenile *Clarias gariepinus* fed different dietary lipid sources. Int. J. Res. Fish. Aquac. 2, 52–55.

Sorbera, L.A, Asturiano, J.F., Carrillo, M., Zanuy, S., 2001. Effects of polyunsaturated fatty acids and prostaglandins on oocyte maturation in a marine teleost, the European sea bass (*Dicentrarchus labrax*). Biol. Reprod. 64, 382–389.

Sotolu, A.O., 2010. Feed utilization and biochemical characteristics of *Clarias gariepinus* (Burchell, 1822) fingerlings fed diets containing fish oil and vegetable oils as total replacements. World J. Fish Mar. Sci. 2, 93–98.

Sperling, P., Heinz, E., 2001. Desaturases fused to their electron donor. Eur. J. Lipid Sci. Technol. 103, 158–180.

Sperling, P., Ternes, P., Zank, T.K., Heinz, E., 2003. The evolution of desaturases. Prostaglandins Leukot. Essent. Fat. Acids 68, 73–95.

Sprague, M., Betancor, M.B., Tocher, D.R., 2017. Microbial and genetically engineered oils as replacements for fish oil in aquaculture feeds. Biotechnol. Lett. 39, 1599–1609.

Sprecher, H., 2000. Metabolism of highly unsaturated *n-3* and *n-6* fatty acids. Biochim. Biophys. Acta 1486, 219–231.

Sprecher, H., 1992. A reevaluation of the pathway for the biosynthesis of 4,7,10,13,16,19-docosahexaenoic acid. Omega-3 News 7, 1–3.

Sprecher, H., Luthria, D.L., Mohammed, B.S., Baykousheva, S.P., 1995. Reevaluation of the pathways for the biosynthesis of polyunsaturated fatty acids. J. Lipid Res. 36, 2471–2477.

Steffens, W., 1997. Effects of variation in essential fatty acids in fish feeds on nutritive value of freshwater fish for humans. Aquaculture. 151, 97–119.

Stukey, J.E., McDonough, V.M., Martin, C.E., 1990. The OLEl Gene of *Saccharomyces cerevisiae* encodes the Δ9 fatty acid desaturase and can be functionally replaced by the rat stearoyl-CoA desaturase gene. J. Biol. Chem. 265, 20144–20149.

Suh, M., Clandinin, M.T., 2005. 20:5n-3 but not 22:6n-3 is a preferred substrate for synthesis of n-3 very-long-chain fatty acids (C_{24}-C_{36}) in retina. Curr. Eye Res. 30, 959–968.

Szabó, A., Romvári, R., Szathmári, L., Molnár, T., Locsmándi, L., Bázár, G., Molnar, E., Horn, P., Hancz, C., 2009. Effects of dietary vegetable oil supplementation on fillet quality traits , chemical and fatty acid composition of African catfish (*Clarias gariepinus*). Arch. Tierzucht 52, 321–333.

Tacon, A.G.J., Hasan, M.R., Metian, M., 2011. Demand and supply of feed ingredients for farmed fish and crustaceans : Trends and prospects, FAO Fisheries and Aquaculture Technical Paper.

Tanomman, S., Ketudat-Cairns, M., Jangprai, A., Boonanuntanasarn, S., 2013. Characterization of fatty acid delta-6 desaturase gene in Nile tilapia and heterogenous expression in *Saccharomyces cerevisiae*. Comp. Biochem. Physiol. Part B Biochem. Mol. Biol. 166, 148–156.

Tidwell, J.H., Allan, G.L., 2001. Fish as food: aquaculture's contribution: Ecological and economic impacts and contributions of fish farming and capture fisheries. EMBO Rep. 2, 958–963.

Tocher, D.R., 2015. Omega-3 long-chain polyunsaturated fatty acids and aquaculture in perspective. Aquaculture 449, 94–107.

Tocher, D.R., 2010. Fatty acid requirements in ontogeny of marine and freshwater fish. Aquac. Res. 41, 717–732.

Tocher, D.R., 2003. Metabolism and functions of lipids and fatty acids in teleost fish. Rev. Fish. Sci. 11, 107–184.

Tocher, D.R., Agaba, M., Hastings, N., Teale, A.J., 2003. Biochemical and molecular studies of the polyunsaturated fatty acid desaturation pathway in fish, in: Browman, H., Skiftesvik, A.B. (Ed.), The Big Fish Bang - Proceedings of the 26th Annual Larval Fish Conference. Institute of Marine Research. Bergen, Norway, pp. 211–227.

Tocher, D.R., Agaba, M.K., Hastings, N., Bell, J.G., Dick, J.R., Teale, A.J., 2002. Nutritional regulation of hepatocyte fatty acid desaturation and polyunsaturated fatty acid composition in zebrafish (*Danio rerio*) and tilapia (*Oreochromis niloticus*). Fish Physiol. Biochem. 24, 309–320.

Tocher, D.R., Bell, J.G., Dick, J.R., Henderson, R.J., McGhee, F., Michell, D., Morris, P.C., 2000. Polyunsaturated fatty acid metabolism in Atlantic salmon (*Salmo salar*) undergoing parr-smolt transformation and the effects of dietary linseed and rapeseed oils. Fish Physiol. Biochem. 23, 59–73.

Tocher, D.R., Glencross, B.D., 2015. Lipids and Fatty Acids, in: Lee, C., Lim, C., Gatlin, D.M., Webster, C.D. (Eds.), Dietary Nutrients, Additives, and Fish Health. John Wiley & sons inc., pp. 47–94.

Tocher, D.R., Leaver, M.J., Hodgson, P.A., 1998. Recent advances in the biochemistry and molecular biology of fatty acyl desaturases. Prog. Lipid Res 37, 73–117.

Turchini, G.M., Francis, D.S., De Silva, S.S., 2006. Fatty acid metabolism in the freshwater fish Murray cod (*Maccullochella peelii peelii*) deduced by the whole-body fatty acid balance method. Comp. Biochem. Physiol. Part B Biochem. Mol. Biol. 144, 110–118.

Turchini, G.M., Torstensen, B.E., Ng, W.K., 2009. Fish oil replacement in finfish nutrition. Rev. Aquac. 1, 10–57.

Uchida, Y., Holleran, W.M., 2008. Omega-O-acylceramide, a lipid essential for mammalian survival. J. Dermatol. Sci. 51, 77–87.

Vagner, M., Santigosa, E., 2011. Characterization and modulation of gene expression and enzymatic activity of delta-6 desaturase in teleosts: A review. Aquaculture 315, 131–143.

Van Weerd, J.H., 1995. Nutrition and growth in Clarias species - a review. Aquat. Living Resour. 8, 395–401.

Vasireddy, V., Uchida, Y., Salem, N., Kim, S.Y., Mandal, M.N.A., Reddy, G.B., Bodepudi, R., Alderson, N.L., Brown, J.C., Hama, H., Dlugosz, A., Elias, P.M., Holleran, W.M., Ayyagari, R., 2007. Loss of functional ELOVL4 depletes very long-chain fatty acids (≥C28) and the unique ω-O-acylceramides in skin leading to neonatal death. Hum. Mol. Genet. 16, 471–482.

Wallis, J.G., Watts, J.L., Browse, J., 2002. Polyunsaturated fatty acid synthesis: What will they think of next? Trends Biochem. Sci. 27, 467–473.

Wang, H., Klein, M.G., Zou, H., Lane, W., Snell, G., Levin, I., Li, K., Sang, B.C., 2015. Crystal structure of human stearoyl-coenzyme A desaturase in complex with substrate. Nat. Struct. Mol. Biol. 22, 581–585.

Wang, M., Chen, H., Gu, Z., Zhang, H., Chen, W., Chen, Y.Q., 2013. ω3 fatty acid desaturases from microorganisms: Structure, function, evolution, and biotechnological use. Appl. Microbiol. Biotechnol. 97, 10255–10262.

Wang, S., Monroig, Ó., Tang, G., Zhang, L., You, C., Tocher, D.R., Li, Y., 2014. Investigating long-chain polyunsaturated fatty acid biosynthesis in teleost fish: Functional characterization of fatty acyl desaturase (Fads2) and Elovl5 elongase in the catadromous species, Japanese eel *Anguilla japonica*. Aquaculture 434, 57–65.

Watters, C., Iwamura, S., Ako, H., Deng, D., Biosciences, M., Resources, H., Feeds, A., 2012. Nutrition considerations in aquaculture: The importance of omega-3 fatty acids in fish development and human health. Foods Nutr. FN-11, UH–CTAHR 1-7.

Wilson, R.P., Moreau, Y., 1996. Nutrient requirements of catfishes (Siluroidei). Aquat. Living Resour. 9, 103–111.

Wirth, M., Steffens, W., Meinelt, T., Steinberg, C., 1997. Significance of docosahexaenoic acid for rainbow trout (*Oncorhynchus mykiss*) larvae. FETT Wiss. Technol. Sci. Technol. 99, 251–253.

Xie, D., Chen, F., Lin, S., Wang, S., You, C., Monroig, Ó., Tocher, D.R., Li, Y., 2014. Cloning, functional characterization and nutritional regulation of Δ6 Fatty acyl desaturase in the herbivorous euryhaline teleost *Scatophagus argus*. PLoS One 9, e90200.

Xue, X., Feng, C.Y., Hixson, S.M., Johnstone, K., Anderson, D.M., Parrish, C.C., Rise, M.L., 2014. Characterization of the fatty acyl elongase (elovl) gene family, and hepatic elovl and delta-6 fatty acyl desaturase transcript expression and fatty acid responses to diets containing camelina oil in Atlantic cod (*Gadus morhua*). Comp. Biochem. Physiol. Part B 175, 9–22.

Yanes-Roca, C., Rhody, N., Nystrom, M., Main, K.L., 2009. Effects of fatty acid composition and spawning season patterns on egg quality and larval survival in common snook (*Centropomus undecimalis*). Aquaculture 287, 335–340.

Zadravec, D., Tvrdik, P., Guillou, H., Haslam, R., Kobayashi, T., Napier, J.A., Capecchi, M.R., Jacobsson, A., 2011. ELOVL2 controls the level of n-6 28:5 and 30:5 fatty acids in testis, a prerequisite for male fertility and sperm maturation in mice. J. Lipid Res. 52, 245–255.

Zhang, K., Kniazeva, M., Han, M., Li, W., Yu, Z., Yang, Z., Li, Y., Metzker, M.L., Allikmets, R., Zack, D.J., Kakuk, L.E., Lagali, P.S., Wong, P.W., MacDonald, I.M., Sieving, P.A., Figueroa, D.J., Austin, C.P., Gould, R.J., Ayyagari, R., Petrukhin, K., 2001. A 5-bp deletion in *ELOVL4* is associated with two related forms of autosomal dominant macular dystrophy. Nat. Genet. 27, 89–93.

Zhang, X.M., Yang, Z., Karan, G., Hashimoto, T., Baehr, W., Yang, X.J., Zhang, K., 2003. Elovl4 mRNA distribution in the developing mouse retina and phylogenetic conservation of Elovl4 genes. Mol Vis 9, 301–307.

Zheng, X., Ding, Z., Xu, Y., Monroig, Ó., Morais, S., Tocher, D.R., 2009. Physiological roles of fatty acyl desaturases and elongases in marine fish: Characterisation of cDNAs of fatty acyl Δ6 desaturase and *elovl5* elongase of cobia (*Rachycentron canadum*). Aquaculture 290, 122–131.

Zheng, X., Seiliez, I., Hastings, N., Tocher, D.R., Panserat, S., Dickson, C.A., Bergot, P., Teale, A.J., 2004. Characterization and comparison of fatty acyl Δ6 desaturase cDNAs from freshwater and marine teleost fish species. Comp. Biochem. Physiol. Part B Biochem. Mol. Biol. 139, 269–279.

Zheng, X., Tocher, D.R., Dickson, C.A., Bell, J.G., Teale, A.J., 2005. Highly unsaturated fatty acid synthesis in vertebrates: New insights with the cloning and characterization of a Δ6 desaturase of Atlantic salmon. Lipids 40, 13–24.